Purinergic signalling in human adipose-derived mesenchymal stromal cells and *in vitro* differentiated adipocytes.

Seema Begum Ali

A Thesis Presented for the Degree of Doctor of Philosophy at the University of East Anglia

Faculty of Science, School of Biological Sciences

February 2019

In the name of Allah, the most Beneficent, the most Merciful

Declaration

I verify that the work presented in this thesis is my own original work and has not been previously submitted for a degree at this or any other university. Where work by other authors has been included, their work has been fully cited and referenced.

In line with the regulations for submission for a degree of Doctor of Philosophy at the University of East Anglia, this thesis has a word count of approximately 76,300 words, which includes all footnotes and references, but excludes an appendix which consists of approximately 1000 words.

The data presented in Chapter 3 were published in a peer-reviewed journal:

Ali S, Turner J and Fountain SJ (2018) $P2Y_2$ and $P2Y_6$ receptor activation elicits intracellular calcium responses in human adipose-derived mesenchymal stromal cells. *Purnergic Signalling.* DOI: 10.1007/s11302-018-9618-3. [Epub ahead of print].

All experimental work and data analysis were performed by S Ali and the manuscript was written by S Ali. Both J Turner and SJ Fountain designed the research. The full manuscript is available open access at https://link.springer.com/article/10.1007/s11302-018-9618-3

The data presented in Chapter 4 and 5 were recently published in a peer-reviewed journal:

Ali SB, Turner JJO and Fountain SJ (2018) Constitutive P2Y2 receptor activity regulates basal lipolysis in human adipocytes. *Journal of Cell Science.* DOI: 10.1242/jcs.221994. [Epub ahead of print].

All experimental work and data analysis were performed by S Ali and the manuscript was written by SJ Fountain and SB Ali. Both JJO Turner and SJ Fountain designed the research. The manuscript is available open access at http://jcs.biologists.org/content/early/2018/10/11/jcs.221994

Abstract

Obesity is now a global epidemic, which represents a significant health problem. Obesity is defined as an excessive accumulation of adipose tissue mass, thus understanding adipose biology has become imperative to uncovering novel drug targets in the fight against obesity. Purinergic signalling has been implicated in a wide variety of physiological functions, however very little is currently known about the role of purinergic signalling in human adipocytes and their progenitor cells. This project aimed to characterise the P2 receptor profiles in both primary human adipose-derived mesenchymal stromal cells (AD-MSCs) and *in vitro* differentiated adipocytes and then determine the functional roles of these receptors in each cell type.

AD-MSCs and *in vitro* differentiated adipocytes express almost all of the known subtypes of P2 receptors and transient elevations of intracellular calcium levels are observed in both cell types in response to exogenous application of ATP, ADP and UTP. However subtype-selective antagonism revealed that only $P2Y_2$ and $P2Y_6$ receptors are functionally active in AD-MSCs, and $P2Y_1$, $P2Y_2$ and $P2Y_{12}$ receptors mediate nucleotide-evoked calcium responses in adipocytes. It is unclear what physiological functions $P2Y_2$ and $P2Y_6$ receptors mediate in AD-MSCs, but in adipocytes, $P2Y_2$ receptors appear to regulate basal lipolysis. Selective antagonism and shRNA-mediated knockdown of $P2Y_2$ receptors resulted in an increase in basal glycerol release. In this study, it was determined that continuous $P2Y_2$ activation suppresses basal lipolysis by maintaining calcium tone within adipocytes to tonicly inhibit calcium-sensitive isoforms of adenylate cyclase. This prevents the cytoplasmic accumulation of cAMP, thus inhibiting the activation of protein kinase A-mediated stimulated lipolytic pathways. These findings imply that $P2Y_2$ receptors may be a novel and interesting drug target for modulating adipose tissue expansion. Further research is required to fully investigate the physiological roles of all of the P2 receptor subtypes expressed in these cells.

Contents

List of Figures

List of Tables

Abbreviations

AC	Adenylate cyclase
AD	Adipose derived
ADP	Adenosine diphosphate
AMP	Adenosine monophosphate
ANGPTL4	Angiopoietin-like 4
ATGL	Adipose triglyceride lipase
ATP	Adenosine triphosphate
BAT	Brown adipose tissue
BM	Bone marrow derived
BMI	Body mass index
Bp	Base pairs
BSA	Bovine serum albumin
Ca^{2+}	Calcium ions
cAMP	Cyclic adenosine monophosphate
C/EBP	CCAAT/enhancer-binding protein
cDNA	Complementary deoxyribonucleic acid
CD	Cluster of differentiation
CGI-58	Comparative gene identification 58
CRP	C-reactive protein
C_T	Cycle threshold
CVD	Cardiovascular disease
DAB	3,3'-Diaminobenzidine
DAG	Diacylglycerol
DG	Diglyceride
DIEP	Deep inferior epigastric perforator
DNL	*De novo* lipogenesis
DMEM	Dulbecco's Modified Eagles medium
DMSO	Dimethyl sulfoxide
EC_{50}	Half-maximal effective concentration
EDTA	Ethylenediaminetetraacetic acid
ER	Endoplasmic reticulum
GH	Growth hormone
FBS	Foetal bovine serum
FFA	Free fatty acids
F_{ratio}	Fluorescence ratio
GPCR	G-protein coupled receptor
HRP	Horse radish peroxidase
HSL	Hormone sensitive lipase
IBMX	3-isobutyl-1-methylxanthine
IC_{50}	Half-maximal inhibitory concentration
IGF	Insulin-like growth factor
IGFBP	Insulin-like growth factor binding protein
IL	Interleukin
IP_3	Inositol 1,4,5-trisphosphate
LDH	Lactate dehydrogenase
MG	Monoglyceride
MGL	Monoglyceride lipase
mRNA	Messenger ribonucleic acids
ORAI1	Calcium release-activated calcium channel protein 1
PBS	Phosphate buffered saline

PDE	Phosphodiesterase
PFA	Paraformaldehyde
PKA	Protein kinase A
PLC	Phospholipase C
PMCA	Plasma membrane Ca^{2+} ATPases
PPARγ	Peroxisome proliferator-activated receptor gamma
PTx	Pertussis toxin
MESC	Mesenchymal stem cells
MOI	Multiplicity of infection
MSC	Mesenchymal stromal cells
qRT-PCR	Quantitative real time polymerase chain reaction
RANTES	Regulated on activation, normal T cell expressed and secreted
RBP4	Retinol binding protein 4
RPLP0	Ribosomal Protein Lateral Stalk Subunit P0
RT-PCR	Reverse transcription polymerase chain reaction
SAA	Serum amyloid A
SAT	Subcutaneous adipose tissue
SBS	Salt buffered solution
SERCA	Smooth endoplasmic reticular Ca^{2+} ATPase
shRNA	Short hairpin ribonucleic acid
SOCE	Store-operated calcium entry
STIM1	Stromal interaction molecule 1
T2DM	Type 2 diabetes mellitus
TNFα	Tumour necrosis factor alpha
TG	Triglyceride
UCP-1	Uncoupling protein 1
UDP	Uridine diphosphate
WAT	White adipose tissue
WHO	World Health Organisation
UTP	Uridine triphosphate
VAT	Visceral adipose tissue

Acknowledgements

There are a number of people that I would like to thank that were pivotal to the success of this project. Firstly, I would like to thank my incredible family and friends for their unfailing support. I would also like to thank my supervisors, Dr Samuel Fountain, Professor Jeremy Turner and Dr Matthew Fenech, for their continuous support and guidance. In particular, I would like to thank Sam for believing in me (at times more than I believed in myself) and for choosing me to pursue this project. I would have been completely lost without his help and guidance over the past four years. I am also incredibly grateful to Jeremy for his boundless enthusiasm and encouragement and Matt for all of his practical guidance at the beginning of my PhD.

In addition, I would also like to express my profound gratitude to all the members, past and present, of Fountain Lab, namely Dr Janice Layhadi, Dr Lisa Burrows, Izzuddin Ahmad, Dr Priscilla Day, Jonny Micklewright, Dr David Richards, Sean Cullum, Dr Maria Gonzalez-Montelongo and Dr Tim Ellison. It was my privilege to work with them all. I want to say a huge thank you for all of their support and for generally making my PhD an incredible experience. I'm not sure how I would have coped without them all. I also want to extend a special thank you to Janice and David for all of their help in the lab and for putting up with my constant stream of questions.

Furthermore, I would like to thank the Biotechnology and Biological Sciences Research Council for funding my project and the Plastic Surgery Team at the Norfolk and Norwich University Hospital for their invaluable expertise and for allowing me to approach their patients for my research project. In particular, I would like to thank the research nurses attached to my project, Georgie, Deirdre and Jill, who have been absolutely amazing at recruiting patients and making sure I always had plenty of cells to work with. Most importantly, I would like to thank all of the lovely women who volunteered to take part in my research, without them this project would not have been possible, so I will be forever grateful for their generosity.

Chapter 1: Introduction

1.1 Obesity

Obesity is a pathological condition characterised by the abnormal or excessive accumulation of body fat capable of effecting an individual's health and wellbeing (WHO, 2018). Obesity is currently a worldwide epidemic with global estimates indicating that more than 1.9 billion adults are classified as overweight, of which 650 million are obese (WHO, 2016). The global prevalence of obesity has been steadily increasing over the past four decades (Afshin *et al.*, 2017). Many countries, including the United Kingdom, now have a greater than 60% prevalence of overweight and obese adults (WHO, 2016) (Figure 1.1A), which is accompanied by a distressing increase in childhood obesity. Most countries that exhibit an abundance of overweight adults have a greater than 30% prevalence of overweight children and adolescents (WHO, 2016) (Figure 1.1B). It is estimated that 41 million children under the age of 5 and 340 million children aged between 5 and 19 worldwide are classified as overweight or obese (WHO, 2016). Although, as a proportion there are less overweight children than adults, the rate of increase in childhood obesity exceeds that of adults in many countries (Afshin *et al.*, 2017). The substantial rise in global obesity is likely to be fuelled by environmental factors, such as the surge in the availability, affordability and accessibility of high calorie foods and a decrease in physical activity due to urbanisation (Swinburn *et al.*, 2011).

Body mass index (BMI) values are the most widely used classification system to identify overweight and obese adults (Table 1.1). BMI values are determined by dividing an individual's weight in kilograms by their height in meters squared (BMI = weight (kg)/height $(m)^2$). The BMI thresholds shown in Table 1.1 only apply to adults. For children and adolescents (five to 19 years old) the thresholds are adjusted according to age, with BMI values of greater than one or two standard deviations above the WHO Growth Reference median being defined as overweight or obese respectively. For children aged between two and five, weight-for-height values of greater than two and three standard deviations above WHO Child Growth Standards median are considered overweight and obese respectively (WHO, 2018). Although widely adopted, the BMI system is criticised for its inability to accurately measure total fat mass and fat distribution (Nuttall, 2015), which are both key indicators of metabolic risk (Kissebah *et al.*, 1982, 1989; Fox *et al.*, 2009). Waist measurements are able to overcome some of these criticisms, as waist circumference and waist-to-hip ratios measure abdominal obesity, which is associated with an increased risk for developing metabolic syndrome (Després and Lemieux, 2006). Waist circumferences of greater than 102 cm and 88 cm for men and women respectively indicate elevated risk (Lean *et al.*, 1995). However, these thresholds cannot be universally applied, as studies indicates that ethnicity can also impact on cardiovascular risk, thus lower cut-offs are required for individuals of Asian descent (Misra *et al.*,

2005). Despite the criticisms of the BMI classification system, it is still the most extensively used system and BMI is a strong predictor of overall mortality in individuals that fall above and below the healthy range (Whitlock *et al.*, 2009).

Table 1.1 International classification of human body weight using body mass index (BMI) values. BMI values are calculated by dividing an individual's weight in kilograms by the square of their height in meters. These values apply to both sexes and all ages, excluding children under the age of 19.

Body mass index (kg/m^2)	Classification
< 18.5	Underweight
18.5 - 24.9	Healthy weight
25.0 - 29.9	Overweight
> 30.0	Obese

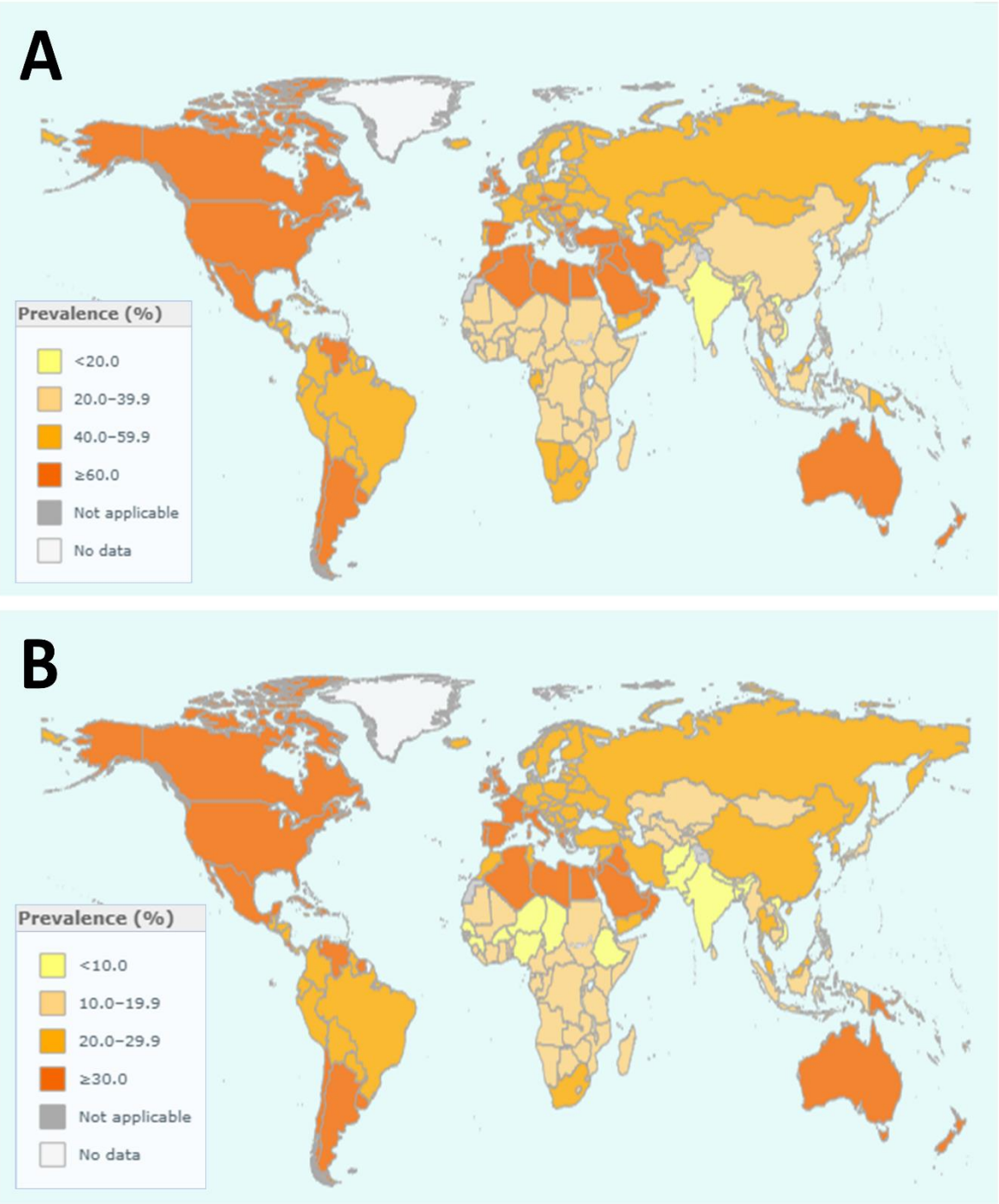

Figure 1.1 Map depicting the prevalence of overweight and obese adults and children per country. (A) Proportion of adults (aged 18 or over) with BMI values of above 25 kg/m^2 in each country. (B) Proportion of children and adolescents (aged 5 to 19 years old) with BMI values of greater than one standard deviation above the WHO Growth Reference median per country. Colour coding refers to different percentages for each map as indicated by the respective keys in each panel. Data shown is from 2016 and was adapted from the World Health Organisation's website. Source: http://www.who.int/gho/ncd/risk_factors/overweight/en/ Last accessed 6.8.18.

1.2 Wider impacts of obesity

The global rise in the incidence of obesity represents a major health and economic issue. It's estimated that a larger overweight population in the United Kingdom costs the National Health Service £3.2 billion (Allender and Rayner, 2007). More importantly, obesity poses a significant health problem, with 7.1% of deaths worldwide attributed to being overweight or obese (Afshin *et al.*, 2017). There is an almost log-linear increase in the risk of death as BMI increases over 25 kg/m^2 (Di Angelantonio *et al.*, 2016), where each 5 kg/m^2 increase in BMI above the healthy range is associated with a 41% increase in risk of vascular mortality and 210% elevated probability of diabetic mortality, as well as a 29% higher risk of overall mortality (Whitlock *et al.*, 2009). Vascular diseases, such as cardiovascular disease (CVD), accounts for almost 70% of all of the deaths associated with being overweight (Afshin *et al.*, 2017). BMI values of between 30 and 35 kg/m^2 are predicted to result in a two to four year reduction in median lifespan, whereas BMI values of 40 to 45 kg/m^2 may reduce median life expectancy by a staggering eight to ten years (Whitlock *et al.*, 2009). Between 1990 and 2015, the total number of deaths associated with being overweight or obese increased by 28.3% (Afshin *et al.*, 2017).

Although the excessive expansion of adipose tissue observed in obesity is an independent risk factor for mortality, obesity is also strongly associated with the development of other metabolic diseases, such as type 2 diabetes mellitus (T2DM) and CVD. This occurs, because adipose tissue plays a prominent role in energy metabolism, and dysfunction of adipose tissue disrupts the carefully balanced homeostatic systems in place to maintain healthy metabolism. Metabolic syndrome is characterised by the concurrent presence of multiple interrelated risk factors for T2DM and CVD. Symptoms include hypertension, hypertriglyceridemia, elevated plasma free fatty acids (FFA), hyperglycaemia and obesity (particularly abdominal obesity). Many obese individuals display liver steatosis, which is known to contribute to insulin resistance and may lead to the development of non-alcoholic fatty liver disease (Bjørndal *et al.*, 2011).

There are numerous factors that are capable of affecting an individual's personal risk for developing obesity and its related comorbities. These include socioeconomic status, counterindications from pharmaceutical treatments, epigenetics, the gut microbiome and endocrine disruptors (McAllister *et al.*, 2009). However regardless of the underlying cause of obesity, obesity and related metabolic disorders are at least in part due to adipose tissue dysfunction caused by overwhelming the body's capacity to safely store excess calories within adipocytes (Zhao, 2013). Thus, a fundamental understanding of adipose tissue functioning is necessary to fully comprehend the molecular mechanisms involved in the pathogenesis of obesity. Currently the best interventions for combating obesity are maintaining a healthy diet and exercising and/or bariatric surgery. Only limited success has been attained with pharmacological inventions (Apovian, 2016). The global increase in the

incidence of obesity and related comorbidities means that new and effective strategies for tackling the problem of obesity are urgently required. Identification of novel mechanisms and drug targets could save or at least improve the quality of life of countless people across the globe, as well as significantly reducing the financial burden of obesity.

1.3 Types of adipose tissue and adipocytes

There are three distinct types of adipocytes: white, brown and beige adipocytes. These adipocytes are contained within two different types of adipose tissue, white and brown adipose tissue (WAT and BAT respectively). As their names suggest, WAT predominantly contains white adipocytes, whereas the primary cell type in BAT is brown adipocytes. Beige adipocytes are found sporadically within WAT depots (Kiefer, 2017).

Although neonates have a relative abundance of BAT, the amount of BAT reduces with age and the vast majority of adipose tissue in adult humans is WAT (Lecoultre and Ravussin, 2011). However, small depots of BAT are present in adults as well (Cypess *et al.*, 2009; van Marken Lichtenbelt *et al.*, 2009; Virtanen *et al.*, 2009). BAT is easily distinguishable by its highly distinctive morphology. Brown adipocytes are multilocular and contain an abundance of mitochondria (Figure 1.2), which contain cytochrome enzymes with iron as a cofactor. The coloured cytochromes and the highly vascular nature of BAT gives rise to the dark red or 'brown' appearance of BAT (Lee *et al.*, 2013). The primary functions of BAT, or brown adipocytes, is to generate heat via non-shivering thermogenesis and to decrease metabolic efficiency by accelerating the rate of food combustion (Cannon and Nedergaard, 2004). Brown adipocytes achieve these functions via uncoupling protein 1 (UCP-1), which is expressed almost exclusively in the inner mitochondrial membrane of brown adipocytes. When humans are exposed to cold temperatures or there is an excess of energy, sympathetic nervous stimulation of BAT leads to activation of β_3-adrenergic receptors expressed on the surface of brown adipocytes, which triggers the breakdown of triglycerides to release FFAs. The FFAs are then transported into the mitochondria and bind to and activate UCP-1. The FFAs also undergo β-oxidation and consequently fuel the electron transport chain to generate a proton gradient between the inner and outer mitochondrial membranes. The protons travel back through the inner membrane via UCP-1, thus rapidly dissipating the gradient to generate heat instead of ATP. After lipolysis is terminated, residual FFA are oxidised and UCP-1 reverts back to its basal inhibited state (Cannon *et al.*, 2004; Nicholls and Rial, 2016). There is an inverse relationship between the abundance of BAT and weight (Cypess et al. 2009; van Marken Lichtenbelt et al. 2009) and in recent years there has been much interest in trying to manipulate BAT to enhance energy expenditure to combat obesity, although this will not be discussed further as this project focuses predominantly on white adipocytes and their progenitor cells.

WAT is the biological caloric reservoir of the body. In times of nutrient excess, adipose tissue is able to expand by storing excess nutrients as triglycerides in specialised lipid droplets within adipocytes (Ahmadian *et al.*, 2010). Like BAT, WAT also has highly distinctive morphology. White adipocytes, the primary cell type in WAT, are very large unilocular cells that contain large lipid droplets that take up more than 90% of the interior of the cells (Sheldon, 2011). The lipid droplets displace all the other organelles, including the nucleus, to the periphery of the cell (Figure 1.2).

WAT also contains beige adipocytes (also known as brite adipocytes), which are dynamic cells that can transition from white (energy storage) to brown (energy expenditure) phenotypes when exposed to certain stimuli, via a phenomenon termed adaptive thermogenesis or 'browning' (Rutkowski *et al.*, 2015; Roh *et al.*, 2018). There are thought to be specific pools of beige adipocytes precursors within WAT, which are induced to differentiate in response to adrenergic, thermogenic or hormonal stimuli (Kajimura *et al.*, 2015). Unlike white adipocytes, which do not express UCP-1, beige adipocytes are capable of upregulating their expression of UCP-1 and adopting a more classical brown adipocyte phenotype (Kalinovich *et al.*, 2017; Roh *et al.*, 2018). Beige adipocytes are morphologically distinct from white adipocytes as they are multilocular and contain more mitochondria (Figure 1.2).

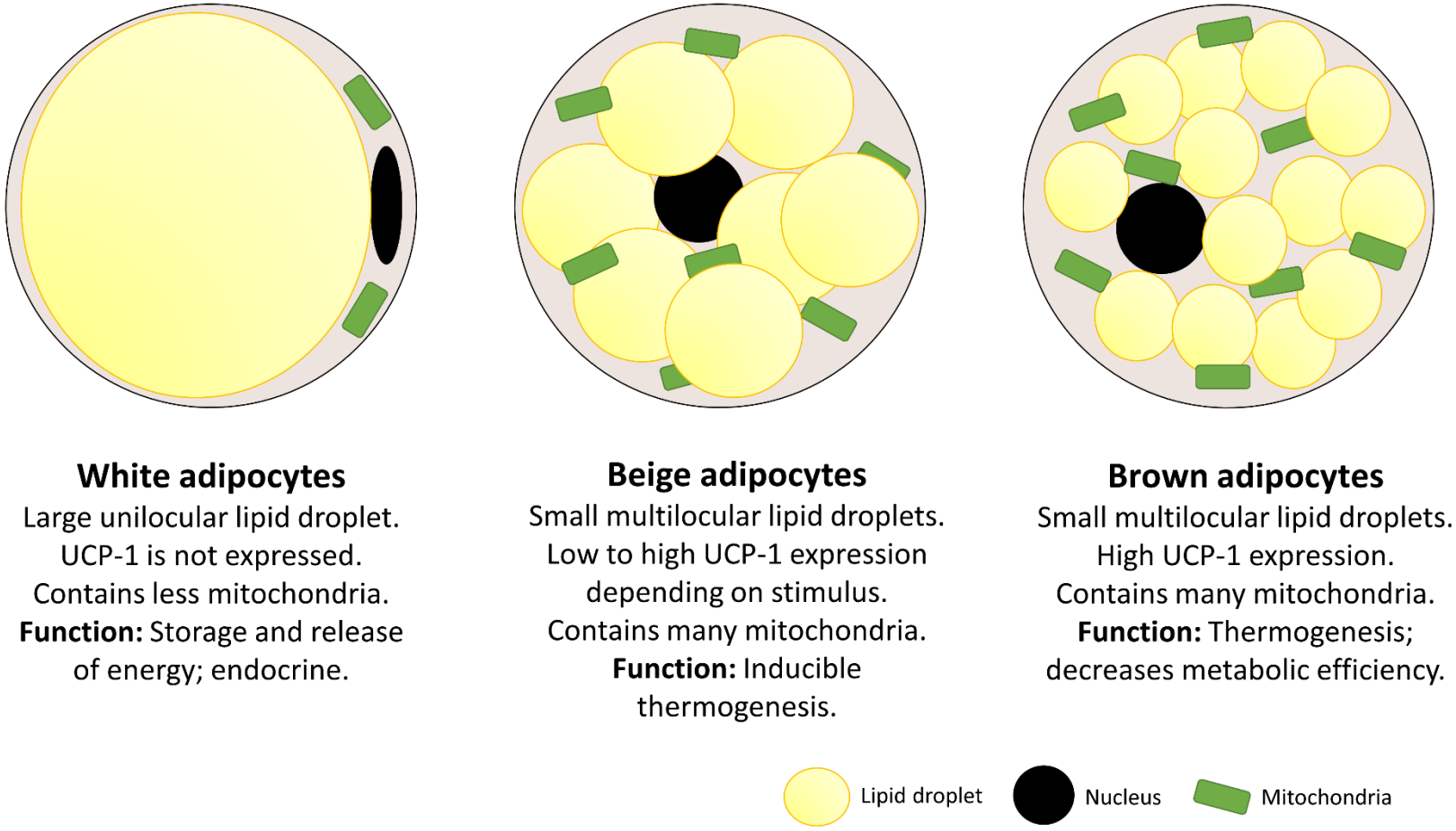

Figure 1.2 Schematic diagrams of the different types of adipocytes, including the major morphological features and functions of each cell type.

1.4 White adipose tissue

WAT consists of tightly packed white adipocytes surrounded by nerves and blood vessels (Figure 1.3). The tissue also contains immune cells, beige adipocytes and adipocyte precursor cells that all contribute to maintaining healthy WAT (Cristancho and Lazar, 2011; Kiefer, 2017). WAT is subdivided into subcutaneous and visceral adipose tissue (SAT and VAT respectively). Although the distribution of SAT and VAT varies from person-to-person and is dependent on a variety of factors including age, sex, ethnicity and diet (Wajchenberg, 2000), on average SAT accounts for 80-90% of total body fat, whereas VAT accounts for 5-20% of total body fat (Karastergiou *et al.*, 2012). SAT is located directly below the skin, with specific depots in the abdominal, subscapular, gluteal and femoral regions (Karastergiou *et al.*, 2012), whereas VAT is located around the vital organs in the mesentery, omentum, pericardium and mediastinum (Kwok *et al.*, 2016). SAT is the primary site of long-term nutrient storage, but it also serves as a barrier against dermal infections, protects against external mechanical stress by cushioning organs and acts as a thermal insulating layer to limit heat loss via the skin (Kwok *et al.*, 2016). Abdominal SAT is anatomically divided by the Scarpa's fascia into two layers: deep SAT (DSAT) and superficial SAT (SSAT) (Kelley *et al.*, 2000; Walker *et al.*, 2007). DSAT and SSAT are metabolically distinct. Expansion of SSAT appears to confer beneficial cardiometabolic effects in diabetic patients (Golan *et al.*, 2012), whereas DSAT enlargement correlates with the development of insulin resistance (Kelley *et al.*, 2000; Smith *et al.*, 2001; Marinou *et al.*, 2014). Like DSAT, increased VAT mass directly correlates with the development of insulin resistance, and VAT expansion is also a risk factor for CVD and T2DM (Wajchenberg, 2000; Ibrahim, 2010). The difference between SSAT and DSAT/VAT may be due to variation in the metabolic activity of white adipocytes in these depots. White adipocytes in both VAT and DSAT are known to more efficiently hydrolyse triglycerides than their SSAT counterparts (Hoffstedt *et al.*, 1997; Karastergiou *et al.*, 2012), which means that DSAT and VAT release more free fatty acids (FFA) and elevate plasma FFA levels which promotes the development of insulin resistance (Björntorp, 1990; Monzon *et al.*, 2002). By contrast, SSAT displays lower lipolytic activity and higher insulin sensitivity, which suggests that white adipocytes in SSAT have a greater capacity to act as a physiological buffering system to store excess FFA in the form of triglycerides and consequently protect other tissues from lipotoxic effects (Frayn, 2002).

There are also regional differences between the properties of white adipocytes within SAT. White adipocytes in abdominal SAT are more sensitive to stimulation of lipolysis than adipocytes in the gluteal regions (Wahrenberg *et al.*, 1989). This is due to a predominance of anti-lipolytic signalling pathways in lower body adipose tissue depots versus their upper body counterparts (Manolopoulos *et al.*, 2012). In addition, femoral SAT depots are prone to expand via hyperplasia, whereas abdominal SAT preferentially expands via hypertrophy (Tchoukalova *et al.*, 2010). Hypertrophy is associated with an increased metabolic risk (Weyer *et al.*, 2000). These depot differences underlie

the assertion that upper body obesity, but not lower body obesity, is associated with metabolic dysfunction (White and Tchoukalova, 2014).

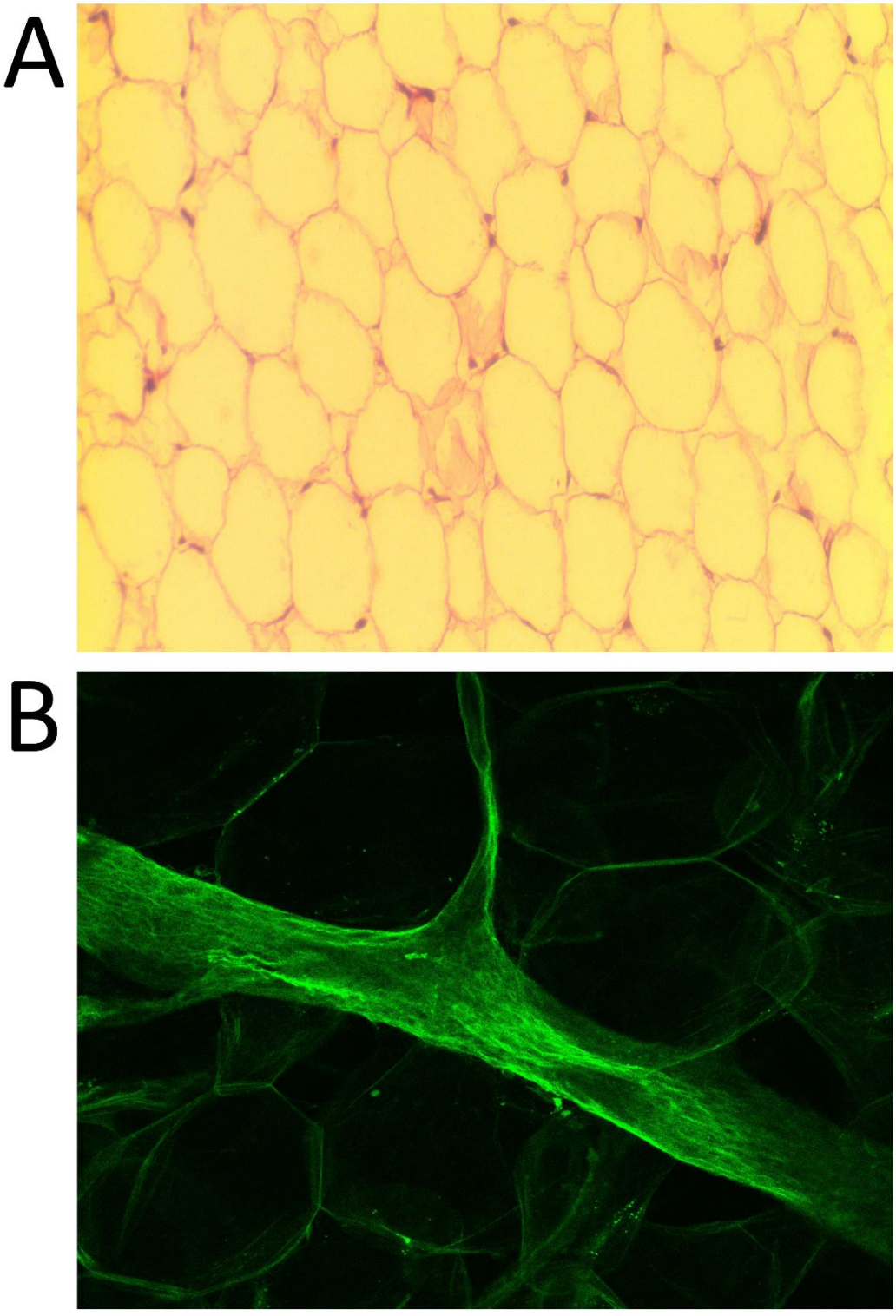

Figure 1.3 Images of primary human subcutaneous abdominal white adipose tissue. (A) Brightfield image of a 6 µm section of human adipose tissue stained with haematoxylin and eosin taken at 100X magnification. (B) Image of human adipose tissue autofluorescence taken using a multiphoton microscope (200X magnification) showing a large blood vessel intersecting through the adipocytes. In both images only the plasma membranes of the adipocytes are visible.

1.5 Mesenchymal stromal cells

Adipocytes, like chondrocytes, osteoblasts and myocytes, are derived from mesenchymal stem cells (MESCs). In adult humans, approximately 10% of mature adipocytes are renewed annually via adipogenesis (Spalding *et al.*, 2008). Adipogenesis, as well as hypertrophy for mature adipocytes, enables the expansion of adipose tissue mass in response to a surplus of energy. Adipogenesis is a very complex process, which begins when MESCs undergo the process of commitment to create preadipocytes, which are morphologically indistinguishable from their progenitors (Cristancho *et al.*, 2011). Wnt signalling, bone morphogenetic proteins and the confluency of the cells are key drivers of commitment. Preadipocytes are then either maintained as progenitor cells by inhibiting further progression of adipogenesis or they are induced to terminally differentiate (Cristancho *et al.*, 2011). Differentiation of preadipocytes commences with the activation of a transcriptional cascade to produce several adipocyte specific proteins, including leptin, adiponectin and fatty acid binding protein 4. There are a huge variety of transcription factors that play a role in adipogenesis, including a pivotal role for peroxisome proliferator-activated receptor γ (PPARγ), as well as CCAAT/enhancer-binding protein-α (C/EBPα), C/EBPβ and C/EBPδ. C/EBPβ and C/EBPδ drive expression of PPARγ during the early stages of differentiation and then C/EBPα maintains expression later in the process (Rosen and Spiegelman, 2006). Lower rates of adipogenesis are associated with increased incidence of visceral obesity, adipocyte hypertrophy and higher fasting blood glucose levels (Lessard *et al.*, 2014). This suggests that efforts to improve the adipogenic potential of progenitor cells may oppose this metabolically unhealthy phenotype.

WAT represents the most abundant and easily accessible source of mesenchymal stromal cells (MSCs) in adult humans. The term MSC refers to the multipotent plastic-adherent cells that can be isolated from bone marrow and other tissues, including adipose tissue (Dominici *et al.*, 2006). As MESCs are morphologically indistinguishable from preadipocytes and dedifferentiated mature cells, it is likely that multipotent cells extracted from adipose tissue (MSCs) are a heterogenous population of cells (Baer and Geiger, 2012). A lack of specific markers for these different cell types means that the multipotent cells extracted from adipose tissue cannot be accurately referred to as MESCs or preadipocytes and must instead be referred to as MSCs. In addition to differentiating to adipocytes, MSCs are also capable of differentiating *in vitro* to osteoblasts, chondrocytes, myocytes and neurons (Ning *et al.*, 2006; Uccelli *et al.*, 2008; Karantalis and Hare, 2015). This has led to several clinical trials to determine whether MSCs can be used therapeutically to regenerate damaged tissue (Thesleff *et al.*, 2011; Houtgraaf *et al.*, 2012; Jo *et al.*, 2014). The initial results are promising and propose that MSCs exert their beneficial effects by migrating to the site of injury and utilising their regenerative capacity, as well as having an immunomodulatory effect at the injury site (Cho *et al.*, 2009; Feisst *et al.*, 2015). However, the process of MSC senescence severely diminishes the

potential benefits of this treatment. Senescence adversely affects migration and proliferation of MSCs, as well as impairing their capacity to differentiate (Turinetto *et al.*, 2016; Kim and Park, 2017). In addition, senescent MSCs secrete pro-inflammatory factors, rather than anti-inflammatory cytokines, thus potentially exacerbating the original injury (Turinetto *et al.*, 2016). A greater understanding of the molecular mechanisms that underline normal MSC functioning is needed to be able to overcome these issues.

1.6 White adipocytes

Unlike other cell types, white adipocytes have specifically developed to accumulate triglycerides without experiencing lipotoxicity (Konige *et al.*, 2014). Their ability to store neutral lipids underlies their distinctive morphology, which consists of greater than 90% of the interior of the cell being occupied by one large lipid droplet which displaces all the other organelles, including the nucleus, to the cell periphery (Figure 1.2 and 1.3). White adipocytes are highly dynamic cells that facilitate both storage and release of nutrients, via lipogenesis and lipolysis respectively, in response to an individual's energy stasis. They are also capable of synthesising and releasing a wide variety of adipokines, which regulate systemic metabolism (Halberg *et al.*, 2008).

White adipocytes can dynamically change their size depending on their lipid content. Hyperplasia of adipocytes occurs when there is a surplus of energy, such as after a meal, and there is a predominance of lipogenesis over lipolysis (Bódis and Roden, 2018). The term lipogenesis encompasses both fatty acid and triglyceride synthesis (Kersten, 2001). Although endogenous *de novo* lipogenesis (DNL) can occur in adipose tissue, in the postprandial state DNL primarily occurs in the liver and then the triglycerides are transported to adipose tissue to be safely stored within adipocytes (Postic and Girard, 2008). However, fatty acids are also acquired directly via dietary intake of fats and indirectly via increased carbohydrate consumption leading to activation of fatty acid synthase (FAS) in adipose tissue, which facilitates conversion of glucose to fatty acids (Hillgartner *et al.*, 1995). It is thought that DNL in adipose tissue promotes a more metabolically healthy phenotype than DNL in the liver, because DNL in WAT generates metabolites, such as FA esters of hydroxy FA, which enable crosstalk between WAT and other organs involved in insulin sensitivity and energy metabolism (Yilmaz *et al.*, 2016), whereas liver DNL is linked to liver hepatosteatosis (Cao *et al.*, 2008). Obesity is associated with a down-regulation of lipogenic genes in WAT and an upregulation of lipogenic genes in the liver, thus promoting metabolic dysfunction (Ranganathan *et al.*, 2006; Eissing *et al.*, 2013; Bódis *et al.*, 2018).

1.7 Lipolysis

In addition to storing energy when there is an excess of nutrients (fed state) via lipogenesis, white adipocytes are also able to release energy via lipolysis when there is an energy deficit (fasting state) (Kersten, 2001; Nielsen *et al.*, 2014). Lipolysis encompasses the sequential hydrolysis of triglycerides (TG) to their component parts of free fatty acids (FFAs) and glycerol. This process is mediated by three lipases: Adipose triglyceride lipase (ATGL), hormone-sensitive lipase (HSL) and monoglyceride lipase (MGL). ATGL catalyses the initial rate-determining hydrolysis of TG to diglycerides (DG) (Zimmermann *et al.*, 2004), then DGs are hydrolysed to monoglycerides (MG) by HSL (Haemmerle *et al.*, 2002) and finally MG is broken down to glycerol by MGL (Fredrikson *et al.*, 1986). Each step yields one FFA molecule, therefore each TG molecule ultimately yields three FFAs. Adipocytes are the only cell type in the body that are capable of secreting FFAs into the bloodstream. These FFAs can subsequently travel to distant peripheral tissues and act as a substrate for β-oxidation to generate ATP to fuel cellular processes (Kolditz and Langin, 2010). Loss of lipid from adipocytes causes a reduction in adipocyte size, which may ultimately lead to weight loss.

In addition to acting as an energy source, it has been determined that many of the products of lipolysis, such as DG, MG and FFAs, are involved in intracellular and systemic signalling mechanisms (Zechner *et al.*, 2012). However augmented concentrations of these intermediate products of lipolysis have been linked to the development of insulin resistance in peripheral tissues (Boura-Halfon and Zick, 2009; Copps and White, 2012). Excessively elevated levels of FFA in the plasma is widely thought to be involved in the development of insulin resistance and T2DM, thus indicating that dysregulation of lipolysis in obese individuals is likely to have adverse effects on insulin sensitivity (Nielsen *et al.*, 2014).

There are two forms of lipolysis: basal and stimulated lipolysis. Basal lipolysis is the omnipresent low levels of triglyceride hydrolysis that occurs spontaneously in the absence of external stimuli, whereas stimulated lipolysis facilitates a more substantial release of FFAs and glycerol in response to external stimuli.

1.7.1 Stimulated lipolysis

There are a variety of substances that are able to initiate stimulated lipolytic pathways in white adipocytes, including hormones, cytokines and nervous stimulation. Fasting initiates sympathetic nervous stimulation of WAT via catecholamine-mediated activation of β-adrenoreceptors on the surface of white adipocytes (Fain, 1973) (Figure 1.4). Similarly, activation of other G_s-coupled receptors, such as thyroid stimulating hormone (TSH) receptors (Endo and Kobayashi, 2012) and melanocortin receptors (Cho *et al.*, 2005; Rodrigues *et al.*, 2013), also stimulate lipolysis. Activation of G_s-coupled receptors stimulates adenylate cyclase (AC) to generate cyclic AMP (cAMP). Cytoplasmic accumulation of cAMP activates protein kinase A (PKA) (Langin, 2006), which in turn

phosphorylates HSL and perilipins on the surface of the lipid droplet to allow translocation of HSL from the cytoplasm to the lipid droplet (Miyoshi *et al.*, 2006). Phosphorylation of perilipins also promotes the release of comparative gene identification-58 (CGI-58) (Sahu-Osen *et al.*, 2015), which is a potent co-activator of ATGL that increases the activity of ATGL by up to 20-fold (Schweiger *et al.*, 2006; Miyoshi *et al.*, 2008). At the surface of the lipid droplet, ATGL begins hydrolyzing TGs and to produce DGs, which act as a substrate for HSL. Then MGL catalyses the breakdown of MG to FFA and glycerol (Figure 1.4). The FFA are recycled or released into the bloodstream where they are able to travel to distant organs to be utilised as a cellular energy source (Ahmadian *et al.*, 2010). ATGL and HSL are the main drivers of TG hydrolysis. Studies indicate that knocking out ATGL or HSL expression in mice leads to an approximately 70% reduction in β-adrenergic stimulated lipolysis. Furthermore, selective inhibition of HSL in ATGL knockout mice results in a 95% reduction in TG hydrolase activity versus wildtype mice (Schweiger *et al.*, 2006).

Cardiac hormones, such as atrial natriuretic peptides (ANP) and B-type natriuretic peptides (BNP), can also stimulate lipolysis (Sengenès *et al.*, 2003). Cardiac hormones are released from the heart in response to myotubal distension and travel via the bloodstream to WAT where they bind to guanylyl cyclase (GC)-linked type-A natriuretic peptide receptors expressed on the surface of white adipocytes. This stimulate the conversion of GTP to cyclic GMP, which in turn activates protein kinase G (PKG), which acts in the same manner as PKA to stimulate lipolysis (Sengenès *et al.*, 2000) (Figure 1.4). In addition, other hormones such as growth hormone (GH) also stimulate lipolysis (Hansen *et al.*, 2002). Although the exact mechanism is not well understood, it is hypothesized that GH renders adipocytes more responsive to β-adrenergic stimulation (Doris *et al.*, 1994; Yang *et al.*, 2004) and less responsive to the anti-lipolytic effects of insulin (Johansen *et al.*, 2003).

Furthermore, cytokines are also capable of stimulating lipolysis in adipocytes. Tumour necrosis factor α (TNFα) significantly decreases the expression of phosphodiesterase (PDE) 3B (H. H. Zhang *et al.*, 2002), thus reducing the breakdown of cAMP to allow cAMP accumulation and consequent activation of PKA-mediated lipolysis. TNFα also increases ATGL activity by initiating remodeling of core components of the lipolytic machinery (Nielsen *et al.*, 2014).

1.7.2 Anti-lipolytic pathways

Although catecholamines stimulate lipolysis via β-adrenergic receptors, they can also inhibit lipolysis via activation of α_2-adrenergic receptors. α_2-adrenergic receptors are G_i-coupled, thus activation of these receptors inhibits AC to prevent the elevation of cytoplasmic cAMP levels and subsequent initiation of lipolysis (Nielsen *et al.*, 2014) (Figure 1.4). Similarly activation of other G_i-coupled receptors, such as adenosine A1 receptors (Fredholm and Sollevi, 1977; Ohisalo, 1981; Johansson *et al.*, 2008) and neuropeptide Y-Y_1 receptors (Serradeil-Le Gal *et al.*, 2000), also has an inhibitory effect on lipolysis.

However, the main anti-lipolytic pathway is mediated by insulin. There is a post-prandial elevation of plasma insulin levels, which is capable of inhibiting lipolysis (Jensen, 1995), while also promoting lipogenesis (Czech *et al.*, 2013). The anti-lipolytic effects of insulin are achieved by activating phosphodiesterases 3B, which leads to degradation of cAMP and subsequent deactivation of PKA-mediated lipolysis. Insulin binding to insulin receptors expressed on the surface of adipocytes induces autophosphorylation of the receptors and subsequent phosphorylation of insulin receptor substrate (IRS) proteins (White, 1998). IRS proteins then activate phosphatidylinositol 3-kinase (PI3K), which generates phosphatidylinositol-3,4,5- triphosphate (PIP3), which in turn activates phosphoinositide-dependent kinase and this activates protein kinase B (PKB)-mediated activation of PDE3B (Alessi *et al.*, 1997; Stokoe *et al.*, 1997; Nielsen *et al.*, 2014) (Figure 1.4).

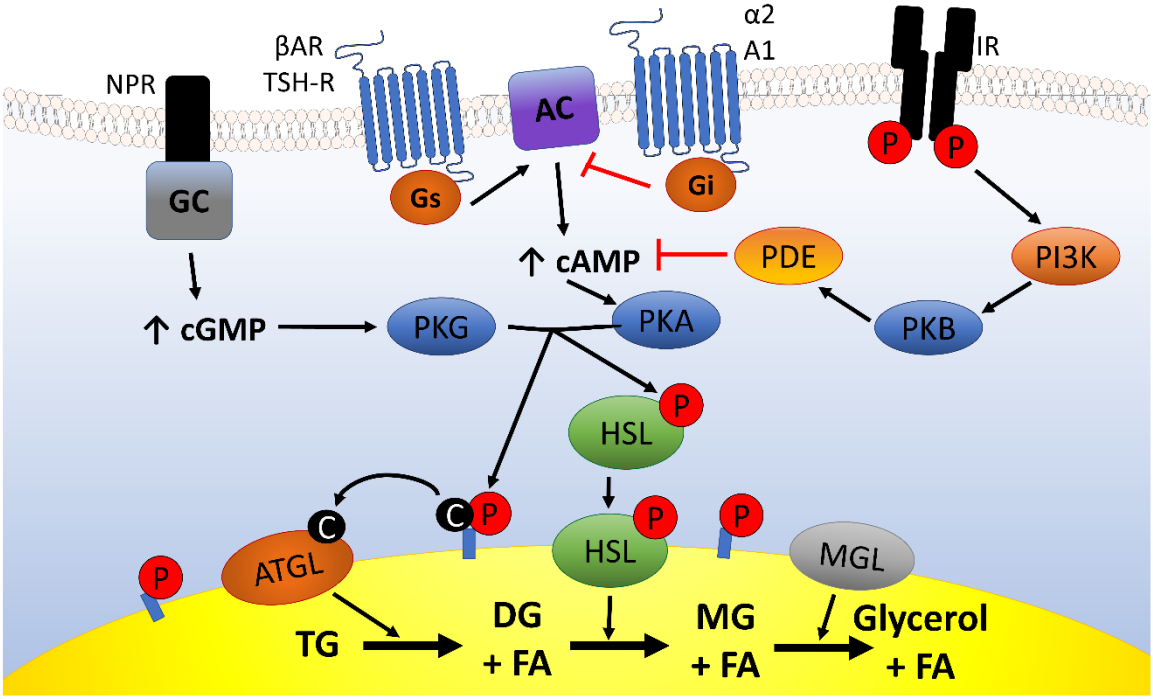

Figure 1.4 Schematic diagram of the molecular mechanisms governing stimulated lipolytic pathways, including some inhibitory pathways. Lipolysis can be stimulated by activation of G_s-coupled receptors, such as β-adrenoreceptors (βAR) and thyroid stimulating hormone receptors (TSH-R). Upon agonist binding, $G\alpha_s$ (Gs) proteins stimulate adenylate cyclase (AC) to produce cyclic AMP (cAMP). The accumulation of cAMP activates protein kinase A (PKA), which then phosphorylates hormone sensitive lipase (HSL) and perilipins (blue rectangle) on the surface of the lipid droplet. This allows HSL to translocate to the lipid droplet and it also causes comparative gene identification-58 (CGI-58) (black circle containing a white C) to dissociate from perilipins and bind to adipose triglyceride lipase (ATGL). ATGL then catalyses the hydrolysis of triglycerides (TG) to diglycerides (DG). DG are then further hydrolysed by HSL to monoglycerides (MG) and finally MGs are broken down to glycerol by monoglyceride lipase (MGL). Each step also yields one fatty acid (FA). Activation of guanylyl cyclase (GC)-linked type-A natriuretic peptide receptors (NPR) also stimulates lipolysis by stimulating accumulation of cyclic GMP (cGMP), which in turn activates protein kinase G (PKG), which acts in the same manner as PKA to stimulate lipolysis. There are also pathways that inhibit stimulated lipolysis, such as via α_2-adrenoceptor (αAR) or adenosine A1 receptor (A1) activation. Both of these receptors are G_i-protein (Gi) coupled receptors, thus their activation leads to an inhibition of AC. In addition, insulin also inhibits lipolysis by binding to insulin receptors (IR) and causing autophosphorylation of IRs, which then phosphorylates insulin receptor substrate (IRS) proteins. IRS proteins then activate phosphatidylinositol 3-kinase (PI3K), which eventually activates protein kinase B (PKB)-mediated activation of phosphodiesterase (PDE), which breaks down cAMP to prevent cAMP accumulation and subsequent induction of stimulated lipolysis.

1.7.3 Basal lipolysis

In comparison to stimulated lipolysis, little is currently known regarding the underlying mechanisms governing basal lipolysis, though it has been suggested that perilipins and ATGL play a prominent role (Miyoshi *et al.*, 2008). Under basal conditions, perilipins expressed on the surface of lipid droplets act as a barrier between the triglycerides within the lipid droplet and the lipases (ATGL and HSL) in the cytoplasm (Miyoshi *et al.*, 2008) (Figure 1.5). Perilipins play an important role in limiting the extent of basal lipolysis. This is evidenced by the fact that perilipin knockout mice have smaller adipocytes and higher rates of basal lipolysis than their wildtype counterparts (Martinez-Botas *et al.*, 2000; Tansey *et al.*, 2001). In addition, CGI-58 reversibly interacts with perilipin A on the surface of the lipid droplet (Figure 1.5), thus preventing CGI-58 from interacting with ATGL and indirectly reducing ATGL activity (Granneman *et al.*, 2007).

In the basal state, ATGL localizes to both the cytoplasm and lipid droplet (Zimmermann *et al.*, 2004; Granneman *et al.*, 2007), whereas HSL predominantly resides in the cytoplasm (Granneman *et al.*, 2007) (Figure 1.5). ATGL Knockout mice display reduced FFA release under basal and stimulated conditions, which suggests that ATGL is likely to play a role in both basal and stimulated lipolysis (Schweiger *et al.*, 2006). In addition, overexpression of ATGL is associated with an approximately two-fold increase in basal glycerol and FFA release (Kershaw *et al.*, 2006), while ATGL silencing substantially decreased basal lipolysis (Bezaire *et al.*, 2009). Interestingly, HSL-null mice display similar rates of basal lipolysis to their wildtype counterparts (Wang *et al.*, 2001; Haemmerle *et al.*, 2002), and HSL overexpression and silencing has no effect on the rate of basal lipolysis in human adipocytes (Bezaire *et al.*, 2009). This suggests HSL has a limited role in basal lipolysis. Much more research is required to fully comprehend the complex molecular mechanisms involved in regulating basal lipolysis.

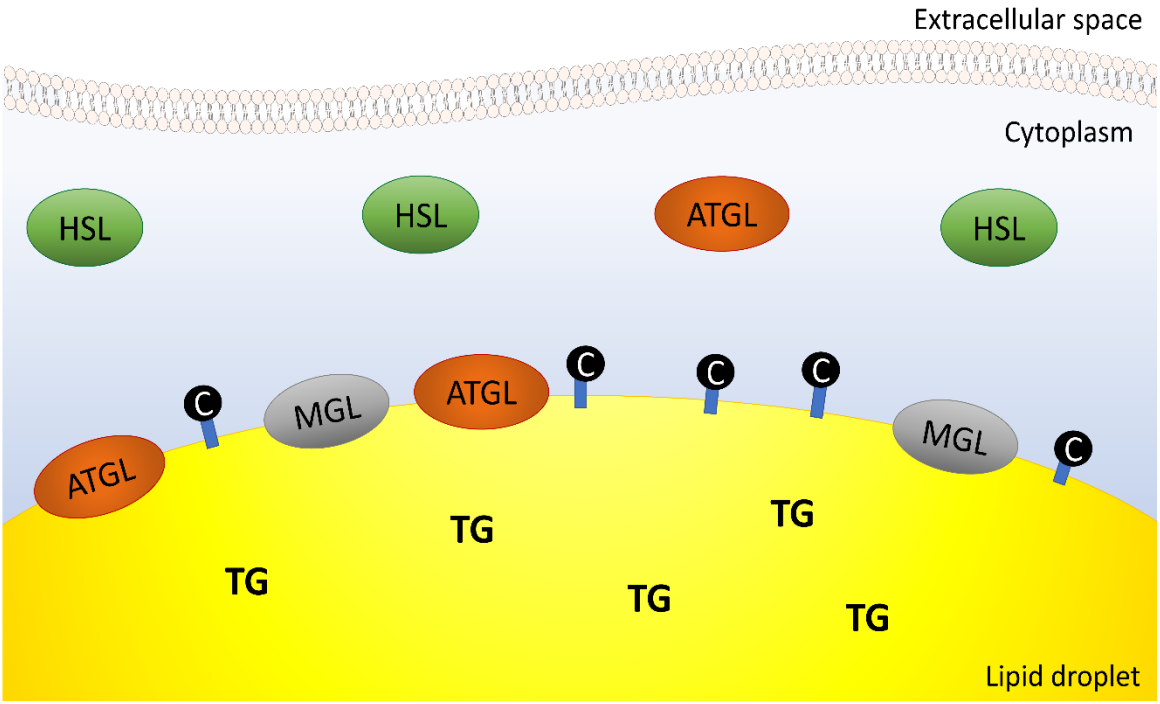

Figure 1.5 Schematic diagram of the molecular mechanisms governing basal lipolytic pathways. Under basal conditions, hormone sensitive lipase (HSL) localizes to the cytoplasm, whereas adipose triglyceride lipase (ATGL) localizes to both the lipid droplet and the cytoplasm and monoglyceride lipase (MGL) localizes to the lipid droplet. In addition, comparative gene identification-58 (CGI-58) (black circle containing a white C) is associated with perilipins (blue rectangle) on the surface of the lipid droplet, which indirectly limits ATGL capacity to hydrolyse triglycerides (TG) stored within lipid droplets.

1.8 Adipokine secretion

In addition to being the primary site of long-term nutrient storage in the body, WAT also has a significant role as an endocrine organ. Adipose tissue is capable of secreting a wide repertoire of substances that are collectively termed adipokines. In recent years, hundreds of adipokines have been identified, some of which act in an autocrine or paracrine fashion within adipose tissue, whereas other adipokines are able to travel to distant sites to influence the metabolic activity of the other organs (Kim & Moustaid-moussa 2000). For example, when lipolysis is initiated, adipocytes release anti-lipotoxic adipokines, such as leptin, adiponectin and fibroblast growth factor 21, to protect peripheral tissues from the lipotoxic effects of lipid accumulation (Unger *et al.*, 2013). Leptin was the first adipokine to be identified (Zhang *et al.*, 1994). It is secreted by adipocytes, but acts at specific leptin receptors within the hypothalamus to signal satiety and prompt an increase in energy expenditure to maintain an optimal adipose tissue volume (Klok *et al.*, 2007). Fasting and catecholamines decrease leptin production, whereas overfeeding, insulin and glucocorticoids all increase levels of circulating leptin (Kim & Moustaid-moussa 2000). In comparison to leptin, adiponectin is produced in relatively large quantities (μg/ml adiponectin versus ng/ml leptin in the plasma) and is able to effect many different tissues, with the liver and skeletal muscle being two major target organs (Wang and Scherer, 2016). Adiponectin inhibits apoptosis, suppresses inflammation, inhibits lipolysis and promotes insulin sensitivity to improve systemic metabolism (Wedellová *et al.*, 2011; Wang *et al.*, 2016). Another example of an adipokine that decreases lipid uptake is angiopoietin-like 4 (ANGPTL4). ANGPTL4 is released in response to fasting and is known to inhibit lipoprotein lipase activity and decrease lipid uptake in rodent adipocytes (Köster *et al.*, 2005; Lafferty *et al.*, 2013).

Adipocytes also secrete a wide variety of inflammatory cytokines and chemokines, such as tumour necrosis factor α (TNFα), interleukin (IL) 6 (Ronti *et al.*, 2006) and RANTES (regulated upon activation normal T cell expressed and secreted) (Skurk *et al.*, 2009). However, adipocytes can also secrete anti-inflammatory factors too, such as IL-1 receptor antagonist and IL-10 (Lago et al. 2007). The adipokine secretion profile alters according to the metabolic and redox state of white adipocytes (Cao, 2014). Although under normal conditions, this feature enables adipocytes to influence systemic metabolism to maintain energy homeostasis, in obese individuals, white adipocyte dysfunction leads to an increase in release of proinflammatory cytokines as well as a decrease in anti-inflammatory adipokines, such as adiponectin (Slawik and Vidal-Puig, 2007; Ibrahim, 2010). This in turn promotes low grade inflammation of adipose tissue, which participates in the development of cardiovascular complications and autoimmune conditions in obese individuals (Lago *et al.*, 2007; Bódis *et al.*, 2018).

1.9 Intracellular signalling mechanisms

Activation of cell surface receptors initiates intracellular signalling cascades, which enables the transmission of extracellular signals from the cell surface to a multitude of intracellular targets in a process known as signal transduction (Cooper, 2000). Signals are transmitted via three different categories of cell surface receptors: ligand-gated ion channels, enzyme-linked receptors and G-protein coupled receptors (GPCRs). Successful ligand binding to ligand-gated ion channels produces a conformational change in the receptor, which results in the receptor switching from its closed state to its open state, thus enabling passage of ions and other molecules through the plasma membrane. Enzyme-linked receptors are often protein kinases, such as tyrosine kinases, thus activation of these receptors leads to downstream phosphorylation of intracellular target proteins. Finally, GPCRs represent the largest family of membrane proteins. All receptors in this family share a common seven transmembrane domain structure and activation of these receptors regulates intracellular function indirectly via GTP-binding protein (G-protein) intermediate molecules or β-arrestin (Purves *et al.*, 2001).

1.9.1 G-protein coupled receptors

GPCRs regulate a diverse range of intracellular signalling cascades triggered by numerous stimuli, including hormones, neurotransmitters, lipids, nucleotides, ions, photons and odorants (Hilger *et al.*, 2018). There are 826 different GPCRs in the human body and they are responsible for the majority of cellular signalling events (Wu *et al.*, 2017). GPCRs are highly attractive therapeutic targets and currently approximately 30% all marketed drugs target GPCRs (Shonberg *et al.*, 2015). GPCRs are subdivided according to their sequence homology into four major categories: rhodopsin-like (class A), secretin-like (class B), metabotropic glutamate/pheromone (class C) and frizzled (class F) (Shonberg *et al.*, 2015). The intracellular responses initiated by GPCR activation are broadly mediated via two different pathways: G-protein mediated and G-protein-coupled receptor kinase (GRK)-mediated phosphorylation and arrestin coupling (Hilger *et al.*, 2018). Determination of the crystal structure of both active and inactive GPCRs has substantially increased our understanding of the conformational changes that occur in response to ligand binding (Shonberg *et al.*, 2015; Zhang, Zhao, *et al.*, 2015; Wu *et al.*, 2017). Most commonly, GPCR activation leads to a major reorganisation and rearrangement of the transmembrane helices to expose an intracellular pocket that can effectively engage the relevant effector proteins (Hilger *et al.*, 2018).

Classical signal transduction via GPCRs is mediated via heterotrimeric G proteins. G proteins are composed of three subunits: Gα, Gβ and Gγ. Based on sequence homology of the α subunit, there are four major categories of G-proteins: G_s, $G_{i/o}$, $G_{q/11}$ and $G_{12/13}$ (Table 1.2). Each class of G-protein activates different effectors and consequently mediates different signalling pathways. In the inactive state, GDP is bound to Gα and Gα associates with the Gβγ dimer to form a heterotrimer.

Upon receptor activation, GDP dissociates from Gα and is rapidly replaced by GTP, which initiates a conformational change in the receptor and the subsequent dissociation of Gα and Gβγ subunits. The Gα subunit is then able to mediate downstream signalling cascades by targeting effectors, which include adenylate cyclases and phospholipase C (Cooper, 2000; Hilger *et al.*, 2018). The liberated Gβγ subunit can also recruit GRKs to the plasma membrane and regulate many downstream effectors too (Hilger *et al.*, 2018). The intrinsic GTPase activity of Gα enables the hydrolysis of GTP to GDP, thus allowing the reassociation of the Gα and Gβγ subunits and terminating signalling.

Table 1.2 Main effectors and actions of G-proteins within each of the four major classes of G-proteins.

G-protein class	G-protein subunits	Main effector	Action	Reference
G_s	$G\alpha_s$ G_{olf}	Adenylate cylases	Stimulation; ↑ cAMP	(Jones and Reed, 1989; Yang *et al.*, 1997)
$G_{i/o}$	$G\alpha_{tr}$, $G\alpha_{tc}$, $G\alpha_g$	Phosphodiesterases	Stimulation; ↓ cAMP	(Pierce *et al.*, 2002) (Kristiansen, 2004)
	$G\alpha_{i1\text{-}3}$	Adenylate cyclases	Inhibition; ↓ cAMP	(Zorina *et al.*, 2010)
	$G\alpha_o$	c-Src	Stimulation	
$G_{q/11}$	$G\alpha_{q,\ 11,\ 14,\ 15/16}$	Phospholipase C	Stimulation; ↑ Ca^{2+}	(Mizuno and Itoh, 2009)
$G_{12/13}$	$G\alpha_{12}$ $G\alpha_{13}$	Rho GTPase nucleotide exchange factors	Stimulation	(Siehler, 2009)

1.9.2 Calcium signalling

Calcium ions (Ca^{2+}) are involved in almost all aspects of cellular functioning. Ca^{2+} acts as a highly versatile and ubiquitous second messenger that plays a vital role in numerous cellular processes (Berridge *et al.*, 2000; Clapham, 2007). For example, calcium plays a central role in mesenchymal stem cell migration and adipogenesis (Shi *et al.*, 2000; Pchelintseva and Djamgoz, 2018). Furthermore in white adipocytes, Ca^{2+} has been shown to be involved in lipolysis, secretion of adipokines and glucose uptake (Xue *et al.*, 2001; Cammisotto and Bukowiecki, 2004; El Hachmane *et al.*, 2018). Cells exert tight regulatory control to maintain a low intracellular concentration of Ca^{2+}

of approximately 100 nM under resting conditions, as calcium overload leads to apoptosis and necrosis (Berridge *et al.*, 2000, 2003; Clapham, 2007). This represents an approximately 20,000-fold gradient between the intracellular and extracellular environment which contains mM concentrations of Ca^{2+}. However, in response to various stimuli, intracellular Ca^{2+} levels can be transiently elevated up to approximately 1 µM to initiate various signalling pathways (Berridge *et al.*, 2000). Ca^{2+} can enter the cell via voltage-gated Ca^{2+} channels and other ionotropic receptors, or activation of receptor tyrosine kinases and G_q-coupled receptors increases intracellular Ca^{2+} via release from intracellular stores. Initial increases in Ca^{2+} via entry from the extracellular space triggers additional release from the endoplasmic reticulum (ER) via Ca^{2+}-sensitive ryanodine receptor (RyR) expressed on the surface of the ER (Clapham, 2007). Receptor tyrosine kinases or GPCRs can activate phospholipase C (PLC), which cleaves phosphatidylinositol 4, 5 bisphosphate (PIP2) into inositol (1,4,5) triphosphate (IP_3) and diacylglycerol (DAG). IP_3 binds to IP_3 receptors expressed on the ER and triggers a conformational change that allows Ca^{2+} to flow out of the ER and into the cytoplasm, thus elevating intracellular calcium. The resulting emptying of the intracellular stores initiates translocation of stromal interaction molecule 1 (STIM1) in the ER to enable interaction between STIM1 and calcium release-activated calcium channel protein 1 (ORAI1) on the plasma membrane, which subsequently results in the opening of the ORAI1 channels to allow Ca^{2+} influx to replenish the intracellular stores (Smyth *et al.*, 2010). ORAI1 channels remain open until the intracellular Ca^{2+} stores have been refilled. These store-operated calcium entry (SOCE) mechanisms have been demonstrated in both preadipocytes and mature adipocytes (Hu *et al.*, 2009; El Hachmane *et al.*, 2018).

Due to the potentially cytotoxic effects of elevated cytoplasmic Ca^{2+} levels, stimulus-induced augmented calcium levels are rapidly lowered by extrusion of Ca^{2+} out of the cell via plasma membrane Ca^{2+} ATPases (PMCA) transporters or into the endoplasmic reticulum cellular Ca^{2+} stores via smooth endoplasmic reticular Ca^{2+} ATPase (SERCA) transporters. In addition, sodium/calcium exchangers and Ca^{2+}-activated potassium (or chloride) channels can also help to decrease intracellular calcium concentrations (Clapham, 2007). Decreasing intracellular calcium levels back to baseline levels terminates Ca^{2+}-mediated signalling pathways.

1.9.3 Cyclic AMP signalling

Like calcium, cAMP is a ubiquitously expressed secondary messenger molecule that plays a pivotal role in a variety of cellular functions, including an essential role in lipolysis in white adipocytes (Section 1.7.1 and 1.7.2). Intracellular cAMP levels are regulated by the balance between the activity of adenylate cyclases (AC) and phosphodiesterases (PDE). There are ten isoforms of ACs. Nine are membrane-bound and regulated by G-proteins (AC1-9) (Sadana and Dessauer, 2009) and the tenth isoform (AC10) is a soluble AC that has unique enzymatic properties and does not respond

to G-proteins (Satrawaha *et al.*, 2011). Activation of ACs leads to an accumulation of cAMP and consequent activation of various effectors, of which protein kinase A (PKA) is the most well characterised (Pierce *et al.*, 2002). In contrast, both inhibition of ACs or activation of PDEs manifests in a reduction of intracellular cAMP and subsequent deactivation of downstream effectors (Sassone-Corsi, 2012). There is also some co-operation between cAMP and Ca^{2+}-mediated signalling pathways, as both ACs and PDEs can be positively or negatively regulated by calcium signalling (Sadana *et al.*, 2009).

1.10 Purinergic signalling

The concept of nucleotides acting as non-adrenergic, non-cholinergic neurotranmitters was first proposed by Professor Geoffrey Burnstock in 1970 (Burnstock *et al.*, 1970). Shortly thereafter this phenomenon was termed 'purinergic signalling' (Burnstock, 1972). Despite previous evidence in support of the concept (Drury and Szent-Györgyi, 1929; Buchthal and Folkow, 1948; Emmelin and Feldberg, 1948; Holton, 1959), initially there was much resistance to the idea and it took a further 20 years before purinergic signalling was truly accepted by the wider scientific community (Burnstock, 2014). Now, it is known that autocrine/paracrine signalling via extracellular nucleosides and nucleotides is one of the most common cell signalling mechanisms and purinergic signalling is implicated in a wide range of physiological processes including smooth muscle contraction, immune responses, embryonic development and maintaining homeostasis (Yegutkin 2014). These signalling pathways are regulated by specific purinergic receptors of which there are two broad categories, P1 and P2 receptors (Spedding & Weetman 1976; Burnstock 1978). P1 receptors are GPCRs activated by the nucleoside adenosine, whereas P2 receptors are activated by nucleotides and they are subdivided into two distinct subclasses known as P2X and P2Y receptors respectively (Burnstock & Kennedy 1985).

1.11 Sources of extracellular nucleosides and nucleotides

There are several different sources of extracellular nucleotides, including release from apoptotic or necrotic cells, secretion in response to various mechanical or chemical stimuli, exocytosis alone or in combination with other neurotransmitters and via ion-channels and transporters. Exocytosis is thought to be the method by which ATP is released by nerves, endocrine cells and platelets (Yegutkin 2014). Cells can also release ATP to mediate autocrine regulation of cellular activity, with some cells demonstrating constitutive release of ATP (Corriden and Insel, 2010; Sivaramakrishnan *et al.*, 2012; Campwala and Fountain, 2013). Data from murine 3T3-L1 adipocytes and adipocytes isolated from pannexin 1 knockout mice suggests that ATP can be released via activated pannexin 1 channels (Adamson *et al.*, 2015). However, Adamson *et al* (2015) also showed that there are basal concentrations of ATP (<500 nM) released by adipocytes, which are not altered in pannexin 1

knockout mice and are unaffected by pharmacological activation and inhibition of pannexin 1, which suggests that additional ATP release mechanisms are also present in murine adipocytes. Irrespective of the source of ATP, when endogenous nucleotides are in the extracellular space they are able to directly interact with P2X and P2Y receptors expressed at the cell surface to initiate purinergic signalling cascades. The extracellular nucleotides can also be (or are subsequently) metabolised by cell surface ectonucleotidases, such as nucleoside triphosphate diphosphohydrolase-1 (CD39) and ecto-5'-nucleotidase (CD73), which produces metabolites that are able to interact with P1 and P2Y receptors. Finally, nucleosides are metabolised further and/or reabsorbed into the cell (Yegutkin 2008).

Rodent white adipocytes maintained *in vitro* secrete small amounts of ATP (<500 nM) into the supernatant under basal conditions (Schödel *et al.*, 2004; Adamson *et al.*, 2015), which raises the possibility of white adipocytes regulating their own purinergic responses in an autocrine manner. As cells are very closely packed within WAT, ATP released from white adipocytes is likely to have paracrine effects on neighbouring cells, potentially including progenitor cells located throughout WAT. In a suspension of white adipocytes harvested from rats, 5 µM ATP had a half-life of 16 minutes, which represents a 500-fold increase in half-life when compared to the metabolism of ATP in the bloodstream (Schödel *et al.*, 2004). This indicates that white adipocytes may employ mechanisms to extend nucleotide viability, thus potentially prolonging activity of purinergic signalling pathways. In addition, adipose tissue is highly innervated, so co-release of ATP and noradrenaline from sympathetic nerves is likely to be another source of ATP in WAT (Fishman and Dark, 1987; Bartness and Bamshad, 1998; Bartness and Song, 2007).

1.12 P1 receptors

P1 receptors are GPCRs that are activated by adenosine. There four subtypes of P1 receptors: A1, A2A, A2B and A3. Adenosine has the highest affinity for A1 and A2A, which have opposing actions. Both A1 and A3 are $G\alpha_i$-coupled receptors, whereas A2A and A2B are $G\alpha_s$-coupled receptors. Thus, activation of A1 or A3 leads to a reduction in adenylate cyclase activity and a decrease in the concentration of intracellular cAMP, whereas A2A or A2B activation elicits an increase in adenylate cyclase activity (Layland *et al.*, 2014). In some cells, A2B receptors can also activate PLC and mitogen-activated protein kinases (MAPK) signalling pathways (Cohen *et al.*, 2010). The four membrane receptors of the P1 family share an average sequence homology of 47%, although this rises to approximately 57% homology when only the transmembrane domains are considered (Jacobson *et al.*, 2012).

Activation and overexpression of A2B receptors is associated with stimulation of osteogenic differentiation in MSCs, whereas adipogenic differentiation is related to an increase in expression of A1 and A2A receptors (Gharibi *et al.*, 2011, 2012). In addition, signalling via P1 receptors has an established role in white adipocytes. Adenosine is known to have an anti-lipolytic effect (Fredholm *et al.*, 1977; Ohisalo, 1981; Johansson *et al.*, 2008), which, as mentioned earlier in Section 1.7.2, is exerted by inhibiting the accumulation of intracellular cAMP. A1 receptor knockout mice display increased fat mass and impaired insulin sensitivity (Faulhaber-Walter *et al.*, 2011), whereas mice overexpressing A1 receptors are protected from obesity-induced insulin resistance (Dong *et al.*, 2001).

1.13 P2X receptors

P2X receptors are ATP-sensitive gated ion-channels (Figure 1.6). There are seven P2X subunits, named P2X1-7. All seven subunits share a common basic structure that consists of intracellular N- and C-termini, two transmembrane domains and a large extracellular ectodomain (Dal Ben *et al.*, 2015). P2X receptors are trimeric receptors that are formed of either homomeric or heteromeric combinations of the seven P2X subunits (Surprenant and North, 2009; Evans, 2010). Upon interaction with ATP a conformational change occurs that facilitates the entry of cations, such as Na^+, K^+ and Ca^{2+}, into the cells via lateral fenestrations (Kawate *et al.*, 2011), thus initiating depolarisation of the cell and induction of downstream signalling pathways (Dal Ben *et al.*, 2015). Some P2X receptors are also capable of allowing larger molecules through the cell membrane after prolonged periods of activation (North, 2002). Signalling via these receptors has already been implicated in processes ranging from cell proliferation and death to inflammation (Dal Ben *et al.* 2015).

Very few studies have investigated the role of P2X receptors in human adipose-tissue derived adipocyte progenitor cells. However, a study conducted by Zippel *et al.* (2012), identified that P2X5, P2X6 and P2X7 were all expressed at the protein level in AD-MSCs. Furthermore, ATP elicits a functional Ca^{2+} response, which is blocked by the generic P2 antagonist, suramin and non-specific concentrations (100 µM) of the selective P2X1 antagonist, NF279 (Zippel *et al.*, 2012). Taken together, these data indicate that P2X receptors are expressed in AD-MSCs and these cells have a functional purinergic response. However, this study only used cells isolated from three donors, so there is currently a need for more comprehensive investigations into the role of P2X receptors in human AD-MSCs. However, additional functional studies in MSCs derived from other tissues, for example dental pulp, demonstrate a role for P2X7 receptors in cell proliferation and migration (Peng *et al.*, 2016). Most studies conducted in cells from mice or bone marrow, suggest that P2X7 receptors are central for driving osteogenesis and suppressing adipogenesis (Noronha-Matos *et al.*, 2014; Li *et al.*, 2015). However, a study using human AD-MSCs suggests P2X7 receptor expression

is actually downregulated during osteogenesis in human AD-MSCs. Instead, there is an upregulation of P2X6 receptor expression during adipogenesis and a downregulation of expression of the receptor during osteogenesis (Zippel *et al.*, 2012). Both findings correlate well with previous data that suggests ATP treatment increases mouse preadipocyte responsiveness to adipogenic hormone stimulation (Omatsu-Kanbe *et al.*, 2006).

Like AD-MSCs, very little is currently known about the role of P2X receptors in human adipocytes. However, expression of P2X3-7 mRNA has been detected in human adipocytes (Zippel *et al.*, 2012) and electrophysiological evidence of ATP-evoked responses in white adipocytes isolated from rats (Lee and Pappone, 1997) suggests that there are functional purinergic receptors present in white adipocytes. Studies investigating the physiological roles of P2X receptors in white adipocytes have focused on P2X7 receptors. P2X7 receptor activity appears to mediate inflammatory responses within adipose tissue (Yu and Jin, 2010). Similar findings have been determined in humans where activation of P2X7 receptors leads to enhanced release of inflammatory cytokines, IL-6 and TNFα, and acute phase reactants, such as plasminogen activator inhibitor-1 (PAI-I). These effects are sensitive to antagonism of P2X7 receptors and/or gene silencing (Madec *et al.*, 2011). However, the P2X7 knockout mouse appears to be heavier and display ectopic lipid deposition, which suggests P2X7 activity may also protect against adipose tissue dysfunction (Beaucage *et al.*, 2014).

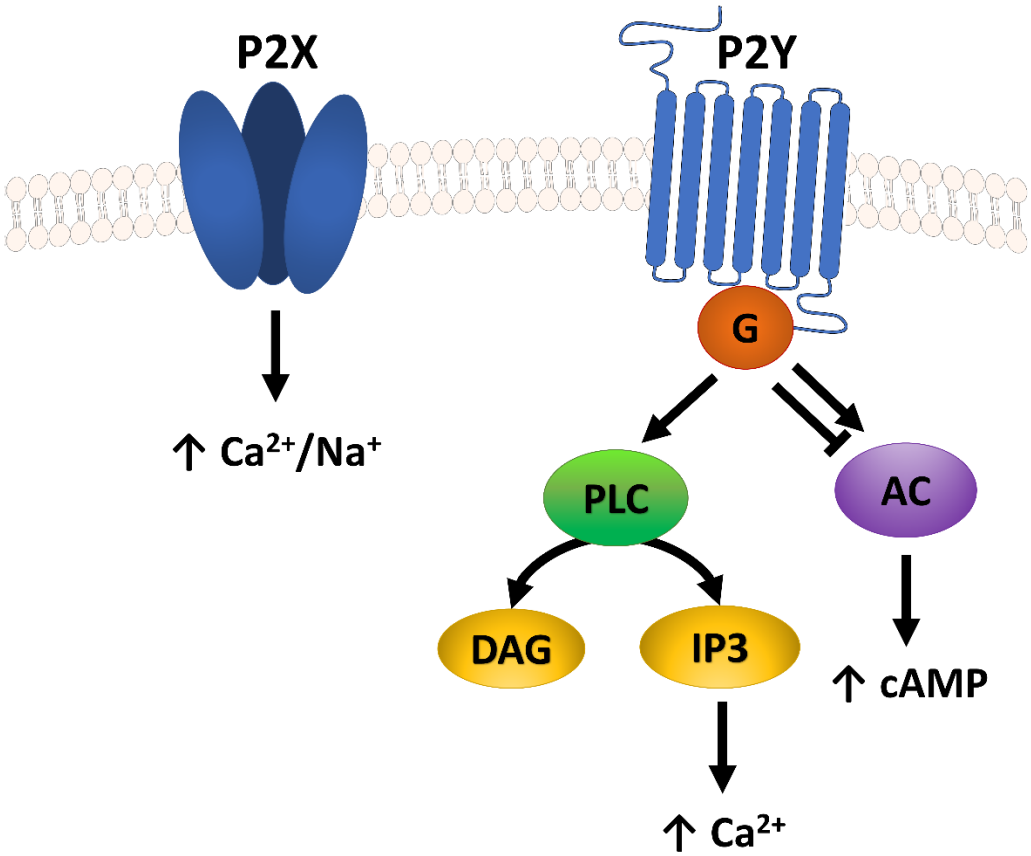

Figure 1.6 Schematic diagram of P2X and P2Y receptors, including downstream signalling pathways. Activation of ionotropic P2X receptors initiates a conformational change in the receptor which enables the opening of lateral fenestrations to allow entry of calcium (Ca^{2+}) and sodium (Na^{+}) ions, whereas activation of metabotropic P2Y receptors leads to different downstream effects depending on which G-protein the receptor is coupled to. $P2Y_1$, $P2Y_2$, $P2Y_4$ and $P2Y_6$ are all primarily coupled to G_q proteins, thus activation of these receptors activates phospholipase C (PLC), which generates diacylglycerol (DAG) and inositol triphosphate (IP_3). IP_3 then binds to receptors on the surface of the endoplasmic reticulum (ER) to initiate release of Ca^{2+} from the ER into the cytosol. $P2Y_{11}$ receptors are G_s-coupled, thus activation of $P2Y_{11}$ stimulates adenylate cyclase (AC) and leads to an accumulation of intracellular cyclic AMP (cAMP). Finally, $P2Y_{12}$, $P2Y_{13}$ and $P2Y_{14}$ are G_i-coupled receptors, thus their activation leads to inhibition of AC and prevents accumulation of cAMP.

1.14 P2Y receptors

The second major class of P2 receptors are the P2Y receptors (Figure 1.6), which are metabotropic receptors. P2Y receptors, like P1 and P2X receptors, are widely distributed throughout the body and are implicated a huge variety of cellular processes, such as platelet aggregation, inflammation and epithelial cell hydration (Boeynaems *et al.*, 2012). Unlike other class A GPCRs, P2Y receptors display limited sequence homology, which may explain the subtype variation in agonist preference and G protein coupling (Conroy *et al.*, 2016) (Table 1.3). However, coupled with phylogenetic information, the sequence homology between the receptor subtypes is sufficient to categorise the eight members of this family of receptors into two groups: $P2Y_1$-like or $P2Y_{12}$-like receptors. $P2Y_1$, $P2Y_2$, $P2Y_4$, $P2Y_6$ and $P2Y_{11}$ are all $G\alpha_{q/11}$-coupled receptors and consequently activate phospholipase C-β, whereas $P2Y_{12}$, $P2Y_{13}$ and $P2Y_{14}$ are $G\alpha_{i/o}$-coupled receptors which inhibit adenylate cyclase and regulate ion channels (Yegutkin 2008) (Figure 1.6 and Table 1.3). $P2Y_{11}$ receptors can also couple to G_s proteins, which means they can activate either adenylate cyclase or phospholipase C-β. In addition, $P2Y_2$ and $P2Y_4$ receptors can couple to both G_q and G_i proteins (Erb and Weisman, 2012).

Table 1.3 P2Y receptor agonist preferences and G-protein coupling. Table adapted from (Jacobson *et al.*, 2012).

Receptor subtype	Preferred agonists (pEC_{50}, human)	G-protein coupling
$P2Y_1$	ADP (5.90)	G_q
$P2Y_2$	ATP (7.07) = UTP (8.10)	G_q, G_i
$P2Y_4$	UTP (5.60)	G_q, G_i
$P2Y_6$	UDP (6.52)	G_q
$P2Y_{11}$	ATP (4.77)	G_q, G_s
$P2Y_{12}$	ADP (7.22)	G_i
$P2Y_{13}$	ADP (7.94)	G_i
$P2Y_{14}$	UDP (6.80), UDP-glucose (6.45)	G_i

Unlike P2X receptors, which are exclusively activated by ATP, both purine and pyrimidine nucleotides are capable of activating P2Y receptors. Although each subtype displays their own agonist preference (Table 1.3). In brief, $P2Y_1$, $P2Y_{12}$, and $P2Y_{13}$ receptors are all preferentially activated by ADP, $P2Y_2$ and $P2Y_4$ are both UTP receptors, while $P2Y_6$ and $P2Y_{14}$ receptors are activated by UDP and $P2Y_2$ and $P2Y_{11}$ are ATP receptors (Boeynaems et al. 2012). $P2Y_{14}$ is also a receptor for UDP-glucose and other nucleotide sugars. Like other GPCRs, P2Y receptors share a basic general structure that consists of an extracellular N-terminus, seven transmembrane domains

that contains the ligand binding pocket, three intracellular loops that enable G-protein coupling and an intracellular C-terminus (Erb *et al.*, 2012).

Gene expression analysis indicates that all eight P2Y receptor subtypes are expressed in primary human AD-MSCs and white adipocytes (Zippel *et al.*, 2012). The literature regarding the role of P2 receptor mediated signalling in human AD-MSCs and mature adipocytes is limited, with the vast majority of the data surrounding these cell two types being derived from rodent models and/or bone marrow derived (BM) MSCs. However, studies indicate that $P2Y_1$, $P2Y_2$, $P2Y_4$ and $P2Y_{11}$ may positively regulate adipogenesis in BM- or AD-MSCs (Kawano *et al.*, 2006; Zippel *et al.*, 2012; Ciciarello *et al.*, 2013; Li *et al.*, 2015). In addition, inhibition of G_i-signalling pathways with pertussis toxin (Katada *et al.*, 1983) prevents ATP-induced increases in PPARγ, a major transcription factor involved in adipogenesis (Ciciarello *et al.*, 2013). It is possible that these G_i-mediated effects are achieved via $P2Y_{13}$ receptor activation, as data from $P2Y_{13}$ knockout mouse models indicate that BM-MSCs isolated from these mice display earlier expression of adipogenic markers, faster lipid droplet formation and augmented numbers of adipocytes within the bone marrow, while also demonstrating a decrease in the development of osteogenic markers in the presence of osteogenic stimuli (Biver *et al.*, 2013). In addition, $P2Y_6$ receptors have been shown to promote osteogenesis in BM-MSCs (Noronha-Matos *et al.*, 2012) and this receptor has also been implicated in increasing IL-6 expression (Satrawaha *et al.*, 2011). It has been suggested that IL-6 is important for maintaining the immunoprivilege stasis of MSCs (Li *et al.*, 2013), so if $P2Y_6$ receptors are involved in IL-6 secretion, $P2Y_6$ receptors may be a valuable target for prolonging MSC viability for therapeutic use. However much more additional work is required to clarify both the molecular mechanism and functional role of $P2Y_6$ receptor activation in these cells.

Currently there are very few studies that have investigated the molecular basis of the role of P2Y receptors in primary human adipocytes, but data gathered from rodent models suggests P2Y receptors may play a role in key adipocyte functions. For example, activation of $P2Y_6$ receptors has been shown to enhance GLUT4 translocation to the membrane and increase glucose uptake in primary mouse white adipocytes. This effect was reversed by selective inhibition of $P2Y_6$ receptors (Balasubramanian *et al.*, 2014). In addition, selective inhibition of $P2Y_1$ receptors or deleting $P2Y_1$ receptor expression leads to a decrease in leptin production (Laplante *et al.*, 2010), whereas $P2Y_4$ knockout mice display augmented secretion of adiponectin (Lemaire *et al.*, 2017).

Despite the limited scope of the research into the role of P2 receptors in human adipocytes and their progenitor cells, progress has been made in targeting P2 receptor-mediated signalling pathways in other cell types. Purinergic receptors are attractive drug targets and success has

already been attained in disrupting P2Y receptor activity for therapeutic gain (as discussed in further in Section 1.14.1 and 1.14.2).

1.14.1 $P2Y_1$ and $P2Y_{12}$ receptors

The crystal structures of both $P2Y_1$ and $P2Y_{12}$ receptors have been published and this revealed that $P2Y_1$ has two distinct agonist binding sites (Zhang, Gao, *et al.*, 2015), whereas $P2Y_{12}$ requires large scale receptor rearrangement to enable agonist binding (Zhang *et al.*, 2014). Both receptors are preferentially activated by ADP, but as mentioned in the previous Section, $P2Y_1$ receptors are G_q coupled, whereas $P2Y_{12}$ receptors are G_i-coupled and thus they activate distinct downstream signalling pathways. Both $P2Y_1$ and $P2Y_{12}$ receptors play important roles in platelet aggregation (Jagroop *et al.*, 2003). Activation of $P2Y_1$ receptors leads to a change in platelet shape and an initiation of platelet aggregation (Jin *et al.*, 1998), and then $P2Y_{12}$ receptor activity sustains platelet aggregation post-initiation (Dorsam and Kunapuli, 2004). Anti-thrombotic drugs are currently the only widely approved therapeutic drug that selectively targets P2Y receptors. Despite the fact that inhibition of $P2Y_1$ receptors significantly decreases platelet aggregation and effectively decreases arterial thrombosis (Fabre *et al.*, 1999; Léon *et al.*, 2001; Lenain *et al.*, 2003), all available therapeutic anti-aggregation treatments specifically target $P2Y_{12}$ receptors (Conroy *et al.*, 2016). Selective antagonists of $P2Y_{12}$ receptors, such as Ticagrelor, are routinely used clinically for the prevention of atherothrombotic events in acute coronary syndrome patients (Wallentin *et al.*, 2009).

Although, there are currently no reports indicating $P2Y_{12}$ receptors may be involved in adipocyte biology, studies using $P2Y_1$ knockout mice have identified that $P2Y_1$ is involved in leptin secretion (Laplante *et al.*, 2010). Upon comparison to wild type mice, preadipocytes and adipocytes isolated from knockout mice secreted less leptin when agonised with ADP despite similarities in mature cell size, lipid content and lipolytic activity between the two model animals. The suppression of leptin secretion could also be mimicked in wildtype cells by incubating them with MRS2500 (a selective $P2Y_1$ antagonist) for 48 hours. A decrease in the plasma concentration of leptin was also noted within the knockout models, but this decrease was overcome when these mice were put on a high fat diet suggesting that when the demand for leptin increases the effects of $P2Y_1$ receptor mediated secretion of leptin are overcome by other compensatory mechanisms. An elevation in cytoplasmic calcium was seen in response to ADP even in the $P2Y_1$ knockout mice, suggesting the contribution of other P2 receptors (Laplante *et al.*, 2010).

1.14.2 $P2Y_2$ receptors

$P2Y_2$ receptors are equipotently activated by both ATP and UTP, and they are able to couple to G_q, G_o and G_{12} proteins, although G_o and G_{12}-coupling requires interaction with αv integrins (Bagchi *et al.*, 2005; Liao *et al.*, 2007). An agonist for $P2Y_2$, Diquafosol, has been approved for therapeutic use as an ophthalmic solution under the trade name Diquas™ (Santen Pharmaceutical Co, Ltd, Osaka, Japan) by the regulatory bodies in Japan and Korea for the clinical treatment of dry eye. However, Diquas™ has not been approved for use in other countries (Lau *et al.*, 2014). In addition, it has been identified that activation of $P2Y_2$ receptors increases the secretion of Cl^-, water and mucin into the trachea in *ex vivo* models (Yerxa *et al.*, 2002), which suggests that $P2Y_2$ receptors could be a potential drug target in cystic fibrosis patients, who exhibit faulty Cl^- secretion. Despite promising results in rodent models (Yerxa *et al.*, 2002) and in Phase II trials (Deterding *et al.*, 2005), the results from early Phase III clinical trials and longer term studies did not display statistically significant improvements in cystic fibrosis patients (Accurso *et al.*, 2011; Ratjen *et al.*, 2012) and consequently this drug was not pursued further.

It has recently been suggested that the $P2Y_2$ receptor may play a role in driving BM-MSC adipogenesis while suppressing osteogenesis, without effecting the rate of cell proliferation (Li *et al.*, 2015). It may be that $P2Y_2$ receptors are involved in a similar role in AD-MSCs. If this was the case, this could provide an opportunity to develop pharmacological tools to target $P2Y_2$ receptors specifically to drive MSCs towards/away from an adipogenic phenotype *in vivo*, thus providing a route to control the number of new adipocytes present in adipose tissue and potentially regulate weight gain. $P2Y_2$ receptor-mediated signalling has also been implicated in the proliferation of keratinocytes (Dixon *et al.*, 1999) and carcinoma cells (Xie *et al.*, 2014; Qiu *et al.*, 2018), as well as neutrophil migration (Chen *et al.*, 2006). Both cell proliferation and migration are key functions of MSCs, so investigating whether $P2Y_2$ receptors play a role in either of these functions in human AD-MSCs would be of significant clinical and physiological interest.

$P2Y_2$ is also a potentially interesting target to investigate within white adipocytes as well, as $P2Y_2$ knockout mice are resistant to diet-induced obesity and display improved glucose tolerance. These effects have been attributed to enhanced metabolic rates in $P2Y_2$ knockout mouse models (Kishore *et al.*, 2016). As adipocytes play a vital role in systemic metabolism, this could be indicative of a role for $P2Y_2$ receptors in white adipocytes.

1.15 Project aims

The global rise in the incidence of obesity has initiated a surge in research into adipose biology to enable attempts to identify novel drug targets that can be of use in the fight against obesity. Purinergic receptors represent a very attractive drug target and they have been successfully targeted in other cell types for therapeutic gain. However, purinergic signalling in adipose tissue

remains a largely unexplored area of research. Through this project, I hope to identify the molecular basis of nucleotide-evoked responses in primary human adipose derived mesenchymal stromal cells (Chapter 3) and in *in vitro* differentiated adipocytes (Chapter 4) and then attempt to uncover the physiological role of these receptors (Chapter 5). Very little is currently known about the role of P2 receptors in both cell types and it is hoped that this study will provide a solid foundation to begin to unpick the complex role of purinergic signalling in cells within human adipose tissue.

Chapter 2: Materials and Methods

2.1 Materials

Chemical reagents used throughout this study were purchased from Sigma Aldrich. In instances where materials from other suppliers were used, the company's name is provided within the text. A list of commonly used products is provided in the following passage (2.1.1) and in Tables 2.1, 2.2 and 2.3.

2.1.1 Cell culture

Unless otherwise stated, this study was conducted exclusively using primary human adipose-derived mesenchymal stromal cells (MSCs) and primary human *in vitro* differentiated adipocytes. All cells were maintained in uncoated tissue culture flasks or multi-well plates (Thermo Fisher Scientific) in a humidified incubator at 37 ^{o}C in the presence of 5% CO_2. Both cell types were maintained in Dulbecco's Modified Eagles medium (DMEM) containing 4.5 g/L glucose, 0.6 g/L L-glutamine and 0.1 g/L sodium pyruvate (Lonza), supplemented with 10% (v/v) foetal bovine serum (FBS) (GE Healthcare), 50 IU/ml penicillin and 50 µg/ml streptomycin (Gibco). This combination will be referred to as culture media throughout this thesis. Any subsequent reference to DMEM henceforth will denote to DMEM containing 4.5 g/L glucose, L-glutamine and sodium pyruvate (Lonza).

Table 2.1 Nucleotides and subtype-selective agonists.

Agonist	Target	Supplier	Purity	Concentration	Reference
ATP	P2X, $P2Y_2$, $P2Y_{11}$	Abcam	> 99%	0.01 – 300 µM	Burnstock, 2007
ADP	$P2Y_1$, $P2Y_{12}$, $P2Y_{13}$	Sigma Aldrich	≥ 95%	0.01 – 300 µM	Chhatriwala *et al.*, 2004
MRS2365	$P2Y_1$	Tocris	99.6%	0.1 µM	Bourdon *et al*., 2006
UTP	$P2Y_2$, $P2Y_4$	Abcam	> 98%	0.01 – 300 µM	Burnstock, 2007
UDP	$P2Y_6$, $P2Y_{14}$	Sigma Aldrich	> 96%	0.01 – 300 µM	Burnstock, 2007
UDP-glucose	$P2Y_{14}$	Abcam	> 98%	0.01 – 600 µM	Abbracchio *et al.*, 2003

Table 2.2 Subtype-selective purinergic receptor antagonists.

Antagonists	Target	Supplier	Concentration	Vehicle	Reference
PSB-12062	P2X4	Tocris	0.003 – 30 µM	DMSO	Hernandez-Olmos *et al.*, 2012
A438079	P2X7	Tocris	0.003 – 10 µM	DMSO	Nelson *et al.*, 2006
MRS2500	$P2Y_1$	Tocris	0.0001 – 1 µM	Water	Kim *et al.*, 2003
AR-C118925XX	$P2Y_2$	Tocris	0.003 – 30 µM	DMSO	Meghani, 2002; Rafehi *et al.*, 2017
MRS2578	$P2Y_6$	Tocris	0.003 – 10 µM	DMSO	Mamedova *et al.*, 2004
NF340	$P2Y_{11}$	Tocris	0.003 – 10 µM	Water	Meis *et al.*, 2010
PSB-0739	$P2Y_{12}$	Tocris	0.003 – 10 µM	Water	Hoffmann *et al.*, 2009
Ticagrelor	$P2Y_{12}$	Cayman	0.3 µM	DMSO	Zech *et al.,* 2012
MRS2211	$P2Y_{13}$	Tocris	0.003 – 10 µM	Water	Kim *et al.*, 2005

DMSO Dimethylsulfoxide

Table 2.3 Other inhibitors and enzymes.

Antagonists	Target	Supplier	Concentration	Vehicle	Reference
Apyrase	Nucleotides	Sigma Aldrich	0.5-4 U/ml	Water	Kettlun *et al.,* 1982
BRL50481	PDE7	Sigma Aldrich	1 µM	DMSO	Smith *et al*., 2004
Cilostramide	PDE3	Sigma Aldrich	1 µM	DMSO	Hidaka *et al*., 1979
IBMX	PDE	Sigma Aldrich	10 µM	DMSO	Morgan *et al*., 1993
Pertussis toxin	G_i, G_o, G_t	Tocris	100 ng/ml	Water	Carbonetti, 2010
PF-05180999	PDE2	Sigma Aldrich	10 µM	DMSO	Helal *et al.,* 2012
Rolipram	PDE4	Sigma Aldrich	10 µM	DMSO	MacKenzie & Houslay, 2000
SQ22,536	AC	Tocris	1 µM	DMSO	Emery *et al.*, 2013
Thapsigargin	SERCA	Santa cruz	3 µM	DMSO	Lytton *et al*., 1991
U-73122	PLC	Santa cruz	10 µM	DMSO	Bleasdale & Fisher, 1993
Vinpocetine	PDE1	Sigma Aldrich	10 µM	DMSO	Dunkern & Hatzelmann, 2007

AC Adenylate cyclase; DMSO Dimethylsulfoxide; IBMX 2-isobutyl-1-methylxanthine; PDE Phosphodiesterase; PLC Phospholipase C; SERCA Sarcoendoplasmic reticulum calcium transport ATPase

2.2 Tissue donation

Ethical approval for this study was obtained from the London-Stanmore Research Ethics Committee (152093) and the Research and Development department at the Norfolk and Norwich University Hospital (NNUH) (2014EC03L). This permitted the recruitment of 51 healthy female volunteers undergoing elective delayed deep inferior epigastric perforator (DIEP) flap operations at the NNUH. Informed consent was obtained from all volunteers prior to their participation in the study. All recruited patients were prior breast cancer sufferers who required mastectomies as part of the cancer treatment. A DIEP flap operation involves the removal of subcutaneous abdominal tissue to allow autologous tissue breast reconstruction (Hamdi and Rebecca, 2006). The nature of this operation means that there is often surplus subcutaneous abdominal adipose tissue that can be utilised for research purposes.

All volunteers were screened to exclude diabetics, patients with current infections or active malignancy and patients on anti-inflammatory medication. Where available, additional information regarding the donors' age, weight, body mass index (BMI), blood pressure and whether they were pre- or post-menopausal was also noted to further characterise the recruited population. All average data is presented as mean ± SEM. Recruited donors had an average age of 56 ± 1.4 years (*N*=48, range 38-75 years), average weight of 73.1 ± 1.3 kg (*N*=38, range 59-89 kg) and mean body mass index (BMI) value of 27.5 ± 0.5 kg/m^2 (*N*=37, range 23-35 kg/m^2). The average BMI value includes nine donors with a healthy BMI of between 18 and 24, 21 overweight donors (BMI 25-29 kg/m^2) and seven obese donors (BMI 30-39 kg/m^2). The BMI data was not available for 14 donors. Donors were largely normotensive with an average mean arterial pressure of 98.5 ± 1.6 mmHg (*N*=46, range 76-132 mmHg). Information about the donors' menopausal status was only available for 21 of the recruited tissue donors, of which only four were pre-menopausal.

2.3 Primary human mesenchymal stromal cell (MSC) isolation

Fresh human subcutaneous abdominal adipose tissue was transported immediately from the operating theatre to the laboratory and the cell isolation protocol was commenced without delay. The tissue samples were dissected to remove blood vessels, fibrous tissue and skin. The samples were then further minced and enzymatically digested with collagenase from *Clostridium histolyticum* (Sigma Aldrich) and bovine pancreatic DNase I (Biomatik) for 30 minutes at 37 °C with regular mixing by inversion. The digested tissue samples were then passed through a 70 µm cell strainer and centrifuged for 5 minutes at 450 x *g*, which separated the sample into a floating fraction containing mature adipocytes and a pellet containing multipotent mesenchymal stromal cells (MSCs) and other cell types. The mature adipocytes were discarded and the MSC fraction was treated with a red cell lysis buffer, washed and then resuspended in fresh culture media. The cells were then left in a T175 flask overnight in a humidified incubator at 37 °C with 5% CO_2. The following day, the cells were washed twice with phosphate-buffered saline (PBS) (Lonza) to remove any non-adherent cells or debris, and then left in fresh culture media until the cells were close to confluence, at which point they were detached from the bottom of the flask using tryspin EDTA (Lonza) and seeded for experimental use. For experimentation, isolated MSCs were plated at an initial seeding density of 2x10^4 cells/well in 96-well plates, unless otherwise indicated. The cells were then maintained in a humidified environment at 37 °C with 5% CO_2 for 48 hours and either directly used for experimentation or allowed to grow to hyper-confluence over the next two days and then differentiated (Section 2.6). MSCs were passaged a maximum of eight times for direct experimental use.

2.4 Cryopreservation and thawing of MSCs

Early passage, most commonly the first passage post-cell isolation, MSCs that were not required for immediate experimental use were stored in liquid nitrogen for future use. This was achieved by detaching MSCs from their culture flasks using trypsin ETDA and then centrifuging the cells at 450 *x g* for 5 minutes. The MSC pellet was then resuspended in cryopreservation media, which consisted of 45% (v/v) DMEM, 45% (v/v) FBS and 10% (v/v) DMSO. The cells were then immediately transferred to cryovials at a density of $1x10^6$ cells/vial. The cryovials were then placed in a Mr Frosty™ freezing container (Thermo Fisher Scientific) containing isopropanol to slow the cooling rate to 1 °C/min while the cells were stored at -80 °C overnight. The following day, the cells were transferred to a liquid nitrogen tank (-196 °C) for longer term storage.

When these cells were required for experimental use, they were removed from the liquid nitrogen and rapidly defrosted in a 37 °C waterbath. The defrosted cells were then immediately diluted with culture media and centrifuged at 450 *x g* for 5 minutes. Next, the cells were washed once, resuspended in fresh culture media and placed in a culture flask overnight at 37 °C in 5% CO_2. The following morning the culture media was removed and the cells were washed with PBS. Fresh culture media was then added and the cells were incubated at 37 °C until they were nearly confluent, at which point, they were passaged and seeded for experimental use.

2.5 Cell surface marker characterisation of MSCs by flow cytometry

Since the discovery of the existence of MSCs, there have been numerous groups working in this field, with different groups adopting different methods of characterising these cells. In an attempt to standardise the characterisation of MSCs, the International Society for Cellular Therapy proposed a set of minimum criteria for defining human MSCs (Dominici *et al.*, 2006):

1. MSCs must be plastic-adherent under standard culture conditions.
2. MSCs must be able to differentiate to adipocytes, osteoblasts and chondroblasts *in vitro.*
3. MSCs must express CD73, CD90 and CD105, but lack CD45, CD34, CD14 or CD11b, CD79α or CD19 and HLA-DR surface molecules.

All the cells used throughout this study were plastic-adherent and the differentiation capacity of these cells was tested in Section 2.6. To address the third criteria, the cell surface marker expression profile was assessed by flow cytometry using an adapted version of a panel of markers outlined by The International Society for Cellular Therapy. To do this, MSCs were trypsinised and centrifuged at 450 x *g* for 5 minutes. The cells were then resuspended in PBS at a density of $2x10^6$ cells/ml and 100 µl of cells was placed in individual Eppendorf tubes for each marker and control required. The cells were then incubated with 5 µg/ml of human BD Fc block™ (BD Pharmingen) for 10 minutes.

Next, PE-conjugated antibodies (1:33) were added to detect cell surface expression of CD14, CD45, CD73, CD90 and CD105 (Table 2.4) and the cells were incubated in the dark for a further 30 minutes. An isotype control (1:33) and an unstained control was also run alongside these markers. The cells were then washed once with PBS and resuspended in 200 µl of fresh PBS. Samples were analysed using a Beckman Coulter CytoFLEX flow cytometer. Living cells were gated according to their forward and side scatter and histograms were plotted to compare the fluorescence signal for each marker versus the isotype control using CytExpert 1.2.11 software (Beckman Coulter). A total of 10,000 events was collected for each marker and control. Flow cytometry was performed on cells isolated from six independent donors. MSCs from all six donors were strongly positive for the expected cell surface markers CD73 (90.2 ± 2.5% positivity), CD90 (89.8 ± 2.9% positivity) and CD105 (83.7 ± 3.3% positivity), while the expression of CD14 (10.0 ± 4.0% positivity) and CD45 (11.8 ± 4.3% positivity) was low (Figure 2.1).

Table 2.4 Phycoerythrin-conjugated anti-human primary antibodies for flow cytometry.

Target	Manufacturer	Product code	Host species
IgG1 κ isotype control	Biolegend	400113	Mouse
CD14	Biolegend	367103	Mouse
CD45	Biolegend	368509	Mouse
CD73	Biolegend	344003	Mouse
CD90	Biolegend	238109	Mouse
CD105	Biolegend	323205	Mouse

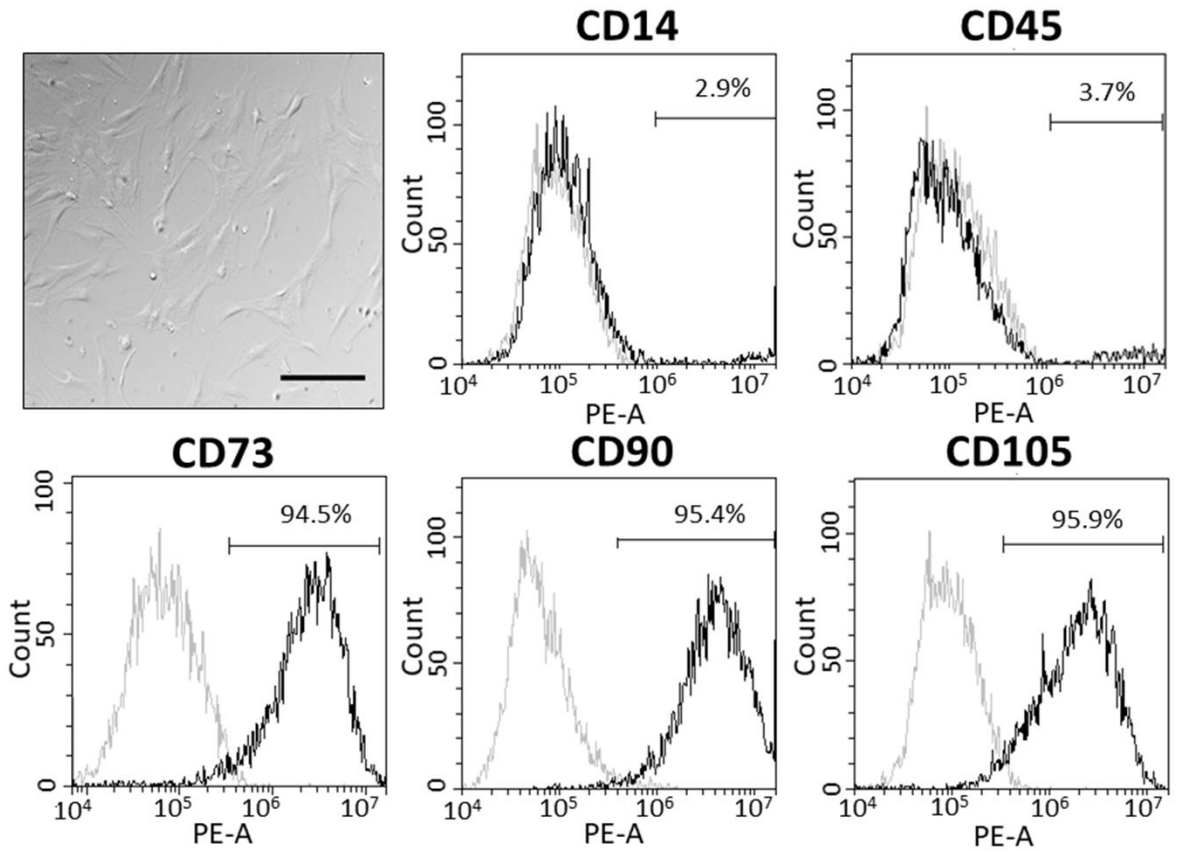

Figure 2.1 Phenotypic characterisation of human adipose-derived mesenchymal stromal cells by flow cytometry. Differential Interference Contrast microscopy of mesenchymal stromal cells in culture. The scale bar represents 200 µm. Flow cytometric analysis of cell surface marker expression in human mesenchymal stromal cells of known positive (CD73, CD90, CD105) and negative (CD14 and CD45) markers. Grey histogram indicates the isotype control (PE-conjugated anti-IgG1) and the black histogram shows the surface antigen expression level. This experiment was conducted on cells from six independent donors, but the data shown here is for one representative donor and the percentages displayed correspond specifically to this one donor.

2.6 Differentiation of primary human MSCs to adipocytes or osteoblasts

MSCs extracted from human adipose tissue can be induced to differentiate *in vitro* by incubating the cells with specific hormone cocktails for two weeks. The ability of MSCs to differentiate diminishes when the cells have undergone multiple passages (Chen *et al.*, 2012; Lee *et al.*, 2014), so in this study only early passage MSCs (P1-4) were differentiated. Freshly isolated mature adipocytes were not used, because they are technically challenging to work with, as they cannot be maintained in culture for extended periods and they are non-adherent. In this study, as is common practice in the field, *in vitro* differentiated adipocytes were utilised.

MSCs were seeded onto plastic or glass-bottom plates/flasks and grown to hyper-confluency by maintaining the cells in a humidified incubator at 37 ^{o}C for four days. The culture media was then removed and replaced with adipogenic or osteogenic media. Adipogenic media consists of culture media supplemented with insulin, dexamethasone, indomethacin and 3-isobutyl-1-methylxanthine (IBMX), whereas osteogenic media consisted of culture media supplemented with sodium β-glycerophosphate, L-ascorbic acid-2-phosphate and dexamethasone (Table 2.5). In both cases, the cells were left in the presence of the adipogenic or osteogenic media for two weeks. During this period the media was replaced every four days. After two weeks in the presence of adipogenic or osteogenic media, the media was removed and exchanged to culture media for three days to allow the cells to habituate. After which, the cells were ready for experimentation. In all instances where *in vitro* differentiated adipocytes (or osteoblasts) are mentioned in this study, they are cells that have undergone the full differentiation and habituation protocol. Only populations of cells that displayed >90% differentiation were deemed adequate for experimental use. There are clear morphological changes that occur that make it easy to distinguish between non-differentiated and mature cells using a microscope, such as the formation of lipid droplets within adipocytes.

Table 2.5 Components of adipogenic and osteogenic differentiation media.

Components	Purpose	Concentration (μM)	Reference
Adipogenic media:			
Dexamethasone	Activates transcription of adipocyte-specific genes	1	Scott *et al.*, 2011
IBMX	Non-selective PDE inhibitor	500	Scott *et al.*, 2011
Indomethacin	Upregulate C/EBPβ and PPARγ2 expression	200	Styner *et al.*, 2010
Insulin	Mimics IGF-1, the main adipogenic inducer, by interacting with the IGF-1 receptor	0.1	Petersen *et al.*, 2008
Osteogenic media:			
Dexamethasone	Activates transcription of osteoblast-specific genes and increase alkaline phosphatase activity	0.01	Lee *et al.*, 2009
L-ascorbic acid-2-phosphate	Increased secretion of collagen type I/ increased Col1/$\alpha_2\beta_1$ integrin-mediated intracellular signalling	172.7	Langenbach and Handschel, 2013
Sodium β-glycerophosphate	Source of phosphate	10,000	Langenbach and Handschel, 2013

2.6.1 Oil red O staining of mature adipocytes

The cells were washed with PBS once and then fixed with 4% paraformaldehyde (PFA) for 5 minutes at room temperature. The cells were then washed once with distilled water and incubated with 60% isopropanol. The isopropanol was removed and replaced with oil red O dye. A working solution of oil red O dye was generated less than two hours before initiating the staining protocol. This was achieved by mixing 30 ml of 3 mg/ml oil red O (dissolved in 99% (v/v) isopropanol) with 20 ml deionised water. The diluted oil red O was passed through filter paper to remove any clumps of dye. The cells were incubated with the dye for 5 minutes at room temperature. The dye was then removed, and the cells were washed with PBS and visualised using an Olympus CKX41 inverted microscope. Oil red O is a neutral lipid stain (Lillie and Ashburn, 1943), which provides an effective method of identifying adipocytes via staining lipid droplets within the cells. MSCs were differentiated in the presence of adipogenic media or incubated with culture media (control cells) and stained with oil red O to confirm the presence of triglyceride-filled lipid droplets within the mature adipocytes that were absent from the non-differentiated control cells (Figure 2.2).

2.6.2 Alizarin red S staining of mature osteoblasts

The cells were washed with PBS lacking Ca^{2+} and Mg^{2+} and then fixed with 4% PFA for 15 minutes at room temperature. Then the cells were washed with deionised water once and incubated with alizarin red S dye (pH 4.1) for 45 minutes at room temperature in the dark. The dye was then removed and the cells were washed four times with deionised water and imaged using an Olympus CKX41 inverted microscope. Red staining indicated the presence of calcium deposition and mineralisation. MSCs were differentiated with osteogenic media to osteoblasts and stained with alizarin red S to detect the presence of calcium deposits in mature osteoblasts, which were not detected in non-differentiated control cells (Figure 2.2).

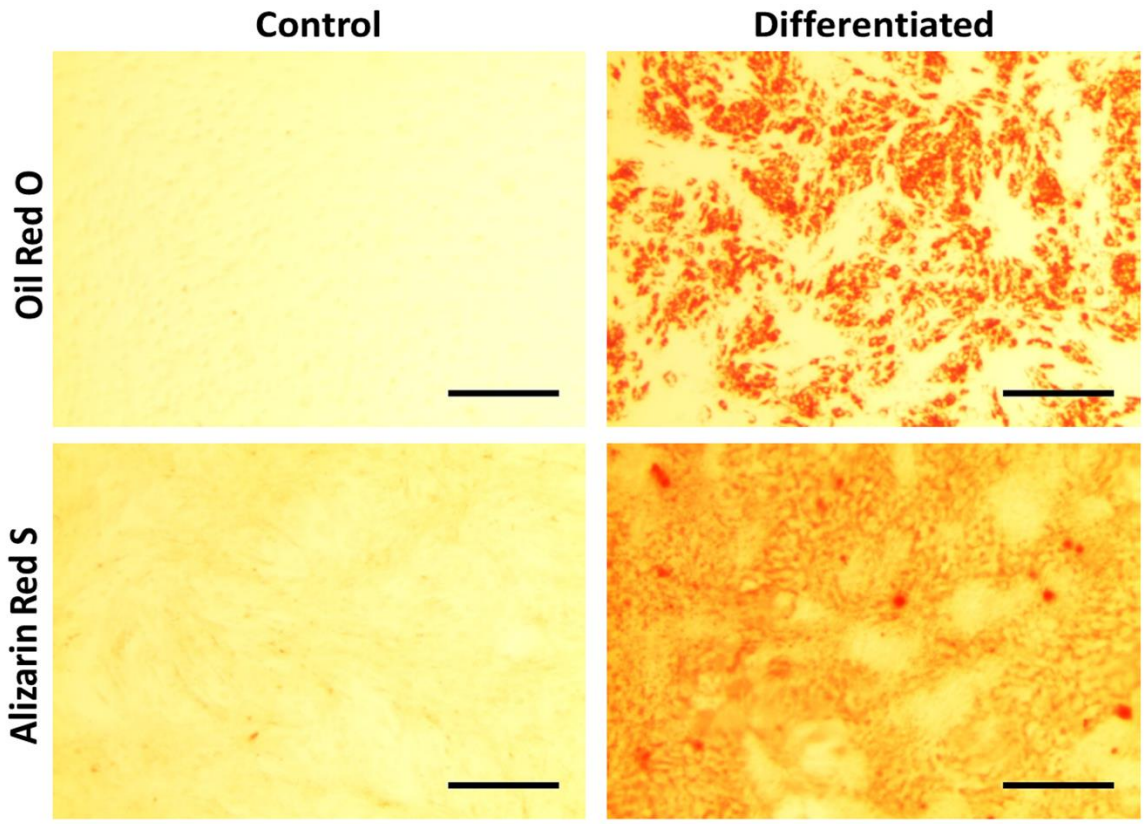

Figure 2.2 Primary human adipose-derived mesenchymal stromal cells can be induced to differentiate to adipocytes and osteoblasts. Cells were cultured in the presence of culture media (controls, left column), adipogenic media (top right) or osteogenic media (bottom right) for two weeks and then the cells shown in the top row (MSCs and adipocytes) were stained with Oil Red O and the cells in the bottom row (MSCs and osteoblasts) were stained with Alizarin Red S. Images shown are for one representative donor, but cells from three independent donors were treated in the same manner to produce nearly identical results. Scale bar represents 150 µm.

2.7 Total RNA extraction

Up to $1x10^6$ cells were lysed with 1 ml of TRI-reagent and transferred into an Eppendorf tube. The lysed cells were then treated with 100 µl 1-bromo-3-chloropropane and centrifuged to partition the sample. The top aqueous phase was then carefully transferred into a fresh tube and the RNA was precipitated with 100% isopropanol and washed with ice-cold 75% (v/v) ethanol. The RNA was then centrifuged at 12,000 x *g* for 10 minutes. The supernatant was removed and the RNA pellet was air dried. The resultant RNA was then resuspended in molecular grade water and heated to 65 °C for 5 minutes to ensure the RNA was fully dissolved. Potential genomic DNA contamination was removed using a DNA-free™ DNA removal kit (Thermo Fisher Scientific) as per the manufacturer's instructions. In brief, the RNA was incubated with 0.1 volume of 10x DNase I buffer and 1 µl of rDNase I for 30 minutes at 37 °C. Then 0.1 volume of DNase inactivation reagent was added and the mixture was incubated at room temperature for two minutes with regular mixture. Finally, the mixture was centrifuged at 10,000 x *g* for 90 seconds and the RNA was transferred to a fresh Eppendorf tube, taking extra care not to disturb the waste pellet at the bottom of the tube. The purity and quantity of RNA was assessed using a Nanodrop 2000 (Thermo Fisher Scientific). An absorbance ratio (260/280 nm) value of 2.0 was regarded as a pure RNA sample. RNA was stored at -80 °C until required.

2.8 Complementary DNA (cDNA) synthesis

Messenger RNA (mRNA) must be converted to complementary DNA (cDNA) by reverse transcriptase, to enable amplification via a polymerase chain reaction (PCR). To do this, 500 ng of RNA for each sample was primed with 100 ng random hexamer primers (Bioline) by heating the mixture to 70 °C for 10 minutes. Each sample was then incubated with 250 µM dNTPs (Bioline), 30 U RNasin ribonuclease inhibitor (Promega), 0.01 M DTT, first strand buffer and 200 U Superscript III reverse transcriptase (RT) (Thermo Fisher Scientific) for 1 hour at 42 °C. A duplicate sample with no RT was run alongside to control for genomic DNA contamination. The reaction was terminated by heating the samples to 70 °C for 10 minutes. cDNA samples were then stored at -20 °C.

2.9 Non-quantitative reverse transcription PCR (RT-PCR)

RT-PCR was used to assess the mRNA expression of human P1 adenosine receptors, adenylate cyclase isoforms and to determine whether functional or non-functional P2X5 receptors were expressed.

2.9.1 Primer design

Primer sequences provided in Table 2.6 were either obtained from previously published sources or designed using the Primer Designing Tool on the National Center for Biotechnology Information (NCBI) website. The primer sequences for the human P2X5 receptor were acquired from Kotnis *et al.* (2010). These primers yield products of varying lengths: 461 bp represents the exon 10-

containing functional P2X5 receptor, whereas the 395 bp product represents the exon 10-less non-function receptor. All the primer sequences for human adenylate cyclase isoforms were obtained from Xu et al. (2001), excluding isoforms 4, 5 and 6, which were manually designed. For manual primer design, accession numbers for mRNA transcript sequences for each gene of interest (GOI) were identified using the Uniprot website. Primer pairs for each GOI were selected using the following criteria:

1. Located within the coding DNA sequence of the GOI.
2. Targets all variants of the GOI.
3. Limited recognition of unintended genes.
4. Spanning exon-exon junctions (where possible).
5. Optimal melting temperature (T_m) of 60 ^oC.

All primers were acquired from Thermo Fisher Scientific in a lyophilised form. The primers were reconstituted to 100 µM stocks with nuclease-free water, and subsequently diluted further to 10 µM working solutions for experimental use. Both the 100 µM stocks and 10 µM working solutions were stored at -20 ^oC. Primer sequences for human P1 adenosine receptors were manually designed by a previous PhD student, Dr Hinnah Campwala.

2.9.2 Polymerase chain reaction (PCR)

cDNA or no RT control samples (1 µg) was mixed with 25 µl of ReadyMix™ Taq PCR Reaction Mix, 0.2 µM forward primers, 0.2 µM reverse primers and water to achieve a total volume of 50 µl. This was done for each of the primer sequences disclosed in Table 2.6. The following PCR conditions were employed for each GOI: Initial denaturation at 94 ^oC for 1 minute, then 35 cycles of 94 ^oC for 30 seconds, variable annealing conditions according to GOI and 72 ^oC for 1 minute to allow robust amplification of the cDNA, followed by 5 minutes at 72 ^oC for the final extension. The annealing conditions were 55 ^oC for 30 seconds for all primer sequences outlined in Table 2.6, excluding ADCY2, ADCY3, ADCY8 and ADCY9 which had an annealing temperature of 52 ^oC for 1 minute and ADCY7 which had an annealing temperature of 45 ^oC for 1 minute. These adjustments were made to gain optimum specific product amplification for each GOI. Commercially available human brain mRNA was transcribed to cDNA (according to the protocol outlined in Section 2.8) and run for each GOI as a positive control. The PCR products were stored at -20 ^oC until needed.

Table 2.6 Primer sequences for human P1 adenosine receptors (ADORA), human P2X5 receptor and human adenylate cyclase isoforms (ADCY).

Gene	Accession number	Primer sequence (5'→3')	Product size (bp)
ADORA1	NM_000674	F: GTGCGAGTTCGAGAAGGTCA	374
		R: GGATGCGGAAGGCATAGACA	
ADORA2A	NM_000675	F: CTACCGTATCCGCGAGTTCC	295
		R: GCTAAGGAGCTCCACGTCTG	
ADORA2B	NM_000676.2	F: CAGAACCCTGGGATGGAACC	277
		R: CAGCACAGGGCAAAAATCCC	
ADORA3	NM_001081976	F: CTGGTGCCGAGGCTATTTCC	302
		R: CCTTGCGGACAACTTTGGGA	
P2RX5	NM_001204520.1	F: CACTATTCTTTTAGCCGTCTGGAC	395/461
		R: TTCTGACTGCTGCTTCCACGCTTC	
ADCY1	L05500	F: CAT GAC CTG CGA GGA CGA T	446
		R: ACA GGA GAC TGC GAA TCT GAA	
ADCY2	X74210	F: GGG GCT GCG TTT CTC T	369
		R: CAG GAA CAC GGA ACA GGA TA	
ADCY3	NM_004036	F: CAC GGG ACC CAG CAA T	263
		R: GCT CTA AGG CCA CCA TAG GTA	
ADCY4	NM_139247.3	F: TCC AAG CTC CCA ATG TGT CC	753
		R: CTT GTC CAG AGG TGG CAT TT	
ADCY5	U65473.1	F: TCT GGT CTA ACG ATG TCA CGC	202
		R: TCT TTC CGC TTC TGG GTG C	
ADCY6	AB007882	F: GGC ATT GAT GAT TCC AGC AAA GAC	380
		R: TGC AGG GCC TTA GGG AAC AGA	

ADCY7	NM_001114.4	F: CCA GTC TGG ATG CAC AGG AG	746
		R: AGC CTC CCA TCA AAG AAC CG	
ADCY8	NM_001115	F: CGG GAT TTG GAA CGC CTC TA	543
		R: CCG GTC TGA CAG GTA ACT GAT AA	
ADCY9	NM_001116	F: CAC CGC AAA ATA CTT AGA TGA CG	497
		R: CCT TCT CCT GCA AGA TCT CAC AC	

2.9.3 Agarose gel electrophoresis

Agarose gel electrophoresis was utilised to separate DNA fragments according to their size (and charge). A 2% (w/v) agarose gel was prepared by dissolving 2 g of agarose (Melford Labs) in 100 ml of 1x Tris-acetate-EDTA (TAE) buffer (Thermo Fisher Scientific). This mixture was heated to ensure the agarose was fully dissolved and 4 µl ethidium bromide (final concentration 0.4 ug/ml) was added. Ethidium bromide intercalates with double stranded DNA and fluorescences under UV light, thus enabling visualisation of DNA fragments separated in an agarose gel. The agarose and ethidium bromide mixture was carefully poured into a gel mould containing a 15 well comb. Any bubbles were removed while the agarose was still molten and then the agarose was left to set for 30 minutes at room temperature. Meanwhile, the PCR products for each GOI, including the no RT controls, were mixed with 6x gel loading dye (New England Biolabs) at a ratio of 6:1 (total volume 20 µl). Once the gel had set, the comb was removed and the gel was placed in an electrophoresis tank containing TAE buffer. More TAE was added until the wells in the gel were filled. Next, the PCR products were carefully loaded into each well. At least one well on each gel was loaded with a 100 bp ladder (New England Biolabs) to enable deduction of the DNA fragment lengths. When all the samples (and ladder) were loaded, electrophoresis was initiated by passing an electrical current at 90 volts through the gel for 90 minutes. DNA is negatively charged and therefore moves towards the anode, with larger fragments travelling at a slower rate than smaller fragments. When the electrophoresis was complete, the DNA fragments were visualised under a UV lamp using a ChemiDoc™ XRS visualizer (Bio-Rad).

2.10 Quantitative real time-PCR (qRT-PCR)

Quantitative RT-PCR was used to characterise the expression of P2 purinergic receptors in human MSCs and *in vitro* differentiated adipocytes. This enabled comparison of relative receptor expression in the two cell types, as well as validation of RNA interference (RNAi) techniques. In qRT-PCR, the primers are tagged with a fluorescent probe to enable real time monitoring of the amplification process.

cDNA or no RT control samples (10 ng) were mixed with 10 µl TaqMan™ fast universal PCR master mix (Applied Biosystems) and 1 µl 20x TaqMan™ gene expression assay primers and probes (Applied Biosystems) for each GOI (Table 2.7) in a total volume of 20 µl. No template control wells were also prepared by substituting cDNA for nuclease-free water to control for DNA contamination of the reagents. Each sample and control was then amplified in a sealed MicroAmp fast optical 96-well reaction plate (Applied Biosystems) using a TaqMan™ 7500 PCR cycler (Applied Biosystems). The following protocol was utilised to amplify DNA: 20 seconds at 50 °C then 10 minutes at 95 °C (initial denaturation), followed by 40 cycles of denaturing the DNA double helix by heating the samples to 95 °C for 15 seconds and cooling to 60 °C for 1 minute to allow primer annealing and DNA amplification.

All TaqMan™ minor groove binder (MGB) probes are tagged with an FAM™ reporter dye at the 5' end and a non-fluorescent quencher (NFQ) at the 3' end. When the primer-probe complex is intact, the NFQ ensures that the fluorescence emitted by FAM is quenched due to fluorescence resonance energy transfer (FRET). However, when the primers anneal successful to the DNA and Taq polymerase begins to create new DNA fragments, the exonuclease activity of Taq polymerase leads to a permanent physical separation of the reporter dye and the NFQ, which prevents the quenching effect and allows a fluorescent signal to be detected. Therefore, the fluorescence signal is directly proportional to primer cleavage and PCR product formation.

The threshold cycle (C_T) values were extracted from amplification plots on the 7500 software (Applied Biosystems) and converted to ΔC_T values by normalising to the expression of endogenous reference gene, ribosomal protein lateral stalk subunit P0 (RPLP0):

$$\Delta C_T = C_T(\text{GOI}) - C_T(\text{reference gene})$$

For relative comparison analyses, the $2^{-\Delta\Delta CT}$ method was employed (Livak and Schmittgen, 2001), which converts the C_T values to a fold-change in gene expression normalised to an endogenous reference gene and a calibrator.

$$2^{-\Delta\Delta CT} = 2^{-(\Delta CT(\text{sample}) - \Delta CT(\text{calibrator}))}$$

For comparing the relative expression of P2 receptors in adipocytes versus MSCs, the calibrator was the ΔC_T value for MSCs, whereas for validating shRNA knockdown, the calibrator was the ΔC_T for the scrambled control cells.

Table 2.7 Assay identification codes for TaqMan™ gene expression assay primers and probes. All primers were minor groove binder (MGB) probes are tagged with an FAM™ reporter dye at the 5' end and a non-fluorescent quencher (NFQ) at the 3' end.

Gene	Assay ID
P2RX1	Hs00175686_m1
P2RX2	Hs04176268_g1
P2RX3	Hs01125554_m1
P2RX4	Hs00602442_m1
P2RX5	Hs01112471_m1
P2RX6	Hs01003997_m1
P2RX7	Hs00175721_m1
P2RY1	Hs00704965_s1
P2RY2	Hs04176264_s1
P2RY4	Hs00267404_s1
P2RY6	Hs00366312_m1
P2RY11	Hs01038858_m1
P2RY12	Hs01881698_s1
P2RY13	Hs03043902_s1
P2RY14	Hs01848195_s1
RPLP0	Hs99999902_m1

2.11 Immunocytochemistry

Confirmation of the P2 receptor expression profile was achieved by performing immunocytochemistry. MSCs were seeded onto glass coverslips and incubated at 37 ^{o}C for 48 hours or differentiated on the coverslips. All subsequent steps were conducted at room temperature unless otherwise stated. Culture media was gently aspirated off the cells and the cells were washed with PBS. They were subsequently fixed with 4% PFA for 15 minutes and permeabilised with 0.25% Triton X-100 for 10 minutes. Non-specific binding was blocked with 1% bovine serum albumin (BSA) and then the cells were incubated with the appropriate primary antibody (1:200 dilution in 1% BSA) (Table 2.8) overnight at 4 ^{o}C. Cells incubated without primary antibodies were used as controls for non-specific secondary antibody staining. The excess primary antibody was removed and successful binding was detected using rabbit anti-goat (Abcam) or goat anti-rabbit (Thermo Fisher Scientific) Alexa Fluor 488-conjugated secondary antibodies (1:1000 dilution in 1% BSA). Finally, cells were mounted onto glass slides using VectaShield containing 1.5 µg/ml DAPI (Vector Laboratories), sealed with clear nail varnish and visualised using a Zeiss AxioPlan 2ie epifluorescent microscope (Carl Zeiss Ltd.). Exposure settings for the green (AF488) and blue (DAPI) channels remained constant throughout the imaging.

2.12 Immunohistochemistry

Fresh human subcutaneous adipose tissue was cut into 1 cm^2 pieces and washed with PBS to remove excess blood. The tissue was then submerged in 4% ice-cold PFA for four hours, then washed with PBS for 30 minutes twice and left overnight at 4 ^{o}C in PBS. The samples were then sequentially submerged in increasing concentrations of ethanol (30, 50, 70, 90, 95 and 100%) for one hour each to dehydrate the tissue. Next, the tissue was submerged in histo-clear (National Diagnostic) for one hour and embedded into paraffin by placing the tissue in molten paraffin for two hours twice. The embedded tissue was placed in a mould, encased in paraffin and left overnight at 4 ^{o}C to set. The tissue blocks were then removed from their moulds and cut into 6 µm sections using a Microm HM355S automatic microtome (Thermo Fisher Scientific) and mounted onto (3-aminopropyl)triethoxysilane coated glass slides and allowed to dry.

The tissue was now ready for staining. To do this, the sections were dewaxed with histo-clear (five minutes twice) and rehydrated by sequentially submerging the slides in decreasing concentrations of ethanol (100, 95, 80, 70, 50 and 30% for 1 minute each), followed by distilled water for 1 minute. The sections were then stained using an Anti-rabbit or Anti-goat HRP-DAB Cell & Tissue Staining Kit purchased from R and D systems as per the manufacturer's instructions. All steps were conducted at room temperature unless otherwise stated. In brief, the rehydrated samples were treated with peroxidase blocking reagent for five minutes and then washed with buffer for five minutes. The sections were then blocked for 15 minutes with the appropriate serum reagent (rabbit or goat)

depending on the kit being used. Excess serum was drained off the slides and avidin blocking reagent was added for 15 minutes. The slides were then rinsed with buffer and biotin blocking reagent was added for 15 minutes. Again, the slides were rinsed with buffer and subsequently the sections were incubated with primary antibodies for $P2Y_1$, $P2Y_2$ or $P2Y_{12}$ (1:200 in PBS with 1% BSA; Table 2.8) or PBS with 1% BSA alone overnight at 4 ^{o}C. The slides were then washed with buffer three times for 15 minutes, drained and incubated with biotinylated secondary antibodies for one hour. The secondary antibody was removed and the slides were washed with buffer three time (15 minutes for each wash). Next, the sections were incubated with high sensitivity streptavidin conjugated to horseradish peroxidase (HSS-HRP) for 30 minutes. The slides were then washed with buffer three times (two minutes each) and incubated with 3,3' Diaminobenzidine (DAB) chromogen for up to 20 minutes. The sections were monitored closely during this incubation period and incubation was terminated early if the appropriate intensity of staining was achieved. However, the same incubation time was maintained for both the primary antibody treated and no primary antibody treated sections. When appropriate, the DAB chromogen was removed and the sections were rinsed and washed with distilled water for five minutes. Subsequently, the sections were dehydrated again by rapidly dipping the slides in increasing concentrations of ethanol, and then histo-clear for 10 minutes and finally mounted with DPX mountant. Once the mountant was dry, images of stained sections and no primary antibody controls were taken using an Olympus CKX41 inverted microscope.

Table 2.8 Polyclonal anti-human primary antibodies for the detection of P2 purinergic receptors.

Target	Manufacturer	Product code	Host species	Application
P2X1	Santa cruz	Sc-31491	Goat	ICC
P2X4	Alomone	APR-002	Rabbit	ICC
P2X5	Santa cruz	Sc-15192	Goat	ICC
P2X7	Alomone	Sc-20123	Rabbit	ICC
$P2Y_1$	Santa cruz	Sc-20123	Rabbit	IHC
$P2Y_1$	Alomone	APR-009	Rabbit	ICC
$P2Y_2$	Santa cruz	Sc-20124	Rabbit	IHC
$P2Y_2$	Abcam	Ab10270	Rabbit	ICC
$P2Y_4$	Alomone	APR-006	Rabbit	ICC
$P2Y_6$	Alomone	APR-011	Rabbit	ICC
$P2Y_{11}$	Alomone	APR-015	Rabbit	ICC
$P2Y_{12}$	Santa cruz	Sc-27152	Goat	IHC
$P2Y_{12}$	Alomone	APR-020	Rabbit	ICC
$P2Y_{13}$	Alomone	APR-017	Rabbit	ICC

ICC immunocytochemistry; IHC immunohistochemistry;

2.13 Calcium mobilisation experiments

For detection of changes in intracellular calcium upon purinergic receptor activation calcium (Ca^{2+}) mobilisation experiments were performed by loading cells with a fluorescent ratiometric Ca^{2+} dye, fura-2 acetoxymethyl (AM) ester (Abcam) (Grynkiewicz *et al.*, 1985). The AM moiety allow fura-2 to traverse the cell membrane to the cytosol, where the AM group is cleaved by cellular esterases, which prevents fura-2 from leaving the cell. The peak excitation wavelength of fura-2 varies according to whether it is bound to Ca^{2+} or not, from 362 nm in Ca^{2+}-free states to 335 nm in Ca^{2+}-bound states, but the emission wavelength remains constant (510 nm). Measurement of fluorescence at 510 nm using two excitation wavelengths, 340 nm and 380 nm respectively, enables calculation of a fluorescence ratio (340/380). Calculating a ratio limits the effects of photobleaching

and neutralises variables, including cell thickness and differing local fura-2 concentrations, thus increases the accuracy and reproducibility of results.

To perform Ca^{2+} mobilisation assays, cells were seeded at $2x10^4$ cells/well in black glass bottom 96 well plates (Molecular Devices, California, USA) and incubated at 37 °C in 5% CO_2 for 48 hours or differentiated *in vitro*. When the cells were ready for experimentation, the growth media was aspirated off and the cells were gently washed with salt buffered solution (SBS), containing 130 mM sodium chloride, 5 mM potassium chloride, 1.2 mM magnesium chloride, 1.5 mM calcium chloride, 8 mM D-(+)-Glucose, 10 mM hydroxyethyl piperazineethanesulfonic acid (HEPES). The cells were then loaded with 2 µg/ml fura-2AM in SBS supplemented with 0.01% (w/v) pluronic acid for 1 hour at 37 °C while being protected from light. The fura-2 loading buffer was then removed and the cells were washed twice with SBS. Where applicable, the cells were incubated for a further 30 minutes with antagonists or calcium-free SBS (SBS lacking 1.5 mM calcium chloride, but containing 2 mM EGTA; pH 7.4). Finally, the cells were challenged with nucleotides administered by a FlexStation III microplate reader (Molecular Devices), which also recorded the fluorescence (excitation 340nm and 380nm, emission 510nm) every three seconds to provide F_{ratio} values. F_{ratio} values at every time point, peak F_{ratios} and area under the curve data were extracted using SoftMax Pro 5.4.5 software (Molecular Devices). Data was analysed using Origin Pro 2018 software (Origin Lab). All dose response data was normalised to the maximal response and all antagonist data was normalised to their respective vehicle controls. Dose response curves were fitted using a modified Hill equation (DoseResp function on Origin) via the following formula:

$$y = A1 + \frac{A2 - A1}{1 + 10^{(Logx0 - x)p}}$$

Where *A*1 is the bottom asymptote (minimum response on the y axis), *A*2 is the top asymptote (maximum response on the y axis), *Logx*0 is the centre (EC_{50}) and *p* is the hill slope.

Analysis of the decay kinetics, τ, was performing using the ExpDecay1 function, which uses the following formula:

$$y = y0 + A1 \text{ x } exp\left(-\frac{x - x0}{t1}\right)$$

Where y0 is the offset, A1 is the amplitude and t1 is the 'time' constant.

2.13.1 Calcium mobilisation experiments using pertussis toxin

Pertussis toxin (PTx) is a exotoxin produced exclusively by *Bordetella pertussis*, the causative agent of Whooping cough (Carbonetti, 2010). PTx is transported across the cell membrane to the cytosol, where it hydrolyses cellular NAD to allow transfer of the released ADP-ribose to cysteine residues on the alpha subunit of heterotrimeric G_i-proteins (Katada *et al.*, 1983), which consequently

terminates any G_i-mediated signalling pathways. In this study, PTx was used to assess whether G_i-proteins were involved in nucleotide-evoked calcium responses in human adipocytes. As the target of PTx is intracellular, it requires a longer incubation time to facilitate entry into the cell and have its an effect, so the calcium mobilisation assay protocol was slightly amended to accommodate this. Cells were seeded and grown in 96-well plates as per the normal protocol (Section 2.13). When the cells were ready for experimentation, instead of directly loading the cells with fura-2 AM, the culture media was removed and replaced with culture media containing 100 ng/ml PTx or vehicle control. The cells were then incubated at 37 ^oC with 5% CO_2 for 4 hours. Then the cells were removed from the incubator and the calcium mobilisation assays was conducted as normal (Section 2.13).

2.13.2 Calcium calibration assay

In vitro differentiated adipocytes were loaded with fura-2AM as per the calcium mobilisation experiment protocol (Section 2.13) and then incubated with SBS or Ca^{2+} free SBS for 30 minutes at 37 ^oC prior to challenging the cells with 2 µM ionomycin and recording the changes in intracellular calcium levels using a Flexstation III microplate reader. The Grynkiewicz formula (Grynkiewicz et al., 1985) was then utilised to convert F_{ratio} values from calcium mobilisation assays to intracellular calcium concentrations:

$$[Ca^{2+}]_i = K_D \times \beta \times (R-Rmin)/(Rmax-R)$$

Where K_D is the K_D for fura2-AM at 37 ^oC which is 224 nM, β is the (maximum fluorescence signal at 380 nm for ionomycin in the absence of calcium)/(the minimum fluorescence at 380 nm for ionomycin in the presence of calcium), R_{min} is the minimum F_{ratio} value for ionomycin in absence of calcium and R_{max} is the maximum F_{ratio} value for ionomycin in the presence of calcium and R is the F_{ratio} value that needs to be converted. β, R_{max} and R_{min} were calculated by averaging the data from three independent donors.

2.14 Lactate dehydrogenase cytotoxicity assay

Lactate dehydrogenase (LDH) is a cytosolic enzyme, which is released into the supernatant when the cell membrane integrity is compromised due to cell damage or death, therefore the amount of LDH in the supernatant equates to the level of cytotoxicity. To exclude the possibility that the pharmacological effects observed with selective antagonism were not due to cytotoxicity, an LDH cytotoxicity assay (Cayman) was performed as per the manufacturer's instructions. In brief, cells were seeded in 96-well plates and treated in the same manner as they are for pharmacological studies (calcium mobilisation and functional studies). MSCs and adipocytes were washed once with SBS and then 200 µl/well SBS was added to each well. An additional 20 µl/well of each antagonist (maximal concentration) or vehicle was added to duplicate wells, including two wells per donor that

contained 10% (v/v) triton X, and the cells were incubated for 30 minutes at 37 °C. The protocol was adjusted slightly for AR-C118925XX in adipocytes to account for the longer incubation times used in the functional studies. For AR-C118925XX, the cells were washed with PBS once and then DMEM was added, in place of SBS, and the cells were incubated with the antagonist for three hours, rather than 30 minutes. When the respective antagonist incubation times had elapsed, the plates were centrifuged at 400 x *g* for five minutes and 100 µl/well of supernatant was removed and placed in a fresh 96-well plate. Then 100 µl/well of LDH reaction solution was added to every well and the plate was incubated at 37 °C for 30 minutes on an orbital shaker. Finally, the absorbance was read at 490 nm using a Flexstation III microplate reader and the percentage cytotoxicity was calculated using the following formula:

$$\% \text{ Cytotoxicity} = ((A490_{\text{Antagonist}} - A490_{\text{Vehicle}}) / (A490_{\text{Triton X}} - A490_{\text{Vehicle}})) \times 100$$

Maximal concentrations of AR-C11892XX, MRS2578 and U73122 did not cause an increase in extracellular LDH levels for MSCs. In addition, treatment of *in vitro* differentiated adipocytes with maximal concentrations of AR-C118925XX, MRS2500, PSB0739, U73122 and Ticagrelor also failed to increase levels of LDH in the supernatant. These results suggested that these antagonists did not cause cytotoxicity in MSCs or adipocytes (Figure 2.3).

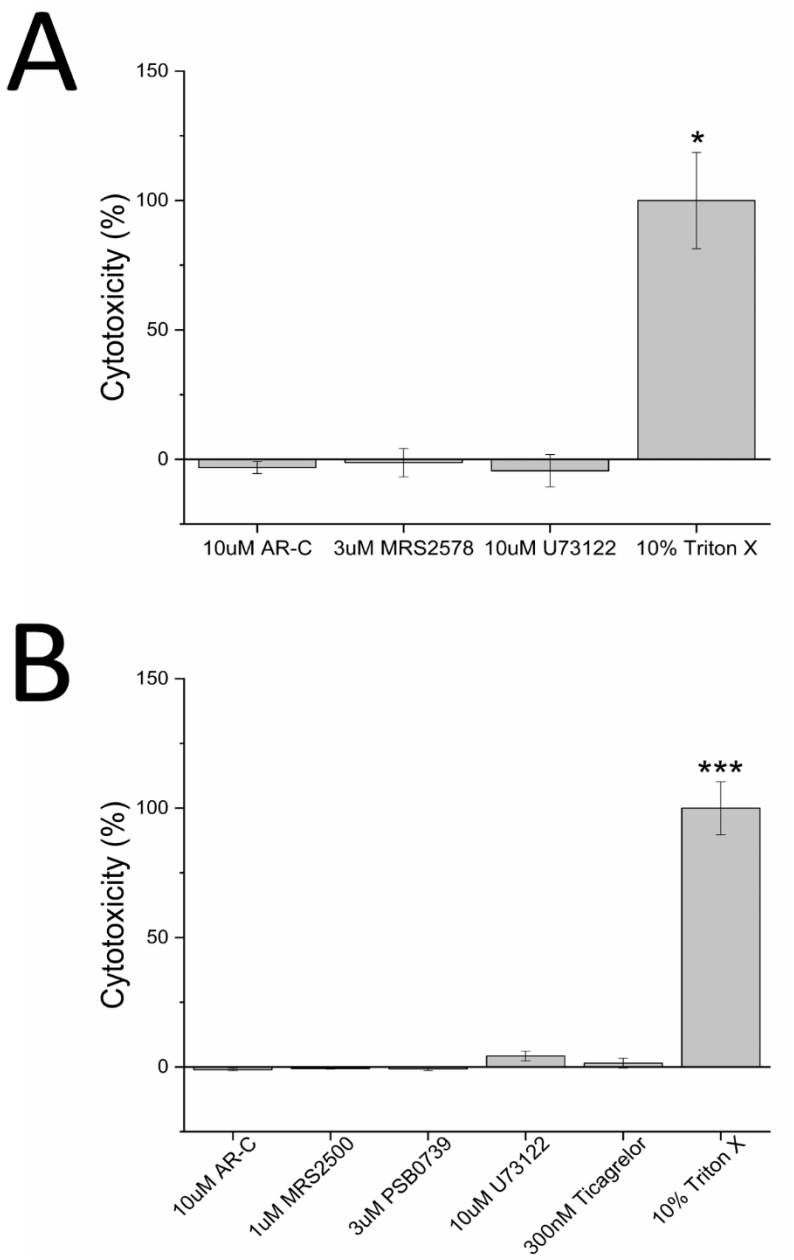

Figure 2.3 Assessment of whether maximal concentrations of antagonists induce cytotoxicity in primary human adipose-derived mesenchymal stromal cells and *in vitro* differentiated adipocytes. Cytotoxicity was determined via measurement of lactate dehydrogenase levels in the supernatants of (A) primary human adipose-derived mesenchymal stromal cells and (B) primary human *in vitro* differentiated adipocytes. Values are normalised to their own vehicle controls and 10% triton X (positive control). Data presented is the mean ± SEM of cells from three independent donors. *p<0.05 and *** p <0.001 versus vehicle control.

2.15 Cell proliferation assay

To ascertain whether activation or inhibition of purinergic signalling influenced proliferation of primary human AD-MSCs, proliferation of AD-MSCs was measured in the presence and absence of nucleotides and subtype selective antagonists. A CellTiter 96® Aqueous one solution cell proliferation assay kit was purchased from Promega and performed as per the manufacturer's instructions. MSCs were diluted to $1x10^4$ cells/ml and 100 µl of cells was added to each well. This lower initial seeding density was selected to provide sufficient space for the MSCs to proliferate within each well. The cells were incubated overnight in humified environment at 37 °C with 5% CO_2 and the following morning, a further 100 µl/well of culture media containing vehicle, nucleotide or antagonist was added to every well and the cells were incubated for 30 minutes at 37 °C. Next, 10 µl of CellTiter 96® Aqueous one solution (MTS reagent) was added to duplicate wells (control and nucleotide/antagonist treated cells) and the cells were incubated for four hours with the reagent at 37 °C. Then the absorbance was measured at 490 nm (4.5-hour reading). The cells were then placed back in the incubator (37 °C) for a further six days, with MTS reagent being added four hours before the absorbance was read at each timepoint (24, 48, 72, 96, 120 and 144 hours). All values were normalised to the absorbance values for the vehicle control at the 144 hour timepoint. The MTS tetrazolium compound is bioreduced by metabolically active cells to produce a coloured formazan product, thus altering the absorbance of culture media. As this reaction can only occur in the presence of viable cells, it is possible to use the formation of formazan as a measure of the number of viable cells present. The number of viable cells, and consequently the amount of formazan produced, should increase as the cells proliferate.

2.16 Cell migration assay (transwell)

Another important function of AD-MSCs is their ability to migrate towards chemotactic agents. To investigate whether nucleotides may play a role in chemotaxis, a transwell assay was performed. MSCs were trypsinised and resuspended at a density of $4x10^5$ cells/ml in Roswell Park Memorial Institute (RPMI) culture media containing HEPES (Lonza), but no FBS or antibiotics. The cells were then incubated for 1 hour at 37 °C in the dark in the presence of 1.5 µM calcein-AM to fluorescently label the cells. A range of concentrations of ATP (0.1, 1, 30 and 100 µM) and a positive control containing 10% FBS (a known chemoattractant) were prepared in RPMI containing HEPES. 200 µl/well of each potential chemotactic agent was placed in the lower clear plate of a Corning Fluoroblok™ 96-multiwell insert system, whereas 50 µl/well of calcein-loaded primary human MSCs were carefully added to the upper wells (black plate). The upper plate was very gently lowered into the lower plate containing the chemotactic agents, avoiding the formation of any bubbles between the two plates. The two-plate structure was then immediately transferred to a Flexstation III microplate reader (maintained at 37 °C) and the fluorescence (excitation 485 nm/emission 530 nm)

was read from the bottom of each well every five minutes for four hours. Corning FluoroBlok multiwell inserts are specifically designed with a polyethylene terephthalate (PET) membrane that efficiently blocks the transmission of wavelengths between 400 and 700 nm, therefore when light is passed through the bottom of the plate, only fluorescence in the lower plate is detected, whereas the cells within the upper plate are protected. Initially the lower plate should be devoid of fluorescence, but the fluorescence signal should increase as the calcein-loaded cells from the upper plate migrate through the PET membrane to the lower plate. Although some cells will spontaneously migrate to the lower plate, the rate of migration should be enhanced in the presence of true chemotactic agents.

2.17 Lentiviral shRNA knockdown

RNA interference techniques are an effective and widely used tool for exploiting cellular microRNA processing mechanisms to reduce expression of a target gene (Cullen, 2005). Short hairpin RNA (shRNA) strategies are often used to produce highly potent and sustained knockdown of a gene of interest (GOI), with minimal off-target effects (Rao *et al.*, 2009). Lentiviral particles based on the human immunodeficiency virus (HIV-1) can be harnessed to effectively deliver plasmids containing shRNA constructs into both dividing and non-dividing cells. When the plasmids enter the cell, they are transported to the nucleus, where the plasmid DNA is transcribed into a single stranded RNA sequence and the complementary regions of the RNA interact to form a stem-loop structure (hairpin) with a two nucleotide 3' overhang (H. Zhang *et al.*, 2002). This pre-shRNA molecule is then transported into the cytoplasm, where the loop region is removed by an enzyme known as DICER. The two strands of the mature shRNA molecule then disassociate, and one strand (the guide strand) is incorporated into the RNA-interfering silencing complex (RISC), where it is used to mediate a conformational change or cleavage of target gene's mRNA, thus preventing the translation of the target gene (Cullen, 2004). The plasmid DNA remains within the nucleus for the lifespan of the cell, which ensures stable production of shRNA and consequently enduring reduction of target gene expression.

In this study, lentiviral particles were used to deliver plasmids containing shRNA constructs capable of knocking down the expression of $P2Y_2$ to further explore the functional role of $P2Y_2$ in primary human MSCs and *in vitro* differentiated adipocytes.

2.17.1 Preparation of plasmid DNA for lentiviral production

Bacterial glycerol stocks of pLKO.1-puro vectors carrying Mission® non-target shRNA control sequences or shRNA sequences that target $P2Y_2$ receptor mRNA were purchased from Sigma-Aldrich (Table 2.9). The base pLKO.1-puro vector (Figure 2.4) was developed as part of the RNAi

consortium at the Broad Institute (Stewart *et al.*, 2003), and it enables antibiotic selection of successfully transduced cells due to the presence of a puromycin-resistance gene within the vector.

In addition to plasmids containing the control and target shRNA sequences, additional plasmids containing viral transgenes are required to facilitate viral particle formation. Bacterial stocks of psPAX2 (viral packaging plasmid) and pMD2.G (viral envelope plasmid) were purchased from Addgene (Trono Lab, unpublished data). All plasmids were purchased in ampicillin-resistant bacteria. Each plasmid DNA sequence was amplified by streaking a small amount of the bacterial stocks on Luria Bertani (LB) agar plates, containing 100 µg/ml ampicillin, and were left at 37 ^{o}C overnight. The following day individual colonies from each agar plate were transferred to tubes containing LB broth (with 100 µg/ml ampicillin) and the tubes were incubated at 37 ^{o}C overnight under constant agitation at 225 rpm. Multiple colonies were inoculated for each plasmid. The plasmid DNA was then purified using an E.Z.N.A Plasmid Mini Kit II (Omega Bio-Tek), performed as per the manufacturer's instructions. The quantity and purity of the resultant DNA was then assessed using a Nanodrop 2000 (Thermo Fisher Scientific). A value of 1.8 for the ratio of absorbance at 260 and 280 nm was regarded as a pure DNA sample.

Table 2.9 Short hairpin RNA plasmid DNA sequences purchased from Sigma-Aldrich.

	Product code		**Sequence**
Non-mammalian shRNA control	SHC002V		CCGGCAACAAGATGAAGAGCACCAACTCGA GTTGGTGCTCTTCATCTTGTTGTTTTT
	TRC number	**Clone ID**	**Sequence**
$P2Y_2$ target shRNA	TRCN0000009481	NM_176072.1-1505s1c1	CCGGGCAGAGGATAGAAGATGTGTTCT CGAGAACACATCTTCTATCCTCTGCTTTTT

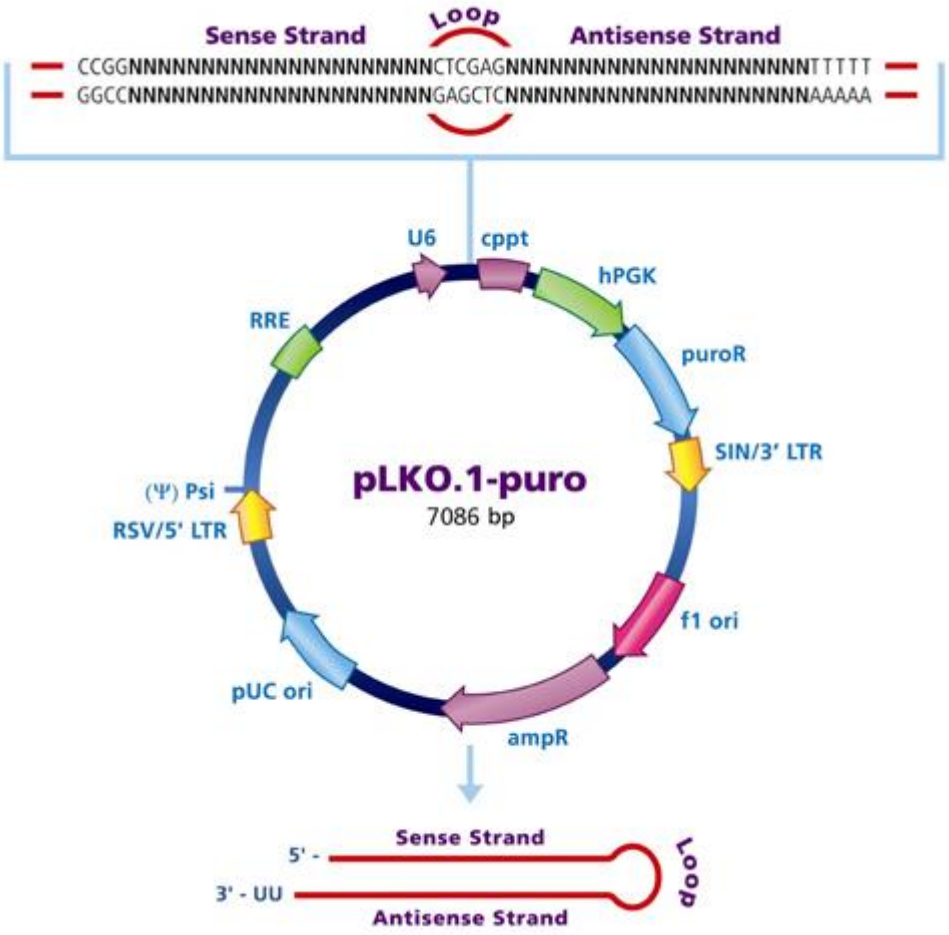

Figure 2.4 Map of an empty pLKO.1-puro vector acquired from the Sigma Aldrich website. https://www.sigmaaldrich.com/life-science/functional-genomics-and-rnai/shrna/library-information/vector-map.html. Last accessed 15.5.18.

2.17.2 Generation of lentiviral particles

Self-inactivating viral particles can be generated via co-transfection of lentiviral genes (psPAX2 and pMD2.G) and shRNA constructs in packaging cells (HEK293T) (Song and Yang, 2010). HEK293 cells are a cell line derived from human embryonic kidney cells that were transformed with adenovirus type 5 DNA (Graham *et al.*, 1977). Transfection of the simian virus 40 large T-antigen and a neomycin resistance gene transformed HEK293 cells to HEK293T cells (DuBridge *et al.*, 1987). HEK293T cells were purchased from the European Collection of Authenticated Cell Cultures (ECACC). HEK293T cells were maintained in culture in the same manner as primary human AD-MSCs (Section 2.1.1). HEK293T cells ($9x10^6$) were seeded in 150 mm petri dishes and left at 37 ^oC overnight in culture media (DMEM with 10% [v/v] FBS, 50 IU/ml penicillin and 50 µg/ml streptomycin). The following morning, the culture media was exchanged for 20 ml of viral collection media (DMEM supplemented with 1% [v/v] FBS and no antibiotics) and the plasmids were prepared for transfection under sterile conditions. Two tubes each containing 1.2 ml serum-free OPTIMEM media (Life Technologies) were prepared: 36 µl Lipofectamine™ 2000 transfection reagent (Life Technologies) was added to one tube, while plasmid DNA was added to the other tube. The following concentrations of plasmid DNA were used: 9 µg of lentiviral vector containing pLKO.1-puro $P2Y_2$ (target) or pLKO.1-puro non-target shRNA (scrambled), 12 µg psPAX2 and 3 µg pMD2.G. Both tubes were then incubated at room temperature for five minutes. The contents of the two tubes were then mixed and incubated for a further 20 minutes at room temperature. The plasmid/transfection reagent mixture was then added drop-wise to the HEK293T cells and the cells were incubated for 6 hours at 37 ^oC in 5% CO_2. The media was then replaced with fresh viral collection media and the cells were left to incubate at 37 ^oC for 72 hours, with the media being collected (and stored at 4 ^oC) and replaced with fresh viral collection media every 24 hours. After 72 hours had lapsed, the virus-containing media was passed through a 0.45 µm filter to remove cell debris and then the virus was concentrated using Lenti-X concentrator solution (Clontech) as per the manufacturer's instructions. The resulting concentrated virus was then immediately aliquoted and stored at -80 ^oC until required. This process was performed in duplicate to produce lentiviral particles containing pLKO.1-puro $P2Y_2$ (target) or pLKO.1-puro non-target (scrambled) shRNA.

2.17.3 Calculation of the Multiplicity of Infection (MOI) using a p24 ELISA

A p24 enzyme-linked immunosorbent assay (ELISA) was performed using a QuickTiter™ Lentivirus Titer Kit (Cell Biolabs Inc) to determine the number of lentiviral particles present for both the scrambled control and $P2Y_2$ target shRNA lentiviruses. These values were then used to ensure that equivalent amounts of control and target lentivirus were used for the subsequent experiments. The QuickTiter™ Lentivirus Titer Kit was designed to specifically detect lentivirus associated HIV-1 p24 core protein, not free p24, thus providing an accurate measurement of the viable viral titre. The assay has a sensitivity limit of 1 ng/ml HIV p24. The assay was performed as per the manufacturer's

instructions. In brief, samples of both the scrambled and $P2Y_2$-shRNA lentiviruses were diluted 1:50 in 1 ml of DMEM and 10 µl ViraBind™ Lentivirus Reagent A and B were added to each tube sequentially with mixing by inversion after each reagent was added. The tubes were then incubated at 37 °C for 30 minutes to inactivate the virus and then centrifuged at 12,000 x *g* for 5 minutes. The supernatant was removed and the pellet was vortexed to resuspend the inactivated virus in 250 µl of sample diluent. 100 µl/well of inactivated lentivirus or p24 antigen standard was added to an anti-p24 antibody coated 96-well plate and the plate was incubated at 4 °C overnight. The next morning, the supernatants were discarded and the wells were washed three times with 1x wash buffer and thoroughly dried. FITC-conjugated anti-p24 monoclonal antibody (100 µl/well) was added to every well and plate was incubated at room temperature on an orbital shaker for one hour. The wells were then emptied and washed three times with 1x wash buffer. Again, the wells were dried and 100 µl/well of substrate solution was added to each well. The plate was incubated on an orbital shaker at room temperature for up to 30 minutes. The colour change reaction was monitored closely to prevent saturation and the reaction was terminated by adding 100 µl/well stop solution. The absorbance was then read at 450 nm using a Flexstation III microplate reader. The p24 standard curve was used to calculate the concentration of virus-associated p24 (ng/ml). This concentration was then converted to a p24 titre (ng/ml) using the following equation:

$$\text{p24 titre (virus associated p24, ng/ml)} = \text{p24 (ng/ml)} \times \text{dilution factor} \times (0.25\ \text{ml}/1.0\ \text{ml})$$

The p24 titre was subsequently converted to the number of lentiviral particles, as 1 ng/ml p24 equates to 1.25×10^7 lentiviral particles. In turn, this value was then used to calculate the Multiplicity of Infection (MOI) for each lentivirus. The MOI is the ratio between the number of viral particles and the number of cells being infected. It was calculated via the following equation:

$$\text{Multiplicity of Infection (MOI)} = \frac{\text{Volume of virus (ml)} \times \text{Number of lentiviral particles}}{\text{Number of cells transfected}}$$

2.17.4 Puromycin kill curve for primary human MSCs

As mentioned previously in Section 2.17.1, the vectors containing the non-target and target shRNA sequences both have a puromycin-resistance gene, which enables selection of successfully transduced cells with puromycin. In order to determine the correct concentration of puromycin to use for selection, a puromycin kill curve was performed. MSCs (2×10^4 cells/well) were seeded in 96 well plates and incubated overnight at 37 °C. The following morning, different concentrations of puromycin were added to quadruplet wells (0, 0.1, 0.3, 1, 3 and 10 µg/ml). Immediately after the puromycin was added (day 0), 10 µl/well of CellTiter 96® AQueous One Solution Reagent (MTS reagent) (Promega) was added to half of the cells and then all the cells were incubated at 37 °C for four hours. Next, the absorbance was read at 490 nm for all the wells containing MTS. All the cells were then placed back in the incubator for five days. On the fifth day, 10 µl/well MTS reagent was

added to the remaining wells and the cells were again incubated at 37 °C for four hours. The absorbance was then read at 490 nm for the remaining well and these values were normalised to the day 0 readings. In primary human MSCs, the absorbance value decreased as the concentration of puromycin increased (Figure 2.5). Little or no effect was observed using ≤ 0.3 µg/ml puromycin, but concentrations of 1 µg/ml and above were sufficient to kill all the cells in the well after five days. Thus 1 µg/ml puromycin was used to select for successful transduction in primary human MSCs.

2.17.5 Direct transfection of primary human *in vitro* differentiated adipocytes

To partially reduce the expression of $P2Y_2$ receptors in primary human *in vitro* differentiated adipocytes, the cells were differentiated and habituated in 96-well plates (Section 2.6). The cells were then washed once with PBS and 200 µl/well of fresh culture media (DMEM with 10% [v/v] FBS, 50 IU/ml penicillin and 50 µg/ml streptomycin) containing 8 µg/ml of hexadimethrine bromide was added to each well. Then lentiviral particles containing either scrambled control or $P2Y_2$ shRNA were added to each well and the cells were incubated for 18 hours at 37 °C in 5% CO_2. A range of different MOIs (1, 10, 100, 500 and 1000) were used in order to identify the optimal MOI for maximum knockdown of $P2Y_2$ receptor expression. The following day, the virus-containing media was removed and replaced with fresh culture media and the cells were incubated for a further four days at 37 °C in 5% CO_2 before they were ready for experimental use. The cells were then lysed with TRI reagent and RNA extraction, cDNA synthesis and quantitative PCR was performed as described in Sections 2.7, 2.8 and 2.10 respectively. The fold-change in $P2Y_2$ mRNA expression was determined using the $2^{-\Delta\Delta CT}$ method, where each value was compared to a scrambled control produced using the same MOI used to knockdown $P2Y_2$ receptor expression. A value of 1 represents no change, but values below 1 represent a decrease in expression (Figure 2.6). From this experiment it was determined that an MOI of at least 500 was required to achieve significant knockdown of $P2Y_2$ expression, however an MOI of 1000 produced the greatest reduction in receptor expression, thus an MOI of 1000 was used for all subsequent experiments in which knockdown of $P2Y_2$ receptor expression was required. Where possible, qPCR was performed to confirm successful shRNA-mediated knockdown of $P2Y_2$ in all subsequent experiments.

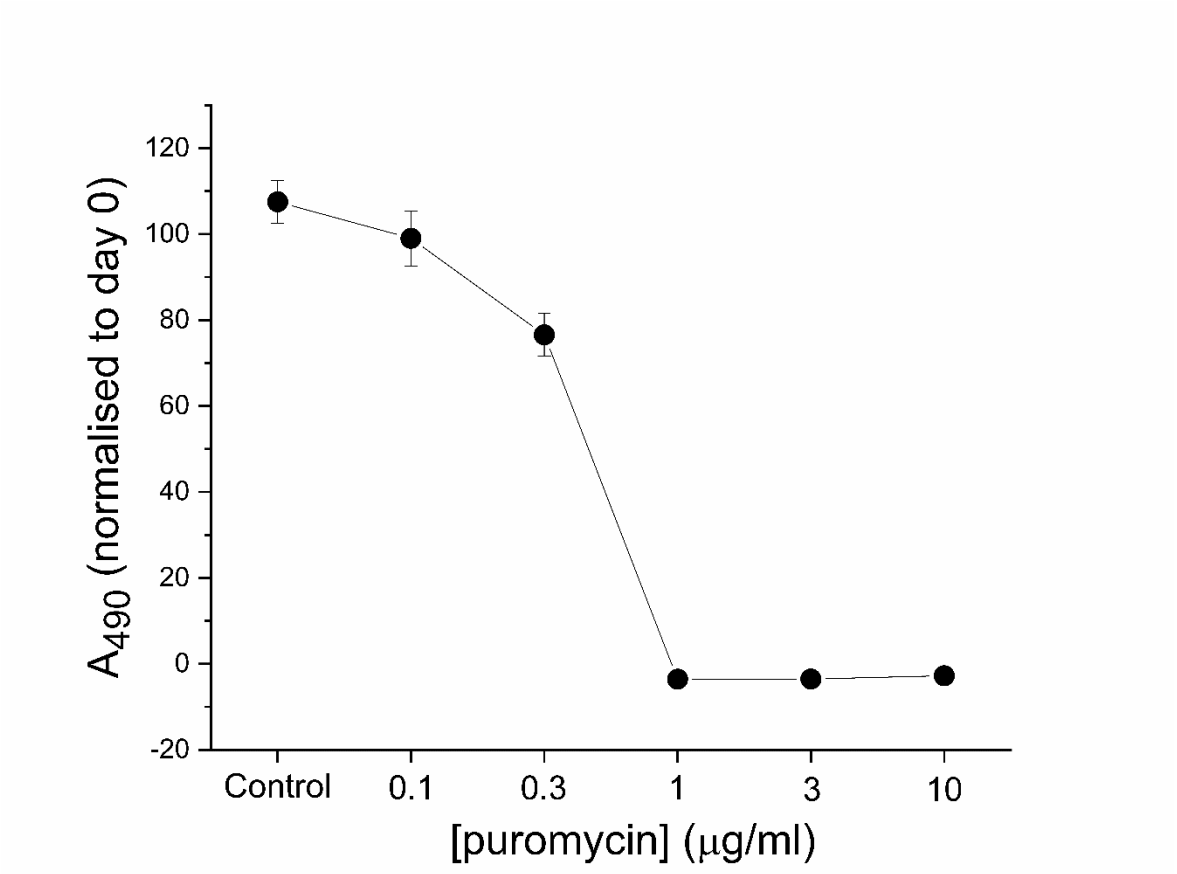

Figure 2.5 Puromycin kill curve for primary human MSCs (N=3). Cells were treated with puromycin for five days and then cell viability was tested by measuring changes in absorbance at 490 nm due to the production of formazan. Absorbance values are normalised to readings taken immediately after puromycin was added on day 0.

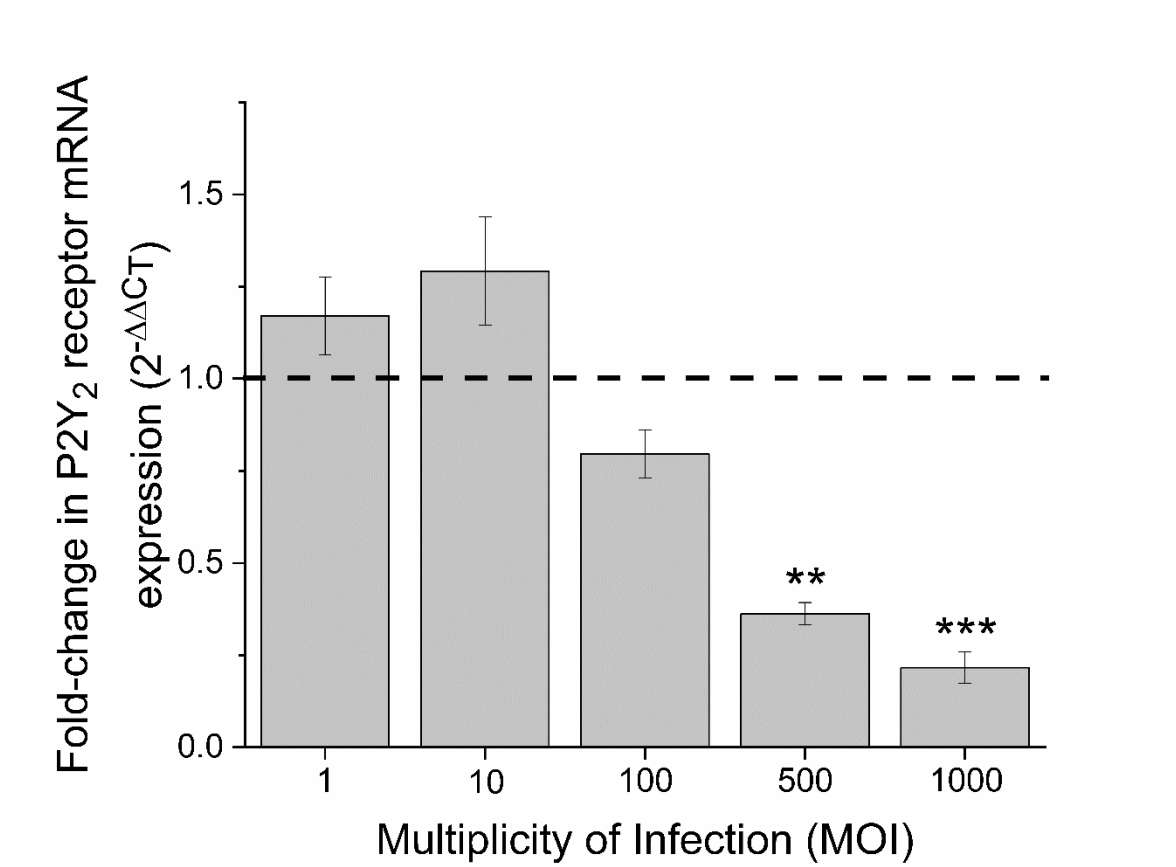

Figure 2.6 Change in $P2Y_2$ receptor mRNA expression in primary human *in vitro* differentiated adipocytes when cells are treated with an increasing number of lentiviral particles (*N*=3). Data was normalised to expression of the endogenous control gene, RPLP0, and then comparisons were made between the ΔC_T values for cells treated with lentivirus containing scrambled non-target control shRNA and lentivirus containing the $P2Y_2$ target shRNA using the $2^{-\Delta\Delta CT}$ method. ** p <0.005 and *** p <0.001.

2.17.5 Transfection of primary human MSCs (spinoculation)

For primary human MSCs it was necessary to adopt a spinoculation protocol to the increase the likelihood of successful transfection (and transduction) of the scrambled and target shRNA sequences (O'Doherty *et al.*, 2000). This involved diluting $2x10^5$ MSCs in 2 ml of culture media containing 8 µg/ml hexadimethrine bromide. Viral particles (control and target; MOI of 1000) were then added to the cells and the mixture was centrifuged at 1,400 x *g* at 32 ^oC for 60 minutes. The supernatant was then carefully aspirated off without disturbing the pellet of cells at the bottom of each tube. The pellet was then gently resuspended in culture media and transferred to a T25 flask. The cells were then incubated at 37 ^oC for 48 hours prior to replacing the culture media with fresh culture media containing 1 ug/ml puromycin. The cells were maintained under puromycin selection until they reached confluence. The media was replaced every four days. The puromycin-resistant cells were then expanded and used for experimentation.

2.18 BODIPY staining

In vitro differentiated adipocytes which were transfected with scrambled control or $P2Y_2$ shRNA lentiviral particles were stained with BODIPY 493/503 lipid dye (Thermo Fisher Scientific) to quantify any changes in total lipid content due to a reduction of $P2Y_2$ receptor expression. To do this, the culture media was removed and replaced with 100 µl/well DMEM (no FBS or antibiotics) and a further 100 µl/well of DMEM containing 2 µM BODIPY 493/503 dye was added and immediately mixed thoroughly by gently pipetting. The cells were then incubated for 30 minutes at 37 ^oC in the dark. The excess dye was then removed and the cells were washed twice with PBS and then the fluorescence at 493/503 nm (excitation/emission) was measured using a Flexstation III microplate reader. Each experiment was normalised for background fluorescence, by measuring and subtracting the fluorescence values for cells in the absence of the dye.

2.19 Lipid droplet quantification

Images of human *in vitro* differentiated adipocytes that had been treated with both scrambled and $P2Y_2$ shRNA lentiviral particles were taken using an Olympus CKX41 inverted microscope for 12 independent donors. These images were then anonymised and given to an independent member of the laboratory for analysis to eliminate operator bias. The number of lipid droplets in 15 individual cells from each image were quantified using the counter plugin on Image J (National Institutes of Health). Once all the counting was complete, the values were sorted according to whether they were calculated from an image of scrambled or $P2Y_2$ knockdown adipocytes to perform statistical analyses.

2.20 Quantification of intracellular cyclic AMP

Cyclic AMP (cAMP) is an important secondary messenger molecule that mediates numerous cellular processes. Increases in intracellular cAMP are mediated by adenylate cyclase (AC), which synthesizes cAMP from ATP. Activation of G_s and G_i-coupled receptors leads to stimulation or inhibition of AC respectively (Reddix and Pacheco, 2007). $P2Y_{12}$ is an G_i-coupled receptor, so quantification of cAMP is a useful method of assessing $P2Y_{12}$ activity (von Kügelgen and Hoffmann, 2016).

2.20.1 CatchPoint cAMP assay

To investigate the functional activity of $P2Y_{12}$, a CatchPoint cAMP Fluorescent Assay Kit was purchased from Molecular Devices and performed as per the manufacturer's instructions. In brief, culture media was gently aspirated off *in vitro* differentiated adipocytes and the cells were washed with Krebs-Ringer Bicarbonate buffer containing 120 mM sodium chloride, 4.6 mM potassium chloride, 0.5 mM magnesium chloride, 0.7 mM dibasic sodium phosphate, 1.5 mM monobasic sodium phosphate, 10 mM D-glucose and 15 mM sodium bicarbonate (KRBG; pH 7.4). The cells were then incubated with vehicle or antagonists (diluted in KRBG; 50 µl/well) for 30 minutes at 37 ^{o}C. An additional 50 µl/well of KRBG containing vehicle or agonist was added to each well and the cells were incubated at 37 ^{o}C for 5 minutes. Finally, a further 50 µl/well of KRBG containing 60 µM forksolin (20 µM final concentration) was added and the cells were incubated for 15 minutes at 37 ^{o}C. The supernatant was then removed and the cells were lysed with 50 µl/well of lysis buffer for 10 minutes on a plate shaker. Then 40 µl of each lysed sample was transferred immediately to a goat anti-rabbit IgG coated microplate and 40 µl/well of rabbit anti-cAMP antibody was also added, excluding two wells where the antibody was replaced with buffer to serve as no antibody control wells. The plate was then placed on a shaker for 5 minutes to mix the lysates and antibody. Next, 40 µl/well of HRP-cAMP conjugate was added to every well and the plate was sealed and placed on an orbital mixer for two hours at room temperature. The supernatant was then removed from all wells and the wells were washed with wash buffer four times. Finally, 100 µl/well Stoplight red substrate was added to each well and the plate was protected from light and incubated at room temperature for 10 minutes, and then the fluorescence intensity (excitation 530 nm/emission 590 nm) was measured. A cAMP standard curve was run on each plate to facilitate conversion of fluorescence intensity readings to intracellular cAMP concentrations. There is an inverse relationship between the fluorescence intensity and concentration of cAMP, because cAMP in the lysates competitively decreases the binding of HRP-cAMP conjugates, consequently decreasing the measured HRP activity.

2.20.2 Cyclic AMP XP® Assay Kit

Measuring intracellular cAMP can also be a useful method of determining intracellular mechanisms. *In vitro* differentiated adipocytes were washed once with PBS and then incubated with 100 µl/well DMEM (no FBS/antibiotics) for two hours at 37 °C and then 1 µl/well vehicle or antagonist was added to each well and the cells were incubated for a further 30 minutes at 37 °C. DMEM alone or agonist (50 µl/well) was added to each well and the cells were incubated for a further 15 minutes at 37 °C. The cells were then washed twice with ice-cold PBS and lysed on ice with 100 µl/well 1x cell lysis buffer containing 1 mM phenylmethylsulfonyl fluoride. The amount of cAMP in the cells was then quantified using a Cyclic AMP XP® Assay Kit (Cell Signalling Technology). The protocol and methodology for this kit is very similar to the CatchPoint cAMP assay described in 2.15.1. In brief, 50 µl/well of the cell lysates and 50 µl/well cAMP-HRP conjugates were placed in microwells coated with anti-cAMP rabbit monoclonal antibodies and incubated at room temperature on an orbital mixer for three hours. The supernatants were then removed and the wells were washed four times with wash buffer. Next, 100 µl/well 3,3',5,5'-Tetramethylbenzidine (TMB) substrate was added to each well and the formation of a coloured product was monitored for up to 30 minutes to prevent saturation. The reaction was terminated by adding stop solution to all the wells and then the absorbance was measured at 450 nm using a Flexstation III microplate reader. A standard curve was run with each experiment.

2.21 ATP quantification assay

An ATP Bioluminescence Assay Kit HS II was purchased from Roche and performed as per the manufacturer's instructions. Luciferase from *Photinus pyralis* (American firefly) catalyses the breakdown of D-luciferin in the presence of ATP and a by-product of this reaction is green light emitted at 562 nm.

$$\text{ATP + D-luciferin + } O_2 \rightarrow \text{oxyluciferin + } PP_i + \text{AMP + } CO_2 + \text{light}$$

At low concentrations of ATP (C_{ATP}), the Michaelis-Menten constant (K_m) is much greater than the concentration of ATP, therefore the Michaelis equation for the reaction (Light intensity = (V_{max} x C_{ATP})/(K_m + C_{ATP})) can be simplified to:

$$\text{Light intensity} = V_{max} \times C_{ATP}/K_m$$

The amount of light produced by the reaction is directly proportional to the concentration of ATP and dependent on the amount of luciferase (V_{max}) present. The working range of the assay is between 10^{-5} and 10^{-12} M ATP.

In vitro differentiated adipocytes were washed once with warm PBS and then incubated with 50 µl/well DMEM (no FBS or antibiotics) for 1 hour at 37 °C. Next, 1 µl vehicle or antagonist was

added directly to each well and the cells were incubated for a further 1 hour at 37 ^{o}C with 5% CO_2. The supernatant was then carefully removed, taking care not to disturb the cells, and placed in a white 96-well plate alongside ATP standard curve samples diluted in DMEM. The plate was then immediately placed in a Flexstation III (Molecular Devices), which automatically added 50 µl luciferase/luciferin reagent to each well and measured the bioluminescence of each well. An integration time of 1 second was used. An ATP standard curve was produced every time the assay was run and this was used to convert the luminescence values to ATP concentrations (nM). Blank DMEM samples were also run to control for background luminescence.

2.22 Glycerol quantification assay

Lipid droplets within white adipocytes are filled with triglyceride molecules, which are composed of three fatty acids (FA) attached to a glycerol backbone. During times of nutrient shortage, triglycerides are hydrolysed to their component parts in a process known as lipolysis (Ahmadian *et al.*, 2010). FA molecules are rapidly reabsorbed and recycled, but glycerol molecules are not metabolised to a significant extent (Vaughan, 1962), which means quantifying glycerol release is a more stable measure of lipolysis. To assess whether purinergic signalling may play a role in lipolysis, glycerol release was measured in the presence and absence of nucleotides and subtype selective antagonists. To do this, *in vitro* differentiated adipocytes were washed once with PBS and then incubated with 100 µl/well DMEM (no serum or antibiotics) for two hours at 37 ^{o}C with 5% CO_2. Immediately following this incubation period, 1 µl/well vehicle or antagonist was added directly to each well and the cells were incubated for a further 30 minutes at 37 ^{o}C with 5% CO_2. Next, a further 50 µl/well DMEM containing vehicle or agonists was added to the cells. For the time series assays, a supernatant sample was collected immediately after the agonist was added by pipetting gently up and down twice and then transferring 100 µl of supernatant to a fresh 96-well plate. Samples were kept on ice for the duration of the experiment. The cells were incubated at 37 ^{o}C between sample intervals. The initial samples were labelled '0 minutes', and then samples were taken after 20, 40, 60, 120 and 180 minutes had lapsed. Alternatively, for all non-time series glycerol experiments, samples were taken three hours after vehicle/agonist was added. After the final sample was collected, all the samples were stored at -80 ^{o}C or used immediately for the glycerol quantification assay.

A glycerol assay kit was purchased from Sigma-Aldrich and was performed as per the manufacturer's instructions. The glycerol concentration is determined via the induction of a series of reactions catalysed by glycerol kinase and glycerol phosphate oxidase resulting in the formation of a fluorometric product proportional to the concentration glycerol present. In brief, 10 µl of each supernatant sample, no cell control or glycerol standard was placed in a glass bottom black 96-well plate. A master reaction mix containing 100 µl assay buffer, 2 µl enzyme mix, 1 µl dye reagent and

1 µl ATP was prepared. These amounts were multiplied by the number of wells required. 100 µl/well of master reaction mix was added to each well and the plate was briefly placed on a plate shaker to allow the reagents to mix well with the samples and then the plate was incubated at room temperature for 20 minutes. The fluorescence was then measured (excitation 535 nm/emission 587 nm) using a Flexstation III microplate reader. A standard curve was run on each plate. The fluorescence intensity (RFU) was converted to a glycerol concentration using the gradient of the linear standard curve:

$$[\text{Glycerol}]\ (\mu M) = (RFU_{sample} - RFU_{no\ cell\ control}) / \text{gradient of the standard curve}$$

Due to variation in basal glycerol levels between donors, the data was normalised to the amount of glycerol produced under the control conditions after 3 hours.

2.23 Measuring glycerol release in primary human subcutaneous adipose tissue *ex vivo*

To investigate whether observations made in *in vitro* differentiated adipocytes were representative of the effects *ex vivo*, an experiment was designed to stimulate adipose tissue *ex vivo* with AR-C118925XX. To do this, two 1 cm^2 pieces of fresh human subcutaneous abdominal adipose tissue were dissected and washed three times with PBS to remove excess blood and lipid. Attempts were made to avoid large blood vessels and areas of fibrous tissue when selecting tissue pieces. The pieces of tissue were then weighed individually. All the tissue pieces used weighed approximately 500-600 mg. Each piece of tissue was then attached to a hook and suspended within a beaker containing 15 ml of gassed DMEM (pH 7.4) for one hour. The DMEM was gassed with a mixture of 5% CO_2 and 95% air). The DMEM was kept at 37 ^oC by incubating the beakers in a 37 ^oC water bath for the duration of experiment. The contents of each beaker were under constant, but gentle, agitation throughout the experiment. After the first hour had elapsed, baseline samples were taken every 20 minutes for 1 hour. Samples were taken in duplicate (20 µl per sample) and kept on ice. When a sample was taken, equivalent amounts of DMEM were replaced in each beaker to maintain a total volume of 15 ml. At the 1 hour timepoint, 15 µl of AR-C118925XX (final concentration 10 µM) was added to one beaker and 15 µl of vehicle (DMSO) was added to other beaker prior to immediately taking the 1 hour sample. Subsequent samples were taken every 20 minutes for two hours for both conditions. Next at the 3 hour timepoint, isoprenaline (final concentration 1 µM) was added to both beakers and the tissue was left for another hour. The final samples were taken one hour later and then the concentration of glycerol in each of the samples was determined using a glycerol assay kit (Section 2.22). Both the vehicle and antagonist treated samples were normalised to their respective initial baseline values (0 minutes).

2.24 Protein array

Adipocytes secrete a wide range of adipokines that are capable of regulating adipocyte metabolism in an autocrine/paracrine manner, as well as adipokines that can control systemic metabolism (Kim and Moustaid-moussa, 2000). In order to determine whether purinergic signalling may be involved in adipokine secretion, a protein array was conducted. *In vitro* differentiated adipocytes were washed once with PBS and then incubated with 100 µl/well DMEM (no serum or antibiotics) for two hours at 37 ^{o}C in 5% CO_2. Next, 1 µl/well of vehicle (DMSO) or AR-C118925XX (10 µM final concentration) was added to each well and the cells were incubated for a further 30 minutes at 37 ^{o}C in 5% CO_2. Then, 1 µl/well of vehicle or ATP (100 µM final concentration) was added to each well and supernatant samples (75 µl/well) were collected immediately for the 0 hour timepoint by gently pipetting up and down. The samples were placed in a fresh 96-well plate and kept on ice for the duration of the experiment. Subsequent samples were taken in the same manner after 3 hours, 6 hours and 24 hours. All the samples were stored at -80 ^{o}C until required.

A Human Obesity Array Q3, which is a multiplexed sandwich ELISA-based quantitative array platform, that has the capacity to detect 40 human adipokine simultaneously (Figure 2.7), was purchased from RayBiotech. The protein array was performed as per the manufacturer's instructions. In brief, supernatant samples and protein array slides coated with adipokine-specific antibodies (16 identical arrays per slide) were equilibrated to room temperature. All subsequent steps were conducted at room temperature, unless otherwise indicated. Each incubation or wash step was conducted on an orbital shaker. Non-specific binding was blocked by adding 100 µl/well of sample diluent to each well for 30 minutes. The sample diluent was then removed and 100 µl/well of undiluted supernatant samples or cytokine standards were added to each well and the array was incubated at 4 ^{o}C overnight to encourage maximum detection. The following morning, the samples/standards were decanted and each well was washed five times with 1x wash buffer I and twice with 1x wash buffer II (five minutes for each wash). The wash buffer was removed, and the arrays were incubated with 80 µl/well of biotin-labelled detection antibodies for two hours, which should create a sandwich complex if the adipokine was present in the sample. Next, the excess antibodies were removed and again, the arrays were washed five times with wash buffer I and twice with wash buffer II. Next, each well was incubated with Cy3 equivalent dye-conjugated streptavidin (80 µl/well) for one hour while being protected from light. The wells were then washed five times with wash buffer I and twice with wash buffer II. The device holding the array was disassembled and the glass slide containing all 16 arrays was carefully transferred to a slide washer tube filled with 1x wash buffer I for 15 minutes. Wash buffer I was removed and the slide was washed with wash buffer II for five minutes. Finally, the slides were dried and sent back to the manufacturer for analysis. Positive adipokine detection was detected using a laser scanner equipped with a Cy3 wavelength. Each adipokine was arrayed in quadruplet for each sample. The

median fluorescence values were used for adipokine quantification analysis and a heat map was generated by normalising the average adipokine concentrations to the vehicle control.

2.25 Statistical analysis

Data were analysed, including statistical analyses, using Origin Student 2018 software (Origin Lab). Data were expressed as mean ± SEM of experiments performed in duplicate using cells from a minimum of three independent donors. However, in most cases cells from six independent donors were used. Throughout this thesis, *N* refers to the number of biological repeats (independent donors). As primary human cells were used throughout this study, unsurprisingly there was often donor-to-donor variation between absolute values, so values were normalised to their respective vehicle controls to minimise the effects of this variation. Data were assessed for normality using a Shapiro-Wilk test. Normally distributed data were assessed using a paired Student's *t*-test or a repeated measures one-way ANOVA with *post hoc* Tukey test, whereas non-normally distributed data were assessed by paired sample Wilcoxon signed rank test or Friedman ANOVA with *post hoc* Dunn's test.

Each antibody is printed in quadruplicate horizontally												
	1	2	3	4	1	2	3	4	1	2	3	4
A	POS1				POS2				Adiponectin			
B	Adipsin				AgRP				ANGPTL4			
C	BDNF				Chemerin				CRP			
D	Growth Hormone				IFN-gamma				IGFBP-1			
E	IGFBP-2				IGF-1				IL-10			
F	IL-12 p40				IL-12 p70				IL-1 beta			
G	IL-1 ra				IL-6				IL-8			
H	Insulin				Leptin				Lipocalin-2			
I	MSP alpha/beta				Osteoprotegerin				PAI-1			
J	PDGF-BB				Pepsinogen 1				Pepsinogen 2			
K	Procalcitonin				Prolactin				RANTES			
L	RBP4				Resistin				SAA			
M	TGF beta 1				Thrombospondin 1				TNF RI			
N	TNF RII				TNF alpha				VEGF-A			

Figure 2.7 Array map acquired from the Ray Biotech website displaying all 40 adipokines in the array. https://www.raybiotech.com/files/images/Maps/QAH-ADI-3.jpg Last accessed 19.5.18

Chapter 3: Characterisation of the purinergic receptor profile in primary human adipose-derived mesenchymal stromal cells

3.1 Introduction

Adipose tissue is an abundant and easily accessible source of mesenchymal stromal cells (MSCs) in adult humans. MSCs are multipotent plastic-adherent cells that can be isolated from bone marrow and other tissues, including adipose (Dominici *et al.*, 2006). These cells exhibit the ability to differentiate into various cell types, such as adipocytes, osteoblasts, chondrocytes, myocytes and neurons (Ning *et al.*, 2006; Uccelli *et al.*, 2008; Karantalis *et al.*, 2015). In adult adipose tissue, a pool of omnipresent MSCs serve to replace approximately 10% of mature adipocytes annually via adipogenesis (Spalding *et al.*, 2008). Both adipogenesis and hypertrophic mechanisms are important for the expansion of adipose tissue and body buffering of glucose and free fatty acids. Lower rates of adipogenesis are associated with increased visceral obesity, adipocyte hypertrophy and higher fasting blood glucose (Lessard *et al.*, 2014). This suggests that efforts to improve the adipogenic potential of MSCs may oppose metabolically unhealthy phenotypes.

In addition to the physiological function of MSCs *in vivo*, adipose-derived (AD)-MSCs have been clinically evaluated for use in regenerative medicine to repair damaged tissue (Thesleff *et al.*, 2011; Houtgraaf *et al.*, 2012; Jo *et al.*, 2014). The initial results suggest that MSCs exert their beneficial effects by migrating to the site of injury and utilising their regenerative capacity as well as having an immunomodulatory effect at the injury site (Cho *et al.*, 2009; Feisst *et al.*, 2015). Despite some promising results in tissue regeneration studies, MSC senescence and induced inflammation are common drawbacks to therapy (Turinetto *et al.*, 2016; Kim *et al.*, 2017). A greater understanding of how MSCs respond to their environment via cell surface receptors will therefore delineate MSC function.

Signalling via extracellular nucleotides has been implicated in cell migration, proliferation, differentiation and inflammation (Burnstock and Verkhratsky, 2010; Yegutkin, 2014). Receptor-mediated intracellular calcium (Ca^{2+}) signals are known to be important for cellular proliferation and differentiation, and studies have demonstrated stem cell sensitivity to extracellular ATP (Tonelli *et al.*, 2012). However, current work has primarily focused on rodent models and bone marrow-derived MSCs (BM-MSC) or has failed to report the molecular basis of purinergic responses (Ferrari

et al., 2011; Jiang, Hao, *et al.*, 2017). For example, extracellular nucleotides elicit reorganisation of actin filaments and cell migration in 3T3-L1 mouse adipocyte precursors (Omatsu-Kanbe *et al.*, 2006), and ATP promotes adipogenic and osteogenic differentiation in BM-MSCs (Ciciarello *et al.*, 2013). This Chapter focuses on the molecular identity of the P2 receptors in human AD-MSCs utilised to respond to physiologically relevant extracellular nucleotides, while also attempting to identify the downstream cellular functions mediated by P2 receptors in these cells.

3.2 Purinergic receptor expression profile in primary human MSCs as determined by analysis of mRNA transcripts

In order to fully identify the profile of purinergic receptors expressed in primary human AD-MSCs, mRNA transcript expression was explored using a mixture of non-quantitative and quantitative PCR.

Although this project primarily focuses on the role of P2 purinergic receptors, for completeness the expression of P1 receptors was confirmed using non-quantitative PCR. Analysis of mRNA transcripts revealed that primary human MSCs expressed all of the known P1 receptor subtypes: A1, A2A, A2B and A3 (*N*=3; Figure 3.1A). P1 receptors are activated by adenosine, which is a product of ATP and ADP cell surface hydrolysis (Yegutkin, 2014), thus it is important to be mindful that exogenous application of nucleotides may indirectly activate P1 receptors, as well as P2 receptors.

For characterising the profile of P2 receptors quantitative PCR was employed, therefore the data are expressed as average cycle threshold (C_T) values (Table 3.1) or relative $1/\Delta C_T$ values (Figure 3.1B) where the expression has been normalised to the expression of an endogenous reference gene, RPLP0, and inverted for analytical ease. Genes with a C_T value of below 35 (or $1/\Delta C_T > 0.06$) were deemed to be present, whereas genes that were not detected or had C_T values of above 35 (or $1/\Delta C_T < 0.06$) were considered absent. Using these principles, it was determined that P2X1, P2X4, P2X5, P2X6, P2X7, $P2Y_1$, $P2Y_2$, $P2Y_4$ and $P2Y_6$ receptors were all present in MSCs, whereas P2X2 and P2X3 receptors were not expressed in any of the donors tested (*N*=6; Figure 3.1B; Table 3.1). It was also identified that there was some heterogeneity in the expression of $P2Y_{11}$, $P2Y_{12}$, $P2Y_{13}$, and $P2Y_{14}$ receptors, as some donors had C_T values above 35 for these receptors (Table 3.1). In the case of the $P2Y_{12}$ receptor, only two of the six donors tested had C_T values below 35, with even these donors displaying average C_T values of 34.1 and 34.7 respectively, which indicates very low expression. On average the $1/\Delta C_T$ for $P2Y_{12}$ was below the cut-off of 0.06.

Table 3.1 Average cycle threshold (C_T) values for each P2 receptor in primary human adipose-derived mesenchymal stromal cells per donor (*N*=6). Only genes with C_T values of <35 were considered present. ND indicates no amplification detected within 40 PCR cycles.

Gene	C_T values					
	Donor 1	Donor 2	Donor 3	Donor 4	Donor 5	Donor 6
P2RX1	31.3	31.5	30.1	31.1	29.7	28.9
P2RX2	ND	ND	ND	ND	ND	ND
P2RX3	37.3	38.5	37.5	ND	36.9	38.6
P2RX4	24.8	26.7	26.5	25.3	26.4	25.2
P2RX5	24.3	31.2	32.5	31.2	33.2	31.4
P2RX6	31.8	32.4	33.5	34.4	33.8	31.6
P2RX7	31.6	32.2	31.3	32.3	31.0	31.4
P2RY1	28.9	30.0	31.9	28.7	28.7	26.0
P2RY2	32.7	31.7	33.0	31.3	31.0	29.9
P2RY4	30.6	31.8	32.8	30.8	30.3	29.3
P2RY6	31.8	29.8	29.3	30.3	29.0	26.0
P2RY11	35.3	35.3	32.0	32.5	31.7	29.3
P2RY12	35.3	35.6	36.9	35.6	34.1	34.7
P2RY13	35.6	33.5	33.8	34.2	32.8	30.9
P2RY14	33.1	32.4	33.8	35.2	33.9	31.0

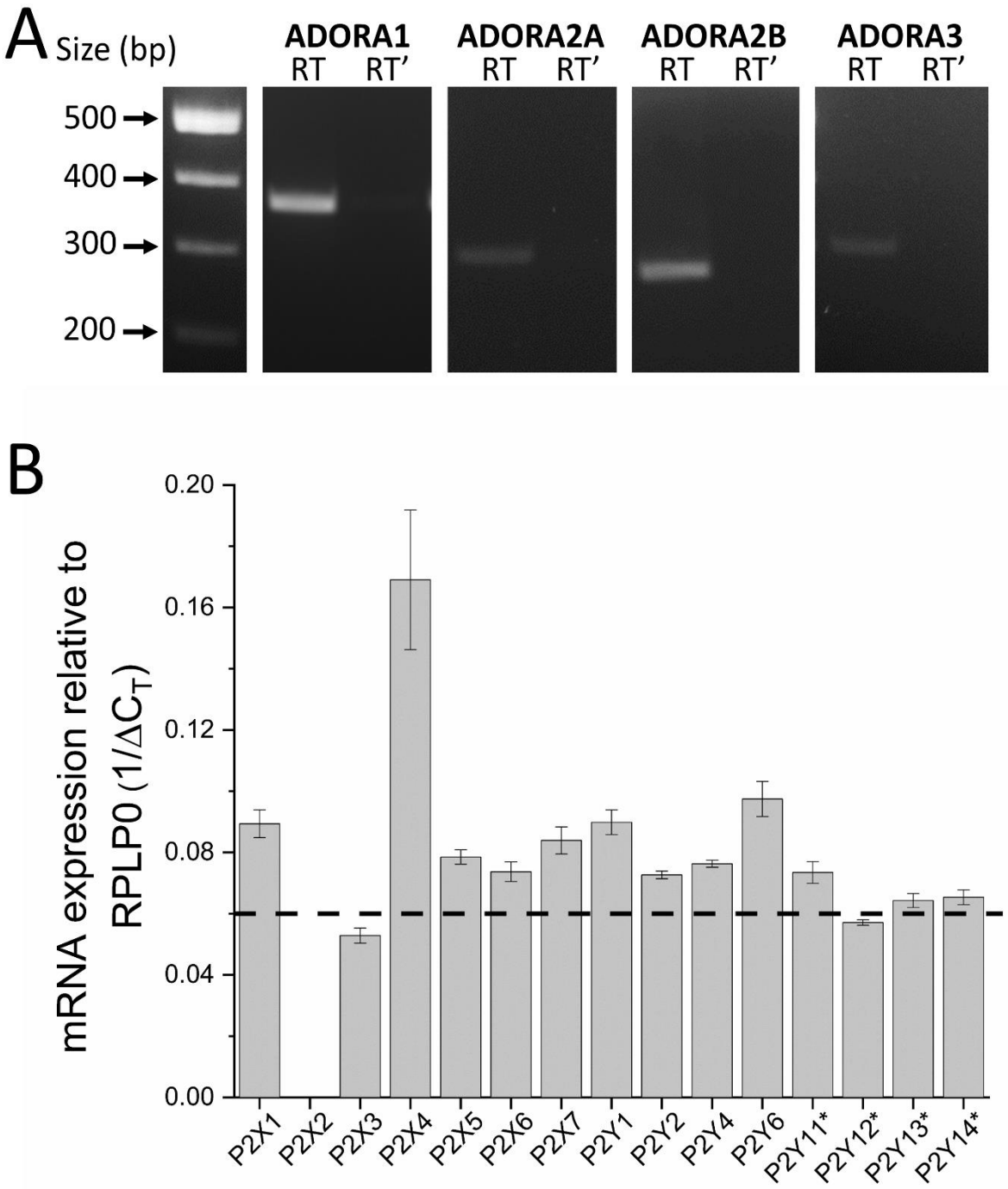

Figure 3.1 Messenger RNA expression profile of purinergic receptors in primary human adipose-derived mesenchymal stromal cells. (A) Non-quantitative RT-PCR analysis of P1 receptor expression showing bands detected for ADORA1 (374 bp), ADORA2A (295 bp), ADORA2B (277 bp) and ADORA3 (302 bp). RT' indicates the no reverse transcriptase control samples. Results are representative of the data for three independent donors. (B) Quantitative real time PCR analysis of the P2 receptor expression profile. Cycle threshold (C_T) values have been normalised to the expression of an endogenous reference gene, RPLP0. The dashed line represents the C_T cut-off, where receptors that had an average $1/\Delta C_T$ value of below 0.06 are classified as not expressed (*N*=6). * indicate variability in expression (above and below the threshold) between donors.

3.3 Protein expression profile of P2 purinergic receptors in MSCs

The protein level expression of the P2 receptors consistently detected at the mRNA level (Section 3.2) were readily confirmed using immunocytochemistry. Immunofluorescence for P2X1, P2X4, P2X5, P2X7, $P2Y_1$, $P2Y_2$, $P2Y_4$ and $P2Y_6$ receptors were all consistently detected in three independent donors. Representative images of the positive staining observed for each receptor are shown in Figure 3.2A. In addition, the heterogeneity in mRNA transcript detection for both the $P2Y_{11}$ and $P2Y_{13}$ receptors was mirrored at the protein level, with positive protein staining detected in only a proportion of the three donors tested (Figure 3.2B). In the donor that $P2Y_{13}$ was detected, the staining is particularly faint, but positive immunofluorescence above the no primary antibody control was evident under the microscope. No staining was observed for the $P2Y_{12}$ receptor (*N*=3). Cells were not stained for P2X2, P2X3, P2X6 or $P2Y_{14}$ either due to lack of mRNA expression or lack of available antibody.

Immunocytochemistry not only confirmed that the mRNA expression profile (Section 3.2) was representative of the protein level expression of P2 receptors in primary human AD-MSCs, it also provided an insight into the cellular localisation and distribution of each receptor. However, it is difficult to definitively distinguish whether the receptors are located intracellularly or on the cell surface, because the cells were permeabilised for staining, cells were not counterstained with a membrane marker and the cells themselves are very flat. Overall, the immunocytochemical staining (Figure 3.2) revealed that P2X4, P2X5, $P2Y_4$ and $P2Y_6$ receptors, as well as $P2Y_{11}$ and $P2Y_{13}$ receptors when they were detected, were distributed relatively uniformly throughout the cytoplasm/cell membrane, although the staining was very faint for P2X5 and $P2Y_{13}$ receptors. The immunofluorescence for $P2Y_2$ receptors displayed a punctate distribution throughout the cell, whereas P2X1 receptors appeared to be particularly pronounced at the edges of the cell. Although immunofluorescence for both P2X7 and $P2Y_1$ receptors was detected throughout the cells, unusually the staining appeared to be particularly intense in the nuclear/perinuclear regions. It was not possible to compare the relative protein expression level of each receptor due to differing antibody affinities.

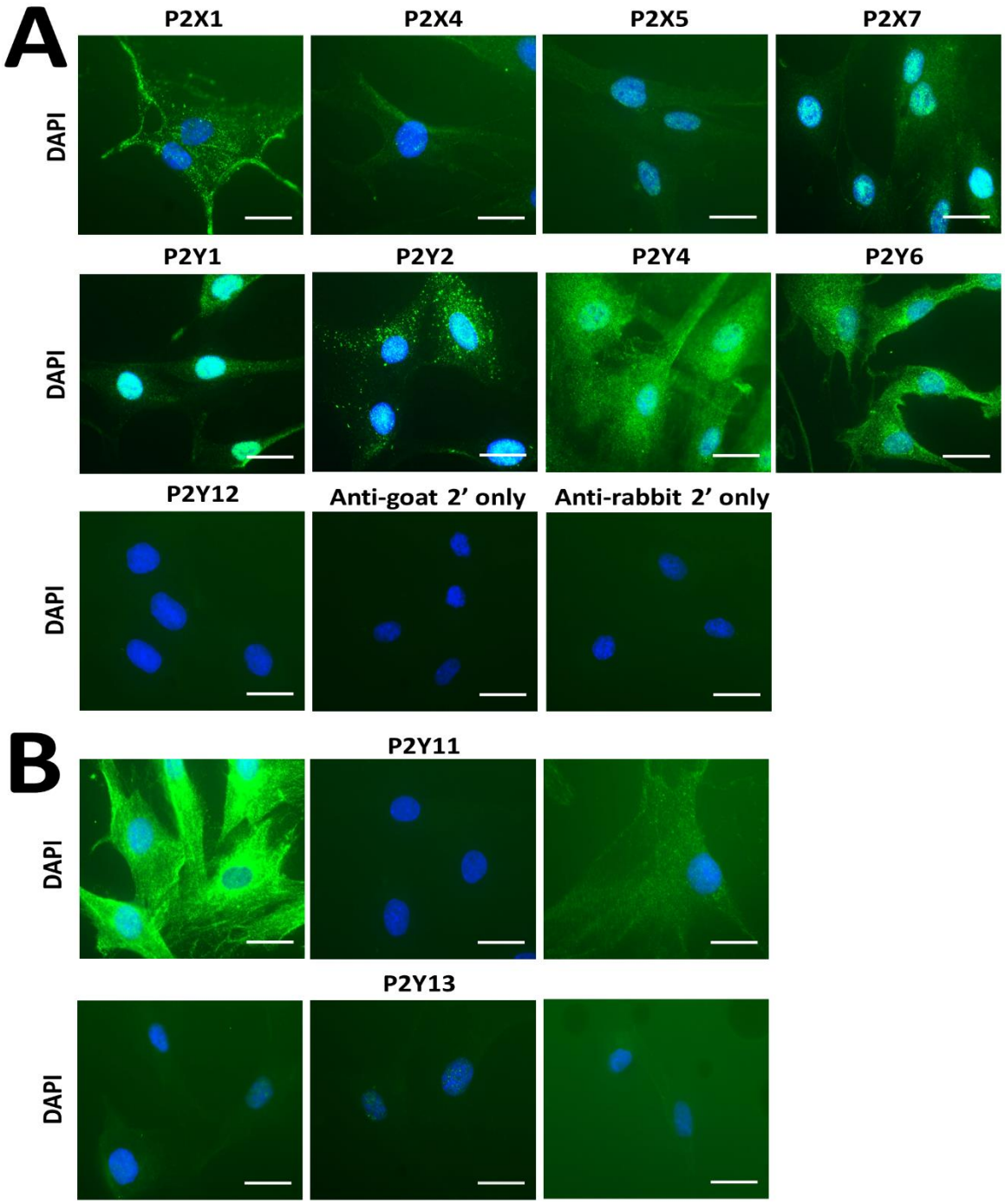

Figure 3.2 Analysis of P2X and P2Y receptor immunofluorescence in human adipose-derived mesenchymal stromal cells (MSCs). (A) Immunocytochemical staining for P2X1, P2X4, P2X5, P2X7, $P2Y_1$, $P2Y_2$, $P2Y_4$, $P2Y_6$ and $P2Y_{12}$ receptors. Images presented are representative of cells from three independent donors. (B) Immunocytochemical staining for $P2Y_{11}$ and $P2Y_{13}$ receptors showing heterogeneity between cells extracted from three independent donors. Images were taken with a 63x objective on a Zeiss AxioPlan 2ie epifluorescent microscope of permeabilised MSCs labelled with primary antibodies against receptor targets and visualized with an Alexa Fluor 488-conjugated secondary antibody (green). Cells are counterstained with DAPI to visualise nuclei (blue). The exposure and camera settings remained consistent across all the images taken for each donor. Images are representative of at least ten fields of view for cells from three independent donors. Scale bar represents 30 µm.

3.4 Nucleotide-evoked calcium responses in primary human MSCs

Activation of P2 receptors leads to a transient elevation of intracellular Ca^{2+} levels due to direct Ca^{2+} entry from the extracellular space via ionotropic P2X receptors or release of Ca^{2+} from intracellular stores due to activation of metabotropic P2Y receptors. To ascertain whether the P2 receptors expressed in MSCs were functionally active, exogenous nucleotides were applied and real-time changes in intracellular Ca^{2+} levels were monitored.

In the presence of extracellular Ca^{2+}, exogenous application of ATP, ADP and UTP elicited concentration-dependent increases in intracellular Ca^{2+} in all donors tested (*N*=7-9) (Table 3.2; Figure 3.3A,C,E). Nucleotides had a rank order of potency ADP (EC_{50} 1.25±1.0μM) > ATP (EC_{50} 2.2±1.1μM) = UTP (EC_{50} 3.2±2.8μM). All three nucleotides elicited an initial rapid response that decayed to approximately 25% above baseline intracellular Ca^{2+} levels within the recording period of 250 seconds (Figure 3.3B,D,F). Between nucleotides the magnitude of responses and net Ca^{2+} movement were comparable at maximal concentrations (Table 3.2), though responses to ADP decayed significantly faster than responses elicited by ATP or UTP ($p<0.05$, *N*=7-9; Table 3.2).

Table 3.2 Characteristics of the calcium responses evoked by maximal concentrations of nucleotides (30 μM) in primary human adipose-derived mesenchymal stromal cells. Mean ± SEM.

Nucleotide	Peak magnitude (F ratio)	Net calcium movement (area under the curve)	Decay time, τ (s)	EC_{50} (μM)
ATP (*N*=9)	0.422 ± 0.05	53.7 ± 5.9	73.4 ± 230.2	2.24 ± 1.1
ADP (*N*=8)	0.385 ± 0.05	39.6 ± 6.2	35.3 ± 6.3[a]	1.25 ± 1.0
UTP (*N*=7)	0.334 ± 0.06	41.9 ± 7.8	122.4 ± 4447.5	3.24 ± 2.8

[a] Decay time was significantly faster for the ADP-evoked calcium response *vs* ATP (*p<0.005*) and UTP (*p<0.005*) as determined by Kruskal-Wallis ANOVA with *post hoc* analysis using a Dunn's Test.

Changes in intracellular calcium were not detected in response to application of 30 μM UDP or below (*N*=6) (Figure 3.4A,B). However, responses were consistently detected in the presence of 300 μM UDP (*N*=6), with some donors displaying very small responses (peak F_{ratio} 0.12 ± 0.04, *N*=3 of 6 donors) with the addition of 100 μM UDP. Agonist concentrations of above 30 μM UDP are not likely to be representative of physiological nucleotide concentrations, so it is unlikely that these results show true activation of UDP-sensitive receptors. It is possible that these responses are instead due to ATP, ADP or UTP contamination of the UDP used, which was the manufacturer states is >96% pure. Similarly, exogenous application of UDP-glucose elicited a Ca^{2+} response in some donors (*N*=3 of 9 donors) (Figure 3.4C,D), but these responses were only evident at very high agonist

concentrations of greater than 100 µM (*N*=1) or 300 µM (*N*=2). No response was detected for 30 µM UDP-glucose (*N*=9). Furthermore, six out of a nine donors tested did not display a response to UDP-glucose at any concentration tested (up to 600 µM) (data excluded from Figure 3.4C,D). The EC_{50} values for both UDP and UDP-glucose could not be accurately calculated as the 'responses' had not plateaued within the range of concentrations tested.

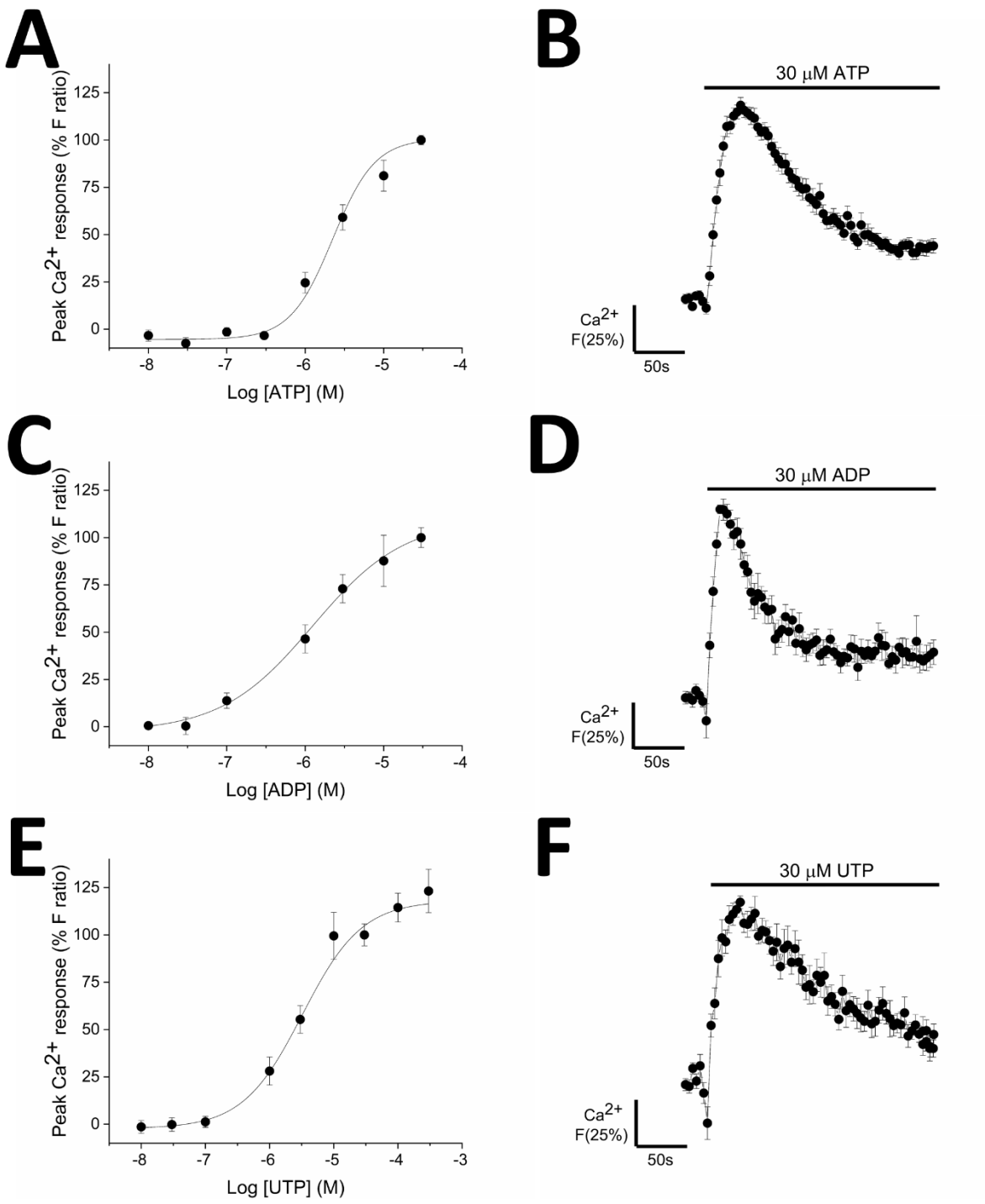

Figure 3.3. ATP, ADP and UTP elicited intracellular calcium responses in human adipose-derived mesenchymal stromal cells. Concentration response curves for the peak magnitude of intracellular Ca^{2+} responses elicited by (A) ATP (*N*=9), (C) ADP (*N*=8) and (E) UTP (*N*=7). Ca^{2+} responses were normalized to the maximal response observed in the majority of donors, which was the response to 30 μM ATP, ADP and UTP respectively. Averaged time-resolved intracellular Ca^{2+} responses elicited by (B) 30 μM ATP (*N*=9), (D) 30 μM ADP (*N*=8) and (E) 30 μM UTP (*N*=7). Traces were normalised to the maximal response within a donor, and averaged across donors. Data points are mean ± SEM.

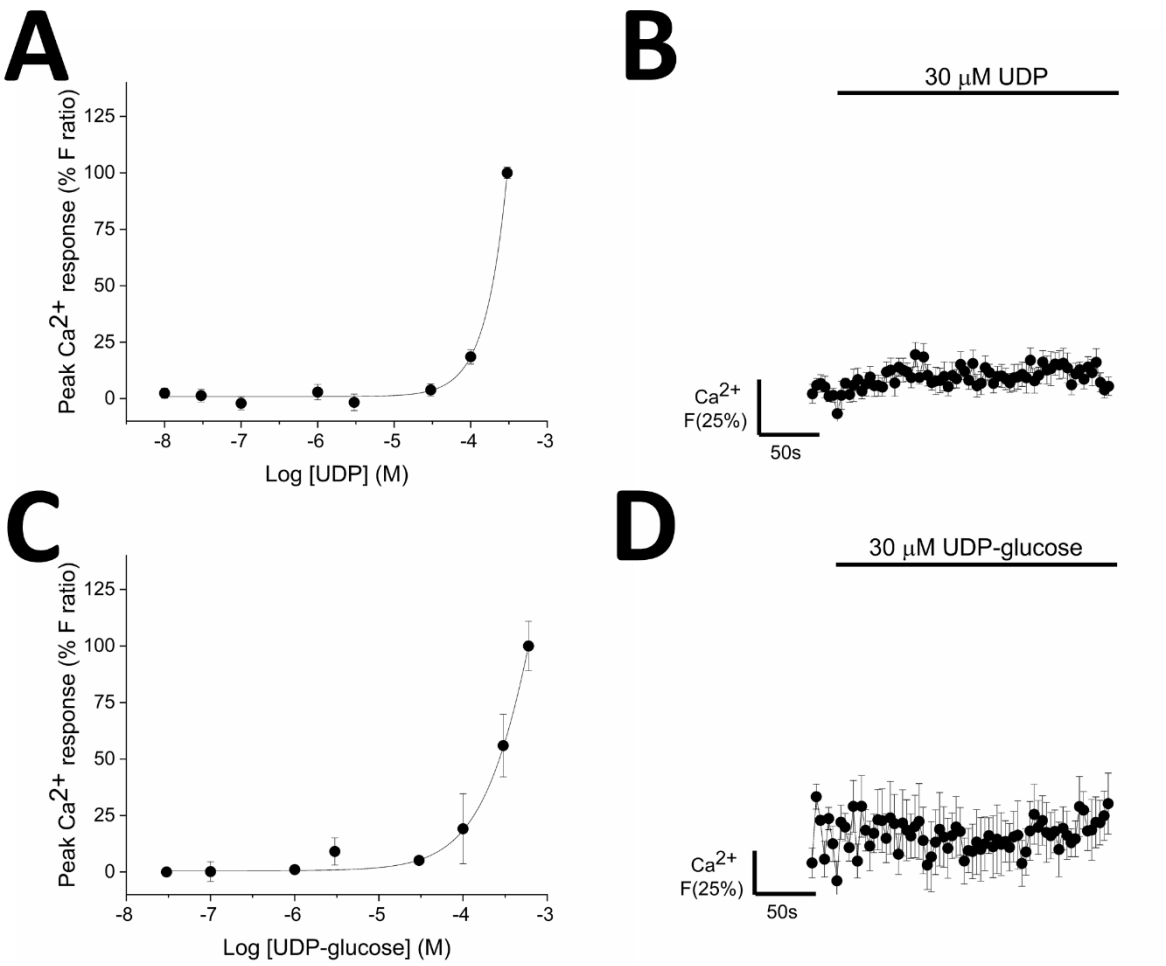

Figure 3.4 Physiological concentrations of UDP and UDP-glucose did not elicit consist intracellular calcium responses in human adipose-derived mesenchymal stromal cells. Concentration response curves for the magnitude of intracellular Ca^{2+} responses elicited by (A) UDP (*N*=6) and (C) UDP-glucose (*N*=3). Ca^{2+} responses were normalized to the maximal response observed in the majority of donors, which was the response to 300 μM UDP and 600 μM UDP-glucose respectively. Average data for donors that responded to nucleotide stimulation are shown. Data for donors that did not respond to nucleotide stimulation were excluded. Averaged time-resolved intracellular Ca^{2+} responses elicited by (B) 30 μM UDP (*N*=6) and (D) 30 μM UDP-glucose (*N*=3). Traces were normalised to the maximal response within a donor, and averaged across donors. Data points are mean ± SEM.

3.5 Nucleotide-evoked calcium responses persisted despite multiple passaging of primary human MSCs

During this study, MSCs were passaged up to eight times for experimental use, so it was important to establish whether the nucleotide-evoked calcium responses remained consistent irrespective of passage number. To do this, the response to super-maximal concentrations of ATP, ADP and UTP were monitored across eight passages. This revealed that all three nucleotides evoked functional calcium responses from passage 1 to 8 and although there were slight fluctuations in the magnitude of the response across the different passages (Figure 3.5), these changes were not significant, suggesting the purinergic response in these cells is not altered by passage.

3.6 Nucleotide-evoked calcium responses persisted, but were significantly diminished in the absence of extracellular calcium

The responses elicited by maximal ATP, ADP and UTP concentrations persisted, but were decreased by 82.7±3.5% (*N*=6, p<0.001), 92.0±4.2% (*N*=3, p<0.05) and 81.8±4.0% (*N*=4, p<0.001; Figure 3.6B,D,F; Table 3.3) respectively following removal of Ca^{2+} from the extracellular solution with 2 mM EGTA. This suggests the magnitude of the nucleotide responses are heavily reliant on extracellular calcium, which may indicate P2X receptor activity. However, the fact that there are concentration-dependent responses to ATP, ADP and UTP (*N*=6; Figure 3.6A,C,E) in the absence of extracellular calcium suggests that nucleotide-evoked calcium responses are at least in part mediated by metabotropic P2Y receptors. If the response was entirely mediated by P2X ion channels, then you would expect the response to be abolished in the absence of extracellular calcium. The small transient increase in intracellular calcium observed with higher concentrations of each agonist must be due to release of calcium from intracellular stores. It is possible that the reduced magnitude of the nucleotide-evoked responses may be due to partial emptying of the intracellular stores due to cellular efforts to maintain intracellular calcium homeostasis in the absence of extracellular calcium.

The nucleotide-evoked responses also all returned to baseline Ca^{2+} levels within the sampling period when extracellular Ca^{2+} was removed, instead of remaining approximately 25% above baseline. In addition, in the absence of extracellular calcium, ATP-evoked responses decayed faster (τ 31.2±5.4 seconds without Ca^{2+} vs τ 55.0±3.6 seconds with Ca^{2+}, p<0.005; *N*=6). Although the responses to ADP and UTP displayed the same trend, the respective alterations in the decay times were not statistically significant (Table 3.3). Also, despite the appearance of a rightward shift in the concentration response curves, particularly for ADP (Figure 3.6C), variation between donors meant

that the EC_{50} values were not significantly altered for any of the nucleotides when extracellular calcium was removed (Table 3.3).

Table 3.3 Changes in the magnitude, decay kinetics and potency of nucleotide-evoked calcium responses in primary human adipose-derived mesenchymal stromal cells in the presence and absence of extracellular calcium, $[Ca^{2+}]_e$. Mean ± SEM.

Nucleotide	Peak magnitude (F ratio)[a]		Decay time, τ (s)		EC_{50} (μM)	
	+ $[Ca^{2+}]_e$	- $[Ca^{2+}]_e$	+ $[Ca^{2+}]_e$	- $[Ca^{2+}]_e$	+ $[Ca^{2+}]_e$	- $[Ca^{2+}]_e$
30 μM ATP (*N*=6)	0.68±0.1	0.11±0.03	55.0±3.6	31.2±5.4[b]	0.9±0.4	5.7±2.6
100 μM ADP (*N*=3)	1.08±0.1	0.17 ± 0.1	30.3±1.4	22.5±72.4	0.8±0.6	28.3±62.1
30 μM UTP (*N*=4)	0.57±0.04	0.12±0.02	59.7±27	41.2±5.9	8.3±1.4	7.8±2.8

[a] The peak magnitude was significantly decreased when extracellular calcium is removed for ATP ($p<0.001$), ADP ($p<0.05$) and UTP ($p<0.001$) as determined by paired T tests or Wilcoxon signed rank test.

[b] The decay time was significantly faster for the ATP-evoked calcium response in the absence of extracellular calcium ($p<0.005$) as determined by a paired T test.

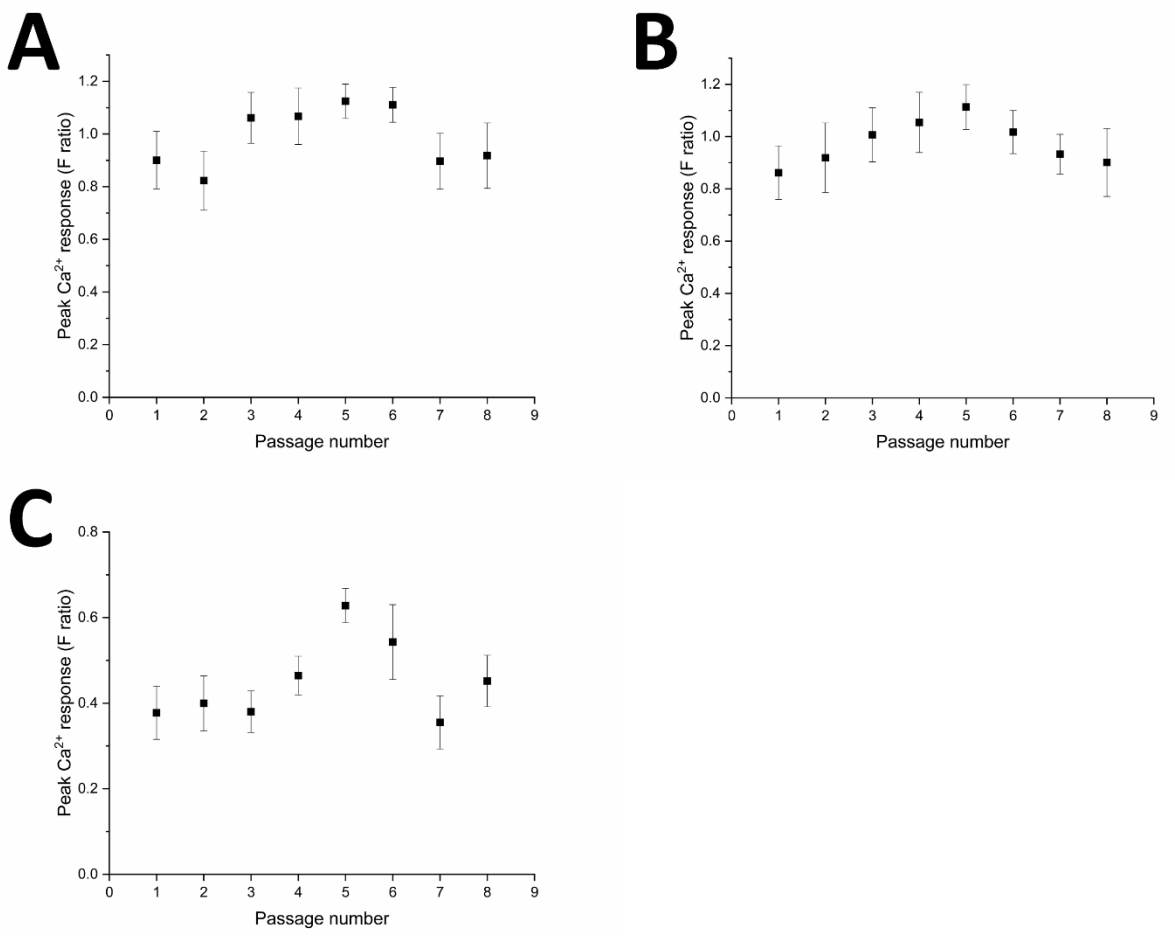

Figure 3.5 Effect of multiple passage of primary human mesenchymal stromal cells on the magnitude of the response to (A) 100 µM ATP, (B) 100 µM ADP and (C) 100 µM UTP.

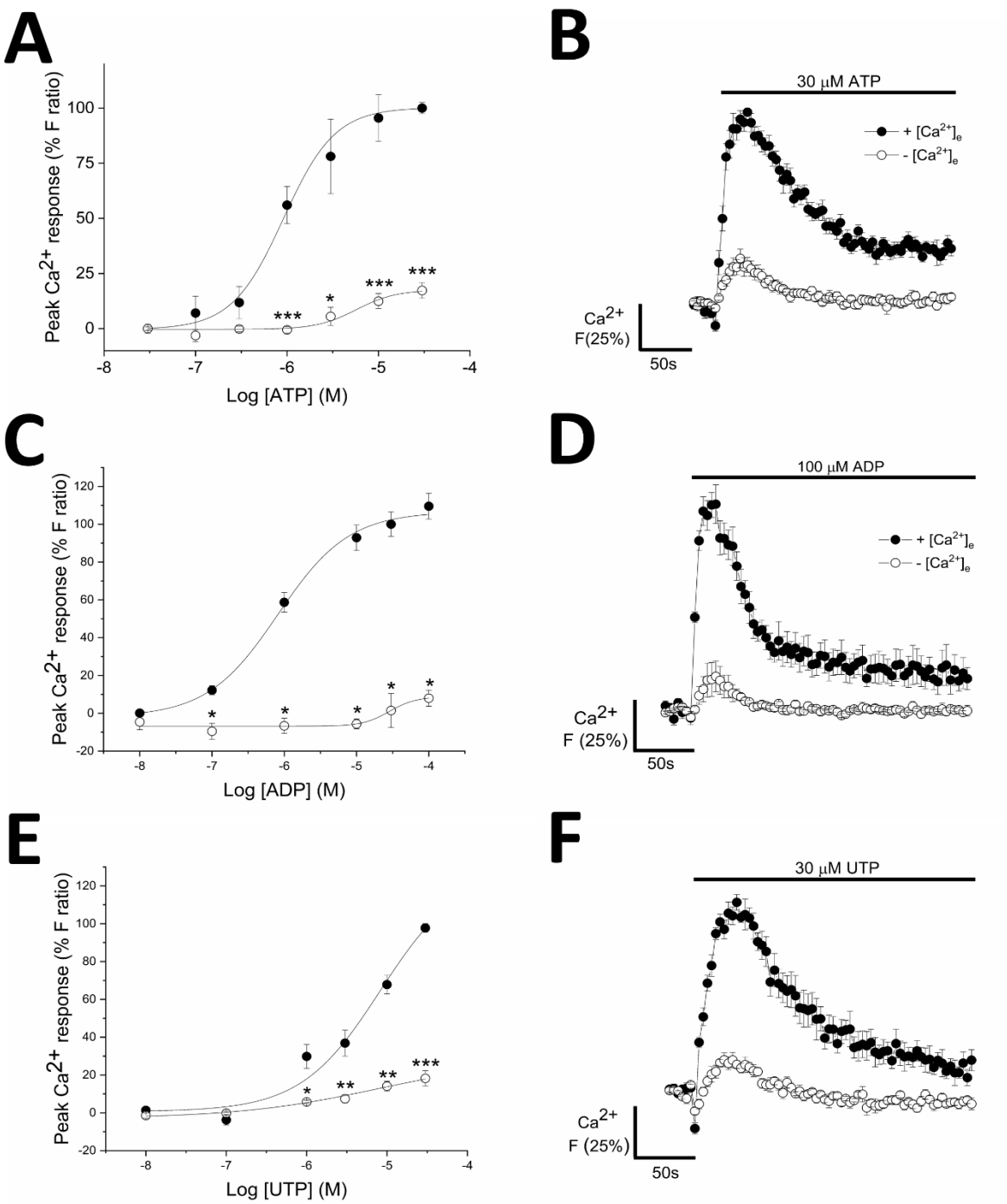

Figure 3.6 Removing extracellular calcium leads to a reduction in the magnitude of the response evoked by ATP, ADP and UTP in primary human adipose-derived mesenchymal stromal cells. Concentration-response curves in the presence (*closed circles*) and absence (*open circles*) of 1.5 mM extracellular calcium for (A) ATP (*N*=6), (C) ADP (*N*=3) and (E) UTP (*N*=4). All responses were normalised to the response to maximal concentrations of each agonist (30 μM ATP and UTP and 100 μM ADP respectively) in the presence of extracellular calcium. Average time-resolved traces showing the response elicited by (B) 30 μM ATP (*N*=6), (C) 100 μM ADP (*N*=3) and (D) 30 μM UTP (*N*=4) in the presence (*closed circles*) and absence (*open circles*) of extracellular calcium (*N*=6). Data points represent the mean ± SEM. **p*<0.05, ***p*<0.01, ****p*<0.001 versus response to equivalent agonist concentration in the presence of extracellular calcium.

3.7 Nucleotide-evoked calcium responses in primary human MSCs are mediated by phospholipase C activation and downstream release of calcium from the intracellular store

Inhibition of phospholipase C (PLC), which is part of the downstream signalling pathway instigated by G_q-coupled P2Y receptor activation, with 10 μM U73122 abolished the responses to ATP (*N*=6), ADP (*N*=4) and UTP (*N*=3) (Figure 3.7). These results suggest a predominance of metabotropic P2Y receptor involvement in the nucleotide-evoked Ca^{2+} responses in primary human AD-MSCs, with little or no contribution from P2X receptors. This hypothesis is supported by the fact that the nucleotide-evoked calcium responses persist in the absence of extracellular calcium (Section 3.6). Furthermore, depleting the endoplasmic reticulum Ca^{2+} stores by inhibiting sarco-endoplasmic reticulum Ca^{2+}-ATPases (SERCA) with 5 μM thapsigargin abolishes the response to ATP (*N*=6) (Figure 3.8). Together these data suggest that the nucleotide responses in human AD-MSCs are mediated primarily by metabotropic P2Y receptors. These results may also indicate that the diminished nucleotide-evoked calcium responses observed in the absence of extracellular calcium (Figure 3.6) are likely to be due to partial emptying of the stores and/or the lack of store-operated calcium entry post-P2Y receptor activation, rather than P2X involvement. However, as the reductions in the magnitudes of the responses are so pronounced (Figure 3.6), it is also possible that P2X receptors act downstream of P2Y receptors and they may be responsible for potentiating the nucleotide-evoked responses in the presence of extracellular calcium.

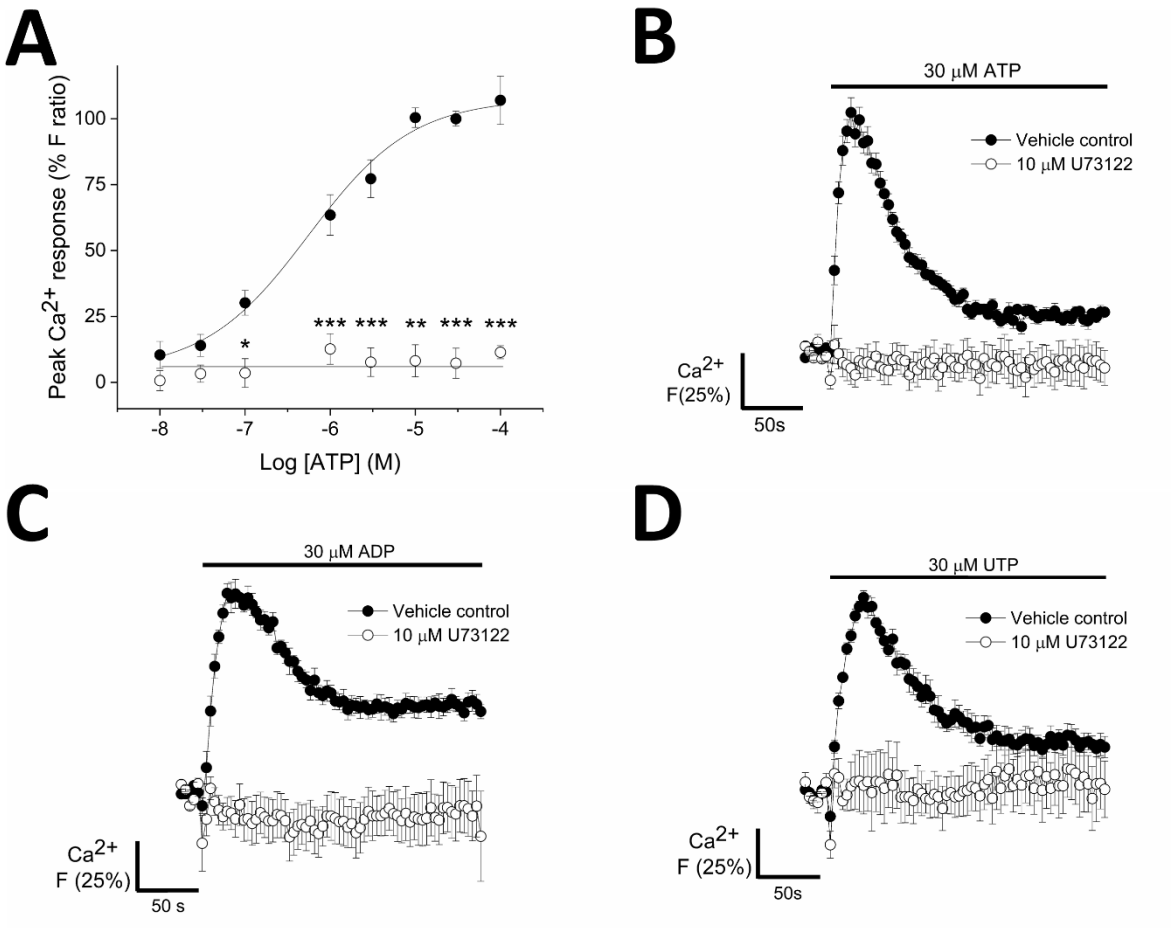

Figure 3.7 Inhibition of phospholipase C with 10 µM U73122 abolishes the response to ATP, 30 µM ADP and 30 µM UTP in primary human adipose-derived mesenchymal stromal cells. (A) ATP concentration response curve in the presence (*open circles*) and the absence (*closed circles*) of 10 µM U73122. Responses were normalised to the response to 30 µM ATP in the absence of U73122. Average time-resolved traces showing the response elicited by (B) 30 µM ATP (*N*=6), (C) 30 µM ADP (*N*=4) and (D) 30 µM UTP (*N*=4) in the presence (*open circles*) and absence (*closed circles*) of 10 µM U73122. Data points represent the mean ± SEM. **p*<0.05, ***p*<0.01, ****p*<0.001 versus response to equivalent concentrations of ATP in the absence of U73122.

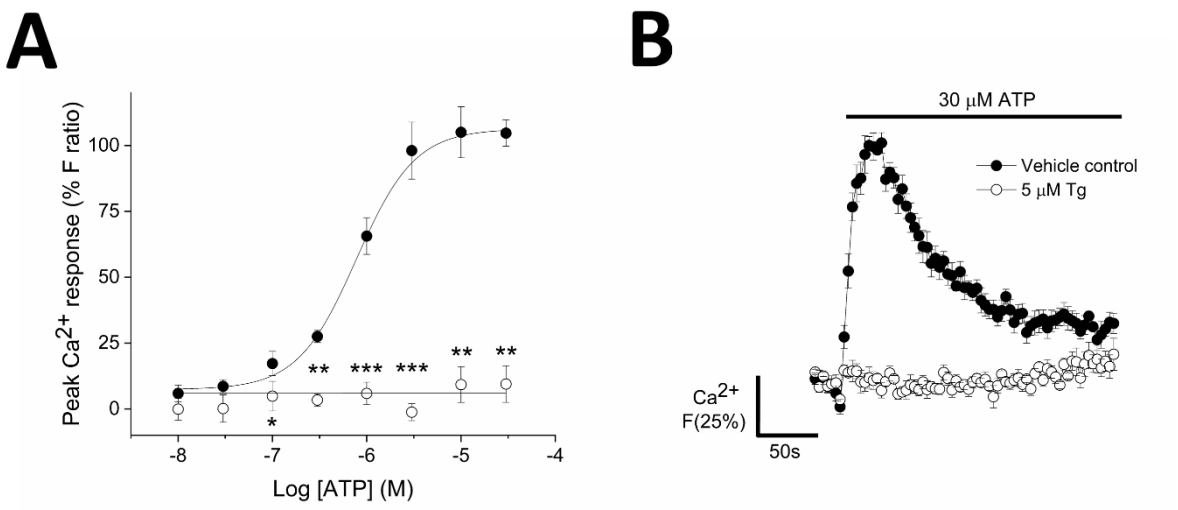

Figure 3.8 Inhibition of sarcoendoplasmic reticulum calcium transport ATPase (SERCA) with 5 μM thapsigargin completely abolishes the response to ATP in primary human MSCs (*N*=6). (A) ATP dose-response curve under control conditions (*closed circles*) or following sarco-endoplasmic reticulum Ca^{2+}-ATPases inhibition induced emptying of the intracellular Ca^{2+} stores with 5μM thapsigargin (*open circles*) (*N*=6). (B) Average time-resolved traces for the response to 30 μM ATP under control conditions (*closed circles*) and following thapsigargin pre-treatment (*open circles*) (*N*=6). Data points represent mean ± SEM. **p*<0.05, ***p*<0.01, ****p*<0.001 versus the response to equivalent concentrations of ATP in absence of thapsigargin.

3.8 P2X receptors are not involved in the ATP-evoked calcium responses in primary human MSCs

Almost all known purinergic receptor subtypes respond to ATP, either directly or via ATP breakdown products, such as ADP or adenosine, however certain subtypes, P2X1-7, $P2Y_2$ and $P2Y_{11}$ receptors, display greater affinity for ATP above other physiological agonists (Burnstock, 2007). All of the known P2X receptor subtypes, excluding P2X2 and P2X3 receptors, were detected in primary human AD-MSCs (Section 3.3 and 3.4). However, only three of the five detected P2X receptors are known to commonly form functional receptors in humans: P2X1, P2X4 and P2X7 receptors. Current evidence suggests both P2X5 and P2X6 receptors are non-functional in humans (Torres *et al.*, 1999; Ormond, 2006; Kotnis *et al.*, 2010). In addition, the response to the P2X1 receptor rapidly desensitises, so it is unlikely to be detected with the equipment used in this study. This narrows the possible P2X receptor candidates to just P2X4 and P2X7 receptors. MSCs were preincubated with selective antagonists for the P2X4 receptor (PSB12062) or the P2X7 receptor (A438079) to see whether either receptor had any effect on the response to ATP. It is important to note that super-maximal concentrations of ATP were used, as P2X receptors, particularly P2X7 receptors, typically require much higher concentrations of ATP to be activated (Gorini *et al.*, 2013), so the agonist concentrations have been adjusted accordingly to facilitate P2X receptor activation. Despite elevating the concentration of agonist, both antagonists failed to significantly alter the response to ATP in these cells (*N*=6; Figure 3.9A-D, Table 3.4), suggesting that neither receptor is involved in the ATP-evoked calcium response. The lack of functional evidence of P2X4 and P2X7 receptor involvement in the response to ATP is in agreement with the evidence put forward in Sections 3.6 and 3.7, which strongly suggests a predominance of metabotropic P2Y receptors.

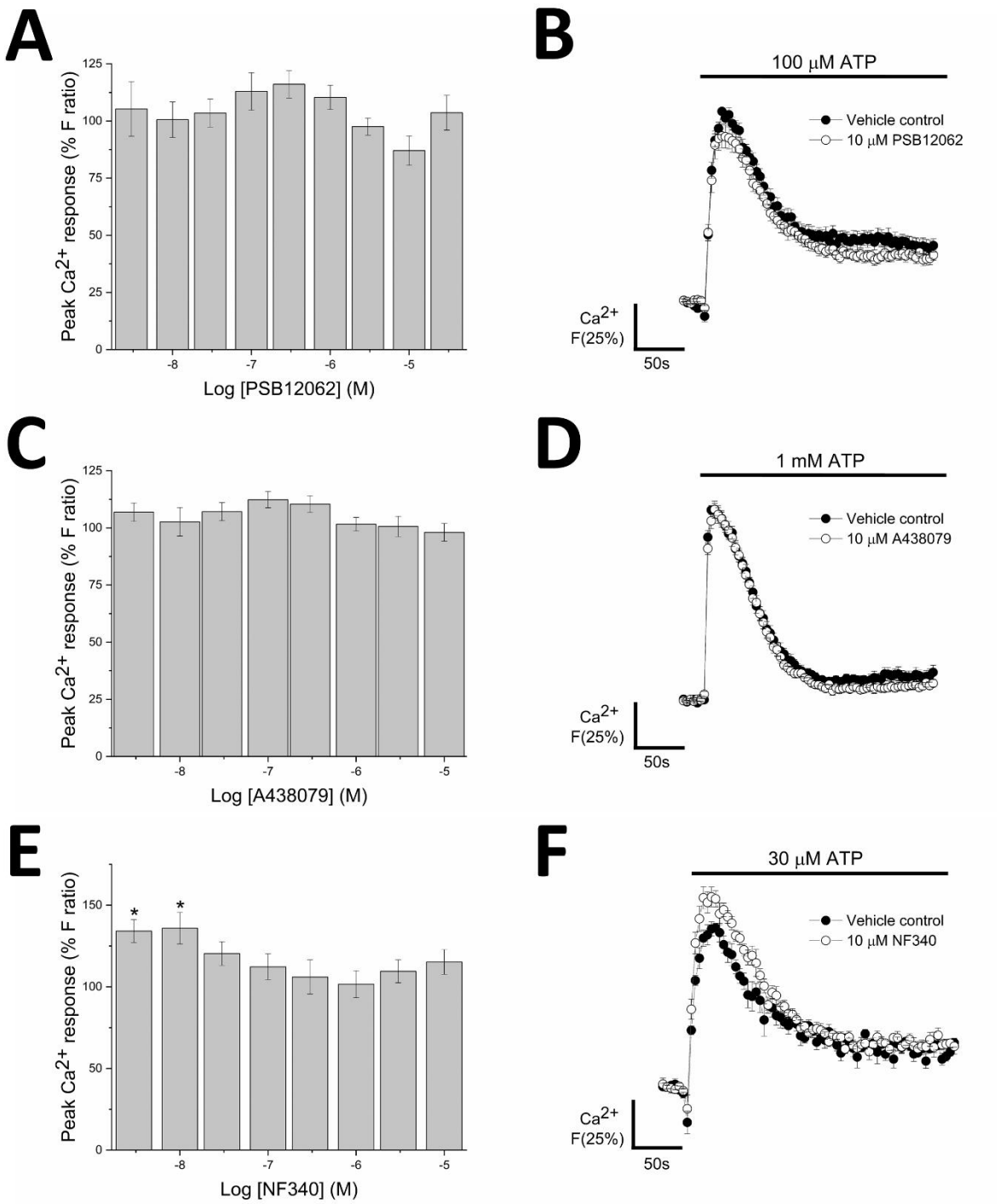

Figure 3.9 Selective antagonism of P2X4, P2X7 and $P2Y_{11}$ receptors had no inhibitory effect on the ATP-evoked calcium response in primary human mesenchymal stromal cells (*N*=6). (A) The response to 100 μM ATP antagonised with increasing concentrations of the selective P2X4 receptor antagonist, PSB12062. (C) The response to 1 mM ATP antagonised with increasing concentrations of the selective P2X7 receptor antagonist, A438079. (E) The response to 30 μM ATP antagonised with increasing concentrations of the selective $P2Y_{11}$ receptor antagonist, NF340. Time-resolved traces showing the response to ATP in the presence (*open circles*) and absence (*closed circles*) of (B) 10 μM PSB12062, (D) 10 μM A438079 or (F) 10 μM NF340. All data points are normalised to their respective peak agonist response in the presence of vehicle only. Data points are expressed as mean ± SEM. * p<0.05 versus the agonist response in the presence of vehicle only.

3.9 ATP and UTP-evoked calcium responses are mediated by $P2Y_2$ receptors in primary human MSCs

In addition to P2X receptors, $P2Y_2$ and $P2Y_{11}$ receptors also display a preference for ATP, so selective antagonists for both receptors were utilised to identify whether either of these receptors were involved in the ATP-evoked Ca^{2+} responses in AD-MSCs. The response to maximal and EC_{50} concentrations of ATP was not inhibited by selective antagonism of $P2Y_{11}$ using NF340 (*N*=6; Figure 3.9E,F; Table 3.4). Although, oddly very low concentrations of NF340 (≤10 nM) caused significant potentiation of the response to ATP. It is unclear what the reason for this may be. Antagonism of other P2Y receptors that display lower affinities for ATP, such as $P2Y_1$ (Figure 3.12A,B), $P2Y_{12}$ and $P2Y_{13}$ receptors (Table 3.4), also failed to have an inhibitory effect on the response to ATP (*N*=6). However, the response to ATP was significantly and dose-dependently inhibited in the presence of a $P2Y_2$ receptor selective antagonist, AR-C118925XX (Figure 3.10A,B). It caused concentration-dependent inhibition of the peak response to ATP (IC_{50} 1.1±0.8μM, *N*=7), reaching a plateau inhibition of 73.0±8.5% on average in the presence of 10 μM antagonist (*N*=7; Figure 3.10A,B). Net elevation in intracellular Ca^{2+} in response to ATP, as calculated by the area under the curve, was inhibited by 81.5±3.3% with maximal concentrations of AR-C118925XX (*N*=5). Although AR-C118925XX had an inhibitory effect on the ATP response in all donors tested, there was some variation between donors. In three of the seven donors tested, the response to ATP was abolished in the presence of 3 μM antagonist, although on average there appears to be a residual response of approximately 20% of the response in the presence of vehicle only. Furthermore, AR-C118925XX abolished UTP-evoked responses with the same potency as the ATP response (IC_{50} 1.6±0.6μM, *N*=6) (Figure 3.10C,D). Together with the observation that ATP and UTP are equipotent agonists in MSCs (Section 3.4), these data strongly suggest that the ATP and UTP responses are mediated primarily by $P2Y_2$ receptor activation.

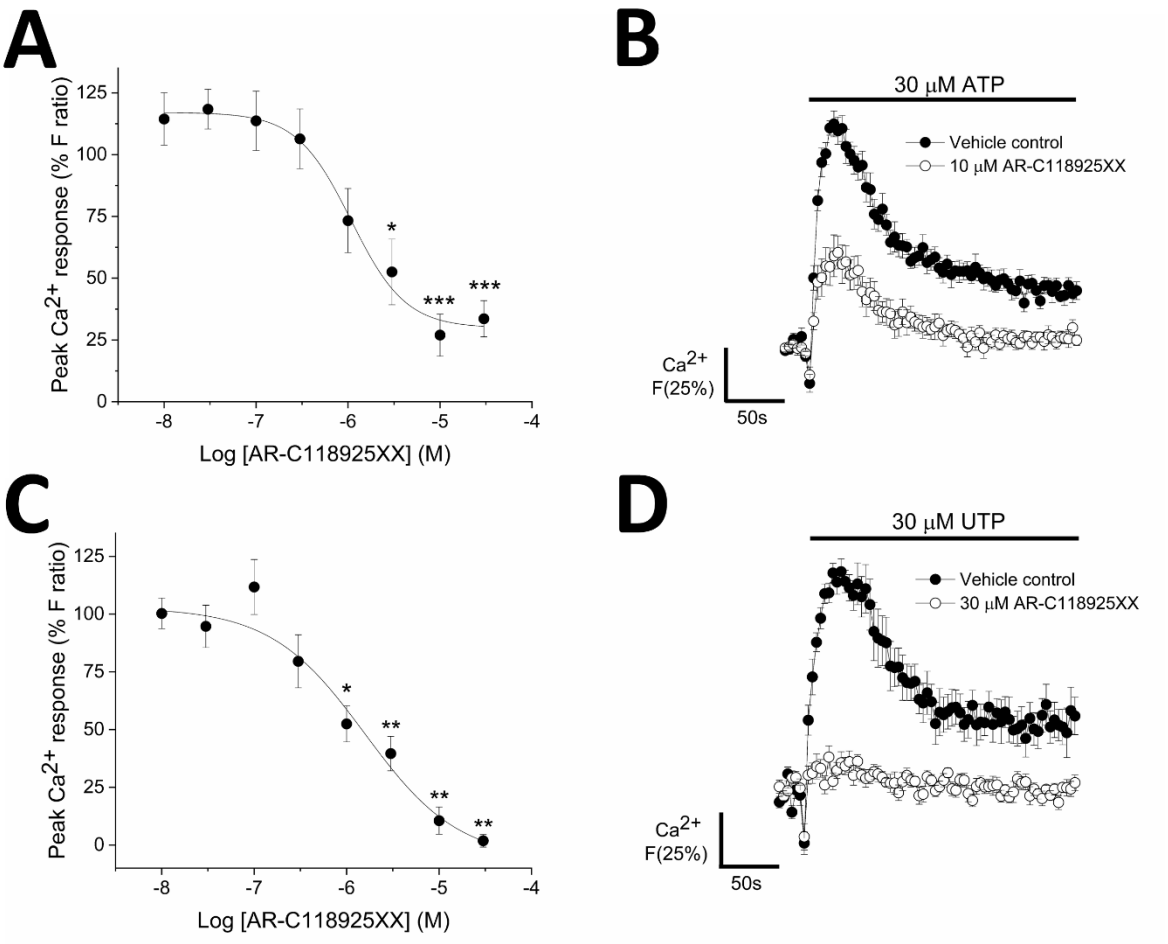

Figure 3.10 Selective antagonism of the $P2Y_2$ receptor with AR-C118925XX has an inhibitory effect on the response to ATP and abolishes the response to UTP in primary human mesenchymal stromal cells. AR-C118925XX inhibition response curves for the response to (A) 30 μM ATP (*N*=7) and (C) 30 μM UTP (*N*=6). (B) Time-resolved traces showing the response to ATP in the presence (*open circles*) and absence (*closed circles*) of 10 μM AR-C118925XX (*N*=7). (D) Time-resolved traces showing the response to UTP in the presence (*open circles*) and absence (*closed circles*) of 30 μM AR-C118925XX (*N*=6). All data points are normalised to their respective agonist responses in the presence of vehicle control. Data points are expressed as mean ± SEM. * $p<0.05$, ** $p<0.005$, *** $p<0.001$ versus the agonist response in the presence of vehicle only.

Table 3.4 The effect of P2 subtype selective antagonism on the nucleotide-evoked calcium responses in primary human adipose-derived mesenchymal stromal cells.

The number of independent donor cells used (*N* number) is indicated within round brackets in the maximum inhibition and IC_{50} columns.

Selective antagonist	Receptor target	Nucleotide [concentration, µM]	Antagonist range, µM	Maximum inhibition (%)[a] [antagonist concentration, µM]	IC_{50}, µM[a]
PSB-12062	P2X4	ATP [100]	0.003 – 30	*NS*	-
A438079	P2X7	ATP [1000]	0.003 – 10	*NS*	-
MRS2500	$P2Y_1$	ATP [3]	1	*NS*	-
		ATP [30]	0.0001 – 1	*NS*	-
		ADP [1]	1	*NS*	-
		ADP [30]	0.0001 – 1	*NS*	-
AR-C118925XX	$P2Y_2$	ATP [30]	0.003 – 30	73.0 ± 8.5 [10] (7)	1.1 ± 0.8 (7)
				81.5 ± 3.3 [10] (5)	2.9 ± 1.1 (5)
		ADP [30]	0.003 - 30	18.2 ± 6.6 [30] (6)	0.64 ± 0.4 (6)
				53.9 ± 5.1 [30] (6)	9.6 ± 1.6 (6)
		UTP [30]	0.003 - 30	100 [30] (6)	1.6 ± 0.6 (6)
				100 [30] (6)	0.84 ± 0.5 (6)
MRS2578	$P2Y_6$	ADP [30]	0.003 - 10	79.4 ± 9.6 [10] (6)	0.44 ± 0.1 (6)

				166.9 ± 27.3 [10] (6)	0.29 ± 0.1 (6)
NF340	$P2Y_{11}$	ATP [3]	10	*NS*	-
		ATP [30]	0.003 - 10	*NS*	-
		ADP [1]	10	*NS*	-
		ADP [30]	0.003 – 10	*NS*	-
PSB-0739	$P2Y_{12}$	ATP [30]	0.003 – 10	*NS*	-
		ADP [30]	0.003 – 10	*NS*	-
MRS2211	$P2Y_{13}$	ATP [30]	0.003 – 10	*NS*	-
		ADP [30]	0.003 – 3	*NS*	-

[a]IC_{50} values and max % inhibition values were calculated with the peak magnitude values (top) and area under the curve data (bottom) for each agonist/antagonist combination. ns indicates no significant inhibition with any concentration of antagonist tested.

3.10 shRNA-mediated knockdown on $P2Y_2$ receptor expression leads to loss of AR-C118925XX sensitivity in primary human MSCs

In an attempt to confirm the pharmacological findings presented in Section 3.9, $P2Y_2$ receptor expression was knocked down in primary human AD-MSCs using shRNA. This method was able to successfully decrease the mRNA expression of $P2Y_2$ by 45.4±22% (*N*=3; Figure 3.11E). The expression of $P2Y_2$ was decreased in all three donors, however, as indicated by the large standard error of the mean associated with the percentage decrease value, there was variability in the amount of knockdown achieved in cells isolated from different donors, ranging from 15.8% to 88.2% knockdown depending on the donor. This variation in the level of knockdown translated to variation in the effects observed, which made it difficult to observe statistically significance.

Surprisingly, knocking down $P2Y_2$ receptor expression lead to a significant increase in the magnitude (Figure 3.11B) and net movement of calcium (Figure 3.11C) of the response to 30 μM ATP, which directly contradicts the results obtained by pharmacologically inhibiting $P2Y_2$ receptors with AR-C118925XX. However, interestingly the $P2Y_2$ knockdown cells were no longer sensitive to AR-C118925XX, whereas AR-C118925XX was able to decrease the peak and area under the curve of the response to ATP in the scrambled cells. In the time-resolved traces (Figure 3.11A), AR-C118925XX appears to accelerate the decay of the response to ATP in the knockdown cells, but this effect was only observed in the donor with the lowest level of $P2Y_2$ receptor knockdown (15.8% knockdown versus scrambled control), which skewed the data. Thus, when the change in net calcium was quantified this effect was not statistically significant. The lack of sensitivity to AR-C118925XX in the knockdown cells indicates that the increase in the magnitude and net movement of calcium in response to ATP in these cells is not mediated by $P2Y_2$ receptors. Instead, it is likely that the reason that the response to ATP increases when $P2Y_2$ receptor expression is knocked down is that redundancy mechanisms are engaged to preserve the response to ATP in AD-MSCs. Although it is unclear what the molecular basis of this heightened response to ATP is, as mentioned in the previous Section (3.7 and 3.8), there are other receptors which are preferentially activated by ATP (P2X receptors and $P2Y_{11}$), so it is likely that the cells engage these alternative receptors to maintain the response to ATP.

Although there appear to be mechanisms in place to preserve the ATP-evoked calcium response, there does not seem to be the same protection for the UTP response. The response to UTP decreased when $P2Y_2$ receptor expression was knocked down, although this decrease was not statistically significant due to variation between donors in the level of decrease in response magnitude. Again, the donor that showed limited $P2Y_2$ receptor knockdown (15.8%) skewed the data. This donor displayed a very small/no effect on the response to UTP in the knockdown cells

versus the scrambled counterparts, which means the decrease in the response to UTP in the knockdown cells was not statistically significant.

Overall, although these data are difficult to interpret due to the variation between donors and the apparent redundancy mechanisms that activate upon receptor knockdown, the results appear to largely support the pharmacological data as the UTP response was decreased, albeit non-significantly, and the ATP response was no longer sensitive to pharmacological inhibition of $P2Y_2$ receptors.

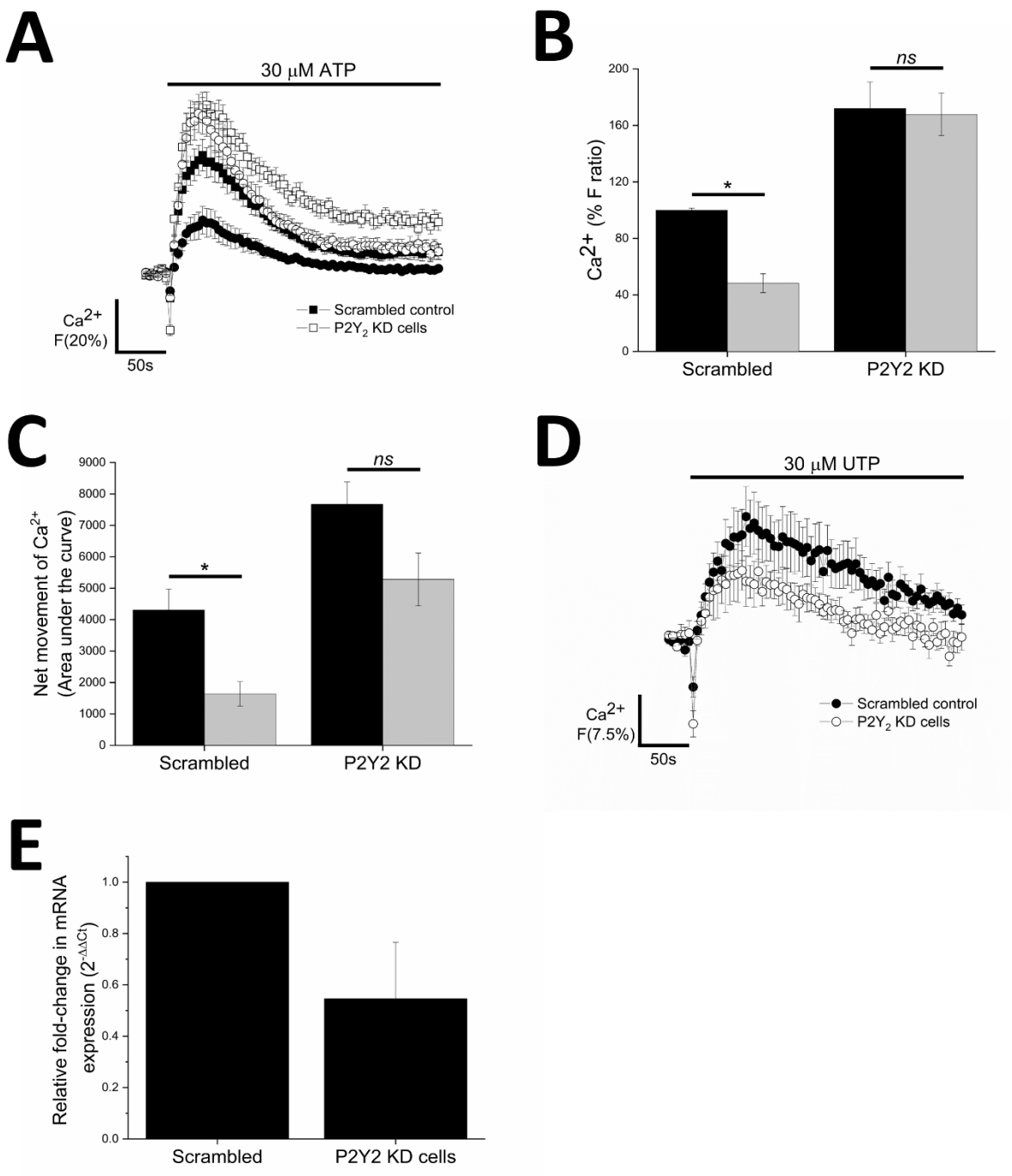

Figure 3.11 shRNA-mediated knockdown of $P2Y_2$ receptors in primary human mesenchymal stromal cells causes a loss of sensitivity to pharmacological inhibition of $P2Y_2$ receptors (*N*=3). (A) Time-resolved traces showing the elevation in intracellular calcium in response to 30 μM ATP in scrambled control cells (*closed symbols*) versus $P2Y_2$ receptor knockdown cells (*open symbols*) in the presence (*circles*) and absence (*squares*) of 10 μM AR-C118925XX. (B) The peak magnitude data and (C) area under the curve data for the ATP-evoked Ca^{2+} response in the presence (*grey bars*) and absence (*black bars*) of 10 μM AR-C118925XX. (D) Response to 30 μM UTP in the scrambled control cells (*closed circles*) and $P2Y_2$ receptor knockdown cells (*open circles*). Responses are normalised to the respective responses to 1 μM ionomycin in each cell type to control for variation in cell number. (E) Relative fold-change in $P2Y_2$ receptor mRNA transcript expression quantified using quantitative PCR. Values were normalised to the expression of an endogenous reference, RPLP0 (*N*=3).

3.11 ADP-evoked calcium responses in primary human MSCs are mediated by $P2Y_6$ receptors

Like ATP, some P2 receptors are preferentially activated by ADP: $P2Y_1$, $P2Y_{12}$ and $P2Y_{13}$ receptors. Of these receptors only $P2Y_1$ receptors are G_q-coupled and therefore expected to directly affect calcium levels via activation of PLC and release of Ca^{2+} from intracellular stores. However, although $P2Y_1$ receptors were detected at the mRNA and protein level, selective antagonism of $P2Y_1$ receptors using MRS2500 had no significant effect on the response to maximal and EC_{50} concentrations of ADP (*N*=6; Figure 3.12B/C; Table 3.4). In addition, application of a selective $P2Y_1$ receptor agonist, MRS2365, did not elicit a detectable change in intracellular calcium levels (*N*=3; Figure 3.12E). Taken together these data strongly suggests that $P2Y_1$ receptors are not functionally active in primary human AD-MSCs under the conditions used in this study. Furthermore, selective antagonism of $P2Y_{12}$ receptors and $P2Y_{13}$ receptors with PSB0739 and MRS2211 respectively had no significant effect on the response to ADP (*N*=6; Figure 3.13). These results are perhaps less surprising, as $P2Y_{12}$ receptors were not detected at the protein level (Figure 3.2) and there was heterogeneity in the expression of $P2Y_{13}$ receptors between donors (Table 3.1), whereas the response to ADP was present in all donors. In addition, $P2Y_{13}$ receptors are G_i-coupled, so activation of $P2Y_{13}$ may instead lead to changes in intracellular cAMP levels that are independent of calcium.

Interestingly, the only subtype-selective antagonists to have an effect were AR-C118925XX and MRS2578 ($P2Y_6$ receptor antagonist). MRS2578 in particular displayed potent antagonism (IC_{50} 437±133nM; *N*=6) of the ADP response and inhibited the peak response elicited by maximal ADP concentrations by >80% (*N*=6; Figure 3.14A,B). Antagonism of $P2Y_6$ receptors also caused the concentration of intracellular Ca^{2+} to drop below baseline Ca^{2+} post agonist stimulation. ADP has been shown to elicit a calcium response in 1321N1 astrocytoma cells over-expressing $P2Y_6$ receptors, but its effects are much less potent than the preferred agonist of $P2Y_6$ receptors, UDP (Communi *et al.*, 1996), so it was surprising that MRS2578 abolished the response to ADP in MSCs, when these cells lack a UDP-elicited Ca^{2+} response (*N*=6; Section 3.4). The ADP-evoked calcium responses were also affected by selective antagonism of $P2Y_2$ receptors with AR-C118925XX. Although, AR-C118925XX (≤10μM) did not affect the magnitude of the response, it altered the decay kinetics which attributed to a decrease in the net movement of Ca^{2+} by 37.3±5.8% (p<0.001, *N*=6) (Figure 3.14C,D). ADP is not the preferred agonist for $P2Y_2$ receptors, so these results may indicate indirect activation of the $P2Y_2$ receptor via ADP-induced release of ATP (Jiang, Mousawi, *et al.*, 2017). Alternatively, this effect may be due to a small amount ATP contamination of the ADP (Mahaut-Smith *et al.*, 2000). The manufacturers state that the ADP utilised in this study is ≥95% pure. 5% ATP contamination would amount to approximately EC_{50} concentrations of ATP being present when a maximal concentration of ADP (30 μM) is applied to the cells.

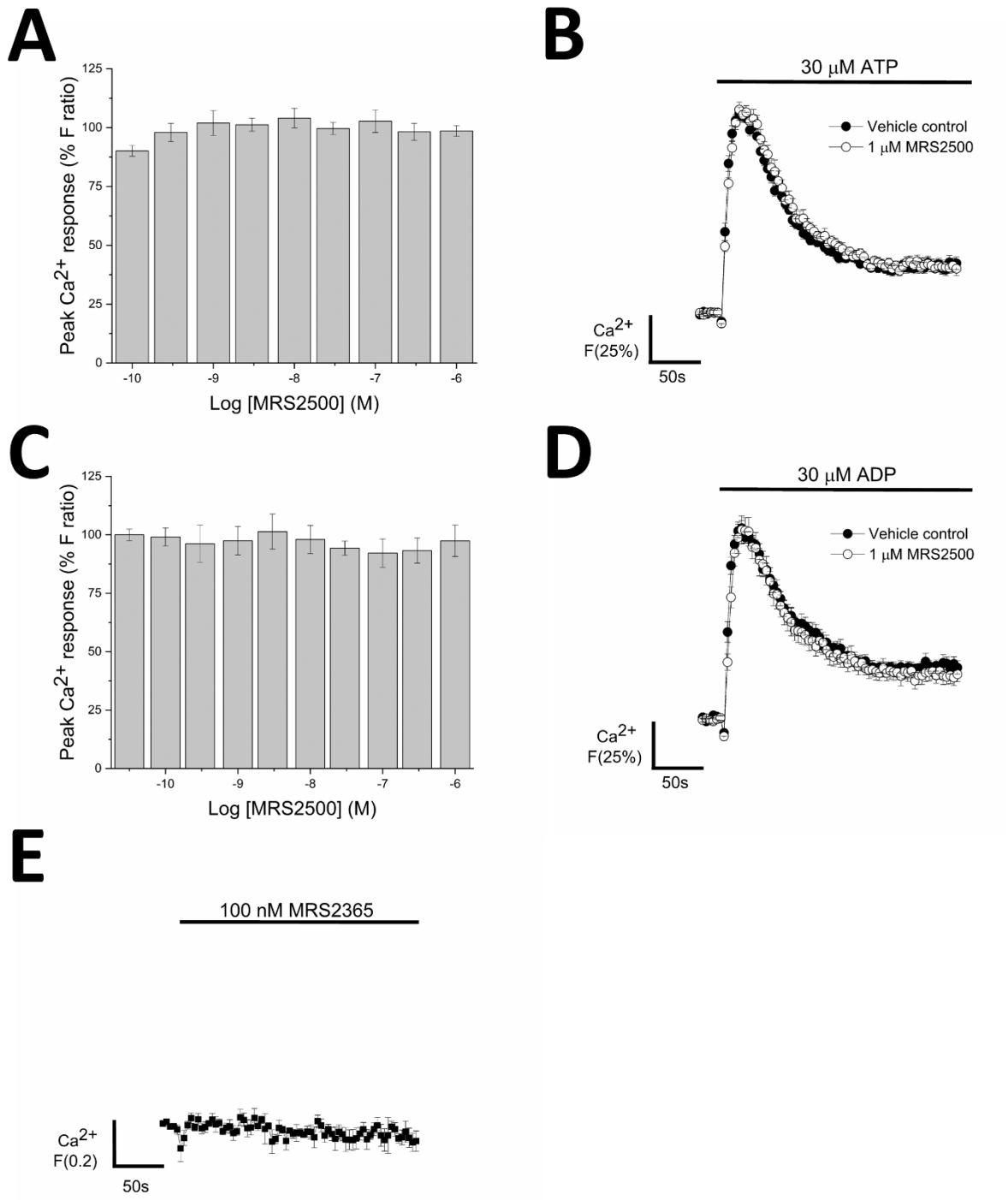

Figure 3.12 $P2Y_1$ receptors do not appear to be functionally active in primary human mesenchymal stromal cells. Effect of increasing concentrations of MRS2500 (a $P2Y_1$ receptor antagonist) on the response to (A) 30 μM ATP (*N*=6) and (C) 30 μM ADP (*N*=6). Time-resolved traces showing the effect of 1 μM MRS2500 on the response to (B) 30 μM ATP (*N*=6) and (D) 30 μM ADP (*N*=6). All data points are normalised to their respective agonist responses in the presence of vehicle control. (E) Non-normalised data showing no detectable change in intracellular calcium upon exogenous application of 100 nM MRS2365 (a $P2Y_1$ receptor agonist) (*N*=3). Data points are expressed as mean ± SEM.

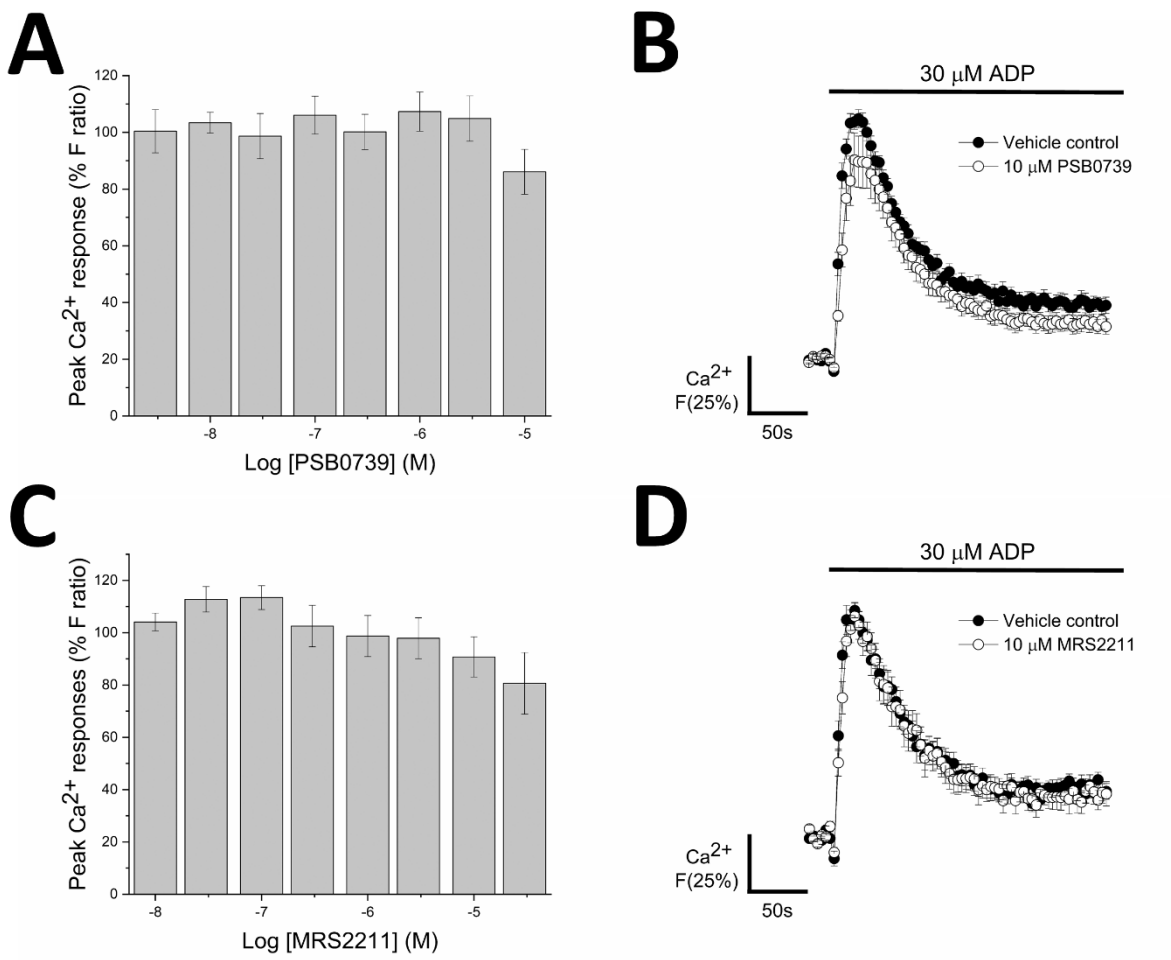

Figure 3.13 The ADP-evoked calcium response in primary human mesenchymal stromal cells is insensitive to selective antagonism of $P2Y_{12}$ and $P2Y_{13}$ receptors with PSB0739 and MRS2211 respectively (*N*=6). Effect of increasing concentrations of (A) PSB0739 (a $P2Y_{12}$ receptor antagonist) or (C) MRS2211 (a $P2Y_{13}$ receptor antagonist) on the response to 30 μM ADP (*N*=6). Time-resolved traces showing the effect of (B) 10 μM PSB0739 or (D) 10 μM MRS2211 on the response to 30 μM ADP (*N*=6). All data points are normalised to their respective agonist responses in the presence of vehicle only. Data points are expressed as mean ± SEM.

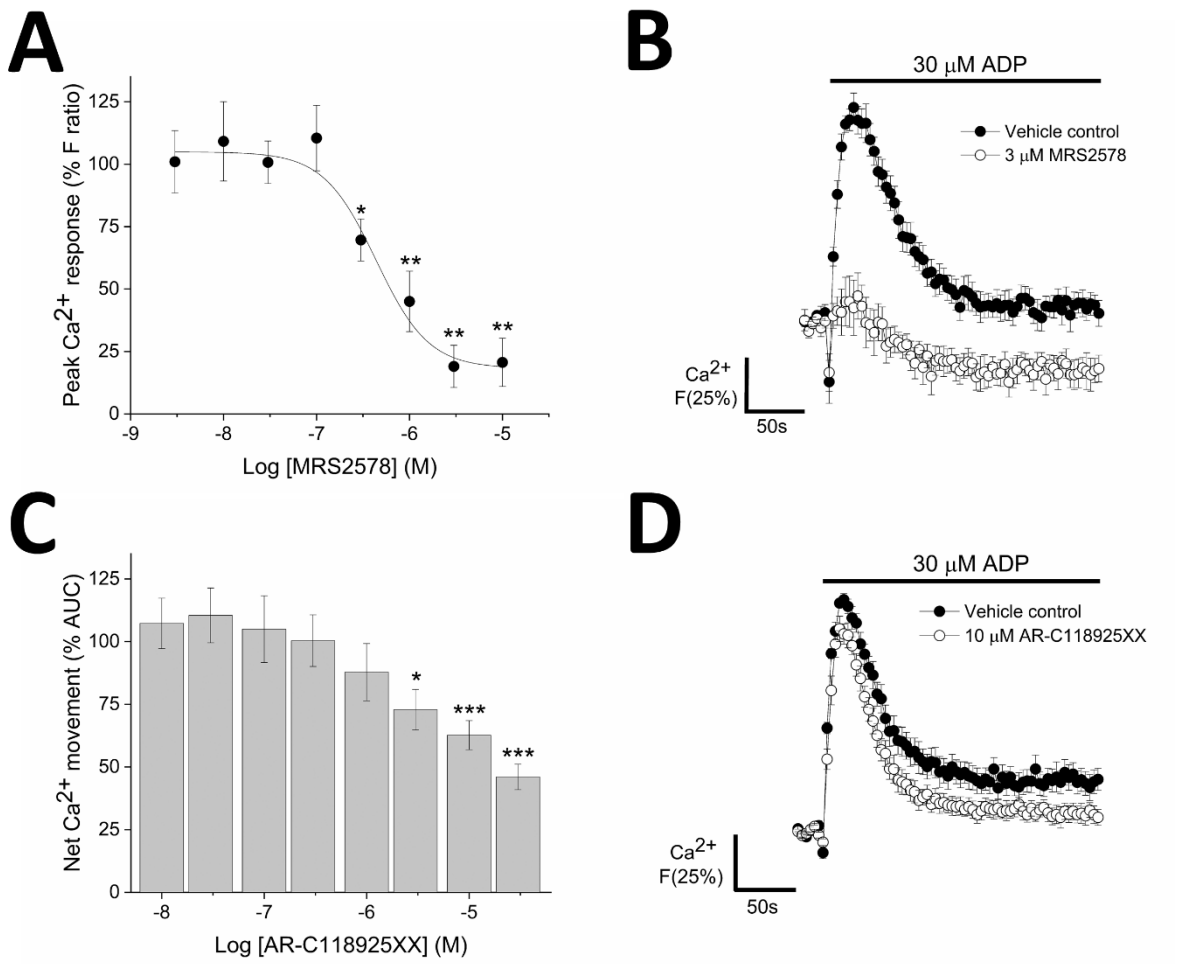

Figure 3.14 Selective antagonism of $P2Y_2$ and $P2Y_6$ cause concentration-dependent inhibition of the ADP-evoked calcium response in primary human mesenchymal stromal cells (*N*=6). (A) Effect of increasing concentrations of MRS2578 (a $P2Y_6$ receptor antagonist) on the peak magnitude of the response to 30 μM ADP (*N*=6). (C) Effect of increasing concentrations of AR-C118925XX (a $P2Y_2$ receptor antagonist) on the net movement of calcium in response to stimulation with 30 μM ADP (*N*=6). Time-resolved traces showing the effect of (B) 3 μM MRS2578 or (D) 10 μM AR-C118925XX on the response to 30 μM ADP (*N*=6). All data points are normalised to their respective agonist responses in the presence of vehicle only. Data points are expressed as mean ± SEM. **p*<0.05, ***p*<0.005, ****p*<0.001 versus the agonist response in the presence of vehicle only.

3.12 Investigating possible downstream functions mediated by purinergic signalling in primary human MSCs

In recent years there has been growing interest in human AD-MSCs, both in research to tackle the growing problem of obesity and for use in regenerative medicine. These cells are able to proliferate to maintain a pool of omnipresent multipotent cells, which are capable of maintaining or expanding adipose tissue via adipogenesis (Spalding *et al.*, 2008). MSCs can migrate to areas where they are required to regenerate adipose tissue post cell death. These homing capabilities can be exploited for use in regenerative medicine, where several chemokines and growth factors have been shown to induce chemotaxis of MSCs to the site of injury and subsequently differentiate to replenish the damaged tissue (Eseonu and De Bari, 2015; Feisst *et al.*, 2015). Although, this technique has been successfully employed in some patients (Feisst *et al.*, 2015), little is known about the molecular mechanisms that underline these functions. Better understanding of these mechanisms could result in a more tailored approach that is able to increase the success rate of these procedures, as well as providing insight into the normal systems that are in place to regenerate and expand adipose tissue, so that we are able to design pharmacological interventions capable of controlling adipose tissue expansion to assist in the fight against the global epidemic of obesity.

Calcium signalling has previously been implicated in the initiation of cell proliferation and migration (Tonelli *et al.*, 2012; Jiang, Mousawi, *et al.*, 2017). As demonstrated earlier in this Chapter, activation of both $P2Y_2$ and $P2Y_6$ receptors in primary human MSCs leads to a transient elevation in intracellular calcium. Thus, these receptors are candidates for mediating calcium signalling pathways controlling cell proliferation and migration within AD-MSCs. The following sections detail the attempts made to identify the functional role of $P2Y_2$ and $P2Y_6$ receptors in primary human MSCs.

3.12.1 Cell proliferation

In comparison to bone marrow derived MSCs, AD-MSCs have an increased capacity to proliferate (Yu *et al.*, 2015), this feature, coupled with the fact that AD-MSCs are more accessible, makes them the ideal resource for regenerative medicine. To test whether purinergic signalling may be involved in cell proliferation, cells were grown in the presence of nucleotides or subtype-selective antagonists and cell proliferation was measured using an MTS assay. As expected the data revealed that MSCs are capable of proliferating *in vitro.* The absorbance steadily increased over the first 72 hours as the cells proliferated and then plateaued due to contact inhibition. However, the results also suggested that a single application of maximal concentrations of ATP, ADP or UTP had no effect on the rate of cell proliferation in primary human AD-MSCs (*N*=3; Figure 3.15). In addition, selective antagonism of $P2Y_2$ and $P2Y_6$ receptors also had no effect on cell proliferation (Figure 3.16). Taken

together these results imply nucleotide-evoked Ca^{2+} responses are not involved in cell proliferation. However, it is important to note that an MTS assay was used to measure cell proliferation in this study and although the reagent is marketed a 'cell proliferation assay kit', the MTS assay is in fact a measure of mitochondrial metabolic activity, which is an indirect indicator of the proportion of viable cells present. In some cases, mitochondrial activity does not accurately reflect proliferation (Wang *et al.*, 2010), so it would be more accurate to draw the conclusion that these results suggest that purinergic signalling does not affect mitochondrial metabolic activity in primary human AD-MSCs. Additional experiments are necessary conclusively determine whether purinergic signalling is involved in MSC proliferation.

3.12.2 Chemotaxis

Chemotaxis of MSCs facilitate normal tissue morphogenesis, homeostasis and repair. Previous studies suggest that regulation of adult stem cell migration is mediated by Ca^{2+} signalling pathways (Jiang, Mousawi, *et al.*, 2017). To investigate whether P2 receptor-mediated changes in intracellular Ca^{2+} are implicated in inducing/enhancing MSC migration, a transwell assay was performed. MSCs migrated towards 10% FBS, a known chemotactic agent (Figure 3.17), however exogenous ATP, at all concentrations tested, had no significant effect on MSC migration. It is unclear what caused the slight dip in the fluorescence after approximately one hour for the cells in the presence of ATP, because the fluorescence would be expected to progressively increase as more cells travel through the PET membrane towards the chemotactic agents. A dip suggests a decrease in the number of cells in the bottom chamber, which may suggest the cells were migrating back into the upper chamber against the ATP gradient or possibly that there was some cell death. Although the MSCs appear to display a slightly reduced capacity to migrate in the presence of ATP (due to this dip), this reduction was not statistically significant and the fact that the effect doesn't demonstrate any concentration-dependence, suggests that this is likely to be artefactual. These results suggest MSCs do not migrate towards ATP, which suggests ATP-evoked calcium responses do not initiate cell migration.

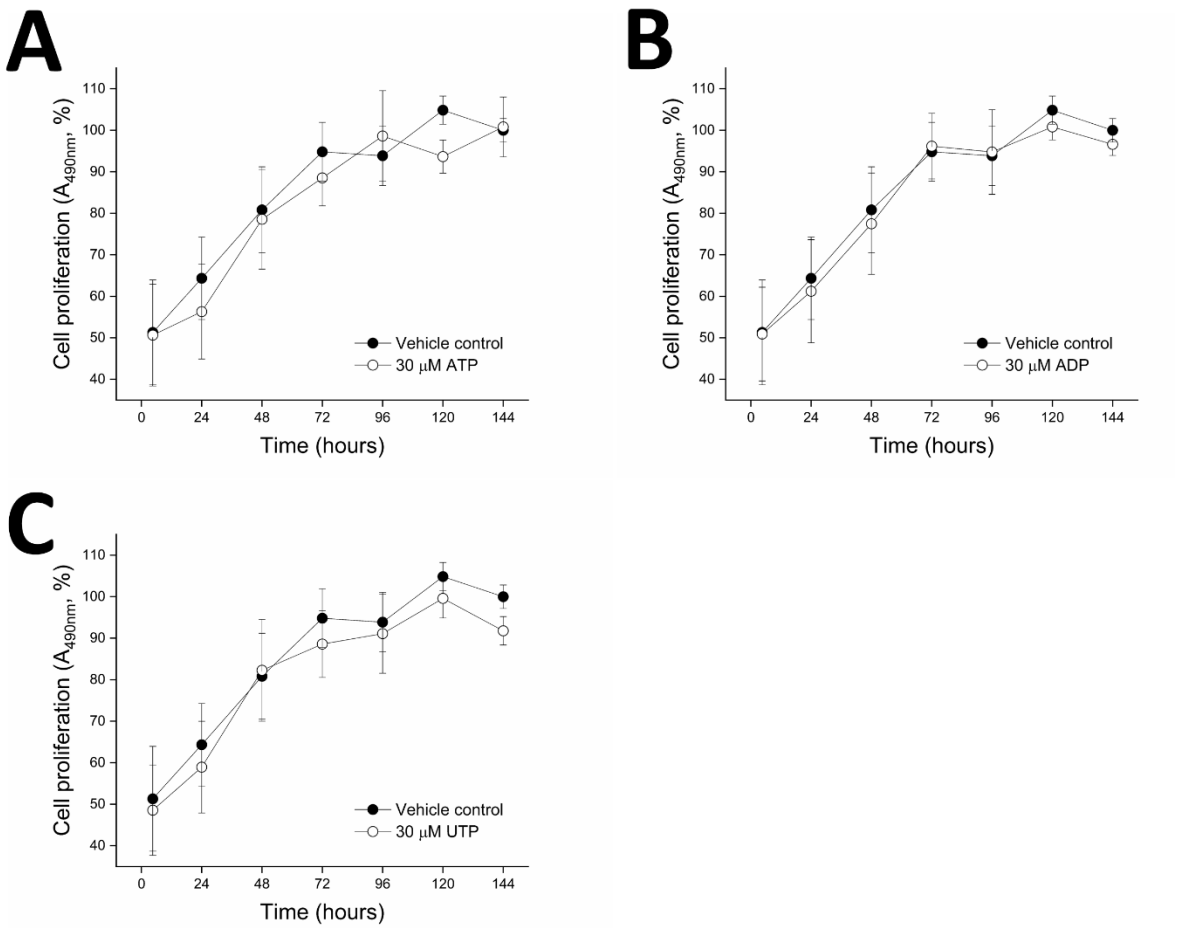

Figure 3.15 Maximal concentrations of exogenous nucleotides have no effect on the rate of cell proliferation in primary human mesenchymal stromal cells over seven days (*N*=3). The absorbance was measured at 490 nm to monitor the formation of a coloured formazan product as an indirect indicator of the number of viable cells present after a single application of (A) 30 μM ATP, (B) 30 μM ADP or (C) 30 μM UTP (*N*=3). Data is normalised to the 144 hour reading for the vehicle control for each respective nucleotide. Data is expressed as mean ± SEM.

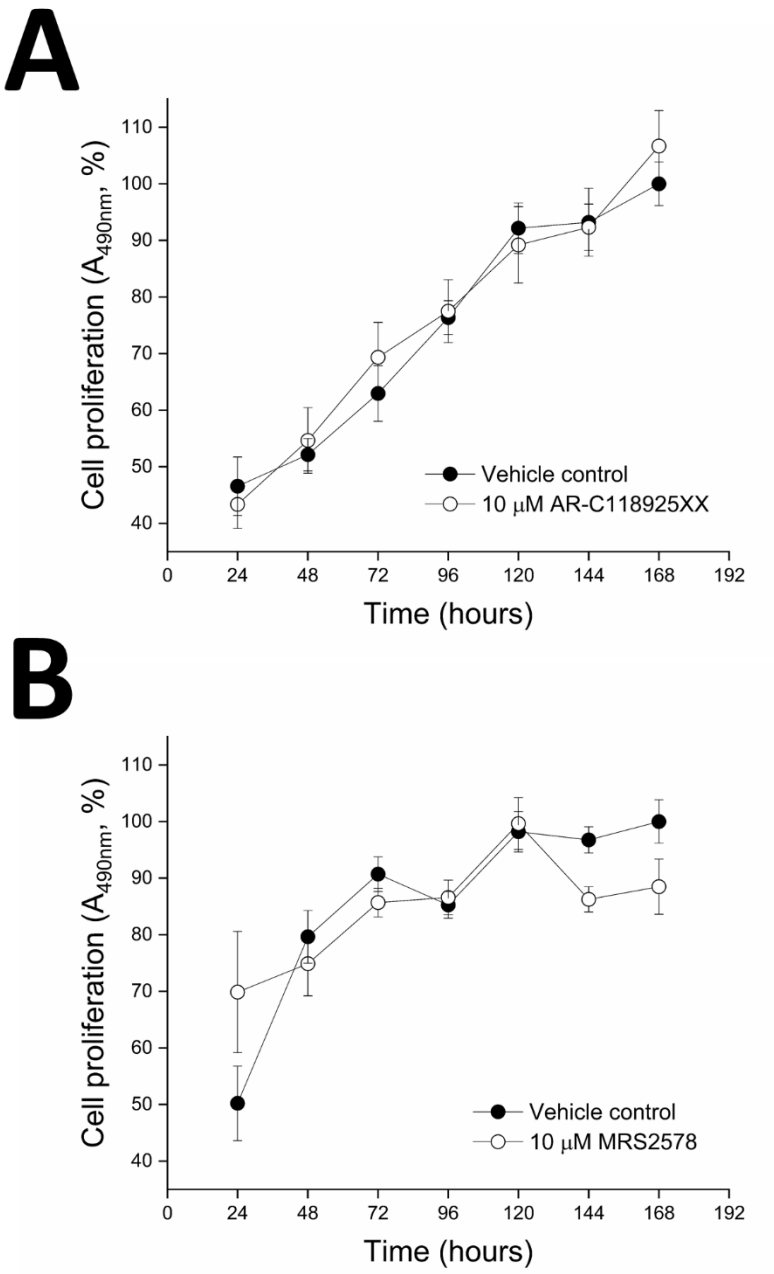

Figure 3.16 Subtype selective antagonism of $P2Y_2$ and $P2Y_6$ receptors have no effect on the rate of cell proliferation in primary human mesenchymal stromal cells over seven days (*N*=3). Absorbance measured at 490 nm to monitor the production of a coloured formazan product as an indirect indicator of the number of viable cells present after a single application of (A) 10 μM AR-C118925XX ($P2Y_2$ receptor antagonist) or (B) 10 μM MRS2578 ($P2Y_6$ receptor antagonist) (*N*=3). Data is normalised to the 168 hour reading for the vehicle control for each antagonist. Data is expressed as mean ± SEM.

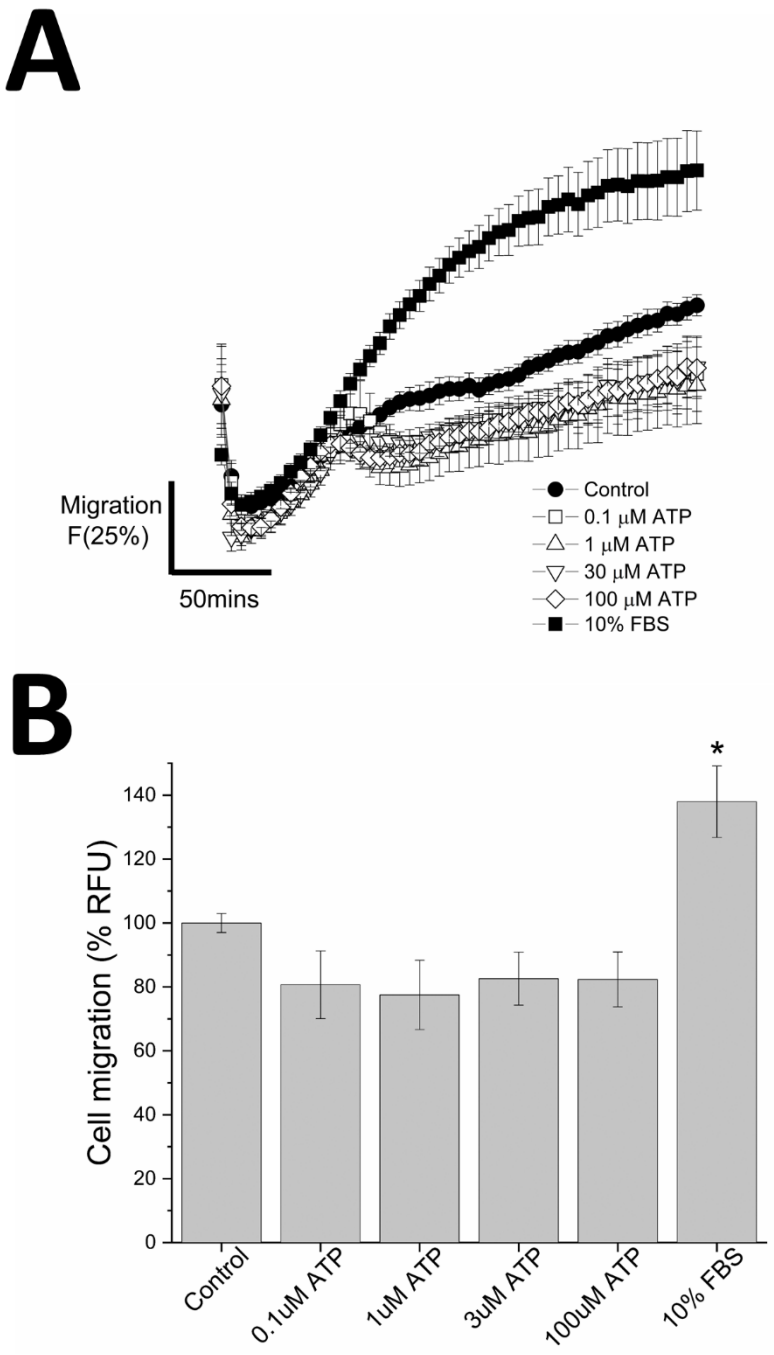

Figure 3.17 Effect of exogenous ATP on primary human mesenchymal stromal cell migration over four hours (*N*=4). Data represents the fluorescence signal (excitation 485nm/emission 530nm) from MSCs labelled with calcein, which have migrated through a polyethylene terephthalate membrane towards the chemotactic agents over time (A) or after 4 hours. 10% foetal bovine serum (FBS) was used as a positive control. Data are normalised to control conditions. **p*<0.05 versus control conditions.

3.13 Summary

Primary human AD-MSCs express all the known subtypes of P2 receptors, excluding P2X2, P2X3 and $P2Y_{12}$, although there is some heterogeneity in the expression of $P2Y_{11}$, $P2Y_{13}$ and $P2Y_{14}$ across donors. In addition, functional evidence of purinergic receptor activation was also acquired, whereby changes in intracellular calcium were detected in response to ATP, ADP and UTP. The nucleotide responses were remarkably consistent across donors and after multiple passages. The ATP response was even resistant to shRNA-mediated knockdown of $P2Y_2$ receptor expression.

Although AD-MSCs appear to express almost all known P2X receptor subtypes, the evidence presented in this Chapter demonstrates a clear predominance of metabotropic G_q-coupled P2Y receptors in the nucleotide-evoked calcium responses. This was demonstrated by the fact that the nucleotide responses persisted (albeit significantly diminished) in the absence of extracellular calcium and were abolished when PLC and SERCA were inhibited. In addition, subtype-selective antagonism of P2X4 and P2X7 receptors had no effect on the response to ATP in these cells. Taken together these data suggest the nucleotide-evoked calcium responses in primary human AD-MSCs are mediated by activation of P2Y receptors, with little/no contribution from the ionotropic P2X receptors present. Although, it is possible that P2X receptors may act downstream of P2Y receptor activation to potentiate the responses, which may explain why the magnitude of the nucleotide-evoked responses is substantially reduced in the absence of extracellular calcium.

All of the known P2Y receptors, excluding $P2Y_{12}$ receptors, were detected at both the mRNA and protein level in primary human MSCs in at least four of the six donors tested. As mentioned previously there was some heterogeneity in the expression of $P2Y_{11}$, $P2Y_{13}$ and $P2Y_{14}$ receptors, however subtype selective antagonism of $P2Y_{11}$ and $P2Y_{13}$ receptors revealed that neither receptor plays a functional role in the nucleotide-evoked calcium responses in these cells. In addition, no response was detected for UDP-glucose, the preferred agonist for $P2Y_{14}$ receptors, suggesting that this receptor was not functionally active either. All of the known G_q-coupled P2Y receptors ($P2Y_1$, $P2Y_2$, $P2Y_4$ and $P2Y_6$ receptors) were consistently detected in primary human MSCs, although subtype-selective antagonism revealed that only $P2Y_2$ and $P2Y_6$ receptors appear to play a functional role in the nucleotide-evoked calcium responses in these cells. $P2Y_2$ receptors mediate the ATP and UTP response in these cells, as evidenced by the equipotent effects of ATP and UTP and the fact that selective antagonism of $P2Y_2$ receptors reduced the response to ATP and abolished the response to UTP. Interestingly, $P2Y_6$ receptors appear to mediate the ADP-evoked calcium response, despite the fact that no response was detected for UDP, the preferred agonist for $P2Y_6$ receptors.

Unfortunately, although the pharmacological evidence presented in this Chapter clearly demonstrates a functional purinergic response in these cells, the downstream functions of these

purinergic signalling pathways were not deciphered during this project. Exogenous nucleotides and/or selective antagonism of $P2Y_2$ or $P2Y_6$ receptors had no effect on the rate of proliferation or chemotaxis in these cells. However, it must be acknowledged that this is far from an exhaustive list of MSC functions, there are many functions that were not explored within the scope of this study. In addition, it is not known whether additional assays or amending assay protocols may have altered these outcomes. Regardless, additional work is required to ascertain the role of purinergic signalling in primary human MSCs, although this study provides a good foundation to build upon.

Chapter 4: Characterisation of the purinergic receptors in primary human *in vitro* differentiated adipocytes

4.1 Introduction

Adipose tissue is the primary site of long-term energy storage in mammals. The tissue contains a wide variety of cell types, but the predominant cell type is white adipocytes. White adipocytes are highly dynamic cells, capable of safely storing excess nutrients as triglycerides in lipid droplets, while also being able to hydrolyse triglycerides to free fatty acids and glycerol in response to a nutrient deficit caused by prolonged fasting or strenuous exercise (Rutkowski *et al.*, 2015). Storage and release of energy was long considered to be the only function of adipose tissue, however approximately 20 years ago it was discovered that adipose tissue is also an endocrine organ that is capable of regulating systemic metabolism via the secretion of a wide variety of adipokines (Barinaga, 1995; Ahima and Flier, 2000). This discovery, in combination with the rise in obesity in society, has fuelled an exponential increase in adipocyte research.

Obesity is defined as the excessive or abnormal expansion of adipose tissue beyond the healthy limits. A crude, but widely used, measurement of obesity are body mass index (BMI) values, which are calculated from an individual's height and weight (Poirier, 2007). A BMI of greater than 25 kg/m^2 indicates that an individual is overweight, whereas a BMI of greater than 30 kg/m^2 denotes obesity. Over the past four decades, there has been an large increase in the number of overweight and obese individuals in the world (Ng *et al.*, 2014). According to the World Health Organisation, in 2016 more than 1.9 billion adults and 380 million children were classified as overweight, of these people more than 30% were obese (WHO, 2018). Being overweight or obese is associated with numerous severe comorbidities, such as cardiovascular disease, diabetes and cancer (Kahn *et al.*, 2006; Van Gaal *et al.*, 2006; Ungefroren *et al.*, 2015), and it is estimated that in 2010 3.4 million deaths occurred due to obesity (Lim *et al.*, 2012). Consequently, the global obesity crisis represents a major clinical and economic problem.

Greater understanding of the molecular mechanisms underlying both healthy white adipocyte functioning, as well as dysfunction of adipocytes during obesity, is required to inform efforts to combat the global obesity crisis. Purinergic signalling has been implicated in a wide range of

physiological processes, including a role for P1 receptors and adenosine in inhibiting triglyceride hydrolysis in adipocytes (Fredholm and Hjemdahl, 1976; Ohisalo, 1981; Johansson *et al.*, 2008). However, thus far limited research has been conducted on the role of P2 receptors in human adipocytes (Tozzi and Novak, 2017). This Chapter outlines my efforts to identify the molecular basis of the P2 purinergic response in primary human *in vitro* differentiated adipocytes (referred to as adipocytes throughout this Chapter) with a view to form a solid foundation for investigating the role of P2 receptors in downstream adipocyte functions.

4.2 Purinergic receptor expression profile in primary human *in vitro* differentiated adipocytes as determined by analysis of mRNA transcripts

Non-quantitative analysis of mRNA transcripts revealed that adipocytes expressed all of the known P1 receptor subtypes: A1, A2A, A2B and A3. No bands were detected in the no RT control lanes suggesting the PCR products were derived from cDNA and not genomic DNA (*N*=3; Figure 4.1A).

Quantitative PCR was used to assess the expression of P2 receptors in primary human adipocytes. Data are expressed as average cycle threshold (C_T) values (Table 4.1) or relative $1/\Delta C_T$ values (Figure 4.1B) where the expression has been normalised to the expression of an endogenous reference gene, RPLP0, and inverted for analytical ease. Genes with a C_T value of 35 or below (or $1/\Delta C_T > 0.062$) were deemed to be present, whereas genes with C_T values exceeding 35 (or $1/\Delta C_T < 0.062$) were considered absent. Applying these parameters revealed consistent expression of P2X4, P2X6, $P2Y_1$, $P2Y_2$, $P2Y_4$, $P2Y_{12}$ and $P2Y_{13}$ receptors, whereas P2X2 and P2X3 receptors were not expressed in any of the donors tested (*N*=6; Table 4.1; Figure 4.1B). Near consistent mRNA expression of P2X5, P2X7 and $P2Y_6$ receptors was also observed with only one donor displaying an average C_T values of above 35 for each receptor. Similarly, C_T values of above 35 were recorded for five out of six donors for P2X1 and $P2Y_{14}$ receptors, and on average the $1/\Delta C_T$ values for both receptors falls below the 0.062 cut-off. The most variation was observed in the expression of $P2Y_{11}$ receptors, with expression being detected in three of the six donors tested, and on average, the $1/\Delta C_T$ value for $P2Y_{11}$ falls below the 0.062 cut-off. Unfortunately, the sample size used in this study is too small to draw conclusions about population level heterogeneity or correlate the variation observed between donors with specific donor traits, such as age, weight or menopausal status.

P2X5 was detected in the majority of donors tested (Table 4.1), but previous studies have elucidated that a single nucleotide polymorphism (SNP) resulting in the substitution of thymine with a guanine at the 3' splice site of exon 10 in the gene for the human P2X5 receptor can result in the exclusion of exon 10 during translation, which renders the receptor non-functional (Kotnis *et al.*, 2010). Non-quantitative PCR, revealed that human adipocytes express the exon-10 less variant of the receptor, indicating that P2X5 is not functional in these cells (Figure 4.1C). This is line-in with the findings

presented by Kotnis et al. (2010), which demonstrated a predominance of the exon-10 less non-functional P2X5 receptor variant in humans

Table 4.1 Average cycle threshold (C_T) values for each P2 receptor in primary human *in vitro* differentiated adipocytes per donor (*N*=6). Only genes with C_T values of <35 were considered present. ND indicates no amplification detected within 40 PCR cycles.

Gene	C_T values					
	Donor 1	Donor 2	Donor 3	Donor 4	Donor 5	Donor 6
P2RX1	35.9	35.1	35.9	37.3	34.6	35.4
P2RX2	ND	ND	ND	ND	ND	ND
P2RX3	36.1	37.9	38.5	ND	37.4	37.3
P2RX4	25.1	27.3	26.6	29.4	26.8	26.3
P2RX5	30.7	29.4	30.4	35.6	30.9	30.3
P2RX6	30.9	29.4	27.6	34.3	30	29.5
P2RX7	31.8	30.9	29.9	36.9	33.2	32.8
P2RY1	28.8	29.3	30.6	29.4	28.2	26.5
P2RY2	33.4	33.6	34.4	31.9	33.7	30.8
P2RY4	31.4	31.4	33	31.6	31.4	29.4
P2RY6	32.8	32.8	35.7	31.4	28.7	26.6
P2RY11	39.9	36.5	34.9	37.8	33.9	33.7
P2RY12	31.4	30.9	30.3	29.1	28	26.5
P2RY13	35	33.9	33.5	34.4	32.6	29.4
P2RY14	35.5	35.2	35.7	36.6	ND	32.1

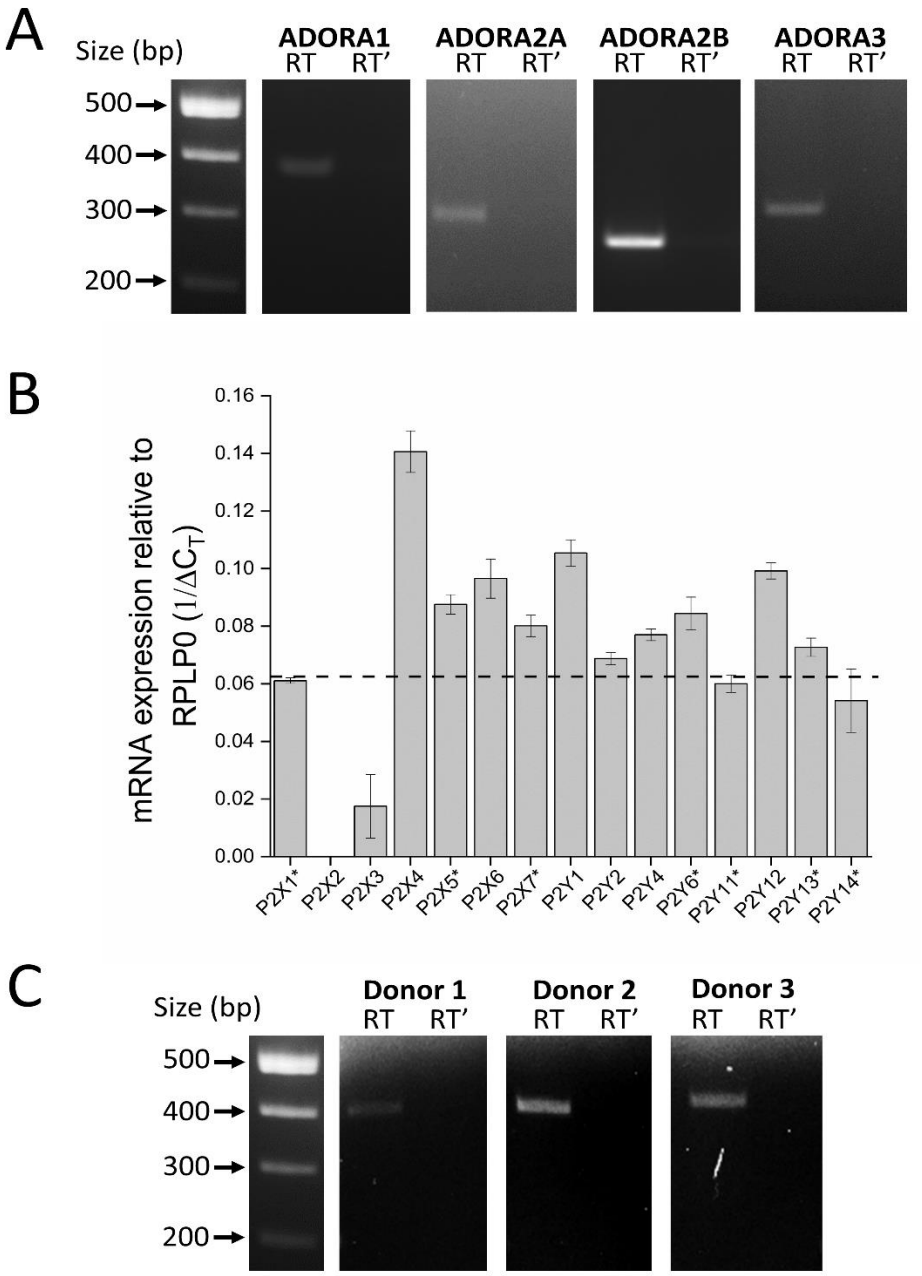

Figure 4.1 Messenger RNA expression profile of purinergic receptors in primary human *in vitro* differentiated adipocytes. (A) Non-quantitative RT-PCR analysis of P1 receptor expression showing bands detected for ADORA1 (374 bp), ADORA2A (295 bp), ADORA2B (277 bp) and ADORA3 (302 bp). RT' indicates the no reverse transcriptase control samples. Results are representative of the data from three independent donors. (B) Quantitative real time PCR analysis of the P2 receptor expression profile. Cycle threshold (C_T) values have been normalised to the expression of an endogenous reference gene, RPLP0. The dashed line represents the C_T cut-off, where receptors that had an average $1/\Delta C_T$ value of below 0.062 are classified as not expressed (*N*=6). *near the tick labels for each receptor indicate variability in expression between donors. (C) Non-quantitative RT-PCR analysis of P2X5 receptor transcript variants in three independent donors showing bands for either exon-10 less non-functional P2X5 receptor (395 bp) or exon-10 containing functional P2X5 receptor transcript (461 bp). RT' indicates the no reverse transcriptase control samples.

4.3 Protein expression profile of P2 purinergic receptors in primary human *in vitro* differentiated adipocytes

Immunocytochemistry was used to confirm that the P2 receptor profile detected at the mRNA level (Section 4.2) correlated well with protein expression. Immunofluorescence for P2X4, P2X5, P2X7, $P2Y_1$, $P2Y_2$, $P2Y_4$, $P2Y_6$, $P2Y_{11}$, $P2Y_{12}$ and $P2Y_{13}$ receptors were all consistently detected in three independent donors. Representative images of the positive staining observed for each receptor are shown in Figure 4.2A. The three donors used for immunocytochemistry were selected at random and do not appear to demonstrate the heterogeneity detected at the mRNA level. Cells were not stained for P2X1, P2X2, P2X3, P2X6 or $P2Y_{14}$ either due to lack of mRNA expression or lack of antibody.

The immunofluorescence for each receptor also provided an insight into the cellular localisation and distribution of each receptor. However, as the cells were permeabilised for staining and not counterstained with membrane or organelle markers, it is not possible to definitively determine the localisations of each receptor. Immunofluorescence was detected for all the receptors investigated and the staining appears to be uniformly distributed throughout the cells. Adipocytes are large cells with a very distinct morphology as the cells are packed with round lipid droplets. Here the *in vitro* model differs slightly from *in vivo* mature adipocytes, which have a unilocular appearance rather than the multilocular phenotype observed with *in vitro* differentiated adipocytes. The edges of round lipid droplets can easily be seen in the images for each receptor, which may indicate that the receptors are present in the cytoplasm. The immunofluorescence for $P2Y_2$ receptors in particular displayed a punctate distribution throughout the cell. Although the intensity of the staining varied slightly inferences about the relative abundance of each receptor cannot be made due to differing antibody affinities.

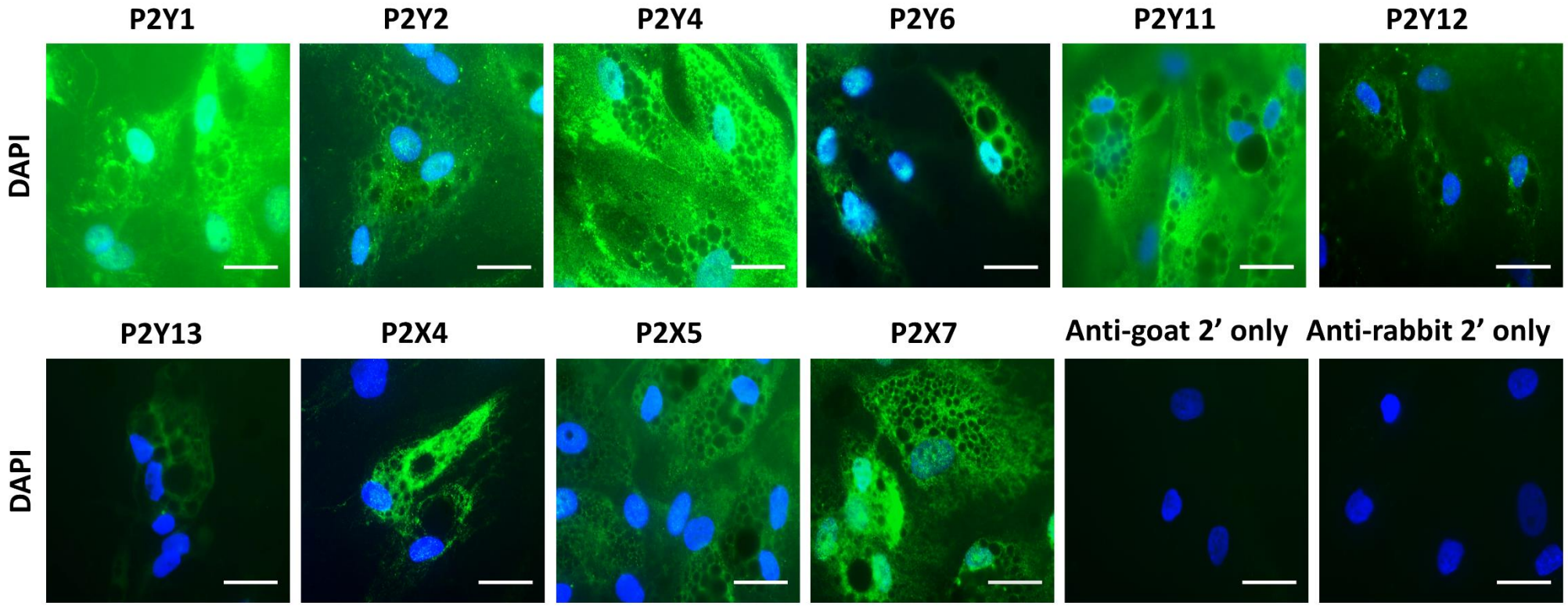

Figure 4.2 Analysis of P2X and P2Y receptor immunofluorescence in primary human *in vitro* differentiated adipocytes. (A) Immunocytochemical staining for $P2Y_1$, $P2Y_2$, $P2Y_4$, $P2Y_6$, $P2Y_{11}$, $P2Y_{12}$, $P2Y_{13}$, P2X4, P2X5 and P2X7 receptors. Images presented are representative of at least ten fields of view for cells extracted from three independent donors. Images were taken with a 63x objective on a Zeiss AxioPlan 2ie epifluorescent microscope of permeabilised *in vitro* differentiated adipocytes labelled with primary antibodies against receptor targets and visualized with an Alexa Fluor 488-conjugated secondary antibody (green). Cells were counterstained with DAPI to visualise nuclei (blue). The exposure and camera settings remained consistent across all the images taken for each donor. Scale bar represents 30 µm.

4.4 ATP, ADP and UTP elicit calcium responses in primary human *in vitro* differentiated adipocytes

Exogenous application of nucleotides can activate purinergic receptors expressed on the surface of cells to initiate transient elevations in intracellular Ca^{2+} levels, due to direct entry of extracellular calcium via P2X receptors or via activation of G_q-coupled P2Y receptors to activate PLC-mediated release of Ca^{2+} from intracellular stores (Burnstock, 2007). To assess whether P2 receptor expressed in primary human adipocytes were functionally active, changes in intracellular calcium levels were monitored while exogenous nucleotides were applied using a Flexstation III microplate reader.

Table 4.2 Characteristics of the calcium responses evoked by maximal concentrations of nucleotides in primary human *in vitro* differentiated adipocytes (*N*=6). Mean ± SEM.

Nucleotide	Peak magnitude (F ratio)[a]	Net calcium movement (area under the curve)[b]	Decay time, τ (s)[c]	EC_{50} (μM)
30 μM ATP	1.37 ± 0.07	72.0 ± 10.2	41.9 ± 1.4	1.84 ± 1.4
10 μM ADP	1.85 ± 0.09	65.5 ± 2.9	21.6 ± 2.1	0.24 ± 0.05
100 μM UTP	0.16 ± 0.04	11.4 ± 3.1	33.6 ± 11.0	13.0 ± 4.6

[a] Peak magnitude was significantly different between the three nucleotides (*p<0.001*) as determined by one-way ANOVA with a post hoc Tukey test. [b] The net calcium movement for UTP was significantly different to ATP and ADP (*p*<0.005) as determined by Kruskal-Wallis ANOVA with a *post hoc* Dunn's test. [C] The decay time was significantly faster for ADP vs ATP (*p*<0.05) as determined using a Kruskal-Wallis ANOVA with a *post hoc* Dunn's test.

Application of ATP, ADP and UTP elicited concentration-dependent increases in intracellular calcium, with a rank order of potency ADP (EC_{50} 0.24±0.05μM) > ATP (EC_{50} 1.84±1.4μM) > UTP (EC_{50} 13.0±4.6μM) (*N*=6; Table 4.2; Figure 4.3A,C,E). Each nucleotide caused a rapid increase in intracellular calcium, which decayed back to baseline calcium concentrations within the recording period of 250 seconds (*N*=6; Figure 4.3B,D,F). The magnitude and kinetics of the responses varied significantly between nucleotides (Table 4.2), with a difference of more than 1.5 F_{ratio} between the magnitude of the response for ADP (F_{ratio} 1.85 ± 0.09 *N*=6) and UTP (F_{ratio} 0.16 ± 0.04 *N*=6). In addition, the time-resolved traces shown in Figure 4.3B and D demonstrate that the response to ADP clearly decays at a faster rate than the response to maximal concentrations of ATP. This difference was quantified by calculating the τ values for the responses, which confirmed that there was a significant difference in the decay times for the two nucleotides (Table 4.2). The small magnitude and shallow decay of the response to UTP, unfortunately meant that the software

struggled to accurately calculate the τ value for some donors, which led to considerable variabilty between donors, which in turn meant that although the average τ value for the response to UTP is higher than the τ value for ADP and the trace appears to mirror the pattern observed for ADP and ATP, the statistical analysis did not reflect this. Instead the statistics suggests there is no significant change in the decay kinetics for ATP or ADP versus UTP.

Adipocytes were insensitive to stimulation with low concentrations of UDP (<30 µM) and UDP-glucose (<100 µM) (*N*=6). However, responses were consistently detected at very high agonist concentrations of above 30 µM UDP (*N*=6; Figure 4.4A,B) or greater than 100 µM UDP-glucose (*N*=6; Figure 4.4C,D). Elevated agonist concentrations are unlikely to be representative of physiological nucleotide concentrations, so it is unlikely that these results truly show activation of $P2Y_6$ and $P2Y_{14}$ receptors, which are preferentially activated by UDP and UDP-glucose respectively (Communi *et al.*, 1996; Abbracchio *et al.*, 2003). It is likely that these responses are due to ATP or ADP contamination of the UDP and UDP-glucose used in this study. The manufacturer's state that the purity of the UDP and UDP-glucose are >96% and >98% respectively.

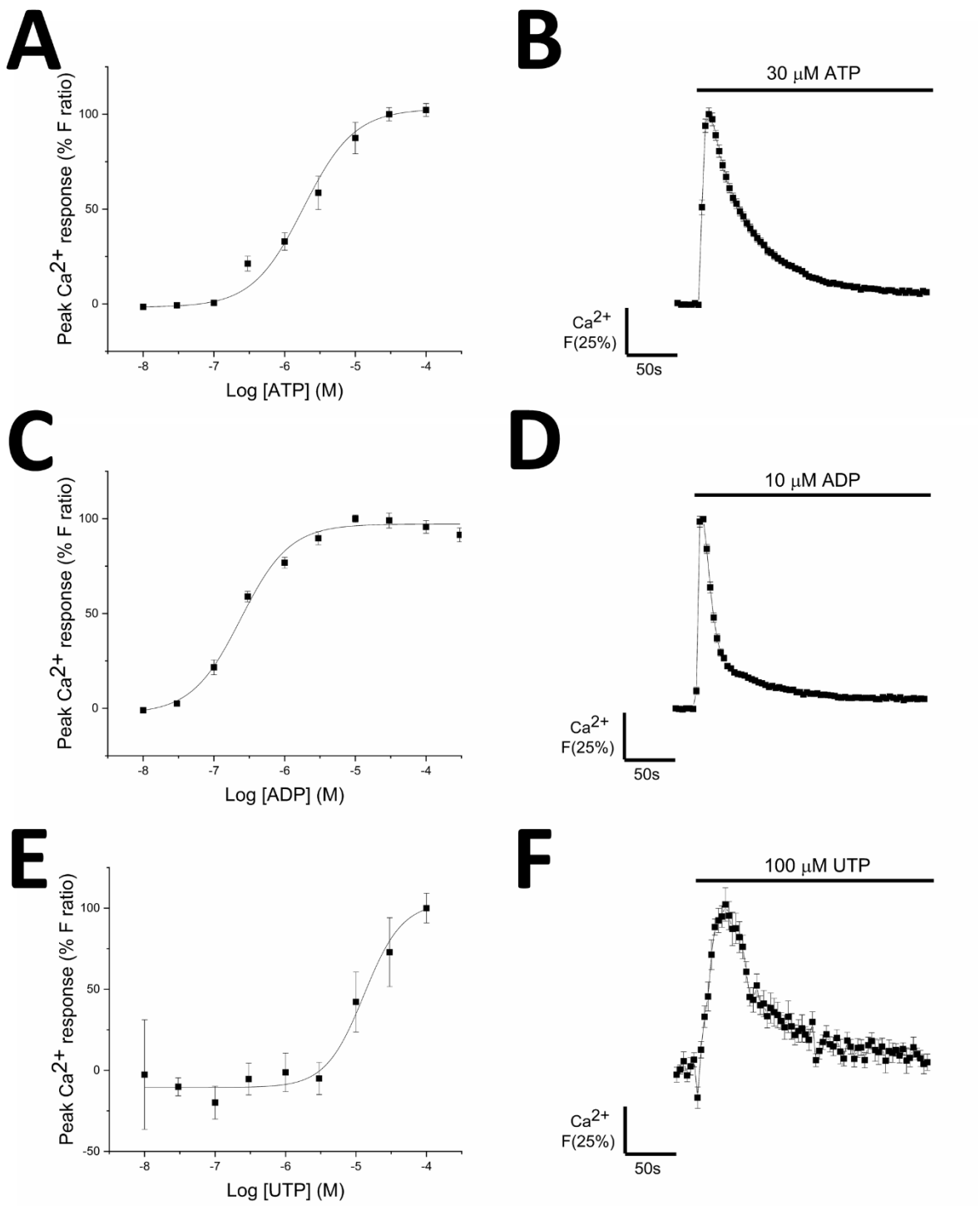

Figure 4.3. ATP, ADP and UTP elicited intracellular calcium responses in primary human *in vitro* differentiated adipocytes. Concentration response curves for the peak magnitude of intracellular Ca^{2+} responses elicited by (A) ATP (*N*=6), (C) ADP (*N*=6) and (E) UTP (*N*=6). Ca^{2+} responses were normalized to the peak magnitude of the agonist concentration that produced the maximal response in the majority of donors, which was the response to 30 μM ATP, 10 μM ADP and 100 μM UTP respectively. Averaged time-resolved intracellular Ca^{2+} responses elicited by (B) 30 μM ATP (*N*=6), (D) 10 μM ADP (*N* =6) and (E) 100 μM UTP (*N* =6). Traces were normalised to the maximal response within a donor and then averaged across donors. Data points represent mean ± SEM.

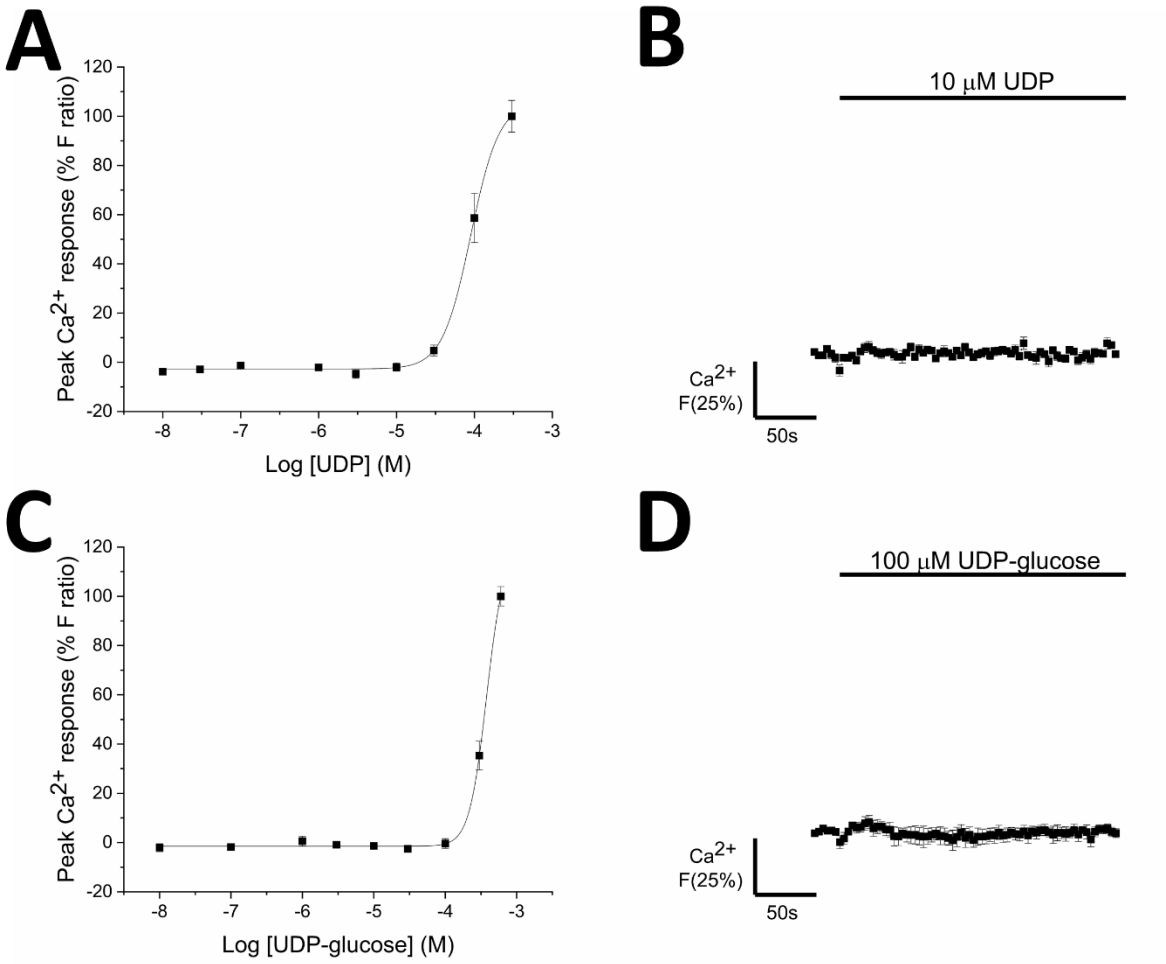

Figure 4.4 Physiological concentrations of UDP and UDP-glucose did not elicit intracellular calcium responses in primary human *in vitro* differentiated adipocytes. Concentration response curves for the magnitude of intracellular Ca^{2+} responses elicited by (A) UDP (*N*=6) and (C) UDP-glucose (*N*=6). Ca^{2+} responses were normalized to the peak magnitude of the agonist concentration that produced the maximal response in the majority of donors, which was the response to 300 µM UDP and 600 µM UDP-glucose respectively. Averaged time-resolved intracellular Ca^{2+} responses elicited by (B) 10 µM UDP (*N*=6) and (D) 100 µM UDP-glucose (*N*=6). Traces were normalised to the maximal response within a donor, and averaged across donors. Data points represent mean ± SEM.

4.5 Nucleotide-evoked calcium responses in primary human *in vitro* differentiated adipocytes are mediated by metabotropic P2Y receptors

Concentration-dependent responses to both ATP and ADP persisted in the absence of extracellular calcium, without a significant change in the potency of the response to each nucleotide: EC_{50} (ATP + Ca^{2+}) 0.89 ± 0.7 µM *N*=6 versus EC_{50} (ATP - Ca^{2+}) 1.37 ± 0.3 µM *N*=6; EC_{50} (ADP + Ca^{2+}) 0.12 ± 0.08 µM *N*=3 versus EC_{50} (ADP - Ca^{2+}) 0.11 ± 0.2 µM *N*=3). However, the magnitude of the responses to both nucleotides were severely diminished when extracellular calcium was removed. The response to 30 µM ATP decreased by 90.3 ± 2.7% (*N*=6; p<0.001; Figure 4.5B) and the response to 10 µM ADP decreased by 81.7 ± 2.2% (*N*=3; p<0.05; Figure 4.5D). The decrease in the magnitude of the responses may be due to partial emptying of the intracellular calcium stores, removal of store-operated calcium entry post-P2Y receptor activation or prevention of downstream P2X receptor activity. Although both responses were significantly decreased, which suggests the magnitude of the responses are dependent on extracellular calcium the fact that the responses persist in the absence of extracellular calcium indicates that at least a component of the ATP and ADP response is mediated by metabotropic P2Y receptors.

There does not appear to be a response to UTP in the absence of extracellular calcium in human adipocytes (*N*=3; Figure 4.5E,F). However, it is likely that the UTP response, like the ATP and ADP response, is diminished, rather than abolished, but as the response to UTP is very small even in the presence of extracellular calcium (F_{ratio} 0.16 ± 0.04 *N*=6), the diminished response in the absence of calcium could not be resolved using a Flexstation III, as the equipment is not sensitive enough to detect a diminished response.

In support of the argument that the nucleotide-evoked calcium responses in adipocytes are mediated by metabotropic receptors, the responses to maximal agonist concentrations are abolished in the presence of a PLC inhibitor, U73122 (Figure 4.6). This suggests that the elevation of intracellular calcium evoked upon P2 receptor stimulation is mediated by PLC-induced release of calcium from the intracellular stores. As the response to UTP is very small, normalisation of the response led to the appearance of a very erratic response in the presence of U73122, but even still it is clear that the response to UTP is completely abolished in the presence of 10 µM U73122 (*N*=4; Figure 4.6D).

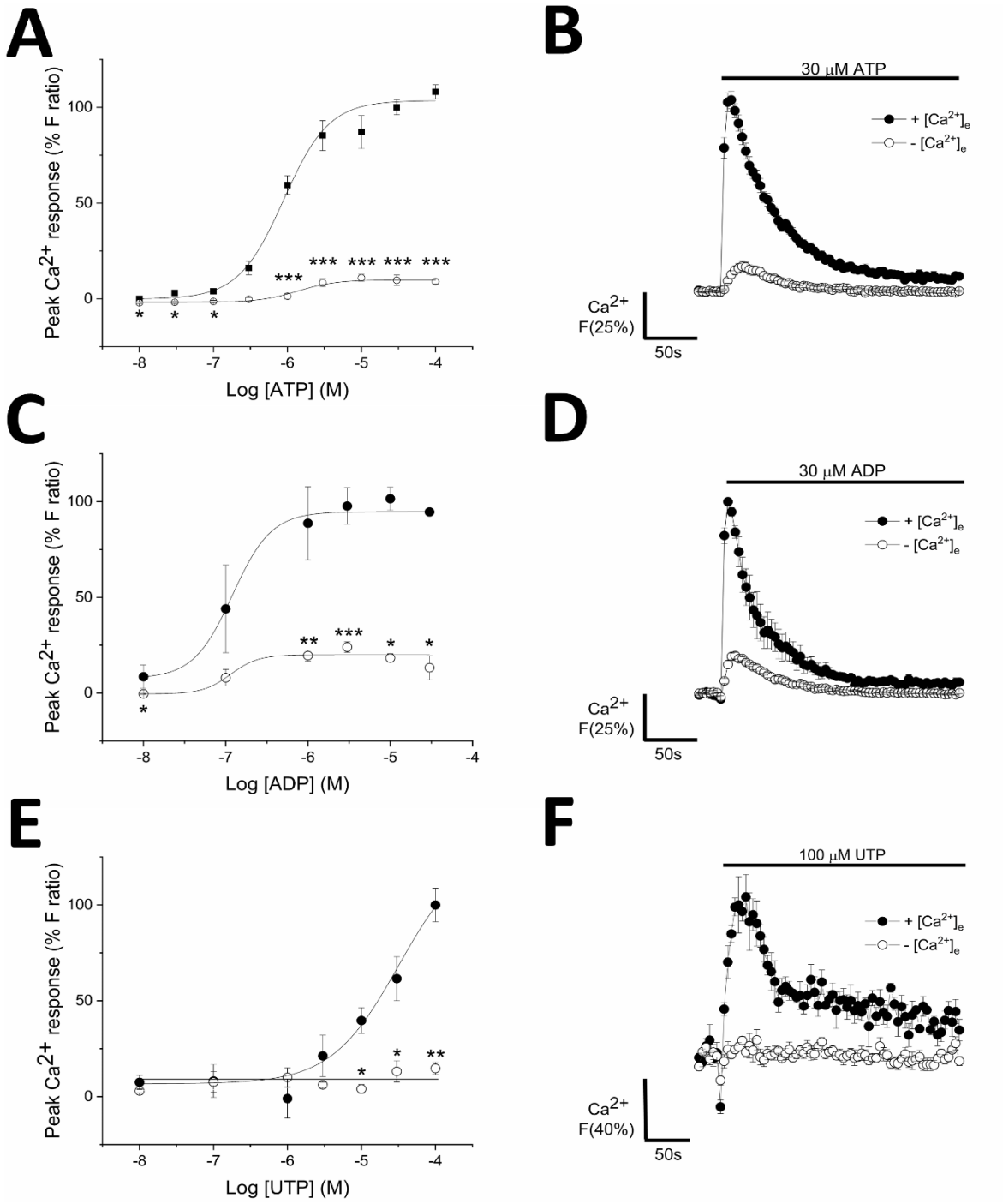

Figure 4.5 Removing extracellular calcium leads to a reduction in the magnitude of the response evoked by ATP, ADP and UTP in primary human *in vitro* differentiated adipocytes. Concentration-response curves in the presence (*closed circles*) and absence (*open circles*) of 1.5 mM extracellular calcium for (A) ATP (*N*=6), (C) ADP (*N*=3) and (E) UTP (*N*=3). All responses were normalised to the response to maximal concentrations of each agonist (30 μM ATP, 10 μM ADP and 100 μM UTP respectively) in the presence of extracellular calcium. Average time-resolved traces showing response elicited by (B) 30 μM ATP (*N*=6), (D) 100 μM ADP (*N*=3) and (F) 30 μM UTP (*N*=3) in the presence (*closed circles*) and absence (*open circles*) of extracellular calcium. Data points represent the mean ± SEM. **p*<0.05, ***p*<0.01, ****p*<0.001 versus the response to equivalent concentrations of agonist in the presence of extracellular calcium.

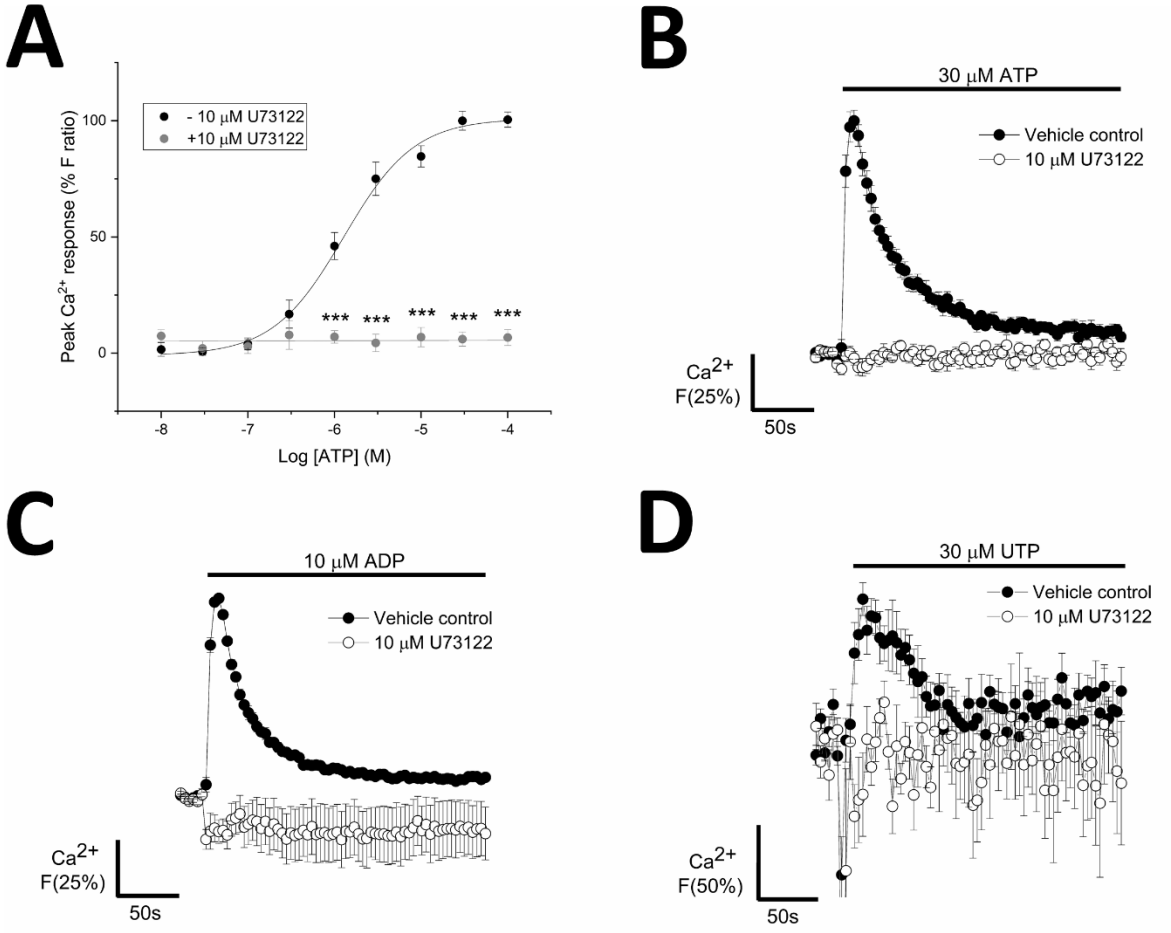

Figure 4.6 Inhibition of phospholipase C with U73122 abolishes the response to ATP, ADP and UTP in primary human *in vitro* differentiated adipocytes. (A) ATP concentration response curve in the presence (*open circles*) and the absence (*closed circles*) of 10 μM U73122. All responses were normalised to the response to 30 μM ATP in the absence of U73122. Average time-resolved traces showing responses elicited by (B) 30 μM ATP (*N*=6), (C) 10 μM ADP (*N*=5) and (D) 30 μM UTP (*N*=4) in the presence (*open circles*) and absence (*closed circles*) of 10 μM U73122. Data points represent the mean ± SEM. ***p<0.001 versus the response to equivalent concentrations of ATP in the absence of U73122.

4.6 ADP-evoked calcium response are mediated by $P2Y_1$ and $P2Y_{12}$ receptors

ADP is the preferred agonist for $P2Y_1$, $P2Y_{12}$ and $P2Y_{13}$ receptors, all of which are expressed in primary human adipocytes (Section 4.2 and 4.3). $P2Y_1$ receptors are G_q-coupled, whereas $P2Y_{12}$ and $P2Y_{13}$ receptors are both G_i-coupled, consequently $P2Y_1$ receptors are the most likely candidate for mediating the ADP-evoked calcium response via activation of PLC and downstream release of calcium from the intracellular stores. Exogenous application of a $P2Y_1$ selective agonist, MRS2365, caused an increase in cytosolic calcium (Figure 4.7D), which suggests that $P2Y_1$ is functionally active in these cells. The response magnitude was approximately half of the peak magnitude achieved with ADP, but the response to MRS2365 bore a striking similarity to the response to ADP: a very fast initial response, that decayed to baseline extremely quickly. In addition, concentration-dependent antagonism of the response to maximal concentrations of ADP were observed using a selective antagonist for $P2Y_1$, MRS2500 (IC_{50} 77.1 ± 37.5 nM *N*=6; Figure 4.7A). MRS2500 (1 µM) achieved a maximum of 45.1 ± 4.7% inhibition of the peak magnitude versus the response in the presence of vehicle only (Figure 4.7B; $p<0.001$, *N*=6). The fact that the response to ADP was not abolished by MRS2500 may indicate that multiple receptors mediate the ADP response or may be due to the competition between ADP and the antagonist. MRS2500 has previously been reported to be a competitive antagonist of $P2Y_1$ receptors (Kim *et al.*, 2003), and this was confirmed here, as there is a clear decrease in the potency of the response to ADP in the presence of 1 µM MRS2500 (EC_{50} (-MRS2500) 13.2 ± 2.5 µM *N*=6 versus EC_{50} (+MRS2500) 466.9 ± 674 nM *N*=6; $p<0.05$), with the response magnitude eventually reaching the same response maxima in the presence and absence of MRS2500 (Figure 4.7C). This pattern is characteristic of a competitive antagonist.

Interestingly the ADP-evoked calcium response was also inhibited in the presence of PSB0739, a $P2Y_{12}$ receptor antagonist. Concentration-dependent inhibition of the response to ADP was observed (IC_{50} 64.0 ± 56.5 nM *N*=6), which plateaued after decreasing the peak response magnitude by approximately 40% (Figure 4.7E,F). PSB0739, like MRS2500, is reported to be a competitive antagonist (Hoffmann *et al.*, 2009). However, although 3 µM PSB0739 caused a shift in the potency of the response to ADP (EC_{50} (-PSB0739) 398 ± 186 nM *N*=3 versus EC_{50} (+PSB0739) 1.4 ± 0.4 µM *N*=3; $p<0.05$; Figure 4.7G), the inhibition caused by the antagonist was insurmountable. An insurmountable decrease in the response is characteristic of non-competitive inhibition. This may suggest a more complex mechanism of action or interplay between receptors activated by ADP.

$P2Y_{12}$ is a G_i-coupled receptor, however it is well documented that there is crosstalk between the signalling pathways activated by $P2Y_1$ and $P2Y_{12}$ receptors in platelets (Hardy *et al.*, 2004), which may be the reason that selective $P2Y_{12}$ antagonism has an unusual effect on the ADP concentration response curve. Simultaneous inhibition of both $P2Y_1$ and $P2Y_{12}$ receptors caused a 62.5 ± 5.3% (*N*=6) decrease in the magnitude of the response to 10 µM ADP, which is more inhibition than was

achieved by inhibiting $P2Y_1$ and $P2Y_{12}$ receptors independently (36.9 ± 7.1% *N*=6 and 39.2 ± 3.8% *N*=6 inhibition respectively) (Figure 4.7H). Although the level of inhibition is greater with combined inhibition, the inhibition achieved is not additive and falls shy of the 76.2% inhibition expected, suggesting that there may be some overlap in the action of $P2Y_1$ and $P2Y_{12}$ in the ADP-evoked calcium response. The fact that the response was not abolished by combined antagonism of both $P2Y_1$ and $P2Y_{12}$ receptors may indicate that additional receptors are involved. However, $P2Y_{13}$ is the only other receptor that is preferentially activated by ADP, and selective inhibition of $P2Y_{13}$ receptors with MRS2211 only significantly inhibited the peak magnitude or area under the curve of response to ADP at very high concentrations of MRS2211 (≥10 µM MRS2211) (Figure 4.8). At these elevated concentrations of antagonist, it is likely that the inhibition observed is due to non-specific inhibition of other P2 receptors, rather than true inhibition of $P2Y_{13}$, which suggests that $P2Y_{13}$ is unlikely to play a role in the ADP-evoked calcium response. In addition, although it is not the preferred agonist for the receptor, ADP can also activate $P2Y_6$ receptors (Communi *et al.*, 1996). Thus, for completeness, the effect of a selective $P2Y_6$ receptor antagonist, MRS2578, was also tested, and this revealed that selective inhibition of $P2Y_6$ (< 10 µM MRS2578) had no significant effect on the response to 10 µM ADP in primary human adipocytes (Table 4.3). Therefore, it is likely that the residual response to ADP after combined antagonism is a consequence of the competitive nature of MRS2500 and PSB0739.

The role of $P2Y_{12}$ receptors was also confirmed using an alternative $P2Y_{12}$ receptor antagonist, Ticagrelor. Currently, Ticagrelor is used clinically for the prevention of atherothrombotic events in acute coronary syndrome patients (Wallentin *et al.*, 2009). Ticagrelor (300 nM) caused a 41.5 ± 7.2% (*N*=6) reduction in the peak magnitude of ADP-evoked Ca^{2+} response (Figure 4.9A), which very closely resembled the maximum amount of inhibition achieved with PSB0739. However, Ticagrelor did not display concentration dependence, with higher concentrations (>300 nM) causing less inhibition than lower concentrations (≤300 nM) of the drug. It is possible that this effect is due to the fact that Ticagrelor also inhibits equilibrative nucleoside transporter 1 (ENT1), an adenosine transporter. Inhibition of ENT1 alone, with NMPBR, caused significant potentiation of the magnitude of the ADP response. It is possible that higher concentrations of Ticagrelor have a greater effect on ENT1, thus reducing the total level of inhibition observed. Slight variability in the potency of the effects of Ticagrelor on ENT1 and $P2Y_{12}$ between donors may also explain the difference in the level of inhibition observed with 300 nM Ticagrelor in Figure 4.9A and 4.9B. Co-application of Ticagrelor and NMPBR neutralises the inhibitory effects of Ticagrelor alone (*N*=7; Figure 4.9B), which eliminates the possibility that the inhibition of the ADP response observed with Ticagrelor is due to inhibition of ENT1 rather than $P2Y_{12}$ receptors. These results confirm $P2Y_{12}$ receptors are involved in the ADP-evoked calcium responses in primary human adipocytes.

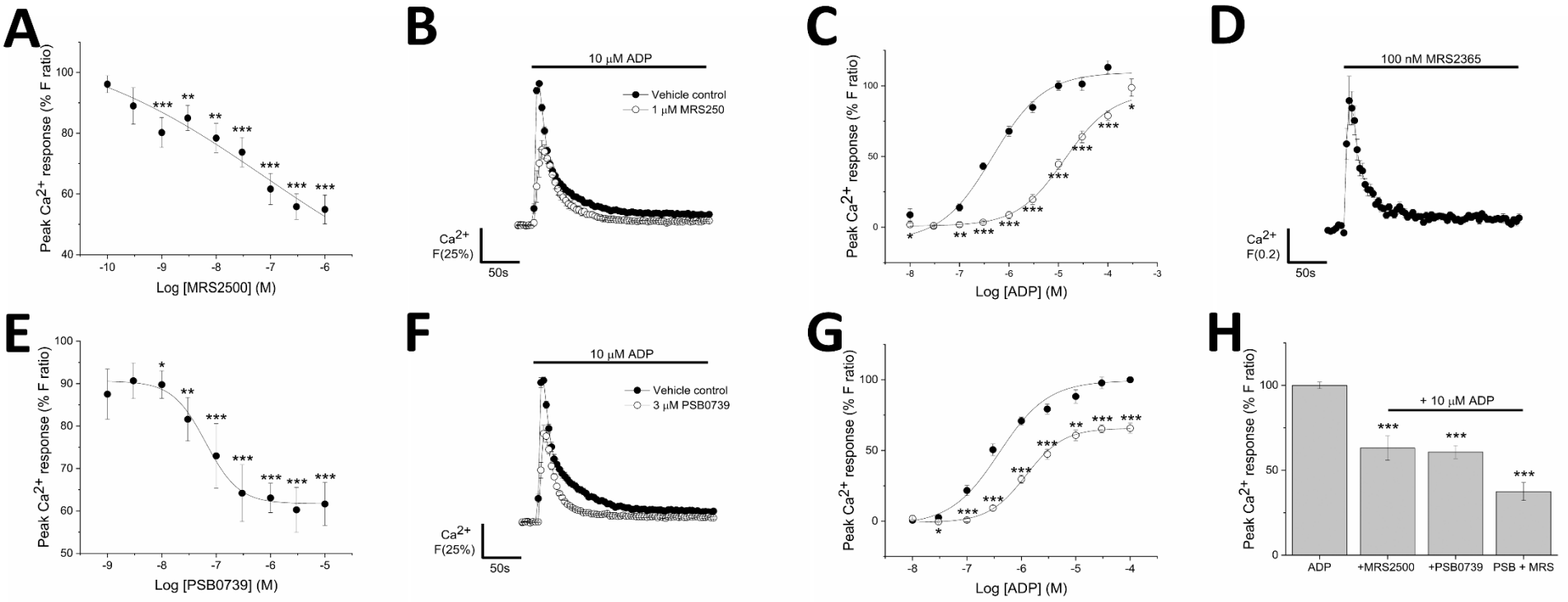

Figure 4.7 The ADP-evoked calcium responses in primary human *in vitro* differentiated adipocytes are mediated by activation of $P2Y_1$ and $P2Y_{12}$ receptors. Concentration-dependent inhibition of the response to 10 μM ADP using (A) MRS2500 (*N*=6) and (E) PSB0739 (*N*=6). Average time-resolved traces showing the response to 10 μM ADP in the presence (*open circles*) or absence (*closed circles*) of (B) 1 μM MRS2500 (*N*=6) or (F) 3 μM PSB0739 (*N*=3). ADP concentration response curves in the presence (*open circles*) or absence (*closed circles*) of (C) 1 μM MRS2500 or (G) 3 μM PSB0739. (D) Average time-resolved trace showing the response to 100 nM MRS2365 (a $P2Y_1$ selective agonist) (*N*=6). (H) Effect of co-inhibition of $P2Y_1$ and $P2Y_{12}$, using 1 μM MRS2500 and 3 μM PSB0739, on the peak magnitude of the response to 10 μM ADP (*N*=6). All data were normalised to their respective vehicle controls in each donor and then averaged across donors, excluding the response to MRS2365 (D) which was not normalised. **p*<0.05, ***p*<0.005, ****p*<0.001 versus the response to equivalent concentrations of ADP in the presence of vehicle alone.

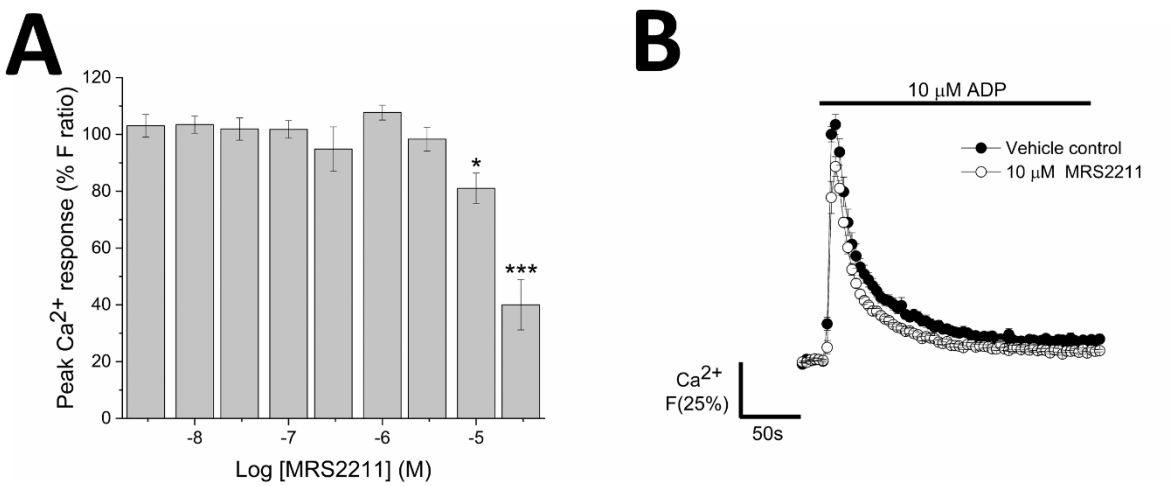

Figure 4.8 Specific concentrations of MRS2211 ($P2Y_{13}$ receptor antagonist) do not significantly inhibit the response to 10 µM ADP in primary human *in vitro* differentiated adipocytes. (A) The effect of increasing concentrations of MRS2211 on the calcium response evoked by 10 µM ADP (*N*=6). (B) Average time-resolved trace showing the response to 10 µM ADP in the presence (*open circles*) or absence (*closed circles*) of 10 µM MRS2211 (*N*=6). All data are normalised to the ADP-evoked calcium response in the presence of vehicle (control) in each donor and then average across donors. **p*<0.05, ****p*<0.001 versus the response to ADP in the presence of vehicle only.

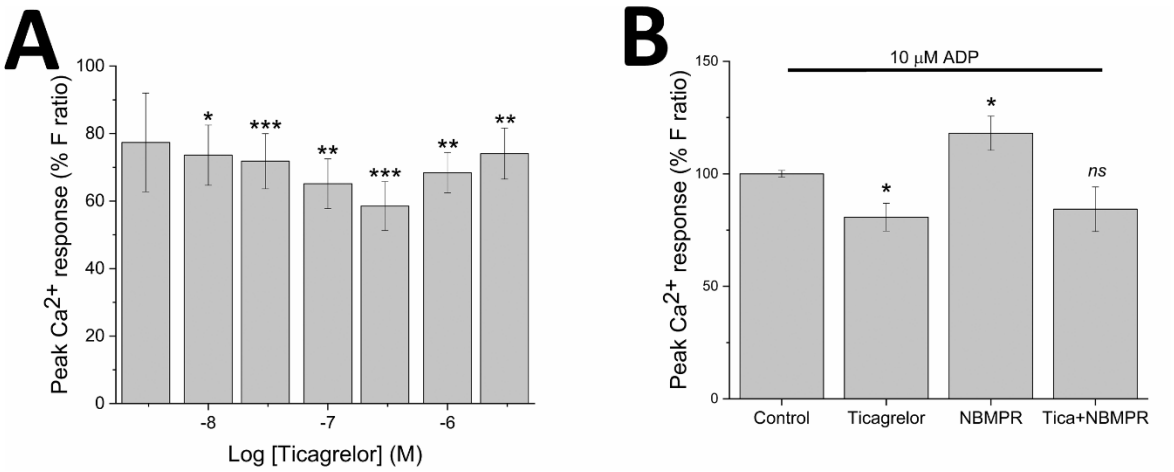

Figure 4.9 The inhibitory effect of Ticagrelor on the ADP-evoked calcium response in primary human *in vitro* differentiated adipocytes is due to inhibition of $P2Y_{12}$ receptors not ENT1. (A) The effect of increasing concentrations of Ticagrelor on the calcium response evoked by 10 µM ADP (*N*=6). (B) Effect of co-application of 300 nM Ticagrelor and 10 nM NBMPR on the response to 10 µM ADP (*N*=7). All data are normalised to the ADP-evoked calcium response in the presence of vehicle (control) in each donor and then average across donors. **p*<0.05, ***p*<0.005, ****p*<0.001, *ns* not significant (*p*>0.05) versus the response to ADP in the presence of vehicle alone.

4.7 Activation of $P2Y_{12}$ with ADP causes a decrease in intracellular cAMP

Activation of G_i-coupled receptors, such as $P2Y_{12}$, leads to inhibition of adenylate cyclase and subsequently a decrease in cAMP production. To identify whether G_i-coupled signalling pathways were being activated by ADP in human adipocytes, the amount of intracellular cAMP was quantified. Forskolin was used to elevate cAMP by directly stimulating adenylate cyclase (Insel and Ostrom, 2003) to amplify any effects observed for analytical ease. Under these conditions, acute stimulation of adipocytes with 10 μM ADP produced a significant reduction in intracellular cAMP, which was unaffected by inhibition of $P2Y_1$, but was reversed when $P2Y_{12}$ receptors were selectively antagonised with PSB0739 (Figure 4.10). Interestingly, pre-incubation of adipocytes with PSB0739 alone caused a significant increase in intracellular cAMP, which suggests that there may be tonic $P2Y_{12}$ receptor activity in these cells. On average the concentration of intracellular cAMP also increased in the presence of PSB0739 and ADP, but the variability between donors was too great for this increase to be statistically significant. Taken together, these results indicate that there are functionally active G_i-coupled P2Y receptors present in primary human adipocytes and this pathway is likely to be mediated by $P2Y_{12}$ receptors, whereas $P2Y_1$ receptors do not play a role in regulating intracellular cAMP levels.

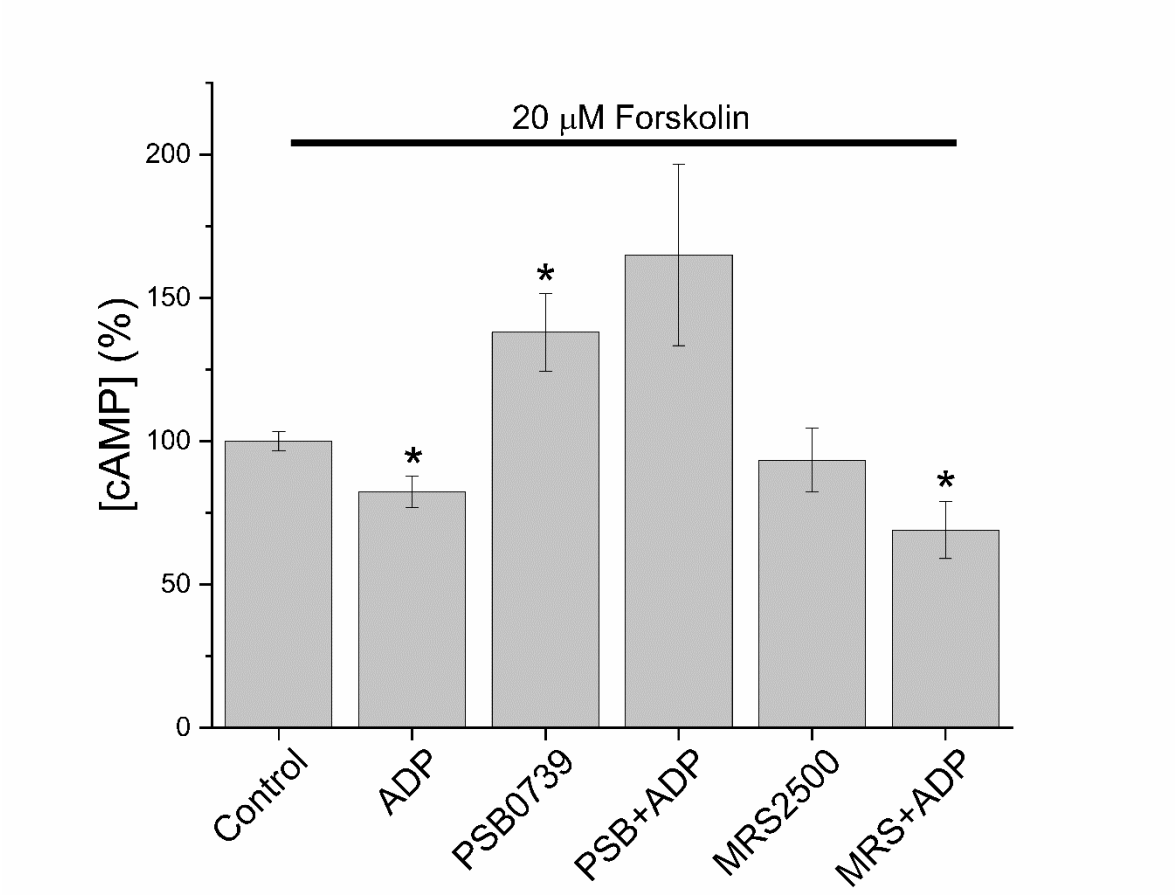

Figure 4.10 ADP causes a reduction in intracellular cyclic AMP that is reversed in the presence of a selective $P2Y_{12}$ receptor antagonist (*N*=5). Primary human *in vitro* differentiated adipocytes were stimulated with 10 μM ADP in the presence and absence of 1 μM MRS2500 ($P2Y_1$ receptor antagonist) and/or 3 μM PSB0739 ($P2Y_{12}$ receptor antagonist) and then the intracellular cAMP levels were quantified using a CatchPoint cAMP assay. Intracellular cAMP levels were artificially augmented by stimulating the cells with 20 μM forksolin. *p<0.05 versus control (cAMP level in the presence of forskolin and vehicle alone).

4.8 G_i-mediated signalling is involved in the ADP-evoked calcium response in primary human adipocytes

$P2Y_{12}$ is a G_i-coupled receptor, thus activation of this receptor is classically associated with causing downstream blockade of intracellular cAMP production. Therefore, at first glance it may appear odd that $P2Y_{12}$ receptors may be involved in ADP-evoked calcium responses. However, there are several studies that show that $P2Y_{12}$ can control intracellular Ca^{2+} levels via modulation of the concentration of cAMP in the cytosol (Sage *et al.*, 2000; Fox *et al.*, 2004; Hardy *et al.*, 2004). Inhibition of G_i signalling pathways using pertussis toxin (PTx) (Katada *et al.*, 1983) decreases the magnitude of the Ca^{2+} response evoked by ADP (Figure 4.11), which supports the hypothesis that a changes in intracellular cAMP may influence the ADP-evoked Ca^{2+} response. It is likely that the G_i-signalling pathways are mediated through $P2Y_{12}$ receptor activation, as equivalent levels of inhibition were achieved by inhibiting $P2Y_{12}$ and G_i-signalling independently, and no further inhibition was observed with combined blockade of both $P2Y_{12}$ receptors and G_i signalling (Figure 4.11B; $p>0.05$). Furthermore, although inhibition of $P2Y_1$ receptors and impeding G_i-signalling caused comparable decreases in the magnitude of the response to ADP, combined antagonism of both $P2Y_1$ and G_i-signalling has an additive effect (Figure 4.11C), which suggests that the $P2Y_1$-mediated component of the ADP response is independent of the G_i-mediated component. Interestingly the combined application of PTx and MRS2500 ($P2Y_1$ antagonist) had a greater inhibitory effect than simultaneous MRS2500 and PSB0739 ($P2Y_{12}$ antagonist) treatment (Figure 4.7H), despite the fact that it is hypothesised here that both of these effects are achieve via blockade of the same receptor-mediated pathways. This discrepancy may point towards the involvement of additional receptors or alternatively it may just be that PTx is more effective than a competitive $P2Y_{12}$ receptor antagonist.

In combination with the data presented in Section 4.6 and 4.7, these data indicate that the ADP-evoked calcium response in primary human adipocytes is mediated via two distinct, but possibly synergistic, pathways. $P2Y_1$ receptors activate G_q-mediated release of Ca^{2+} from the intracellular stores, while activation of $P2Y_{12}$ receptors cause G_i-mediated inhibition of cAMP, which subsequently potentiates the Ca^{2+} response. This proposed mechanism suggests roles for both G_i and G_q-mediated signalling pathways. However, although blockade of G_i-signalling diminishes the response to ADP, blockade of G_q-mediated pathways, via inhibition of PLC (Figure 4.6), abolishes the response to ADP, which suggests a predominant role for G_q-signalling in ADP-evoked calcium responses.

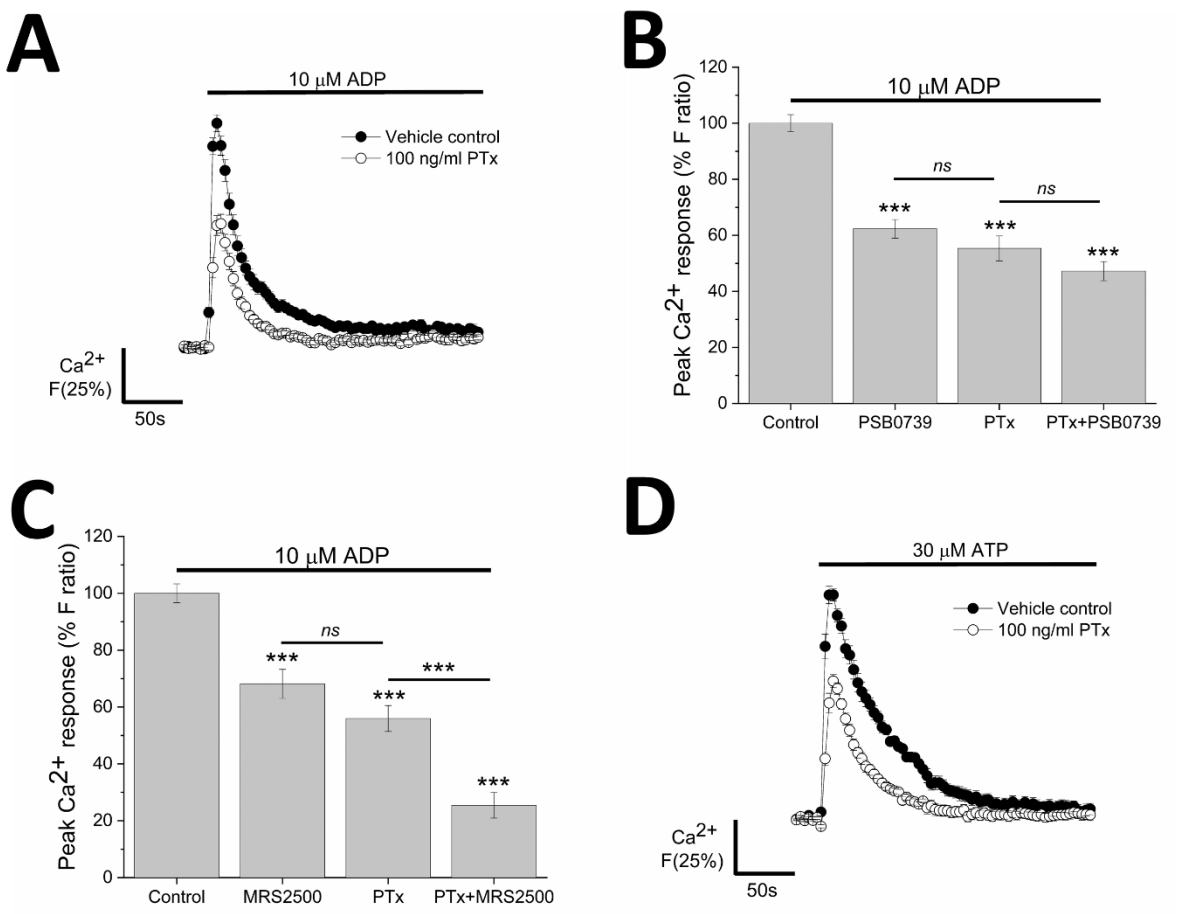

Figure 4.11 Inhibition of G_i-signalling using pertussis toxin (PTx) diminishes the response to ATP and ADP-evoked calcium responses in primary human *in vitro* differentiated adipocytes. Average time-resolved traces showing the response to (A) 10 μM ADP (*N*=7) or (D) 30 μM ATP (*N*=6) in the presence (*open circles*) or absence (*closed circles*) of 100 ng/ml PTx. The effect of PTx in the presence and absence of (B) 3 μM PSB0739 ($P2Y_{12}$ antagonist) (*N*=6) or (C) 1 μM MRS2500 ($P2Y_1$ antagonist) (*N*=6) on the peak magnitude of the ADP-evoked calcium response. All data are normalised to the ADP-evoked calcium response in the presence of vehicle (control) in each donor and then averaged across donors. ***p<0.001 versus the response to ADP in the presence of vehicle control or ***p<0.001 or *ns* (not significant; p>0.05) between the two conditions under the bar.

4.9 ATP and UTP-evoked calcium response are mediated by $P2Y_2$ receptors

In addition to having a functional response to ADP, primary human adipocytes also exhibit ATP and UTP-evoked calcium responses (Figure 4.3). To identify the molecular basis of these responses, the nucleotide responses were antagonised with subtype-selective antagonists. This revealed that neither P2X4 nor P2X7 receptors were involved in ATP-evoked calcium responses (Figure 4.12A-D). The lack of ionotropic P2X involvement in the ATP response is supported by the fact that the ATP response is abolished when PLC is inhibited (Figure 4.6A,B), which strongly suggests a predominance of metabotropic P2Y receptors. Furthermore, selective antagonism of $P2Y_{11}$ receptors also revealed that $P2Y_{11}$ receptors were not involved in the ATP-evoked calcium response (Figure 4.12E,F). This again is perhaps not surprising, as the mRNA transcript analysis revealed heterogeneity in the expression of $P2Y_{11}$ between donors, whereas the ATP response is consistently detected across all donors tested.

Selective antagonism of $P2Y_2$ receptors, using AR-C118925XX, caused a concentration-dependent decrease in the peak magnitude (IC_{50} 683 ± 116 nM (*N*=6); Figure 4.13A) and the area under the curve (IC_{50} 434 ± 133 nM (*N*=6); Figure 4.13B) of the response to 30 µM ATP. Although the IC_{50} values calculated from the magnitude and area under the curve data are almost identical, the amount of inhibition of the magnitude and net movement of calcium observed varied greatly (Table 4.3). The magnitude was diminished by 20.4 ± 3.6% (*N*=6) using 10 µM AR-C118925XX, whereas the same concentration of antagonist caused a 47 ± 1.7% (*N*=6) reduction in the area under the curve. Selective antagonism of $P2Y_2$ receptors compelled the response to ATP to decay faster than the response in the presence of vehicle alone (Figure 4.13C). In fact, in the presence of 10 µM AR-C118925XX, the response to 30 µM ATP greatly resembles the very fast response observed with ADP. These data strongly support the hypothesis that a component of the ATP response, particularly the latter decay phase of the response, is mediated by activation of $P2Y_2$ receptors, although approximately 50% of the response is resistant to the effects of AR-C118925XX, which indicates that other receptors may also play a role.

The UTP response is abolished when $P2Y_2$ receptors are selectively antagonised with AR-C118925XX (Figure 4.13D-F). AR-C118925XX causes concentration-dependent inhibition of the peak magnitude (IC_{50} 318 ± 399 nM (*N*=6); Figure 4.13D) and the area under the curve (IC_{50} 474 ± 527 nM (*N*=6); Figure 4.13E). Although 10 µM AR-C118925XX was sufficient to abolish the response to 30 µM UTP in all six donors tested, the effects of AR-C118925XX were more potent in some donors. In four of six donors, 3 µM AR-C118925XX caused 100% inhibition of the response to UTP. One donor was particularly sensitive to AR-C118925XX and 1 µM was able to eliminate the response to UTP. Irrespective of the potency of the effect, these data strongly suggest that the UTP-evoked calcium response is mediated by $P2Y_2$ receptors.

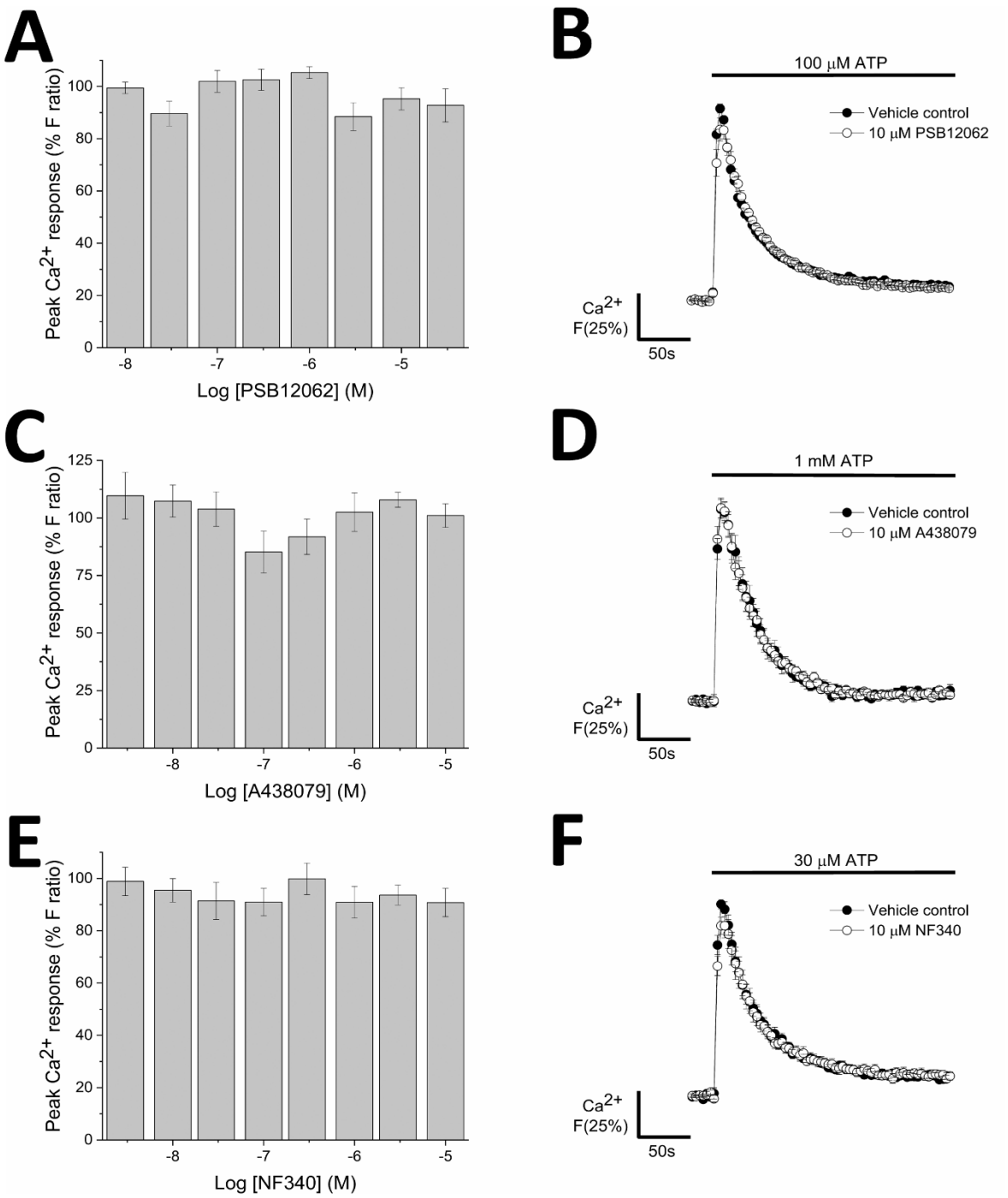

Figure 4.12 Selective antagonism of P2X4, P2X7 and $P2Y_{11}$ receptors had no inhibitory effect on the ATP-evoked calcium response in primary human *in vitro* differentiated adipocytes (*N*=6). (A) The response to 100 μM ATP antagonised with increasing concentrations of the selective P2X4 receptor antagonist, PSB12062. (C) The response to 1 mM ATP antagonised with increasing concentrations of the selective P2X7 receptor antagonist, A438079. (E) The response to 30 μM ATP antagonised with increasing concentrations of the selective $P2Y_{11}$ receptor antagonist, NF340. Average time-resolved traces showing the response to ATP in the presence (*open circles*) and absence (*closed circles*) of (B) 10 μM PSB12062, (D) 10 μM A438079 or (F) 10 μM NF340. All data points are normalised to their respective agonist responses in the presence of vehicle alone. Data points are expressed as mean ± SEM.

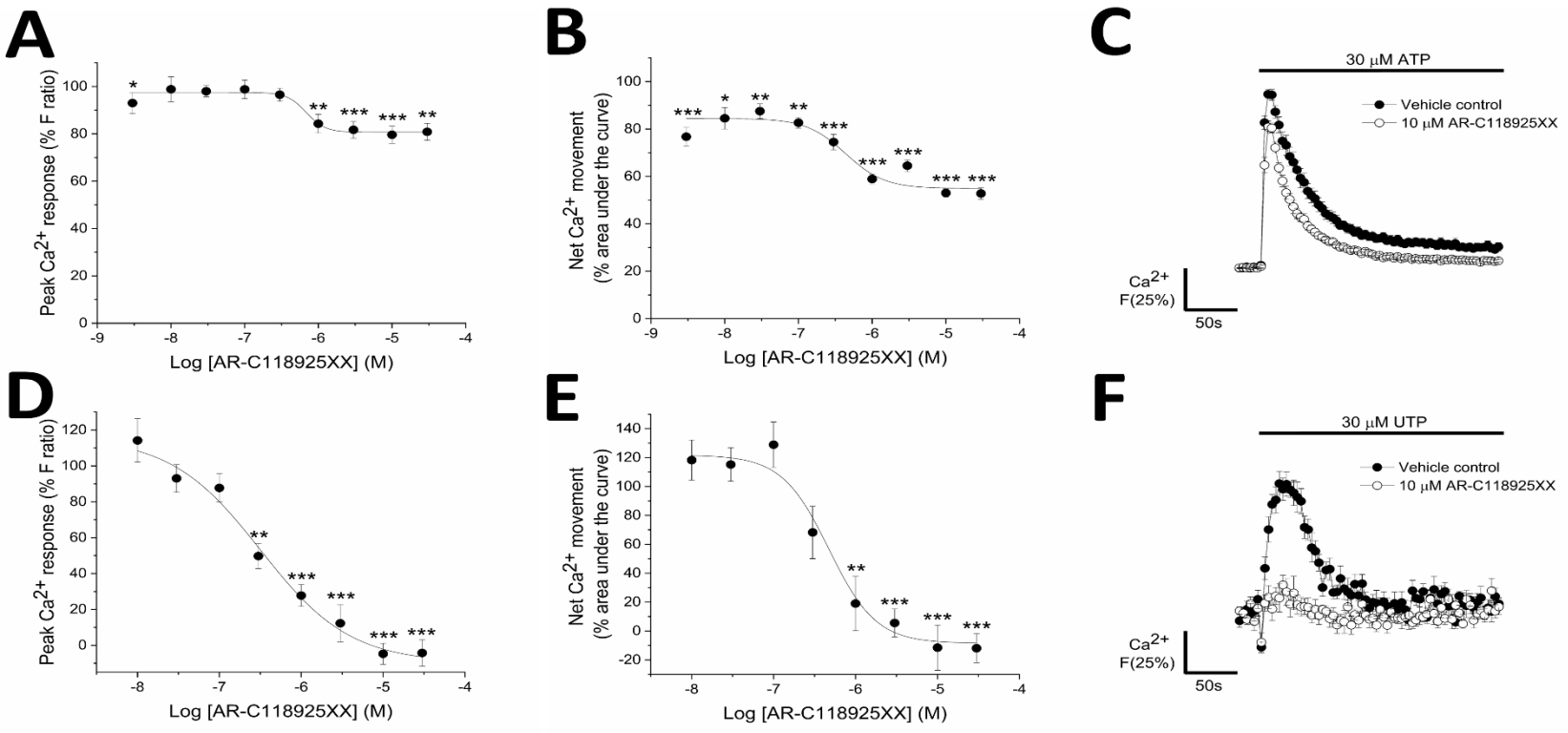

Figure 4.13 Selective antagonism of $P2Y_2$ receptors with AR-C118925XX has an inhibitory effect on the response to ATP and abolishes the response to UTP in primary human *in vitro* differentiated adipocytes. Effect of AR-C118925XX on the peak magnitude of the response to (A) 30 µM ATP (*N*=6) and (D) 30 µM UTP (*N*=6). Effect of AR-C118925XX on the net movement of calcium caused by (B) 30 µM ATP (*N*=6) and (E) 30 µM UTP (*N*=6). (C) Time-resolved traces showing the response to ATP in the presence (*open circles*) and absence (*closed circles*) of 10 µM AR-C118925XX (*N*=6). (F) Time-resolved traces showing the response to UTP in the presence (*open circles*) and absence (*closed circles*) of 30 µM AR-C118925XX (*N*=6). All data points are normalised to their respective agonist responses in the presence of vehicle alone. Data points are expressed as mean ± SEM. * $p<0.05$, ** $p<0.005$, *** $p<0.001$ versus the response to ATP or UTP in the presence of vehicle only.

4.10 shRNA-mediated knockdown of $P2Y_2$ receptor expression mimics the trends observed with pharmacological inhibition of $P2Y_2$ receptors

Lentivirus delivery of shRNA was used to successfully decrease the expression of $P2Y_2$ receptors in primary human *in vitro* differentiated adipocytes. Quantitative PCR analysis revealed that receptor expression was decreased by 63.5 ± 4.5% (*N*=4). Most of the general trends observed with pharmacological inhibition of $P2Y_2$ on the ATP and UTP-evoked Ca^{2+} responses were also observed with shRNA-mediated knockdown of $P2Y_2$ receptor expression in primary human adipocytes (Figure 4.14). However, unlike selective antagonism of $P2Y_2$ receptors with AR-C118925XX, shRNA-mediated knockdown of the receptor does not cause a significant decrease in the peak magnitude of the response to ATP. This is perhaps unsurprising as the effect of AR-C118925XX on the peak magnitude is quite subtle (Table 4.3; Figure 4.13) and 100% receptor knockdown was not achieved. However, it is clear from the time-resolved traces (Figure 4.14A) and the τ values (Figure 4.14C) that the response to ATP decayed faster than the response in the scrambled cells, which mirrors the effects observed with pharmacological inhibition of $P2Y_2$ receptors (Figure 4.13C). In addition, the response to 30 μM UTP was diminished when $P2Y_2$ receptor expression was decreased (Figure 4.14D-F). As with the ATP response, the effects of shRNA-mediated receptor knockdown are more subtle than the effects of pharmacological inhibition. The inhibitory effect on the peak magnitude of the UTP was not statistically significant (Figure 4.14E), but the area under the curve was significantly decreased post receptor knockdown (Figure 4.14F). Taken together, these data support the pharmacological evidence for a role for $P2Y_2$ in the ATP and UTP-evoked calcium responses in primary human adipocytes. The slight discrepancies between the pharmacological and shRNA-mediated knockdown data are likely to be due to incomplete knockdown of $P2Y_2$ receptor expression.

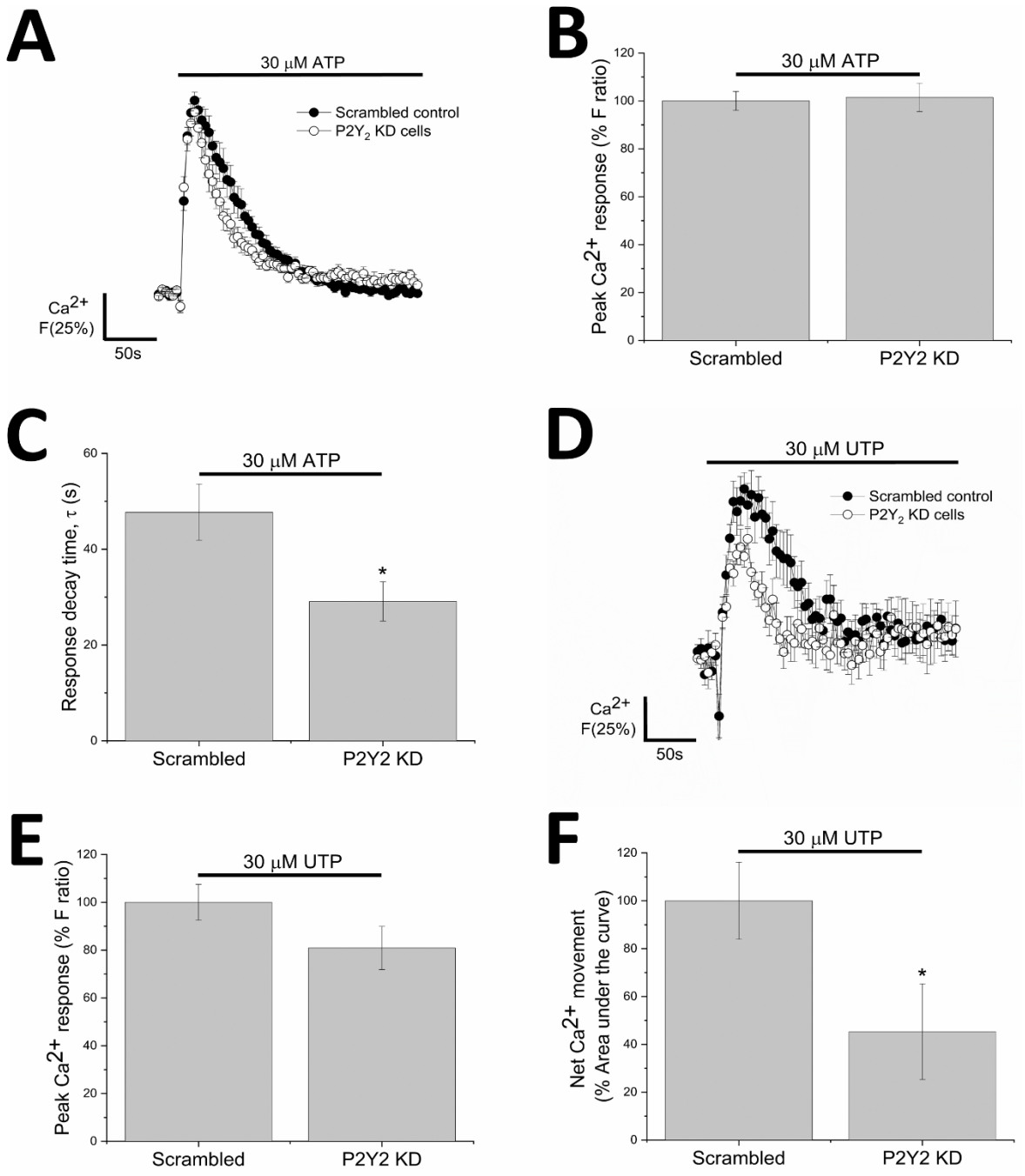

Figure 4.14 shRNA-mediated knockdown of $P2Y_2$ receptors in primary human *in vitro* differentiated adipocytes mimic many of the effects of pharmacological inhibition of $P2Y_2$ (*N*=4). (A) Average time-resolved traces showing the elevation in intracellular calcium in response to 30 μM ATP in scrambled control cells (*closed symbols*) versus $P2Y_2$ receptor knockdown cells (*open symbols*). (B) The peak magnitude and (C) decay time (τ) for the ATP-evoked Ca^{2+} response. (D) Average time-resolved traces for the response to 30 μM UTP in the scrambled control cells (*closed circles*) and $P2Y_2$ receptor knockdown cells (*open circles*). (E) The peak magnitude data and (F) area under the curve data for the UTP-evoked Ca^{2+} response. All data points are normalised to their respective agonist responses in the scrambled control cells, excluding the decay time for the ATP response (C) which was not normalised. Data points are expressed as mean ± SEM. * $p<0.05$ versus the agonist response in the scrambled control cells.

4.11 ATP-evoked calcium responses are inhibited by selective inhibition of $P2Y_1$ and $P2Y_{12}$ receptors

As demonstrated in Section 4.9 and 4.10, $P2Y_2$ receptors mediate part of the response to ATP, but greater than 50% of the response is resistant to the effect of $P2Y_2$ inhibition, which suggests that other purinergic receptors may be involved in this response. P2X receptors and $P2Y_{11}$ receptors are not involved in the response to ATP (Table 4.3; Figure 4.12), but the responses are sensitive to pertussis toxin (Figure 4.10D) and in the presence of AR-C118925XX, the response to ATP resembles the response to ADP (Figure 4.13C), which suggests that ADP receptors may play a role in the response to ATP. This hypothesis was readily confirmed as selective antagonism of $P2Y_1$ receptors (IC_{50} 415 ± 160 nM *N*=6) caused concentration-dependent antagonism of the response to 30 µM ATP, with a decrease of 32.3 ± 3.8% (*N*=6) being observed with maximal concentrations of MRS2500 (1 µM; $P2Y_1$ antagonist) (Figure 4.15A,B). However, the potency and extent of inhibition was lower for the ATP response than the effects observed on the ADP response (Table 4.3). In addition, the ATP-evoked calcium response was also inhibited in a concentration dependent manner by the selective $P2Y_{12}$ antagonist, PSB0739 (Figure 4.15C,D; IC_{50} >10 µM *N*=6). Maximal concentrations of PSB0739 (10 µM) caused a 46.8 ± 4.5% (*N*=6) decrease in the peak magnitude and a 44.5 ± 5.2% (*N*=6) decrease in the net movement of calcium in response to 30 µM ATP (Table 4.3). Although, PSB0739 inhibited the responses to ATP and ADP to the same extent, the effects of PSB0739 were less potent on the ATP response than the ADP response (Table 4.3). The most probable explanation for the role of ADP receptors in the ATP response is that cell surface ectonucleotidases hydrolyse exogenous ATP to ADP, which then activates $P2Y_1$ and $P2Y_{12}$ receptors (Zimmermann, 2001; Yegutkin, 2014).

Unlike the ADP response, there does not appear to any overlap in the action of $P2Y_1$ and $P2Y_{12}$ receptors in the response to ATP, as combined antagonism of $P2Y_1$, $P2Y_2$ and $P2Y_{12}$ had an additive effect (Figure 4.15E). Totalling the average inhibition of the response to ATP caused by each antagonist independently suggests that combined antagonism should result in a 61.6% decrease in the response magnitude. This value is almost identical to the average amount of inhibition achieved by combined antagonism experimentally: 63.0 ± 3.4% (*N*=6) inhibition. It is important to note that the effect of each antagonist (MRS2500, PSB0739 and AR-C118925XX) alone was lower for the combined antagonism experiments than the inhibition curve experiments, but these differences are likely to be due to donor-to-donor variability, as cells from different donors were used for these two experiments.

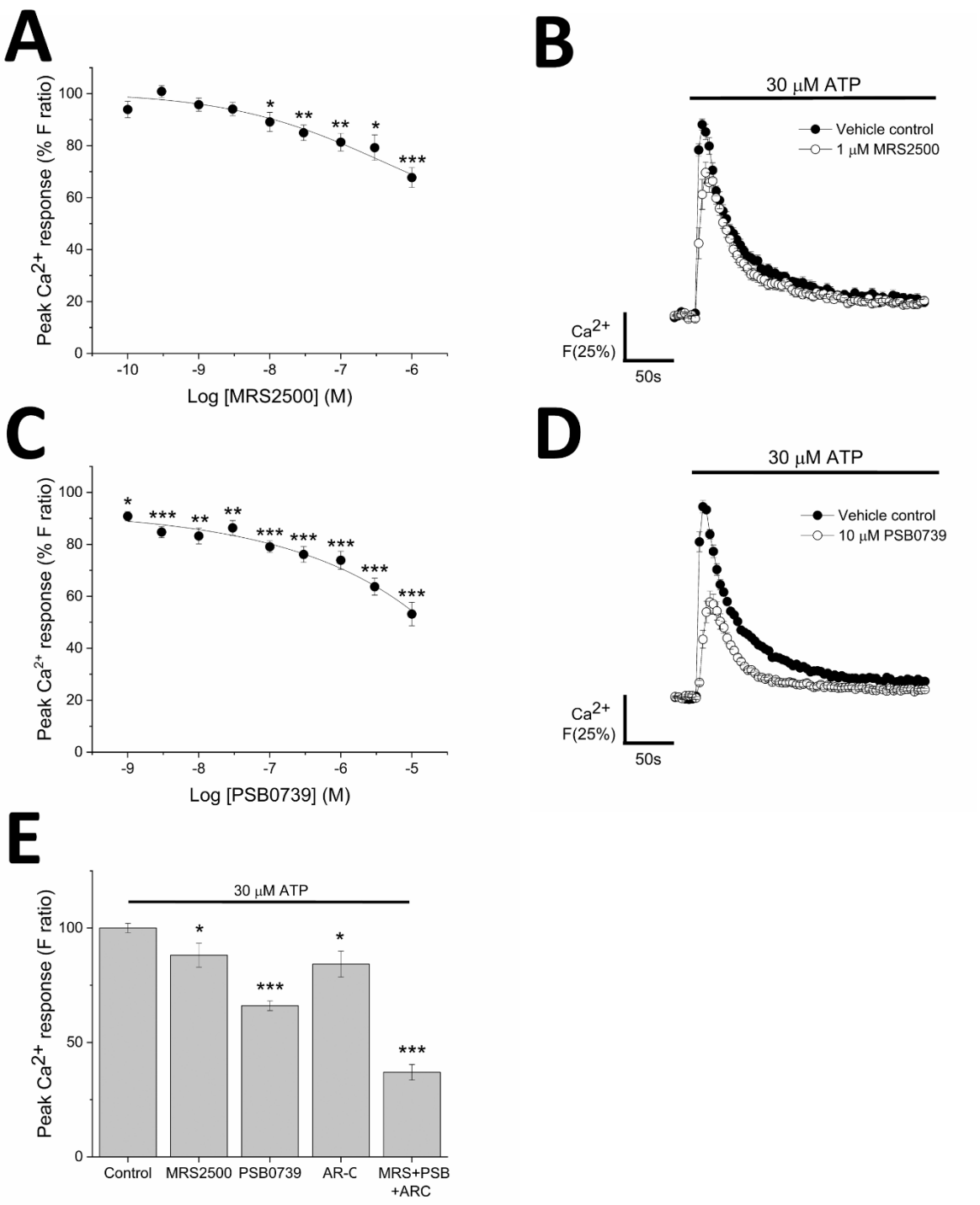

Figure 4.15 Selective antagonism of $P2Y_1$ and $P2Y_{12}$ receptors has a concentration-dependent inhibitory effect on the ATP-evoked calcium response in primary human *in vitro* differentiated adipocytes (*N*=6). The response to 30 μM ATP antagonised with increasing concentrations of (A) MRS2500 (selective $P2Y_1$ antagonist) or (C) PSB0739 (selective $P2Y_{12}$ antagonist). Average time-resolved traces showing the response to ATP in the presence (*open circles*) and absence (*closed circles*) of (B) 1 μM MRS2500 or (D) 10 μM PSB0739. (E) Effect of combined antagonism of $P2Y_1$, $P2Y_2$ and $P2Y_{12}$ receptors. All data points are normalised to the response to ATP in the presence of vehicle (control response). Data points are expressed as mean ± SEM. * p<0.05, ** p<0.005, *** p<0.001 versus the response to ATP in the presence of vehicle only.

Table 4.3 The effect of P2 subtype selective antagonism on the nucleotide-evoked calcium responses in primary human *in vitro* differentiated adipocytes. All the values in the maximum inhibition and IC_{50} columns were determined using cells from six independent donors.

Selective antagonist	Receptor target	Nucleotide [concentration, µM]	Antagonist range, µM	Maximum inhibition (%)[a] [antagonist concentration, µM]	IC_{50}, nM[a]	Reference
PSB-12062	P2X4	ATP [100]	0.003 – 30	*NS*	-	(Hernandez-Olmos *et al.*, 2012)
A438079	P2X7	ATP [1000]	0.003 – 10	*NS*	-	(Nelson *et al.*, 2006)
MRS2500	$P2Y_1$	ATP [30]	0.0001 – 1	32.3 ± 3.8 [1]	415 ± 160	(Kim *et al.*, 2003)
				33.6 ± 3.6 [1]	>1000	
		ADP [10]	0.0001 – 1	45.1 ± 4.7 [1]	77.1 ± 37.5	
				45.4 ± 6.9 [1]	>1000	
AR-C118925XX	$P2Y_2$	ATP [30]	0.003 - 30	20.4 ± 3.6 [10]	683 ± 116	(Rafehi *et al.*, 2017)
				47 ± 1.7 [10]	434 ± 133	
		UTP [30]	0.003 - 30	100%	318 ± 399	
				100%	474 ± 527	
MRS2578	$P2Y_6$	ADP [10]	0.003 – 10	*NS*	-	(Mamedova *et al.*, 2004)
NF340	$P2Y_{11}$	ATP [30]	0.003 - 10	*NS*	-	(Meis *et al.*, 2010)

		ADP [10]	0.003 – 10	*NS*	-	
PSB-0739	$P2Y_{12}$	ATP [30]	0.003 – 10	46.8 ± 4.5 [10]	<10,000	(Hoffmann *et al.*, 2009)
				44.5 ± 5.2 [10]	<10,000	
		ADP [10]	0.003 – 10	38.4 ± 5.1 [10]	64.0 ± 56.5	
				55.4 ± 4.4 [10]	162 ± 25.4	
MRS2211	$P2Y_{13}$	ATP [30]	0.003 – 3	*NS*	-	(Kim *et al.*, 2005)
		ADP [10]	0.003 – 3	*NS*	-	

[a]IC_{50} values and max % inhibition values were calculated with the peak magnitude values (top) and area under the curve data (bottom) for each agonist/antagonist combination. *NS* indicates no significant inhibition at any concentration of antagonist tested.

4.12 $P2Y_1$, $P2Y_2$ and $P2Y_{12}$ are expressed in mature adipocytes in human subcutaneous adipose tissue

In order to confirm that the functional P2 receptors detected in the *in vitro* model of mature human adipocytes were also expressed in mature adipocytes in human adipose tissue, immunohistochemistry was performed. This revealed that all three receptors were indeed expressed (Figure 4.16). Although, it was not possible to confirm that these receptors are functional in human adipocytes *in vivo* within the scope of this study, positive confirmation of $P2Y_1$, $P2Y_2$ and $P2Y_{12}$ receptors in adipose tissue suggests that there is some symmetry between the cells in human adipose tissue and the *in vitro* differentiated model. However, unlike the *in vitro* model (Figure 4.2), all three receptors are clearly detected at the edge of cell, rather than throughout the cells. This may be due to the unilocular morphology of mature adipocytes in human adipose tissue, where the large lipid droplet pushes all the other components of the cell to the periphery, thus making it difficult to distinguish between true membrane staining and intracellular staining.

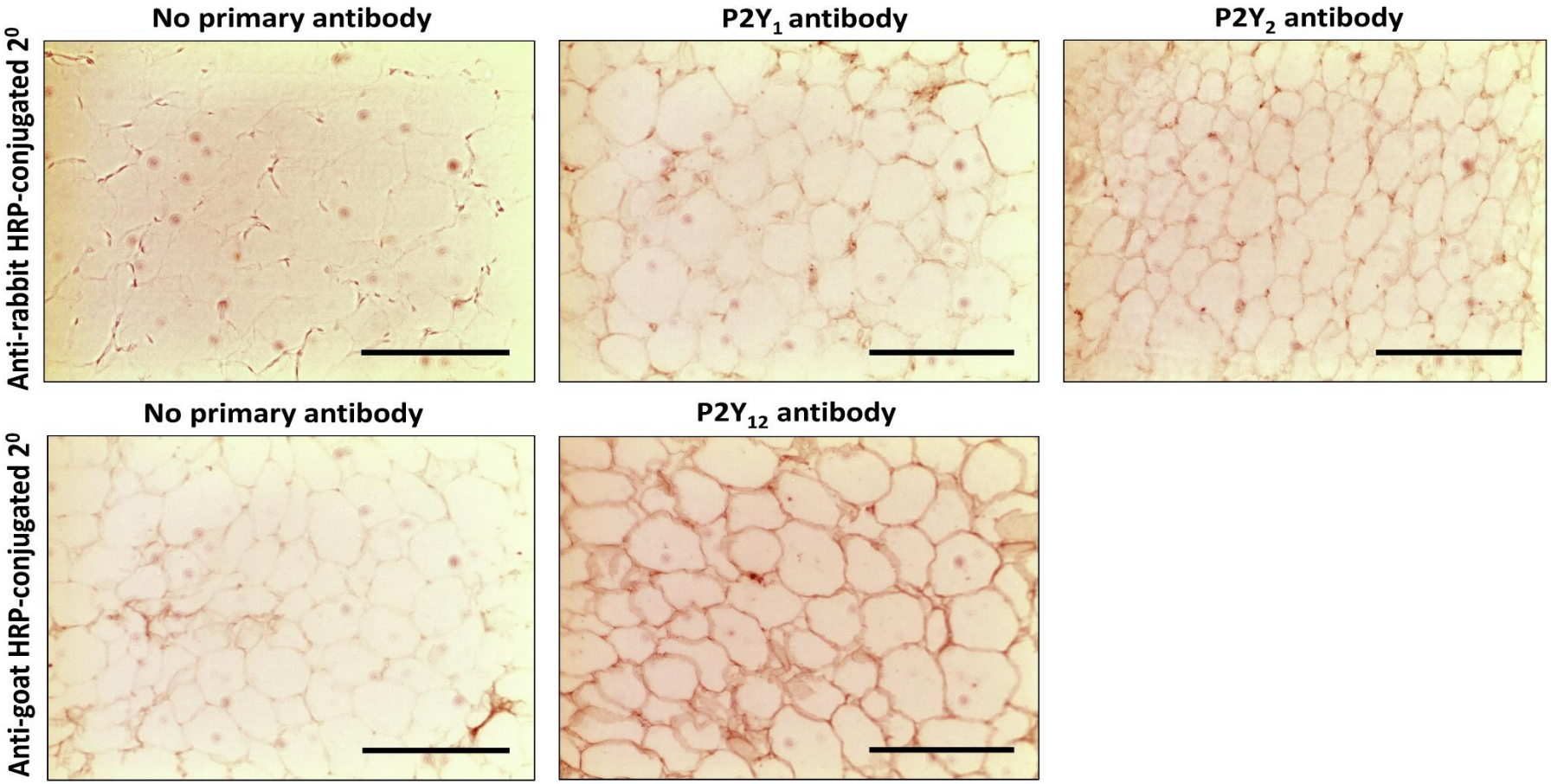

Figure 4.16 Immunohistochemical staining for $P2Y_1$, $P2Y_2$ and $P2Y_{12}$ receptors in 6 µm sections of paraffin-embedded primary human subcutaneous abdominal adipose tissue. Immunoreactivity visualized using anti-rabbit or anti-goat HRP-conjugated secondary antibodies. Non-specific secondary binding was controlled for in the absence of anti-P2Y receptor antibodies (*no primary controls*). Scale bar represents 200µm.

4.13 Summary

Primary human *in vitro* differentiated adipocytes express a wide variety of P2 receptors, including P2X4, P2X5, P2X6, P2X7, $P2Y_1$, $P2Y_2$, $P2Y_4$, $P2Y_6$, $P2Y_{11}$, $P2Y_{12}$ and $P2Y_{13}$, but lack P2X1, P2X2, P2X3 and $P2Y_{14}$ receptors. Although there was some heterogeneity in the expression P2 receptor profile amongst donors, there was remarkably consistent functional evidence of nucleotide-evoked calcium responses in human adipocytes. Exogenous application of ATP, ADP and UTP produced transient increases in the concentration of intracellular calcium, whereas physiological concentrations of UDP and UDP-glucose did not alter intracellular calcium levels. The lack of a functional response to UDP-glucose is perhaps unsurprising as $P2Y_{14}$ was not detected in the majority of donors.

Although human *in vitro* differentiated adipocytes appear to express four of the seven known P2X receptor subtypes, these P2X receptors do not appear to play a functional role in the ATP-evoked Ca^{2+} responses under the conditions used in this study. This is evidenced by the fact that the response to ATP persisted in the absence of extracellular calcium, inhibition of PLC abolished the response and selective antagonism of P2X4 and P2X7 had no effect on the response. These results may be due to the use of sub-optimum conditions for the activation of P2X receptors, such as the use of insufficiently elevated ATP concentrations to activate P2X7 (North, 2002). Alternatively, it is possible that the receptors are not expressed at the cell surface, thus exogenous application of nucleotides is unable to activate the receptors. For example, P2X4 receptors are known to localise to lysosomes and traffic to and from the plasma membrane in other cell types (Ashour and Deuchars, 2004; Stokes, 2013). Although P2X receptors do not appear to be directly involved in initiating ATP-evoked calcium responses, the magnitude of the response to ATP is heavily dependent on the presence of extracellular calcium, so it is conceivable that the initial metabotropic response to ATP is potentiated by subsequent Ca^{2+} entry via P2X receptors.

All of the known P2Y receptors, excluding $P2Y_{14}$ receptors, were detected at both the mRNA and protein level in adipocytes. However, subtype-specific antagonism of $P2Y_6$, $P2Y_{11}$ and $P2Y_{13}$ receptors had no effect on nucleotide-evoked responses, which suggests that these receptors are not functionally active under the conditions used in this study. The UTP response was completely abolished by selective antagonism of $P2Y_2$, which indirectly suggests $P2Y_4$ receptors are also non-functional in these cells. It is not possible to conclusively rule out a role for $P2Y_4$ receptors, as there is currently no commercially-available selective antagonist for this receptor (Jacobson *et al.*, 2009).

The responses to ATP, ADP and UTP were all abolished by inhibition of PLC, which indicates a predominance of G_q-mediated signalling, however the responses to ADP and ATP were also substantially decreased, but not abolished, when G_i-signalling pathways were inhibited. This suggests that multiple signalling pathways may be involved in the nucleotide-evoked calcium

responses in human adipocytes. Indeed, subtype-selective antagonism revealed that a combination of G_q and G_i-coupled receptors were involved in the ATP and ADP response: $P2Y_1$, $P2Y_2$ and $P2Y_{12}$ receptors. It is proposed here that the ATP response is partially mediated by $P2Y_2$ receptor activation, but the majority of the increase in intracellular calcium is produced by activation of ADP receptors, via liberation of ADP from ATP by cell surface ectonucleotidases (Yegutkin, 2014). The ADP is then able to cause PLC-mediated release of Ca^{2+} from the intracellular stores via activation of $P2Y_1$ receptors, while simultaneously activating $P2Y_{12}$ receptors to potentiate the level of intracellular calcium indirectly via modulation of cytosolic cAMP levels (Hardy *et al.*, 2004).

The data outlined in this Chapter identifies three purinergic receptors that are functionally active in primary human *in vitro* differentiated adipocytes: $P2Y_1$, $P2Y_2$ and $P2Y_{12}$. These data will be used as a foundation for exploring the downstream role of purinergic signalling in human adipocytes. Efforts to identify the cellular functions of these receptors will be outlined in Chapter 5.

Chapter 5: Determining the role of purinergic signalling in basal lipolysis and adipokine secretion

5.1 Introduction

Adipocytes are highly dynamic cells, which are able to respond to external cues, such as nervous or hormonal stimulation, to either store energy as triglycerides via lipogenesis or release energy in the form of free fatty acids (FFA) and glycerol via lipolysis (Rutkowski *et al.*, 2015). Prolonged fasting induces lipolysis to ensure that FFA are available for β-oxidation to provide energy when glucose availability is limited. Fasting initiates sympathetic nervous stimulation of adipose tissue via catecholamine-mediated activation of β-adrenoreceptors on the surface of the adipocyte (Fain, 1973). Activation of β-adrenoreceptors initiates G_s-mediated stimulation of adenylate cyclase to elevate cytoplasmic cyclic AMP (cAMP) levels, which then activates protein kinase A (PKA). Activated PKA phosphorylates hormone sensitive lipase (HSL) and perilipins on the surface of the lipid droplet to allow translocation of HSL from the cytoplasm to the lipid droplet (Miyoshi *et al.*, 2006). PKA also phosphorylates comparative gene identification-58 (CGI-58) (Sahu-Osen *et al.*, 2015), a co-activator of adipose triglyceride lipase (ATGL), which increases the activity of ATGL by up to 20-fold (Schweiger *et al.*, 2006; Miyoshi *et al.*, 2008). At the surface of the lipid droplet, ATGL, HSL and monoglyceride lipase (MGL) catalyse the sequential hydrolysis of triglycerides to diglycerides, monoglycerides and finally glycerol. This process also yields three FFA molecules per triglyceride. The FFA are recycled or released into the bloodstream where they are able to travel to distant organs and be utilised as a cellular energy source (Ahmadian *et al.*, 2010). However, lipolysis also occurs spontaneously in the absence of hormonal or nervous stimulation and this is known as basal lipolysis. In comparison to stimulated lipolysis, little is currently known regarding the underlying mechanisms governing basal lipolysis, though it has been suggested that ATGL plays a prominent role (Miyoshi *et al.*, 2008).

Although storage and release of energy is the primary function of white adipocytes, they are also capable of synthesising a wide variety of adipokines that are capable of regulating immunity and systemic metabolism (Halberg *et al.*, 2008). Adipokine is a collective term for hormones and cytokines secreted by cells within adipose tissue, including, but not limited to, white adipocytes. The first adipokine to be identified was leptin (Zhang *et al.*, 1994). Leptin activates receptors in the hypothalamus to signal satiety, initiate decreased food intake and increased energy expenditure to

maintain an optimal adipose tissue volume (Klok *et al.*, 2007). Other examples of adipokines, include adiponectin which inhibits apoptosis, suppresses inflammation and promotes insulin sensitivity to improve systemic metabolism (Wang *et al.*, 2016). Adipocytes, and immune cells within adipose tissue, are also capable of secreting cytokines to promote tissue inflammation. The increase in fat mass associated with obesity leads to an increase in the production of proinflammatory cytokines. The resultant chronic inflammatory response has been causally linked to the development of metabolic diseases (Hotamisligil, 2006). Adipokine release is tightly regulated, however abnormal fat mass accumulation, such as in obesity, is associated with a dysregulation of adipokine production. Furthermore, elevated serum FFA levels in obese individuals, due to enhanced basal lipolysis, further stimulates inflammation and insulin resistance (Wang *et al.*, 2003; Jiao *et al.*, 2011). Additional research is required to fully appreciate the molecular mechanisms underlying adipokine release in order to facilitate safe and effective interventions to prevent or counteract the dysregulation evident in obesity.

White adipose tissue is highly innervated (Bartness *et al.*, 2014) and it is well documented that ATP is released as a co-transmitter with noradrenaline from sympathetic nerves (Kennedy, 2015). ATP is also released physiologically from cells during inflammation and injury, where it acts as a danger-associated molecular pattern (Gorini *et al.*, 2013). In addition, ATP can be constitutively released by cells (Corriden *et al.*, 2010; Sivaramakrishnan *et al.*, 2012). ATP is able to activate a wide repertoire of purinergic P2X and P2Y receptors to initiate a diverse range of physiological functions (Burnstock, 2007). In Chapter 4, it was determined that primary human *in vitro* differentiated adipocytes express functional $P2Y_1$, $P2Y_2$ and $P2Y_{12}$ receptors. In this Chapter, attempts are made to determine whether these P2 receptors have a physiological role in regulating two important functions of adipocytes: lipolysis and adipokine secretion. A greater understanding of the molecular basis of these functions is vital for the development of novel therapies to combat the global crisis of obesity and its myriad of associated comorbidities.

5.2 Human adipocytes release ATP into the extracellular space and modulate cytoplasmic calcium tone via constitutive $P2Y_2$ receptor activity

Cells can regulate purinergic responses in an autocrine manner by constitutively releasing ATP (Corriden *et al.*, 2010; Sivaramakrishnan *et al.*, 2012; Campwala *et al.*, 2013). A previous study by Adamson et al. (2015) demonstrated that 3T3-L1 mouse adipocytes are capable of secreting ATP into the extracellular space. To confirm that primary human *in vitro* differentiated adipocytes are also capable of releasing ATP, the amount of ATP in the supernatant was quantified in the presence and absence of apyrase. Apyrase is a highly active ecto-ATPase that catalyses the hydrolysis of ATP to AMP. A population of $2x10^4$ adipocytes were capable of conditioning 50 µl of supernatant with

approximately 50 nM ATP, which was successfully scavenged by apyrase treatment (*N*=3; Figure 5.1). These are bulk phase measurements of ATP and it is likely that the concentration of ATP is much higher at the cell surface, which means that under basal conditions human adipocytes secrete sufficient concentrations of ATP to activate most P2Y receptor subtypes (Gorini *et al.*, 2013).

The fact that adipocytes secrete ATP under basal conditions suggests that they are capable of constitutively activating P2 receptors expressed on the cell surface (here, and throughout this thesis, constitutive receptor activation refers to the continuous activity of a receptor due to the omnipresence of agonist achieved via constitutive agonist release, it does not refer to the receptor becoming agonist-independent). However, selective antagonism of $P2Y_1$ and $P2Y_{12}$ receptors, with MRS2500 and PSB0739 respectively, did not have a significant effect on resting intracellular calcium levels (*N*=6; *p*>0.05; Figure 5.2A,B). On average, there was a slight reduction in the concentration of cytoplasmic calcium in the presence of MRS2500, however this trend was not consistently observed across donors and consequently this change was not statistically significant (Figure 5.2A). This suggests that although there may be some constitutive $P2Y_1$ receptor activity in some donors, tonic $P2Y_1$ receptor activity is not a universal trait shared by all donors tested. As a limited number of donors were used in this study, it was not possible to fully explore the potential explanations for this variability between donors. In addition, although these results suggest persistent $P2Y_{12}$ receptor activity does not modulate intracellular calcium levels, this does not definitively rule out constitutive $P2Y_{12}$ receptor activity, as it is possible that $P2Y_{12}$ is regulating an alternative secondary messenger molecule, such as cAMP, rather than calcium (see Section 4.7).

Unlike $P2Y_1$ and $P2Y_{12}$ receptors, selective antagonism of $P2Y_2$ receptors with 10 µM AR-C118925XX (Figure 5.2C) caused a significant reduction in the concentration of cytoplasmic calcium. Inhibition of $P2Y_2$ receptors led to the concentration of intracellular calcium decreasing from 125 ± 19 nM to 47 ± 9 nM (*N*=6; *p*<0.005 vs vehicle control). Furthermore, removal of extracellular ATP with apyrase also instigated a significant reduction in intracellular calcium levels (*N*=3; *p*<0.05 vs vehicle control; Figure 5.2D). Taken together, these data suggest primary human *in vitro* differentiated adipocytes are capable of releasing ATP to act in an autocrine and/or paracrine manner to modulate intracellular calcium tone via constitutive activation of $P2Y_2$ receptors.

It is important to note that there was some variability between donors and the presence of different vehicles (water or 0.1% DMSO) appeared to influence the resting cytoplasmic calcium concentrations in adipocytes. This meant that the intracellular calcium concentration under control conditions varies between approximately 50 and 200 nM calcium in Figure 5.2. Unfortunately, it was not possible to avoid this variability, however pairwise comparisons of the effect of each antagonist versus their respective vehicle control per donor were conducted to minimise the impact of this variation.

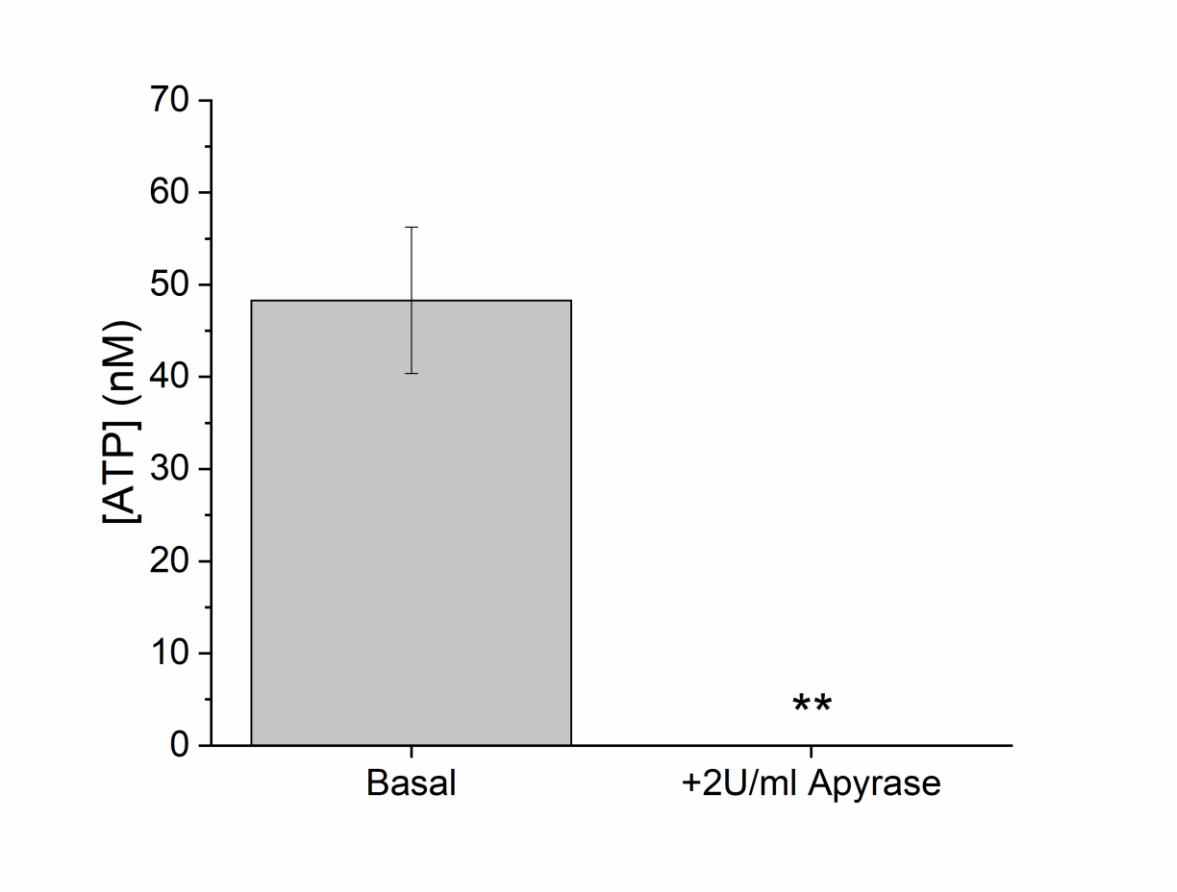

Figure 5.1 Primary human *in vitro* differentiated adipocytes secrete ATP which can be scavenged by apyrase (*N*=3). Bulk-phase measurements of ATP released into medium conditioned by human *in vitro* differentiated adipocytes. The ATP concentration was quantified using a luciferase ATP Bioluminescence Assay Kit HS II purchased from Roche and performed as per the manufacturer's instructions. Data are expressed as mean ± SEM. ** $p<0.005$ versus basal ATP release.

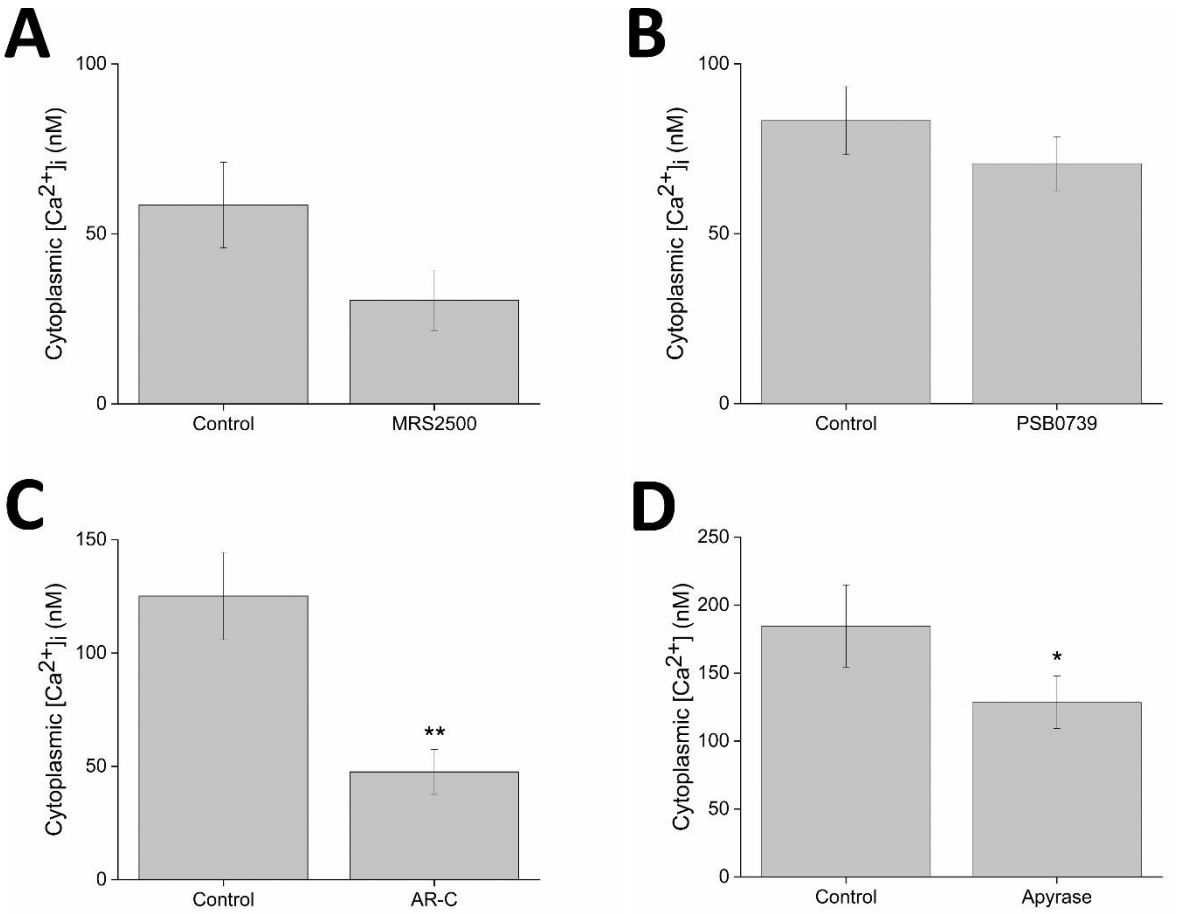

Figure 5.2 Inhibition of $P2Y_2$ receptors and removal of extracellular ATP significantly decreases the concentration of cytoplasmic calcium in primary human *in vitro* differentiated adipocytes. Effect of selective antagonism of (A) $P2Y_1$ receptors with 1 µM MRS2500 (*N*=6), (B) $P2Y_{12}$ receptors with 1 µM PSB0739 (*N*=6) and (C) $P2Y_2$ receptors with 10 µM AR-C118925XX (*N*=6) on resting cytoplasmic calcium levels. (D) Effect of scavenging extracellular ATP with 4 U/ml apyrase on resting cytoplasmic calcium levels (*N*=3). Data are expressed as mean ± SEM. **p*<0.05, ***p*<0.005 versus cytoplasmic calcium levels in the presence of vehicle only (control).

5.3 Pharmacological antagonism and shRNA-mediated knockdown of $P2Y_2$ receptor expression causes an increase in intracellular cAMP

In Section 5.2, it was demonstrated that constitutive $P2Y_2$ receptor activity regulates cytoplasmic calcium tone in primary human adipocytes. However, there are some reports that suggest that activation of $P2Y_2$ receptors can also influence intracellular cAMP levels (Post *et al.*, 1998; Gorini *et al.*, 2013). To investigate whether tonic $P2Y_2$ activation effects cytoplasmic cAMP levels, the total amount of cAMP was measured after pharmacological Inhibition of $P2Y_2$ receptors with 10 μM AR-C118925XX and shRNA-mediated knockdown of $P2Y_2$ receptor expression. This determined that both pharmacological blockade of $P2Y_2$ receptors (Figure 5.3A) and reduced receptor expression (Figure 5.3B) instigated an increase in intracellular cAMP in primary human adipocytes. Inhibition of $P2Y_2$ receptors resulted in a 23.3 ± 5.8% increase in cAMP above cells treated with vehicle only (N=4; p<0.05). However, shRNA-mediated knockdown of $P2Y_2$ receptor expression had a much more pronounced effect and caused a 177.2 ± 51.0% increase in cAMP when compared to scrambled control counterparts (N=3; p<0.05). As demonstrated by the large standard error of the mean associated with the average data for the $P2Y_2$ knockdown cells, there was considerable variability in the extent of the increase in cAMP observed per donor. One donor displaying a more muted rise of only 33.3 ± 14.6%, whereas the other two donors exhibited increases of greater than 200%. This variation may be due to varying degrees of $P2Y_2$ receptor knockdown per donor. The disparity between the average increase caused by pharmacological inhibition of the receptor versus shRNA-mediated knockdown of expression may be due to the fact that knockdown of $P2Y_2$ receptor expression is a longer-term change in $P2Y_2$ activity than pharmacological inhibition of $P2Y_2$ receptors, thus receptor knockdown is able to have a more marked effect.

In combination with the data presented in Section 5.2, these results suggest that $P2Y_2$ receptors are constitutively active and function to regulate both calcium and cAMP tone within primary human *in vitro* differentiated adipocytes. This means that in addition to the transient calcium responses evoked by exogenous application of nucleotides (Chapter 4), human adipocytes are also capable of regulating their own purinergic response in an autocrine and/or paracrine manner.

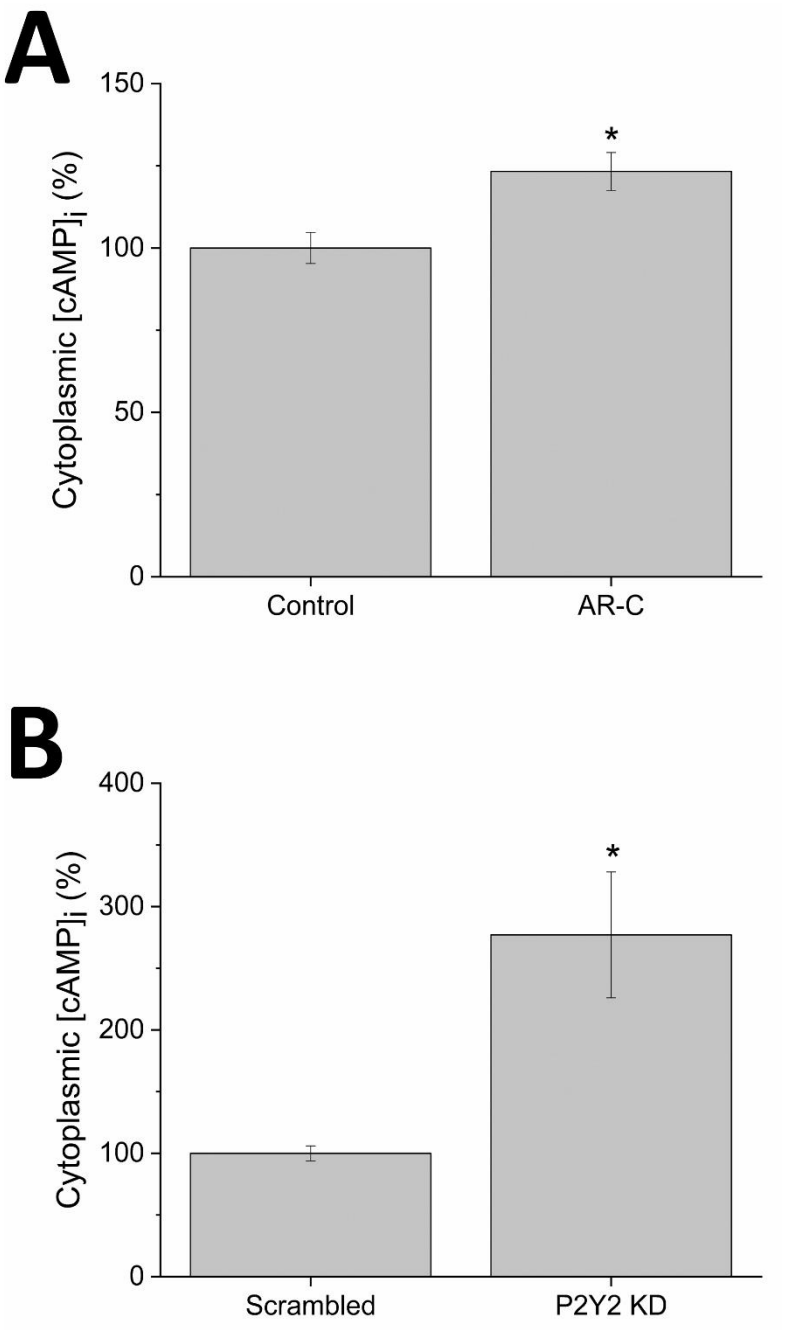

Figure 5.3 Selective antagonism of $P2Y_2$ receptors and shRNA-mediated knockdown of $P2Y_2$ receptor expression in primary human *in vitro* differentiated adipocytes causes an increase in cytoplasmic cAMP concentrations. (A) Effect of selective inhibition of $P2Y_2$ receptors with 10 µM AR-C118925XX on intracellular cAMP levels (*N*=4). (B) Effect of shRNA-mediated knockdown of $P2Y_2$ receptor expression via lentiviral delivery on intracellular cAMP levels (*N*=3). All data are normalised to the basal concentration of cAMP under control (vehicle only) conditions or in cells treated with scrambled non-target shRNA. *p<0.05 versus control or scrambled cells.

5.4 Human adipocytes have both basal and stimulated lipolytic capabilities

It is well established that human adipocytes are capable of performing lipolysis both in the presence (stimulated) and absence (basal) of external stimuli (Nielsen *et al.*, 2014). To reconfirm the assertions made in the literature, the rates of basal and stimulated lipolysis were measured in human *in vitro* differentiated adipocytes by quantifying the concentration of glycerol released into the supernatant. Glycerol is a more stable measure of lipolysis than FFA release, as FFA reuptake occurs and FFAs are reesterified to create new triglyceride molecules, whereas glycerol is not metabolised to a significant extent (Vaughan, 1962). Nervous stimulation was mimicked by applying isoprenaline, a β-adrenergic agonist, and forskolin, an adenylate cyclase activator (Litosch *et al.*, 1982). In line with the previous literature (Nielsen *et al.*, 2014), primary human *in vitro* differentiated adipocytes are capable of releasing glycerol under basal and stimulated (with isoprenaline or forskolin) conditions (*N*=3; Figure 5.4A). The amount of glycerol in the supernatant accumulates over time in all three conditions, however the total amount of glycerol is significantly higher in the presence of isoprenaline or forskolin versus basal conditions. After three hours, under basal conditions the supernatant contained 7.7 ± 1.6 µM glycerol (*N*=3), whereas cells stimulated with forskolin produced 28.9 ± 2.8 µM glycerol (*N*=3) and similarly, cell treated with isoprenaline produced 34.4 ± 4.7 µM glycerol (*N*=3). Thus, representing an approximately four-fold increase in glycerol release under stimulated conditions versus basal conditions ($p<0.05$). Both isoprenaline (Figure 5.4B) and forskolin (Figure 5.4C) treatment caused concentration-dependent increases in glycerol release, with EC_{50} values of 11.2 ± 10.9 nM (*N*=3) and 3.59 ± 11.7 nM (*N*=3) respectively.

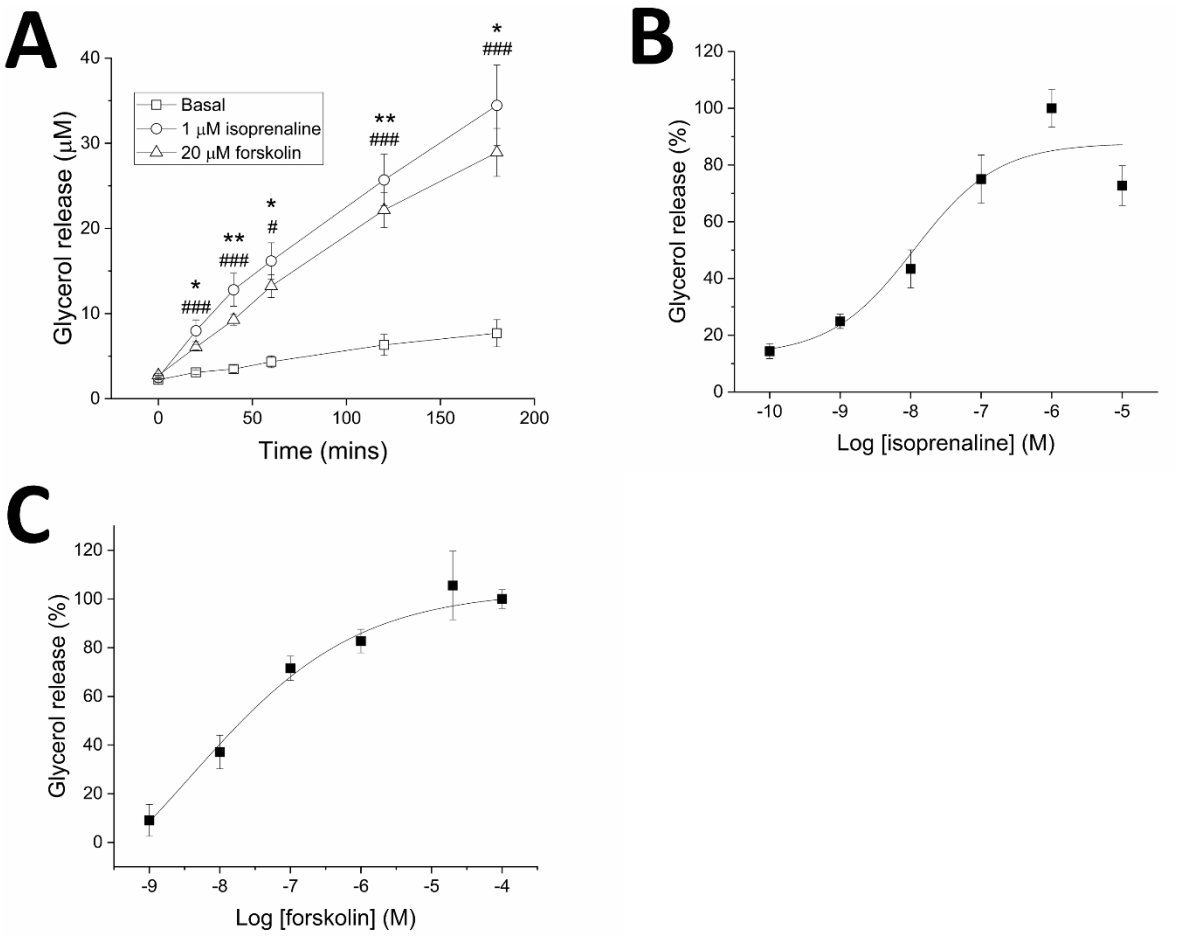

Figure 5.4 Primary human *in vitro* differentiated adipocytes are capable of both basal and stimulated lipolysis (*N*=3). (A) Basal and stimulated (with 1 µM isoprenaline or 20 µM forskolin) glycerol accumulation in the supernatant over three hours. *p<0.05, **p<0.005 isoprenaline-stimulated glycerol release versus basal glycerol release at the equivalent time point. # p<0.05, ### p<0.001 forskolin-stimulated glycerol release versus basal glycerol release at the equivalent time point. The effect of increasing concentrations of (B) isoprenaline or (C) forskolin on the amount of glycerol released after three hours. Data are normalised to the maximum amount of glycerol released per donor and then averaged across donors.

5.5 Exogenous nucleotide application and pharmacological blockade of $P2Y_1$ receptors have no effect on basal or stimulated lipolysis

Lipolysis has previously been shown to be altered by fluxes in intracellular calcium levels (Xue *et al.*, 2001). In Chapter 4, it was determined that exogenous application of ATP and ADP elicited transient increases in intracellular calcium levels, so here attempts were made to test the hypothesis that calcium signalling pathways initiated by P2 receptor activation may affect lipolysis. To this end, it was identified that singular application of maximal concentrations of both ATP and ADP (as determined via calcium mobilisation assays in Chapter 4) do not significantly alter basal glycerol release in human adipocytes (Figure 5.5A,D). Furthermore, exogenous nucleotide application had no statistically significantly effect on isoprenaline- (Figure 5.5 B,E) or forskolin-stimulated (Figure 5.5C,F) lipolysis over a three hour period, despite the fact that EC_{80} concentrations of both isoprenaline (75 nM) and forskolin (60 nM) were used in an attempt to optimise the probability of detecting an effect above the lipolytic effects of both stimulants. There appeared to be a slight increase in the amount of isoprenaline-stimulated glycerol release in the presence of ADP after three hours, however this increase was not statistically significant. It is not known whether this trend would have become significant if glycerol release was monitored over a longer time period (> 3 hours), but if this was the case, it is unlikely that this effect would have been specifically due to ADP, as ADP is rapidly degraded (Slakey *et al.*, 1997; Yegutkin, 2014).

In addition, subtype selective inhibition of $P2Y_1$ receptors with MRS2500 had no significant effect on basal or stimulated glycerol release in human adipocytes (Figure 5.6A-C). This lack of effect was evident both in the presence and absence of exogenous ADP, which suggests that neither activation (with ADP) nor inhibition of $P2Y_1$ receptors (with MRS2500) had any effect on lipolysis under the conditions used in this study. The fact that inhibition of $P2Y_1$ receptors with MRS2500 alone had no effect on lipolysis, is perhaps unsurprising as MRS2500 had no effect on cytoplasmic calcium (Figure 5.2A), which suggests that there is no constitutive activity of $P2Y_1$ in primary human adipocytes.

During the assay, the adipocytes were incubated with serum-free media for two hours prior to the addition of vehicle or antagonists, as foetal bovine serum contains a wide variety of hormones and other substances that can affect lipolysis. The cells are then incubated with vehicle or antagonist for 30 minutes and then the first samples were collected immediately post-nucleotide and DMEM (basal) or stimulant (isoprenaline or forskolin) application. This means that the '0 hour' reading shown in the time-resolved glycerol release graphs represent 0 hours after agonist/stimulant addition, but these supernatant sample have also been conditioned with basal glycerol release for 2.5 hours (including 30 minutes with vehicle/antagonist) prior to agonist addition. Therefore, small quantities of glycerol are present in the supernatant even at '0 hours'. This applies to all subsequent glycerol quantification data, unless otherwise stated. The glycerol release data presented in this

Section, and throughout this Chapter unless otherwise stated, were normalised to the amount of glycerol released into the supernatant after three hours to minimise the effects of donor-to-donor variation. All the data are relative to the 3 hour timepoint, including 0 hours. This means that the relative amount of glycerol at 0 hours under basal conditions appears to be greater than the 0 hour concentrations for the stimulated cells. This is, because basal lipolysis occurs at a slower rate and with a lower magnitude than stimulated lipolysis (Figure 5.4A), thus when the data are normalised to the 3 hour values, the amount of glycerol produced in 2.5 hours (prior to agonist addition) is almost equal to the amount of glycerol produced during the time series, thus it appears as if the proportion of glycerol at 0 hours is approximately 40% for the basal samples, but only 20% for stimulated cells.

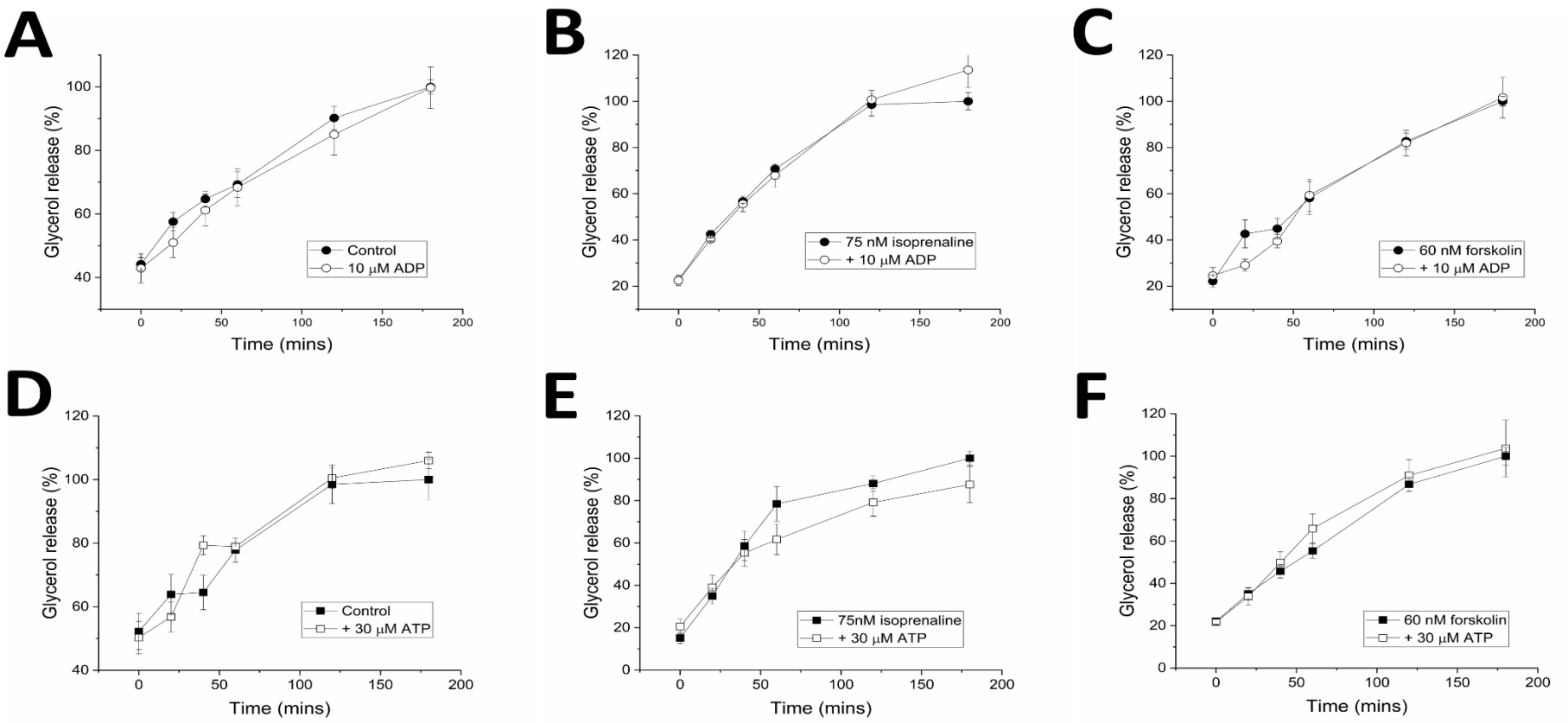

Figure 5.5 Exogenous nucleotide application has no effect on basal or stimulated lipolysis in primary human *in vitro* differentiated adipocytes. Effect of a singular application of maximal concentrations of exogenous ADP (10 μM; *open circles*) on (A) basal (*N*=7), (B) isoprenaline-stimulated lipolysis (*N*=4) and (C) forskolin-stimulated lipolysis (*N*=4) (*closed circles*) over a three hour period. Effect of a singular application of maximal concentrations of exogenous ATP (30 μM; *open squares*) on (D) basal (*N*=3), (E) isoprenaline-stimulated lipolysis (*N*=4) and (F) forskolin-stimulated lipolysis (*N*=3) (*closed squares*) over a three hour period. All data are normalised to the amount of glycerol released in the absence of nucleotide addition (control) after three hours.

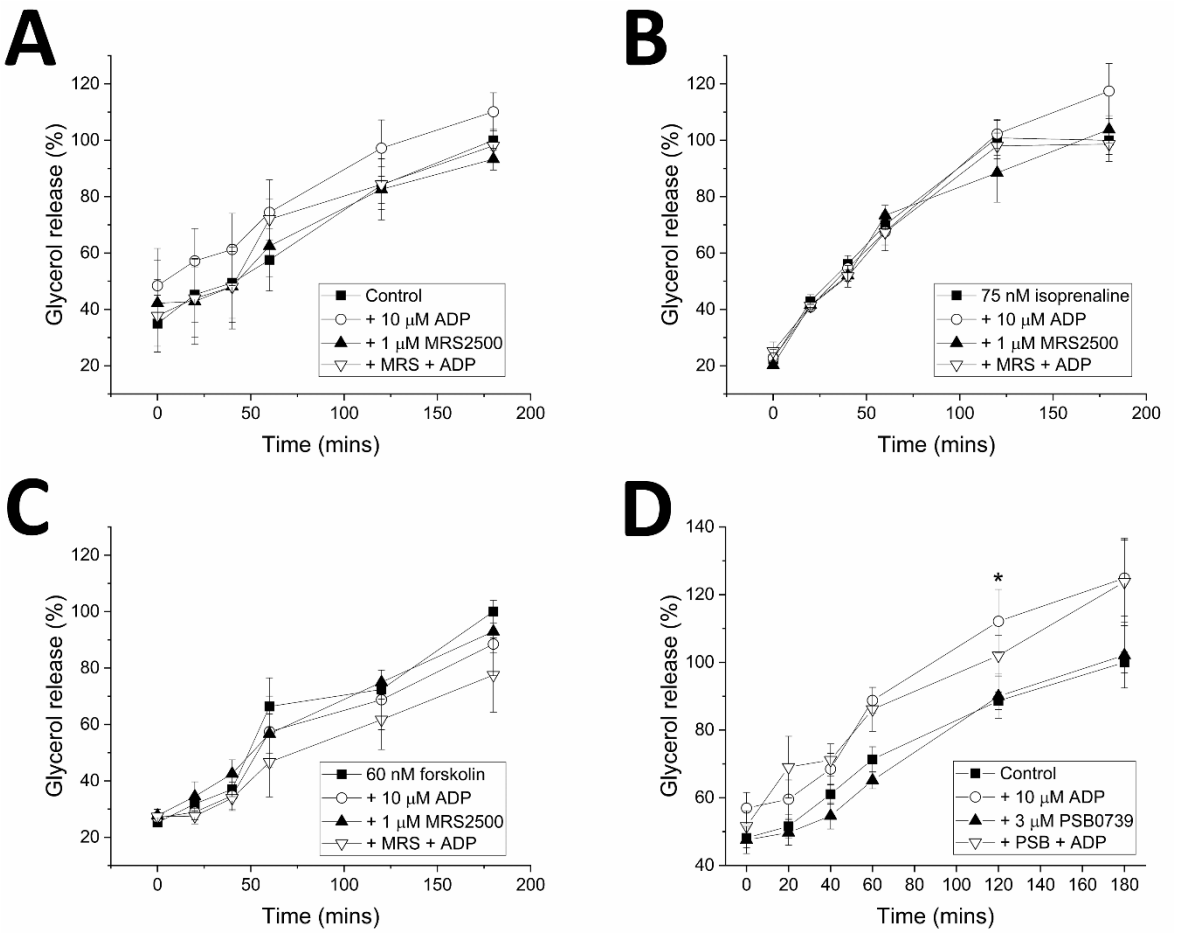

Figure 5.6 Selective inhibition of $P2Y_1$ and $P2Y_{12}$ receptors have no effect on basal lipolysis and inhibition of $P2Y_1$ also has no effect on stimulated lipolysis in primary human *in vitro* differentiated adipocytes (*N*=3). Effect of a singular application of maximal concentrations of exogenous ADP (10 μM; *open circles*) and selective inhibition of $P2Y_1$ receptors with 1 μM MRS2500 in the presence (*open downward triangles*) or absence of 10 μM ADP (*closed triangles*) on (A) basal, (B) isoprenaline-stimulated lipolysis or (C) forskolin-stimulated lipolysis (*closed squares*) over a three hour period. (D) Effect of a singular application of maximal concentrations of exogenous ADP (10 μM; *open circles*) and selective inhibition of $P2Y_{12}$ receptors with 3 μM PSB0739 in the presence (*open downward triangles*) or absence of 10 μM ADP (*closed triangles*) on basal lipolysis (*closed squares*). All data are normalised to the amount of glycerol released in the absence of nucleotide and antagonist addition (control) after three hours. **p*<0.05 ADP only vs vehicle only (control) at each timepoint.

5.6 Effect of inhibition of $P2Y_{12}$ receptors on basal and stimulated lipolysis in human adipocytes

It is well established that adenosine has an anti-lipolytic effect, which is mediated via activation of G_i-coupled P1 receptors to initiate a reduction in cytoplasmic cAMP levels (Fredholm *et al.*, 1977; Ohisalo, 1981; Sollevi *et al.*, 1981; Johansson *et al.*, 2008). $P2Y_{12}$ receptors are also G_i-coupled and ADP was shown to decrease forskolin-stimulated intracellular cAMP levels (Figure 4.10). This led to the hypothesis that activation of $P2Y_{12}$ receptors in human adipocytes may have a similar anti-lipolytic effect to adenosine. In order to test this hypothesis, $P2Y_{12}$ receptors were selectively antagonised with PSB0739 in the presence and absence of ADP. Although, 3 μM PSB0739 had no effect on basal lipolysis, ADP alone caused a significant increase in basal lipolysis after 60 minutes (Figure 5.6D). Although the data for the 120 minute timepoint was the only statistically significant change, the amount of glycerol released trended higher for samples in the presence of ADP (with or without PSB0739) at all timepoints. Contrary to the hypothesis that ADP may act in a similar manner to adenosine, this result suggests ADP may have a lipolytic effect, rather than an anti-lipolytic effect. Although the lack of statistical difference between the effect of ADP and PSB0739 plus ADP, would suggest that the effect of ADP is not mediated via $P2Y_{12}$ receptors. However, the fact that statistical significance was only demonstrated at one timepoint and data from other donors (Figure 5.5A and 5.6A) did not display a significant increase in basal glycerol release in the presence of ADP, suggests that this data is unlikely to be a true representation of the effects of ADP and that it is more likely that ADP does not alter basal lipolysis, at least in the majority of donors tested. Although it may be possible that there is an effect in a subset of donors, but as there is no clear indication of which donors may respond to ADP and the number of donors used in this study was limited, it was not possible to adequately explore a possible role for ADP in a subset of the population within the scope of this study.

ADP had no effect on forskolin- (Figure 5.7D) or isoprenaline-stimulated lipolysis (Figure 5.7A), but selective antagonism of $P2Y_{12}$ with 3 μM PSB0739 had an anti-lipolytic effect on isoprenaline-stimulated lipolysis (Figure 5.7A). These results are surprising, because they do not correlate with previous data illustrating that PSB0739 increases cAMP (Figure 4.10). However, it appears that the anti-lipolytic effects of PSB0739 are only observed with 3 μM PSB0739 and lower concentrations of PSB0739 have no inhibitory effect on isoprenaline-stimulated lipolysis after 3 hours (Figure 5.7B). In addition, selective inhibition of $P2Y_{12}$ with an alternative antagonist, Ticagrelor, did not mimic the results observed with 3 μM PSB0739. In fact, Ticagrelor did not significantly alter isoprenaline-stimulated lipolysis at any timepoint (Figure 5.7C), which suggests that the effect of 3 μM PSB0739 may be due to off-target effects, such as interference with isoprenaline binding. Furthermore, 3 μM PSB0739 had no effect on forskolin-stimulated lipolysis, which activates the same pathway as

isoprenaline, which again indicates that the effects of 3 µM PSB0739 are likely to be due to off-target effects. Although, it is unclear what the true causes of these discrepancies are, it is likely that the effect of 3 µM PSB0739 on isoprenaline-stimulated lipolysis are anomalous and are not representative of the true phenotype.

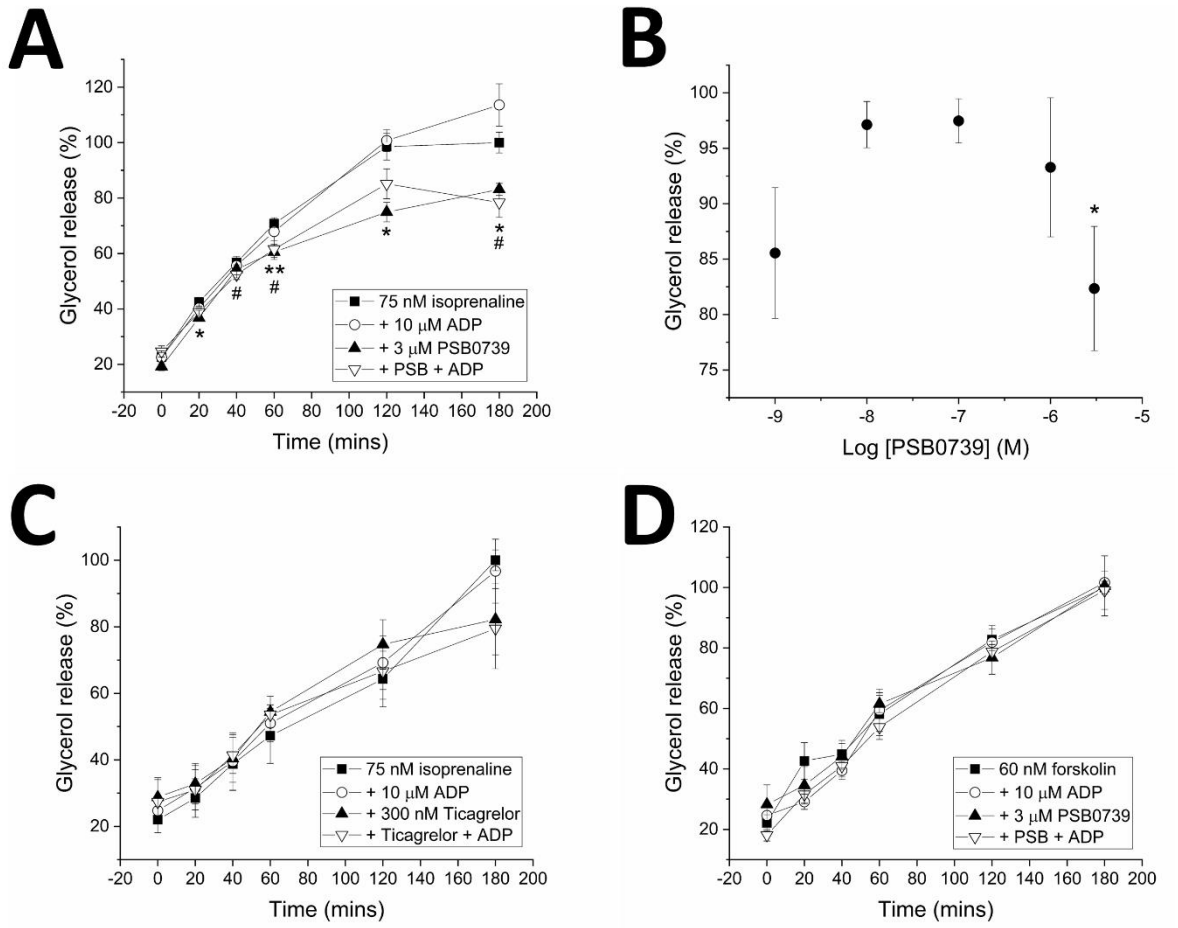

Figure 5.7 Effect of selective inhibition of $P2Y_{12}$ receptors on isoprenaline- and forskolin-stimulated glycerol release in primary human *in vitro* differentiated adipocytes (*N*=3). (A) Effect of a singular application of maximal concentrations of exogenous ADP (10 μM; *open circles*) and inhibition of $P2Y_{12}$ receptors with 3 μM PSB0739 in the presence (*open downward triangles*) or absence of 10 μM ADP (*closed triangles*) on isoprenaline-stimulated lipolysis (*closed squares*) over a three hour period. (B) Effect of increasing concentrations of PSB0739 on isoprenaline-stimulated glycerol release after 3 hours. (C) Effect of a singular application of maximal concentrations of exogenous ADP (10 μM; *open circles*) and inhibition of $P2Y_{12}$ receptors with 300 nM Ticagrelor in the presence (*open downward triangles*) or absence of 10 μM ADP (*closed triangles*) on isoprenaline-stimulated lipolysis (*closed squares*) over a three hour period. (D) Effect of a singular application of maximal concentrations of exogenous ADP (10 μM; *open circles*) and inhibition of $P2Y_{12}$ receptors with 3 μM PSB0739 in the presence (*open downward triangles*) or absence of 10 μM ADP (*closed triangles*) on forskolin-stimulated lipolysis (*closed squares*) over a three hour period. All data are normalised to the maximum glycerol release after 3 hours in the presence of vehicle only. Data are expressed as mean ± SEM. **p*<0.05, ***p*<0.005 PSB0739 only vs vehicle only at each timepoint; # *p*<0.05 PSB0739 and ADP vs vehicle only at each timepoint.

5.7 Pharmacological inhibition of $P2Y_2$ receptor activity enhances basal and stimulated lipolysis

$P2Y_2$ receptors are expressed by primary human *in vitro* differentiated adipocytes and activation of these receptors leads to an appreciable increase in intracellular calcium, as shown in Chapter 4. In addition, it is evident that $P2Y_2$ receptors are constitutively active in human adipocytes and they control both cytoplasmic calcium and cAMP tone within the cell (Figure 5.2 and 5.3). Although exogenous application of ATP had no effect on basal or stimulated lipolysis (Figure 5.5D-F), pharmacological inhibition of the $P2Y_2$ receptor with 10 µM AR-C118925XX enhances both basal and stimulated lipolysis (Figure 5.8). The effects are particularly pronounced under basal conditions, where 10 µM AR-C118925XX generated a significant and sustained increase in basal glycerol release after 40 minutes (Figure 5.8A). Selective antagonism of $P2Y_2$ receptors caused a 32.2 ± 7.8% (*N*=3) increase in basal glycerol release after 3 hours. It is important to note that the cells were preincubated with vehicle or antagonist for 30 minutes prior to collection of the first sample, thus the 40 minute timepoint actually represents 70 minutes in the presence of antagonist. The fact that the cells were preincubated with the antagonist may also explain why the concentration of glycerol in the supernatant trended higher for the AR-C118925XX-treated cells even at the 0 hour timepoint. Although the general trend suggests that AR-C118925XX caused a very rapid increase in glycerol release (from the 0 hour timepoint), these increases were not statistically significant until the 40 minute timepoint. Selective inhibition of $P2Y_2$ receptors enhanced basal lipolysis both in the presence and absence of ATP (Figure 5.8A), which is indicative of tonic $P2Y_2$ receptor activity in these cells.

Inhibition of $P2Y_2$ receptors enhanced basal (Figure 5.8D) and forskolin-stimulated (Figure 5.8B,E) lipolysis in a concentration-dependent manner. After 3 hours, 10 µM AR-C118925XX generated a total increase in glycerol release of 41.1 ± 9.4% above cells stimulated with forskolin alone (*N*=3; $p<0.05$; Figure 5.8B). This increase is comparable to the effect observed on basal lipolysis. However, although the effects of $P2Y_2$ inhibition on basal and forskolin-stimulated lipolysis share many similarities, unlike basal lipolysis, exogenous application of ATP appears to neutralise the effects of AR-C118925XX, particularly at the latter timepoints, which suggests that there may be some redundancies in the system to allow ATP to limit the amount of glycerol released even after $P2Y_2$ receptors are inhibited. It is possible that the reason that this rescue phenotype is evident for forskolin-stimulated lipolysis, but not basal lipolysis, is that total concentration of glycerol released in the presence of forskolin and AR-C118925XX is much higher than under basal conditions. Lipolysis is a very tightly regulated process, so it is possible that when a certain threshold of glycerol release is surpassed, alternative signalling pathways are engaged to limit the loss of triglyceride and maintain stores (Yu and Li, 2017).

AR-C118925XX enhances isoprenaline-stimulated lipolysis in a concentration dependent manner, with maximal concentrations of AR-C118925XX (10 µM) causing a 15.5 ± 5.7% (*N*=3) increase in isoprenaline-stimulated glycerol release (Figure 5.8F). Although the total level of enhancement caused by AR-C118925XX is comparatively less than the effects observed on basal and forskolin-stimulated lipolysis, the effects of AR-C118925XX were more potent, with 1 µM AR-C118925XX causing a small, but significant increase in isoprenaline-stimulated glycerol release, whereas equivalent concentrations of AR-C118925XX had no effect on basal or forskolin-stimulated lipolysis. However, although a subtle, but clear increase in isoprenaline-stimulated glycerol release was observed in Figure 5.8F, when the effects of AR-C118925XX on isoprenaline-stimulated lipolysis was monitored over time (Figure 5.8C) no significant increase in glycerol release was observed at any timepoint. On average, there did appear to be an increase in glycerol release when the cells were treated with AR-C118925XX for two or more hours, but variation between donors meant that this increase was not statistically significant. Again, like forskolin-stimulated lipolysis co-application of AR-C118925XX and ATP appears to neutralise the slight, albeit non-significant, increase in glycerol release.

There are different mechanisms governing basal and stimulated lipolytic pathways (Miyoshi *et al.*, 2008). Basal lipolysis is omnipresent, but certain external stimuli can dramatically increase the production of FFA and glycerol to augment those released via basal lipolysis. As the effects of $P2Y_2$ inhibition are largely comparable for both basal and stimulated lipolysis, it is likely that in both cases the effect is due to a mechanism that enhances basal lipolysis. Consequently, from this point onwards attempts were made to identify the molecular mechanisms underlying the effects on basal lipolysis only.

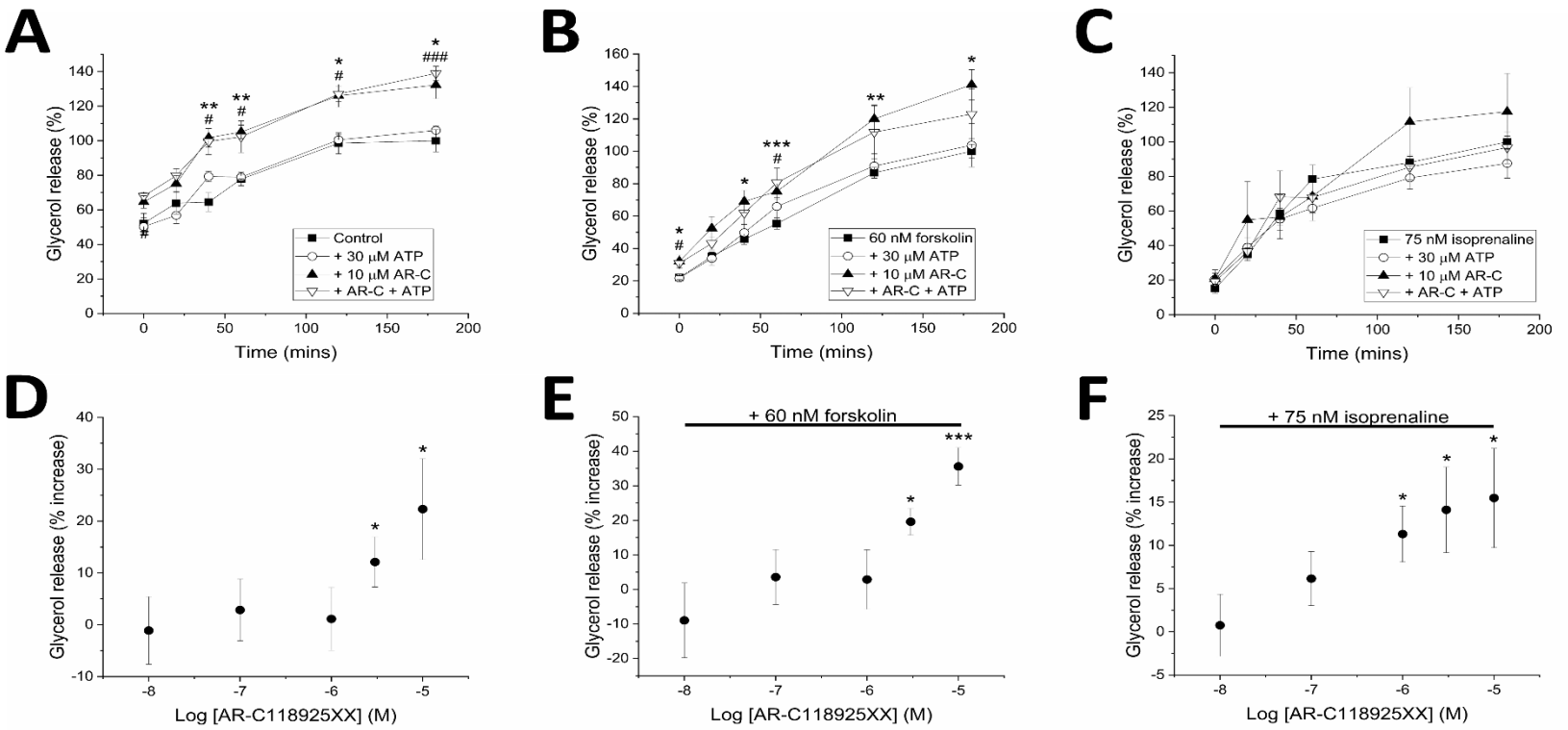

Figure 5.8 Selective inhibition of $P2Y_2$ receptors enhances basal and stimulated lipolysis in primary human *in vitro* differentiated adipocytes (*N*=3). Effect of selective inhibition of $P2Y_2$ receptors with 10 µM AR-C118925XX in the presence (*open downward triangles*) and absence (*closed trianges*) of a singular application of 30 µM ATP (*open circles*) on (A) basal, (B) forskolin-stimulated and (C) isoprenaline-stimulated glycerol release (*closed squares*). **p*<0.05, ***p*<0.005, ***p<0.001 AR-C118925XX only versus vehicle only at each timepoint; # *p*<0.05, ### *p*<0.001 AR-C118925XX and ATP vs vehicle only at each timepoint. Increase in glycerol release caused by increasing concentrations of AR-C118925XX on (D) basal, (E) forskolin-stimulated and (F) isoprenaline-stimulated lipolysis after 3 hours. **p*<0.05 vs glycerol release in the presence of vehicle only. All data are normalised to maximum glycerol release after 3 hours in the presence of vehicle only. Data are expressed as mean ± SEM.

5.8 shRNA-mediated knockdown of $P2Y_2$ receptor expression also enhances basal lipolysis

The increase in glycerol release observed with pharmacological inhibition of $P2Y_2$ was replicated via shRNA-mediated knockdown of $P2Y_2$ receptor expression. Lentiviral delivery of shRNA was used to successfully decrease mRNA expression of $P2Y_2$ by approximately 50%. Knocking down $P2Y_2$ expression caused a 31.6 ± 8.6% (*N*=3) increase in basal glycerol release ($p<0.05$ versus scrambled control cells) (Figure 5.9). Interestingly in addition to causing an increase in glycerol release, decreasing expression of $P2Y_2$ receptors in primary human adipocytes produced a phenotypic change in the cells. $P2Y_2$ knockdown adipocytes had a greater number of smaller lipid droplets when compared to their scrambled counterparts (Figure 5.10). Smaller lipid droplets are consistent with an increase in metabolic activity (Khor *et al.*, 2013). Quantification of the average number of lipid droplets per adipocyte indicate that there was an approximately 60% increase in the number of lipid droplets in $P2Y_2$ knockdown cells versus scrambled cells (Figure 5.10B). In addition, on average $P2Y_2$ knockdown cells contain less neutral lipid than their scrambled counterparts, as quantified using BODIPY neutral lipid stain (Figure 5.10C). These phenotypic changes are in line with the hypothesis that decreasing $P2Y_2$ receptor activity causes an increase in lipolysis, which would consequently correspond with a decrease in triglyceride storage.

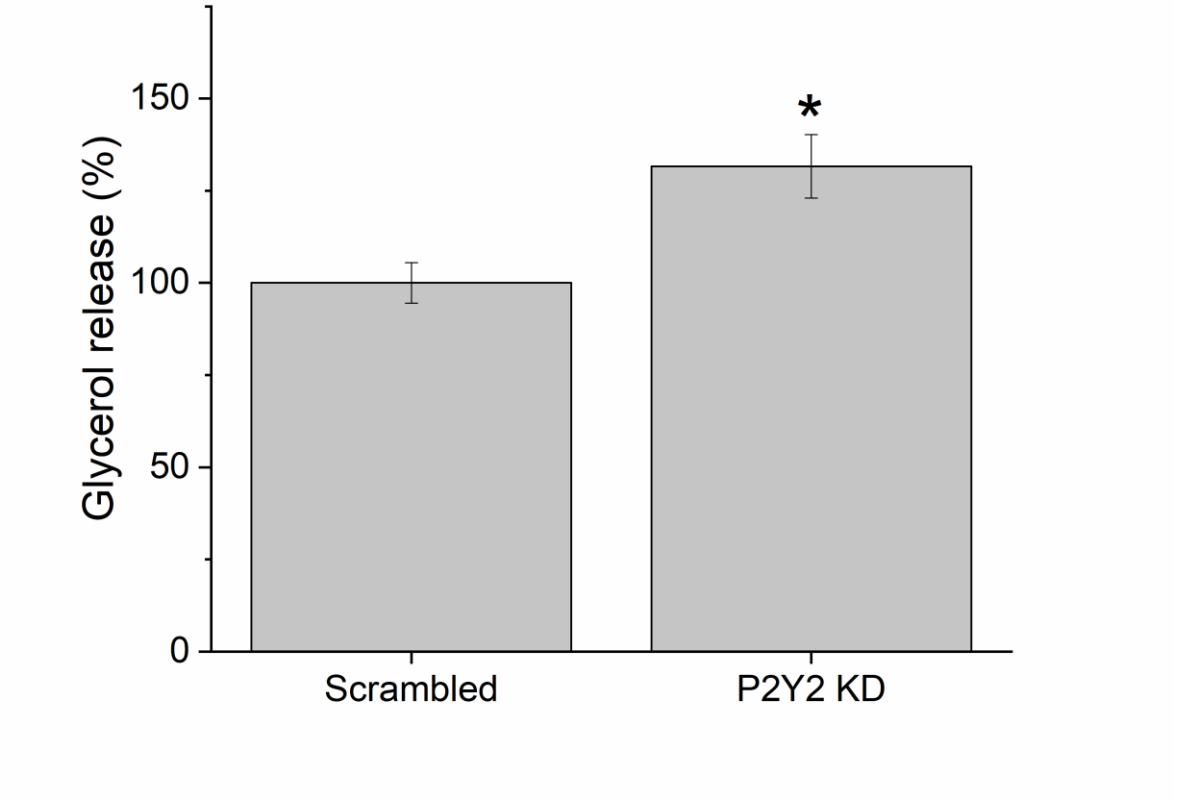

Figure 5.9 shRNA-mediated knockdown of $P2Y_2$ receptor expression causes an increase in basal glycerol release in primary human *in vitro* differentiated adipocytes after 3 hours (*N*=3). Data are normalised to the amount of glycerol released by adipocytes treated with scrambled non-target shRNA per donor and then averaged across donors. Data are expressed as mean ± SEM. **p*<0.05 versus scrambled control cells.

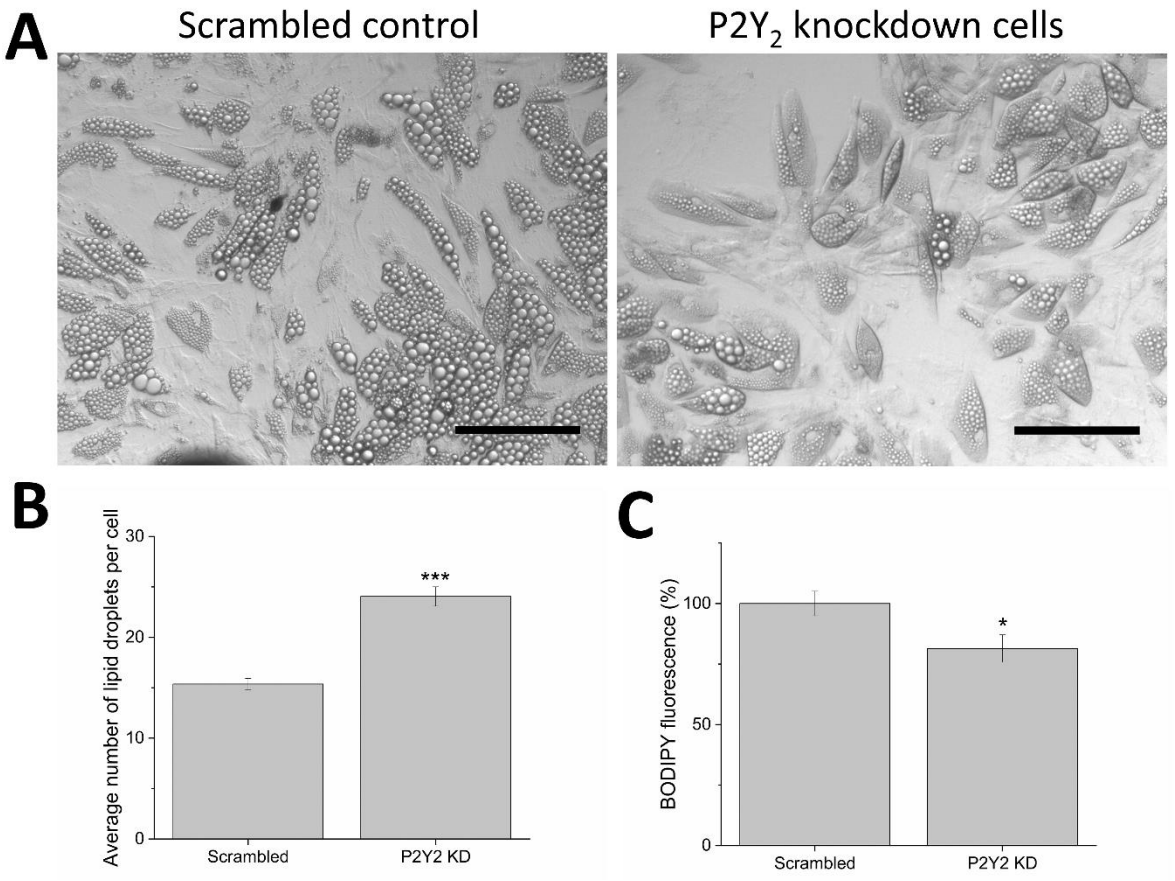

Figure 5.10 shRNA-mediated knockdown of $P2Y_2$ receptor expression causes a phenotypic change in primary human *in vitro* differentiated adipocytes. (A) Representative images of primary human adipocytes treated with non-target scrambled control shRNA (left) or $P2Y_2$ target shRNA (right). (B) Average number of lipid droplets per cell. (C) Amount of neutral lipid present in a population of scrambled control and $P2Y_2$ knockdown cells as determined by staining the lipids with BODIPY dye and then quantifying the fluorescence produced. Fluorescence readings are proportional to the amount of neutral lipid present. All data are normalised to the fluorescence reading for the scrambled control adipocytes per donor and then averaged across donors. Data is expressed as mean ± SEM. *p<0.05, ***p<0.001 versus scrambled control.

5.9 Enhancement of basal lipolysis caused by inhibition of $P2Y_2$ receptors is replicated by removal of extracellular ATP with apyrase

Removal of extracellular ATP with apyrase causes a 59.9 ± 20.0% (*N*=4) increase in basal lipolysis, which is equivalent to the 41.1 ± 16.0% (*N*=4) increase in glycerol release achieved with 10 μM AR-C118925XX. In addition, simultaneous inhibition of $P2Y_2$ receptors and scavenging extracellular ATP produces a 54.1 ± 17.2% (*N*=4) rise in basal glycerol release, which is comparable to the amount of glycerol released with AR-C118925XX and apyrase alone (Figure 5.11). This implies that both pharmacological blockade of $P2Y_2$ receptors and removal of extracellular ATP may enhance lipolysis via the same mechanism. It is proposed that in both cases, the augmentation of basal lipolysis observed is due to inhibition of $P2Y_2$ receptor activity, either via direct inhibition or removal of the physiological agonist. This hypothesis corresponds well with earlier data (Figure 5.2) that demonstrates that both AR-C118925XX and apyrase are able to modulate basal cytoplasmic calcium levels.

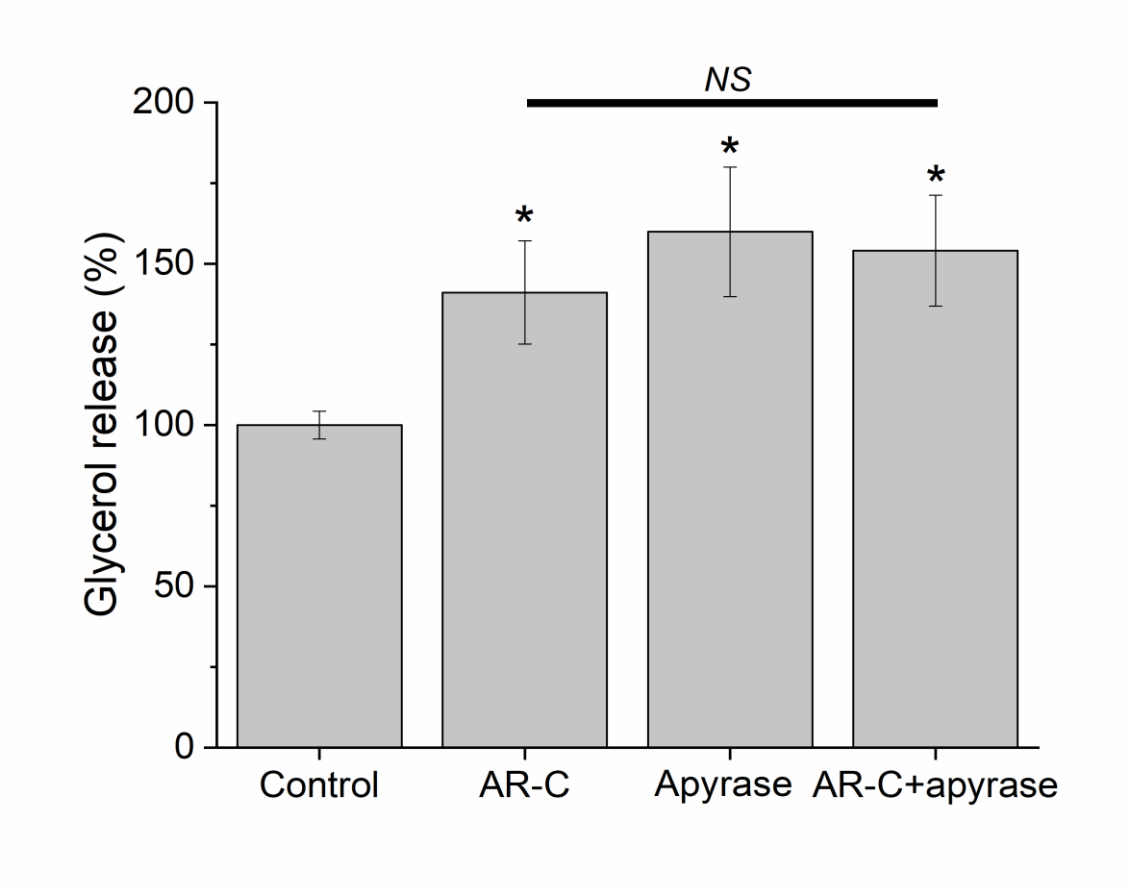

Figure 5.11 Scavenging extracellular ATP enhances basal glycerol release to the same degree as inhibiting $P2Y_2$ receptor activity after 3.5 hours (*N*=4). $P2Y_2$ receptors were selectively antagonised with 10 µM AR-C118925XX and extracellular ATP was removed with 2 U/ml apyrase. Data are normalised to basal glycerol release in the presence of vehicle alone. Data are expressed as mean ± SEM. **p*<0.05 versus control; *NS* implies no significant difference between the conditions under the line.

5.10 Attempting to determine the mechanism by which $P2Y_2$ inhibition leads to an increase in cAMP and subsequent enhancement of basal lipolysis

Throughout this Chapter, it has been determined that inhibition of $P2Y_2$ receptors causes a decrease in cytoplasmic calcium (Figure 5.2), an increase an intracellular cAMP (Figure 5.2) and an enhancement of basal glycerol release (Section 5.7 and 5.8). In this Section, three potential mechanisms are explored in order to attempt to uncover the molecular mechanism connecting $P2Y_2$ receptors and basal lipolysis. Firstly, it is possible that $P2Y_2$ receptors in human adipocytes may couple to G_i proteins, thus inhibition of $P2Y_2$ receptor activity would alleviate G_i-mediated inhibition of adenylate cyclase to encourage cAMP production. Alternatively, elevated cytoplasmic calcium due to $P2Y_2$ receptor activation may enhance phosphodiesterase (PDE) activity, therefore blockade of $P2Y_2$ receptor would limit cAMP breakdown. Finally, increases in intracellular calcium via $P2Y_2$ receptor activation may inhibit calcium-sensitive isoforms of adenylate cyclase (AC), which means that inhibition of $P2Y_2$ receptors would lower calcium tone and subsequently activate adenylate cyclase to increase cAMP production.

5.10.1 Augmented glycerol release due to $P2Y_2$ receptor inhibition is not achieved via G_i-mediated signalling

To determine whether the increase in basal lipolysis observed when $P2Y_2$ receptor activity is inhibited is due to reduced G_i-mediated blockade of adenylate cyclase, basal glycerol release was measured in the presence and absence of AR-C118925XX and pertussis toxin (PTx). The protocol was modified slightly to extend the antagonist incubation time to 4 hours in these experiments to allow PTx sufficient time to enter the cells and terminate G_i-mediated signalling pathways. This method demonstrated that 100 ng/ml PTx alone did not alter basal glycerol release (Figure 5.12), which implies that constitutive G_i-mediated signalling does not suppress basal lipolysis in primary human adipocytes. Although PTx alone did not affect basal lipolysis, inhibition of $P2Y_2$ receptors with 10 µM AR-C118925XX did increase basal glycerol release irrespective of the presence and absence of PTx (Figure 5.12). Taken together, these data indicate that $P2Y_2$ inhibition-induced lipolysis is not achieved via blockade of G_i-mediated signalling.

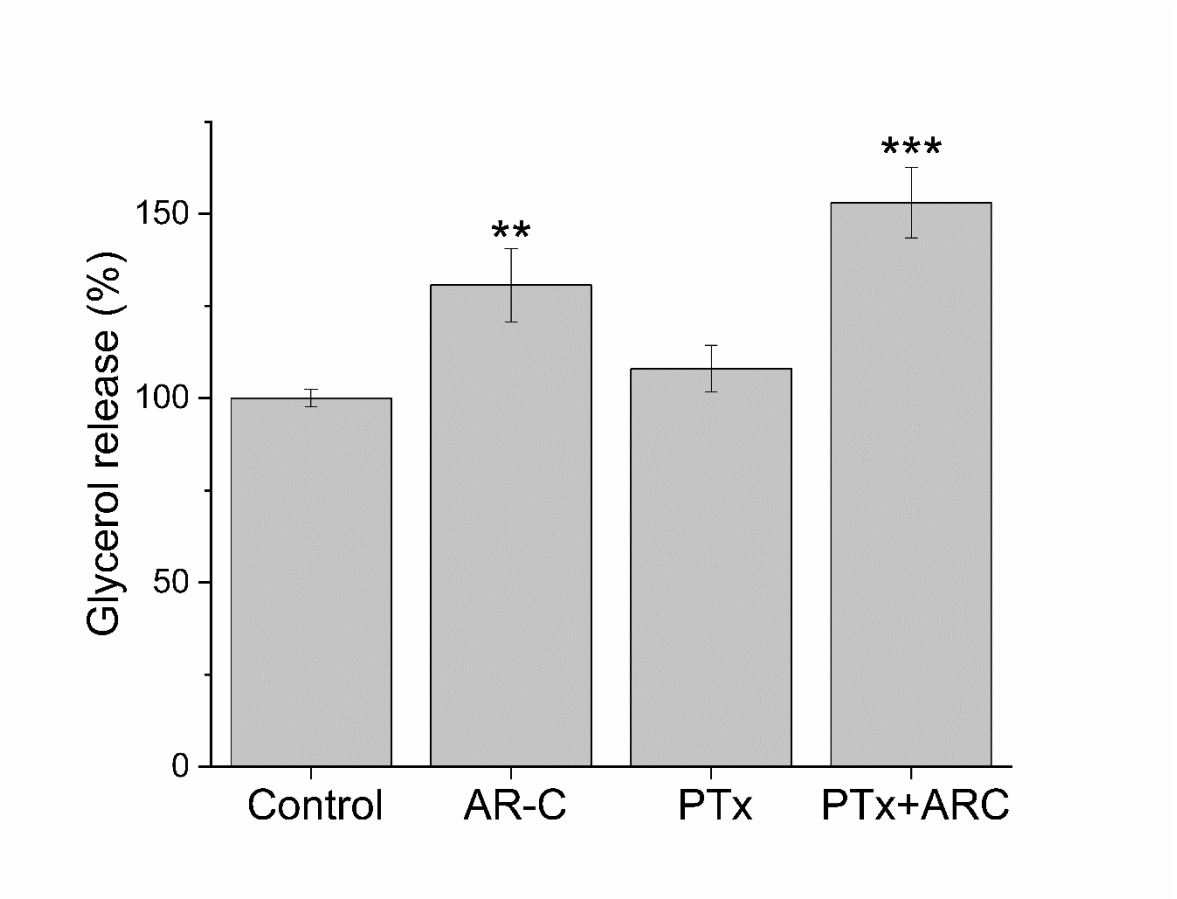

Figure 5.12 Enhanced basal glycerol release via selective antagonism of $P2Y_2$ receptors in primary human *in vitro* differentiated adipocytes is not achieved via inhibition of G_i-mediated signalling (*N*=6). $P2Y_2$ receptors were selectively antagonised with 10 µM AR-C118925XX (AR-C) and G_i-mediated signalling was blocked with 100 ng/ml pertussis toxin (PTx). Cells were preincubated with antagonists for four hours prior to assessment of glycerol concentration in the supernatants. Data are normalised to basal glycerol release in the presence of vehicle alone. Data are expressed as mean ± SEM. ** p<0.005, *** p<0.001 versus glycerol release in the presence of vehicle only (control).

5.10.2 Simultaneous inhibition of $P2Y_2$ receptors and phosphodiesterase isoforms 3 and 4 has a synergistic effect on basal lipolysis

Previous reports describing increases in lipolysis due to changes in intracellular calcium indicated that low intracellular calcium levels may inhibit calcium sensitive phosphodiesterase (PDE) isoforms, such as PDE1, to facilitate accumulation of cytoplasmic cAMP and downstream enhancement of lipolysis (Xue *et al.*, 2001). To ascertain whether $P2Y_2$ inhibition-induced lipolysis is due to inhibition of PDE activity, glycerol release was measured in the presence of PDE isoform-selective antagonists and/or AR-C118925XX. This revealed that selective antagonism of PDE3 (1 µM cilostramide) and PDE4 (10 µM rolipram), as well as non-selective PDE blockade with 10 µM 3-isobutyl-1-methylxanthine (IBMX), caused an increase in basal glycerol production, whereas selective inhibition of PDE1 (vinpocetine), PDE2 (PF-05180999) and PDE7 (BRL50481) had no effect on basal lipolysis (*N*=3; Figure 5.13). It is well-known that inhibition of PDE3 increases lipolysis (Degerman *et al.*, 1997; Snyder *et al.*, 2005) and there are also some reports that demonstrate that inhibition of PDE4 with rolipram also enhances lipolysis (Grønning *et al.*, 2006). It is important to note that IBMX is a component of the differentiation media used throughout this study to differentiate MSCs to adipocytes, however the differentiation media was removed, and the cells were incubated with culture media without IBMX (or the other differentiation media components) for three days prior to experimental use. In addition, the cells are washed immediately before commencing glycerol release assays to ensure no residual IBMX or other differentiation media components are present to affect the functioning of the *in vitro* differentiated adipocytes.

Inhibition of $P2Y_2$ was able to enhance spontaneous glycerol release to comparable degrees in the presence and absence of PDE1, PDE2 and PDE7 antagonists (Figure 5.13). However, when AR-C118925XX was coapplied with IBMX, cilostamide or rolipram, more glycerol was released into the supernatant than due to $P2Y_2$ receptor or PDE inhibition alone (Figure 5.13). This implies that inhibition of $P2Y_2$ does not enhance basal lipolysis by inhibiting PDE-mediated breakdown of cAMP. It also indicates that there is synergism between the pathways mediated by $P2Y_2$ and PDEs in enhancing basal lipolysis.

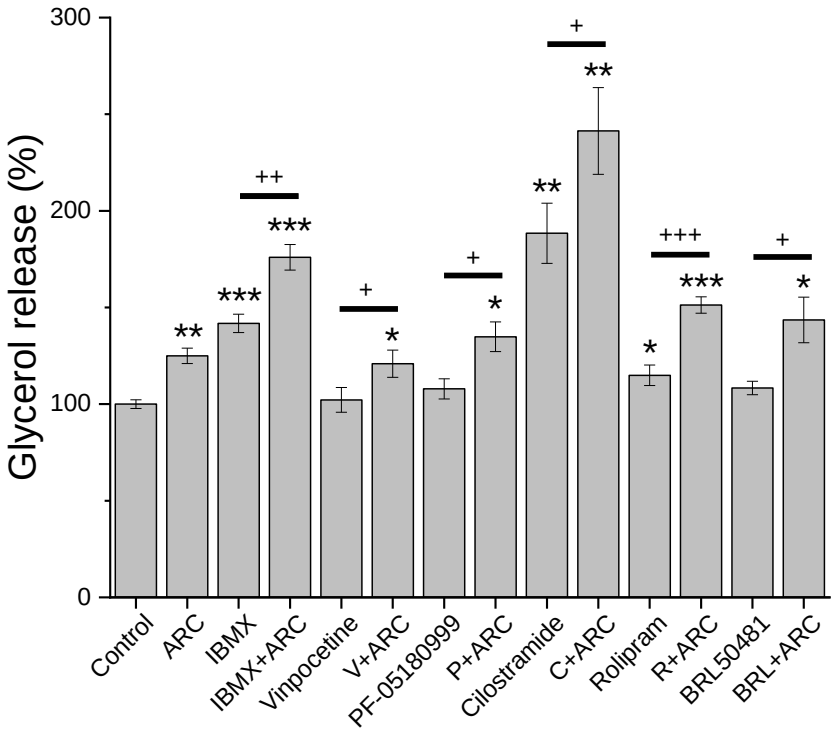

Figure 5.13 Simultaneous inhibition of $P2Y_2$ receptors and phosphodiesterase isoforms 3 or 4 has a synergistic effect on basal glycerol release from primary human *in vitro* differentiated adipocytes (*N*=3). $P2Y_2$ was inhibited with 10 µM AR-C118925XX, phosphodiesterase (PDE) isoforms were inhibited with 10 µM IBMX (pan-PDE inhibitor), 10 µM vinpocetine (PDE1 inhibitor), 10 µM PF-05180999 (PDE2 inhibitor), 1 µM cilostramide (PDE3 inhibitor), 10 µM rolipram (PDE4 inhibitor) and 1 µM BRL50481 (PDE7 inhibitor). Glycerol release was measured after the cells were exposed to antagonists for 3.5 hours. All data are normalised to glycerol release in the presence of vehicle only (control). **p*<0.05, ***p*<0.005, ****p*<0.001 versus control. + *p*<0.05, ++ *p*<0.005, +++ *p*<0.001 denotes a significant difference between the two conditions below the line.

5.10.3 Inhibition of $P2Y_2$ activates calcium-sensitive isoforms of adenylate cyclase to encourage basal lipolysis

There are nine known membrane-bound isoforms of adenylate cyclase, named adenylate cyclase (AC) 1-9 respectively. There is also an additional 'soluble' isoform, AC10, which has distinct catalytic and regulatory properties (Kamenetsky *et al.*, 2006). Non-quantitative RT PCR analysis revealed that all of the membrane-bound isoforms of AC were expressed by primary human *in vitro* differentiated adipocytes, excluding AC9 (Figure 5.14). However, there was some heterogeneity in expression for AC2, which was only expressed in two of the three donors tested.

Calcium has been shown to activate and inhibit different isoforms of AC (Sadana *et al.*, 2009), with AC5 and AC6 being shown to be directly inhibited by submicromolar concentrations of free calcium (Guillou *et al.*, 1999). Previous reports suggest concentrations of below 10 µM SQ22,536 (an AC antagonist) are selective for calcium-sensitive isoforms of AC (AC5 and AC6) (Brand *et al.*, 2013). Using 1 µM SQ22,536, it was shown that inhibition of AC alone had no effect on basal lipolysis, whereas inhibition of $P2Y_2$ receptors enhanced basal lipolysis (Figure 5.15). Interestingly, simultaneous inhibition of both AC and $P2Y_2$ receptors abolished the enhancement of basal glycerol release observed with AR-C118925XX alone (Figure 5.15). This suggests $P2Y_2$ inhibition-induced lipolysis occurs via activation of AC5 and/or AC6. As 1 µM SQ22,536 inhibits both AC5 and AC6, it was not possible to distinguish between AC5 and AC6 within the scope of this study. This mechanism also explains the synergism between PDE inhibition and $P2Y_2$ receptor inhibition (Section 5.10.2). Inhibition of $P2Y_2$ receptors increases production of cAMP, while inhibition of PDEs reduces the breakdown of cAMP, thus facilitating a larger accumulation of cytoplasmic cAMP.

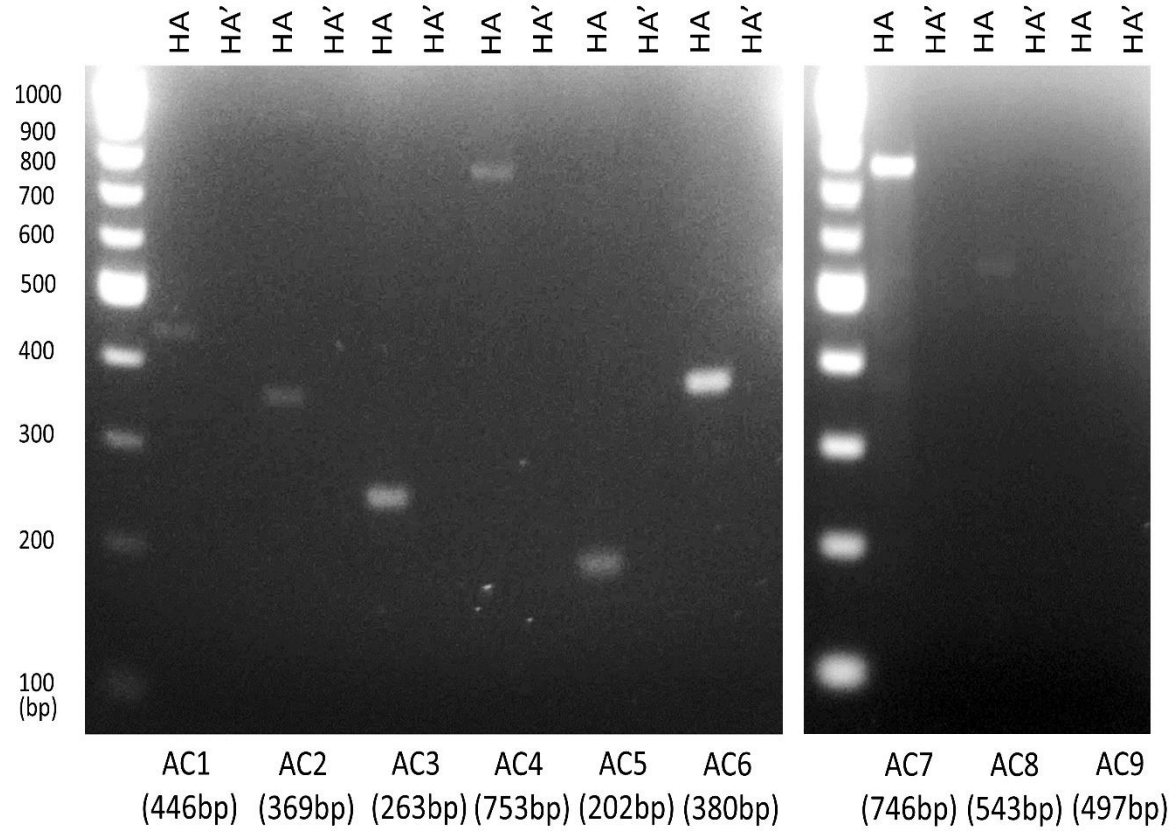

Figure 5.14 Primary human *in vitro* differentiated adipocytes express mRNA transcripts for all membrane-bound isoforms of adenylate cyclase (AC), excluding isoform 9, as detected by non-quantitative RT-PCR. Results are representative of the expression patterns for three independent donors, although there was some heterogeneity for AC2, which was only expressed in 2 of the 3 donors tested. HA = human adipocytes, HA' = control for genomic DNA contamination (no reverse transcriptase control).

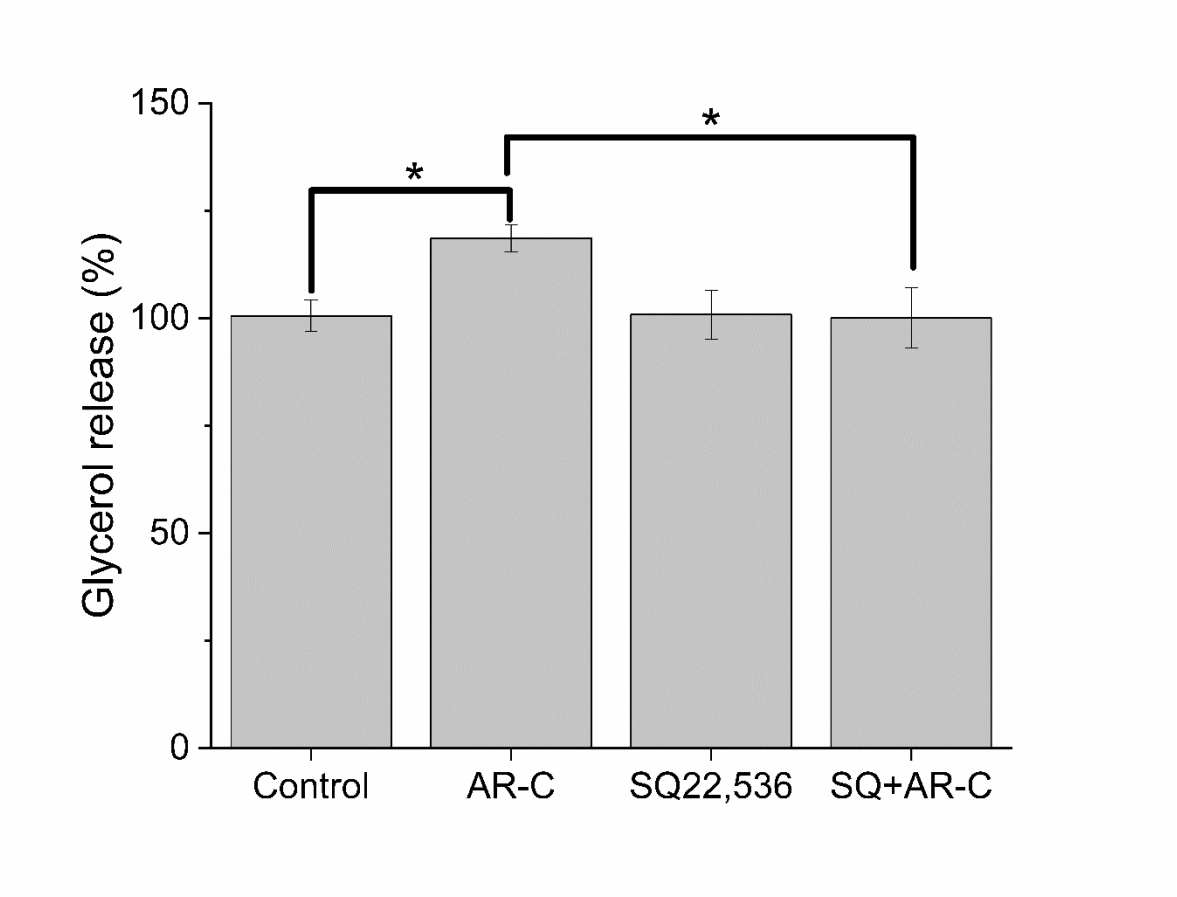

Figure 5.15 Inhibition of calcium-sensitive isoforms of adenylate cyclase abolishes $P2Y_2$-inhibition induced enhancement of basal glycerol release from primary human *in vitro* differentiated adipocytes (*N*=6). $P2Y_2$ receptors were inhibited with 10 µM AR-C118925XX, calcium-sensitive isoforms of adenylate cyclase were inhibited with 1 µM SQ22,536. Glycerol release was measured after the cells were exposed to antagonists for 3.5 hours. All data are normalised to the glycerol release in the presence of vehicle only (control). *p<0.05 signifies a significant difference between the two conditions indicated with the line above the bars.

5.11 Proposed mechanism for the role of $P2Y_2$ receptors in regulating basal lipolysis

The data presented in this Chapter enables the proposal of a molecular mechanism that links $P2Y_2$ receptor activity to basal lipolysis in human *in vitro* differentiated adipocytes. It is proposed that a reduction of constitutive $P2Y_2$ receptor activity causes a decrease in intracellular calcium, which then negates the inhibitory action of resting cytoplasmic calcium levels on AC5 and/or AC6. This in turn leads to an accumulation of cAMP in the cytosol, thus activating PKA, which phosphorylates enzymes associated with lipolysis to enhance basal lipolysis and consequently increase glycerol release from primary human adipocytes. If this mechanism is correct, then it signifies that the physiological role of $P2Y_2$ in primary human adipocytes is to constitutively maintain intracellular calcium levels to perpetuate inhibition of AC5 and/or AC6 and limit basal lipolysis in adipocytes, thus maintaining triglyceride stocks within the cells. This would imply that $P2Y_2$ receptor activity promotes an energy conservative phenotype within primary human *in vitro* differentiated adipocytes. A summary of the proposed mechanism is denoted in Figure 5.16.

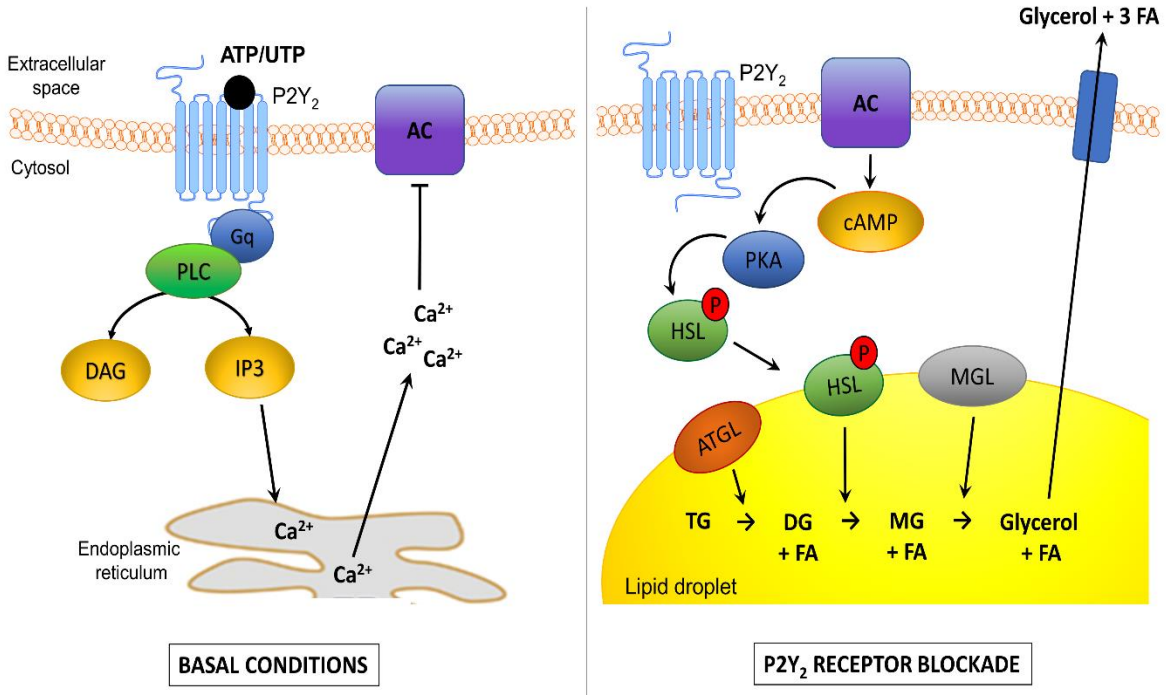

Figure 5.16 Schematic diagram of the proposed mechanism by which $P2Y_2$ receptor activation causes acute suppression of lipolysis in primary human *in vitro* differentiated adipocytes. Under basal conditions (left hand panel), $P2Y_2$ receptors are activated by ATP or UTP released by the adipocytes into the extracellular space, which then subsequently activates phospholipase C (PLC) mediated production of diacylglycerol (DAG) and inositol triphosphate (IP_3). The IP_3 then binds to receptors on the surface of the endoplasmic reticulum (ER) to initiate release of calcium ions (Ca^{2+}) from the ER into the cytosol. This elevation of cytoplasmic calcium causes tonic inhibition of calcium-sensitive adenylate cyclase (AC) isoforms. However, in the absence of $P2Y_2$-receptor mediated inhibition of AC due to blockade of $P2Y_2$ receptor signalling (right hand panel), intracellular calcium concentrations are lower and therefore AC is not inhibited and consequently free to convert ATP to cyclic AMP (cAMP). The increase in intracellular cAMP activates protein kinase A (PKA), which is then able to phosphorylate cytoplasmic hormone sensitive lipase (HSL). This allows HSL to translocate the lipid droplet. Here, adipose triglyceride lipase (ATGL) catalyses the hydrolysis of triglycerides (TG) to diglycerides (DG) and free fatty acid (FA) molecules, then HSL catalyses the conversion of DG to monoglycerides (MG) and FAs, finally monoglyceride lipase (MGL) catalyses lipolytic breakdown of MG to glycerol and FA. The glycerol and three FA molecules can then be transported out of the cell and released into the bloodstream, where they can travel to the liver or other organs to be utilised as an energy source.

5.12 Exogenous application of ATP and inhibition of $P2Y_2$ receptors alters the profile of adipokines secreted by human adipocytes

In addition to storage and release of energy, adipocytes are also capable of secreting a wide variety of adipokines that are capable of regulating immune responses and metabolism (Halberg *et al.*, 2008). To determine whether there is a role for purinergic signalling in adipokine secretion, a Human Obesity Array Q3 multiplex ELISA protein array was used to the assess the secretion of 40 obesity-related adipokines in the presence and absence of super-maximal concentrations of ATP. High concentrations of ATP were used to ensure that sufficient ATP was present to activate most of the P2X and P2Y receptor subtypes expressed in human adipocytes (Gorini *et al.*, 2013). Furthermore, the effect of selective antagonism of $P2Y_2$ receptors using 10 μM AR-C118925XX was ascertained in order to determine whether $P2Y_2$ receptors exerted additional 'energy-conservative' activity to complement the effects observed on basal lipolysis.

To mimic the conditions used for the glycerol release experiments, supernatant samples were collected from adipocytes that were incubated with DMEM (no serum) for two hours, then exposed to a singular dose of vehicle or antagonist for 30 minutes, finally ATP or vehicle was added and the first samples were collected immediately (0 hour sample). Subsequent samples were then taken after a further 6 and 24 hours had elapsed. Although after 6 hours, samples were only collected for cells treated with vehicle or ATP alone and no samples were tested for cells treated with antagonist. Supernatant samples from four independent donors were utilised and the data presented in Sections 5.12, 5.13 and 5.14 are averaged across all four donors. The data from the array is summarised in Table A1, Table A2, Table 5.1 and Figure 5.17.

Although data was collected for samples taken after 0 and 6 hours, the focus here will be on the results for the samples collected after 24 hours. In brief, only 13 adipokines were detected at the 0 hour timepoint. Of these 13 adipokines, secretion of adiponectin, insulin-like growth factor (IGF) 1, IGF binding protein (IGFBP) 2, interleukin (IL) 8, retinol binding protein 4 (RBP4) and tumour necrosis factor (TNF) α were not significantly altered, whereas secretion of adipsin, IL-6, osteoprotegerin (OPG), plasminogen activator inhibitor-I (PAI-I), thrombospondin 1 (TSP-1), TNF receptor II (TNF RII) and vascular endothelial growth factor (VEGF) were significantly affected by ATP and/or AR-C118925XX addition. However, although it is possible that activation/inhibition of purinergic receptors may have an immediate effect on the secretion of these adipokines, it is not very probable, and it is more likely that these results are anomalies. All the data for the 0 hour timepoint is displayed in Table A1 in the appendix. After 6 hours, only 21 adipokines were detected, of which eleven were not affected by nucleotide or antagonist addition: adipsin, IGF-1, IGFBP1, IGFBP2, IL-6, IL-8, PAI-I, RBP4, serum amyloid A (SAA), TNFα and VEGF. However, the secretion of TSP-1 and adiponectin were both augmented, whereas expression of chemerin, growth hormone

(GH), IL-12p40, leptin, lipocalin-2, OPG, resistin and TNF RII were reduced in the presence of 100 µM ATP after 6 hours (Table A2). This suggests that purinergic signalling may be involved in modulating the secretion of these ten adipokines. Although it is interesting that these adipokines are affected by singular exogenous ATP application, it is not possible to ascribe these effects to a specific receptor, as supernatant samples treated with subtype-selective antagonists were not analysed. Thus, the primary purpose of this data is to highlight potential targets for future exploration. However, it was noteworthy that the secretion of anti-lipolytic adiponectin significantly increased (Wedellová *et al.*, 2011), whereas the release of lipolytic adipokines, such as chemerin (Fu *et al.*, 2016), GH (Sakharova *et al.*, 2008), leptin (Ruud and Brüning, 2015) and resistin (Chen *et al.*, 2014) significantly decreased in the presence of ATP. This implies purinergic signalling may promote an anti-lipolytic phenotype after 6 hours, which complements the earlier findings in this Chapter that suggest that constitutive purinergic receptor activity via $P2Y_2$ limits basal lipolysis.

The secretion of almost all of the adipokines in the array increased over time, excluding eight adipokines that were not detected regardless of the presence or absence of ATP and/or AR-C118925XX or timing. These eight adipokines were as follows: Agouti-related peptide (AgRP), brain-derived neurotrophic factor (BDNF), interferon γ (IFNγ), IL-12p70, pepsinogen I, pepsinogen II, platelet-derived growth factor-BB (PDGF-BB) and tumour necrosis factor receptor I (TNF RI). It is not possible to definitively state that these adipokines were not secreted by adipocytes, as it is possible that these adipokines were expressed at levels that fell below the assay detection limit. However, it was not surprising that these eight adipokines were not detected at any time point as previous studies suggest that these adipokines are not expressed by adipocytes or display limited expression in adipose tissue (Fagerberg *et al.*, 2014; Uhlén *et al.*, 2015; Onogi *et al.*, 2017). An additional nine adipokines were detected after 24 hours, but did not appear to be affected by either ATP or AR-C118925XX addition. These adipokines were chemerin, IL-1β, IL-1 receptor antagonist (IL-1ra), IL-12p40, insulin, lipocalin-2, leptin, MSPα and resistin (Table 5.1). There were a few adipokines that were excluded from further study due to technical issues. This included TSP-1, which was omitted, because the concentration of TSP-1 exceeded the assay detection limits after 24 hours, which rendered it impossible to determine whether nucleotide or antagonist addition had an effect. This issue could have been overcome by diluting the supernatant samples to ensure the concentration of TSP-1 fell within the dynamic range of the assay. Furthermore, the data for prolactin was removed, as samples that had undergone multiple freeze-thaw cycles had artifactually reduced quantities of prolactin. Repetition of this experiment with fresh sample would be a good method of ascertaining whether ATP or AR-C118925XX treatment influenced prolactin secretion, but unfortunately time-constraints meant that it was not possible to repeat the experiment for TSP-1 or prolactin within the timeframe of this study.

Of the remaining adipokines, only five were significantly affected by exogenous ATP application, whereas expression of 20 adipokines was altered by selective antagonism of $P2Y_2$ receptors (Table 5.1, Figure 5.17). It is important to be cautious when interpreting the data produced from this protein array. Adipocytes are highly dynamic cells that can adjust their activity in response to changes in their environment. Earlier in this Chapter, it was demonstrated that inhibition of $P2Y_2$ receptors enhances basal lipolysis. It has previously been shown that FFAs can inhibit lipolysis (Burns *et al.*, 1975) and cause inflammation (Jiao *et al.*, 2011). This is just one example, but it is important to note that the evident changes in adipokine secretion due to inhibition of $P2Y_2$ receptors may not be due to direct inhibition of $P2Y_2$-mediated pathways. They may be as a result of activation of feedback mechanisms triggered by $P2Y_2$ inhibition-induced enhanced lipolysis.

Table 5.1 Adipokines secreted by primary human *in vitro* differentiated adipocytes after 24 hours following singular treatment with vehicle, 100 µM ATP and/or a $P2Y_2$ receptor antagonist (10 µM AR-C118925XX (AR-C)) (*N*=4). Adipokines were quantified by protein array and the data are presented as mean ± SEM for four donors. % increase and decrease values show the statistically significant changes in expression versus the vehicle control levels. *NS* indicates no significant change. Cases of donor variation are indicated by an * near the adipokine's name.

	Vehicle control (pg/ml)	100 µM ATP (pg/ml)	% increase or decrease	10 µM AR-C (pg/ml)	% increase or decrease	ATP and AR-C (pg/ml)	% increase or decrease
Adiponectin	8542.1 ± 1404	12018.2 ± 931	*NS*	16001.1 ± 1156	↑ 87%	15533.5 ± 1492	↑82%
Adipsin	1360.5 ± 208	2114.5 ± 337	↑ 55%	5024.4 ± 1468	↑ 269%	5334.3 ± 1549	↑ 292%
AgRP	<14	<14	-	<14	-	<14	-
ANGPTL4	432.4 ± 45	670.4 ± 68	*NS*	119.7 ± 30	↓ 72%	173.5 ± 20	↓ 60%
BDNF	<55	<55	-	<55	-	<55	-
Chemerin	602.1 ± 140	1328.1 ± 458	*NS*	374.6 ± 70	*NS*	311.3 ± 66	*NS*
CRP*	<27	<27	-	12.6 ± 4	*NS*	18.7 ± 5	*NS*
GH	<27	59.5 ± 17	↑ 100%	45.1 ± 11	*NS*	75.7 ± 12	↑ 100%
IFNγ	<14	<14	-	<14	-	<14	-
IGFBP-1	15.3 ± 5	39.6 ± 7	*NS*	346.8 ± 28	↑ 2162%	390.2 ± 33	↑ 2446%
IGFBP-2	756.4 ± 57	1040.1 ± 93	*NS*	262.9 ± 20	↓ 65%	292.6 ± 32	↓ 61%
IGF-1	4921.0 ± 1077	6558.2 ± 1140	*NS*	41515.3 ± 2087	↑ 743.6%	53555.4 ± 2911	↑ 988.3%
IL-10*	1.8 ± 0.5	5.9 ± 1	*NS*	8.5 ± 2	↑ 369%	17.2 ± 4	↑ 857%
IL-12p40	220.2 ± 95	80.2 ± 26	*NS*	32.2 ± 9	*NS*	40.0 ± 10	*NS*
IL-12p70	<3	<3	-	<3	-	<3	-
IL-1β	3.0 ± 0.9	4.3 ± 1	*NS*	6.1 ± 1	*NS*	4.8 ± 0.8	*NS*
IL-1Ra	358.0 ± 64	421.0 ± 59	*NS*	188.6 ± 48	*NS*	204.1 ± 46	*NS*
IL-6	836.4 ± 150	1837.0 ± 113	↑ 120%	1547.0 ± 145	↑ 85%	1383.1 ± 168	*NS*
IL-8	102.4 ± 21	119.6 ± 25	*NS*	181.4 ± 23	↑ 77%	238.9 ± 30	↑ 133%
Insulin	1127.1 ± 381	5006.0 ± 802	*NS*	3767.1 ± 1673	*NS*	668.0 ± 369	*NS*

Leptin	271.1 ± 54	273.2 ± 35	*NS*	151.4 ± 25	*NS*	88.3 ± 24	*NS*
Lipocalin-2	3.0 ± 0.6	4.0 ± 0.7	*NS*	4.9 ± 1	*NS*	2.6 ± 1	*NS*
MSPα	182.3 ± 55	237.6 ± 55	*NS*	121.1 ± 39	*NS*	99.1 ± 26	*NS*
OPG	2309.1 ± 351	1862.0 ± 143	*NS*	1775.1 ± 264	*NS*	828.8 ± 166	↓ 64%
PAI-I	6450.2 ± 1172	6707.2 ± 621	*NS*	1738.6 ± 322	↓ 73%	1355.1 ± 292	↓ 79%
PDGF-BB	<3	<3	-	<3	-	<3	-
Pepsinogen 1	<27	<27	-	<27	-	<27	-
Pepsinogen 2	<55	<55	-	<55	-	<55	-
Procalcitonin	393.7 ± 120	896.2 ± 339	*NS*	<137	↓ 100%	<137	↓ 100%
RANTES	282.4 ± 98	541.6 ± 191	↑ 92%	53.5 ± 15	*NS*	89.1 ± 23	*NS*
RBP4	6459.1 ± 751	6158.5 ± 628	*NS*	2739.7 ± 90	↓ 58%	2045.0 ± 253	↓ 68%
Resistin	579.2 ± 203	1118.3 ± 350	*NS*	70.3 ± 21	*NS*	21.6 ± 10	*NS*
SAA	<137	<137	*NS*	1816.1 ± 186	↑ 100%	1839.5 ± 341	↑ 100%
TGFβ1*	<137	<137	*NS*	278.4 ± 66	↑ 100%	269.6 ± 70	*NS*
TSP-1	>200,000	>200,000	-	>200,000	-	>200,000	-
TNF RI	<137	<137	-	<137	-	<137	-
TNF RII	70.7 ± 7	141.5 ± 11	*NS*	24.7 ± 4	*NS*	18.3 ± 4	↓ 74%
TNFα	98.8 ± 16	319.8 ± 125	*NS*	48.1 ± 8	*NS*	21.9 ± 8	↓ 78%
VEGF	1593.2 ± 73	2039.7 ± 118	↑ 28%	979.0 ± 39	↓ 39%	842.4 ± 113	↓ 47%

*CRP and IL-10 were only detected in 2 of 4 donors tested; TGFβ1 was only detected in 3 of 4 donors tested.

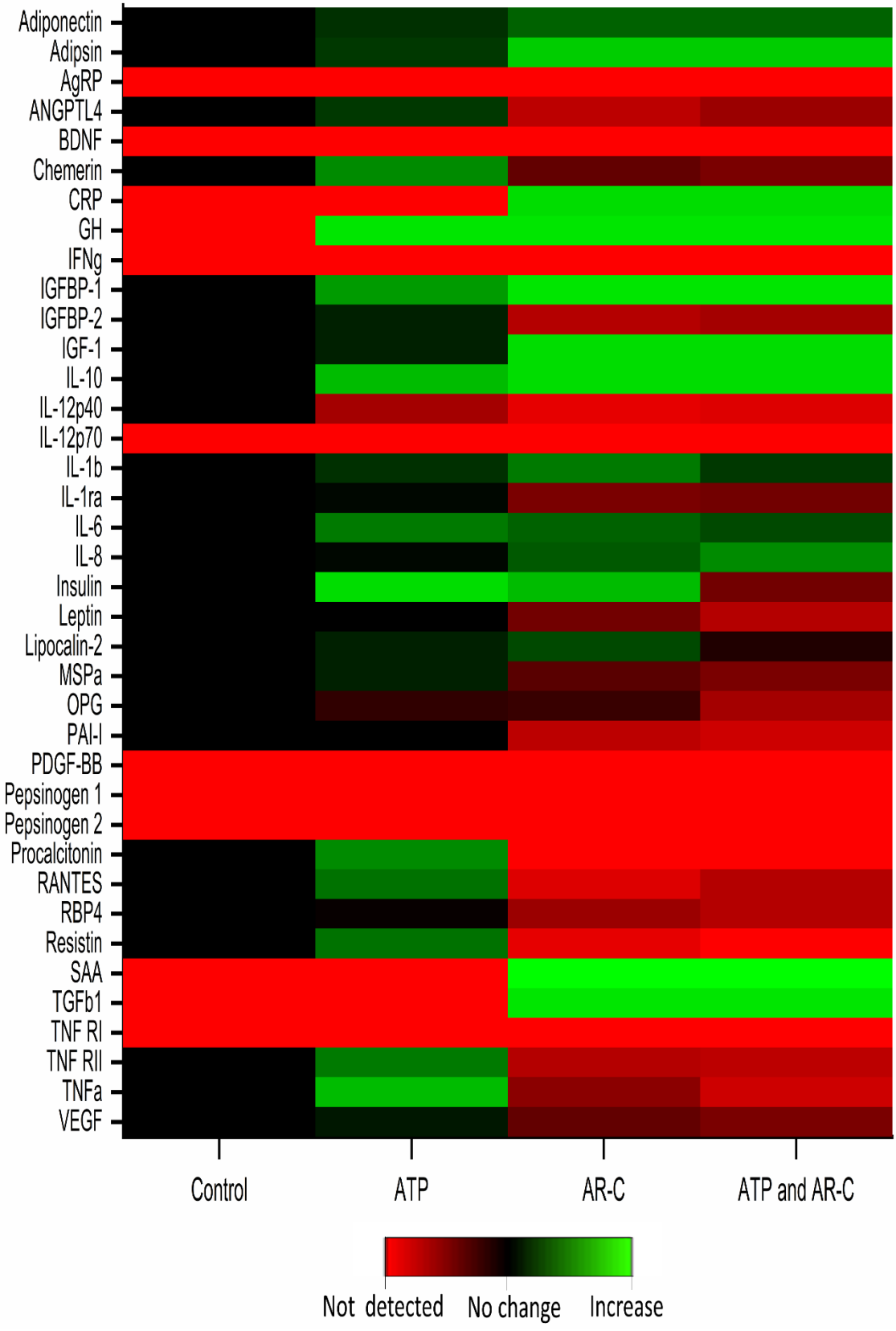

Figure 5.17 Heatmap summarising the changes in adipokine secretion after 24 hours following singular treatment with 100 µM ATP and/or 10 µM AR-C118925XX (AR-C) (*N*=4). Data are shown relative to the control levels of each respective adipokine. Red represents low secretion/not detected, black represents no change and green represents an increase in secretion. Heatmap was generated using Origin Pro software.

5.13 Inhibition of $P2Y_2$ receptors promotes release of chemokines, cytokines and acute phase proteins

Obesity is associated with an increase in adipocytokine production (Halberg *et al.*, 2008; Fain, 2010), that contributes to chronic low grade inflammation of adipose tissue, which in turn is thought to influence the development of obesity-related comorbidities (Després *et al.*, 2006; van Greevenbroek *et al.*, 2013). Obesity is also associated with elevated fasting FFA levels due to an increased rate of basal lipolysis (Wang *et al.*, 2003) and FFA are known to promote inflammation and insulin resistance (Jiao *et al.*, 2011). Earlier in this Chapter, it was determined that inhibition of $P2Y_2$ causes an acute increase in basal glycerol release. Although FFA release was not directly measured, it can be assumed that enhanced glycerol release would be accompanied by augmented FFA production too, thus it was hypothesised that blockade of $P2Y_2$ receptors may promote secretion of proinflammatory cytokines. In support of this theory, inhibition of $P2Y_2$ receptors for 24 hours appears to increase secretion of proinflammatory cytokines and acute phase proteins, such as IL-6, IL-8, C-reactive protein (CRP), serum amyloid A (SAA) and transforming growth factor (TGF) β1, as well as causing a decrease in secretion of TNF RII, thus reducing its capacity to block the proinflammatory action of TNFα (Table 5.1; Figure 5.18). IL-6 secretion was also significantly increased in the presence of 100 μM ATP for 24 hours (Figure 5.18A), which suggests that other purinergic receptors are also involved in modulating IL-6 secretion. CRP, SAA and TGF β1 were only detected when $P2Y_2$ receptors were inhibited (Figure 5.18C-E). However, CRP secretion was only observed in two of the four donors tested, so when the data for all four donors was analysed, the increase in CRP secretion was not deemed statistically significant (Figure 5.18C). On average, TNF RII secretion appears to increase in the presence of ATP alone and decrease in the presence of AR-C118925XX, however these changes were not statistically significant, although co-application of ATP and AR-C118925XX did cause a significant reduction (Figure 5.18F). Taken together, this data suggests that inhibition of $P2Y_2$ receptors promotes inflammation, which may be indirectly due to $P2Y_2$-inhibition induced enhancement of basal lipolysis or directly due to inhibition of tonic $P2Y_2$ activity. If it is the latter explanation, then this would imply that tonic activation of $P2Y_2$ receptors act to reduce inflammation via suppression of proinflammatory adipokine release.

However, in addition to AR-C118925XX treatment inducing an increase in proinflammatory cytokines, blockade of $P2Y_2$ receptors for 24 hours also appears to increase the release of anti-inflammatory cytokines, such as IL-10, as well as diminishing the secretion of some acute phase reactants, including PAI-I and procalcitonin (Whicher *et al.*, 2001). Pharmacological blockade of $P2Y_2$ receptors increases the secretion of IL-10 from 1.8 ± 0.5 pg/ml to 17.2 ± 4 pg/ml (N=4; p<0.005) and 8.5 ± 1.9 pg/ml (N=4; p<0.05) in the presence and absence of 100 μM ATP respectively (Figure 5.19A). Furthermore, ATP increases the secretion of RANTES (regulated on activation, normal T cell

expressed and secreted), a chemotactic factor that encourages the recruitment of immune cells (Appay and Rowland-Jones, 2001), but this increase is neutralised when $P2Y_2$ receptors are inhibited, which suggests that the ATP-induced secretion of RANTES is mediated by $P2Y_2$ receptor activity. Constitutive activity of $P2Y_2$ receptors appears to have no effect on RANTES secretion as AR-C118925XX alone did not significantly alter the concentration of RANTES produced. Together these findings suggest that in addition to encouraging the secretion of proinflammatory cytokines, inhibition of $P2Y_2$ receptors also endorses an anti-inflammatory phenotype. Within the scope of this study, it was not determined whether the increase in anti-inflammatory cytokines was directly due to $P2Y_2$ inhibition or due to activation of homeostatic pathways to manage the effects of the increased presence of pro-inflammatory mediators or vice versa.

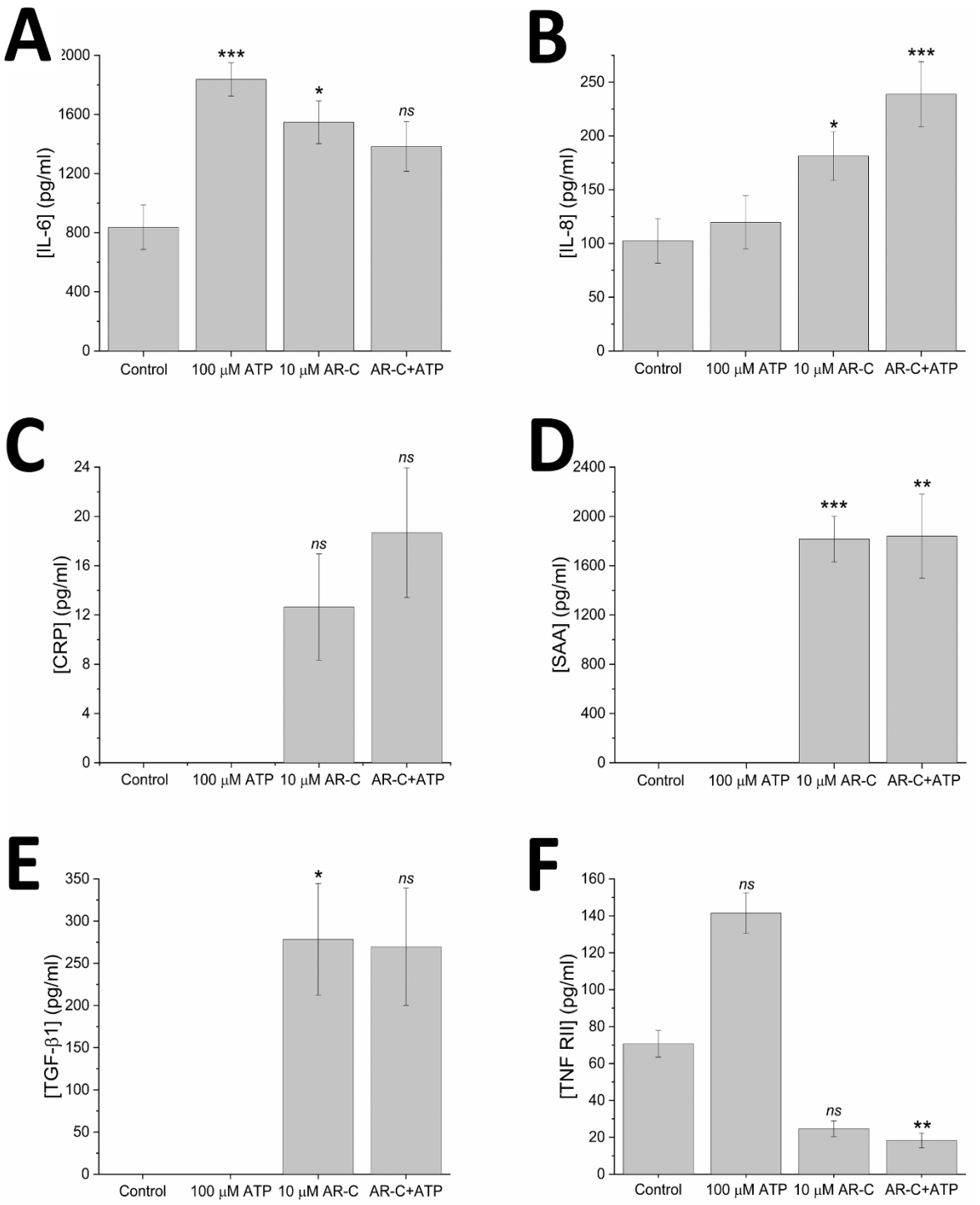

Figure 5.18 Inhibition of $P2Y_2$ receptors enhances the secretion of proinflammatory adipokines, as well as reducing the secretion of some anti-inflammatory adipokines (*N*=4). Effect of singular treatment with 100 μM ATP, 10 μM AR-C118925XX ($P2Y_2$ receptor antagonist) and co-application of ATP and AR-C118925XX on the secretion of (A) interleukin 6 (IL-6), (B) interleukin 8 (IL-8), (C) C-reactive protein (CRP), (D) serum amyloid A (SAA), (E) transforming growth factor (TGF) β1 and (F) tumour necrosis factor receptor II (TNF RII) from primary human *in vitro* differentiated adipocytes after 24 hours. All adipokines were quantified using a Human Obesity Array Q3 multiplex ELISA protein array from Ray Biotech. All data are expressed as mean ± SEM. **p*<0.05, ***p*<0.005, ****p*<0.001, *ns p*>0.05 versus secretion of each adipokine under control conditions (vehicle only).

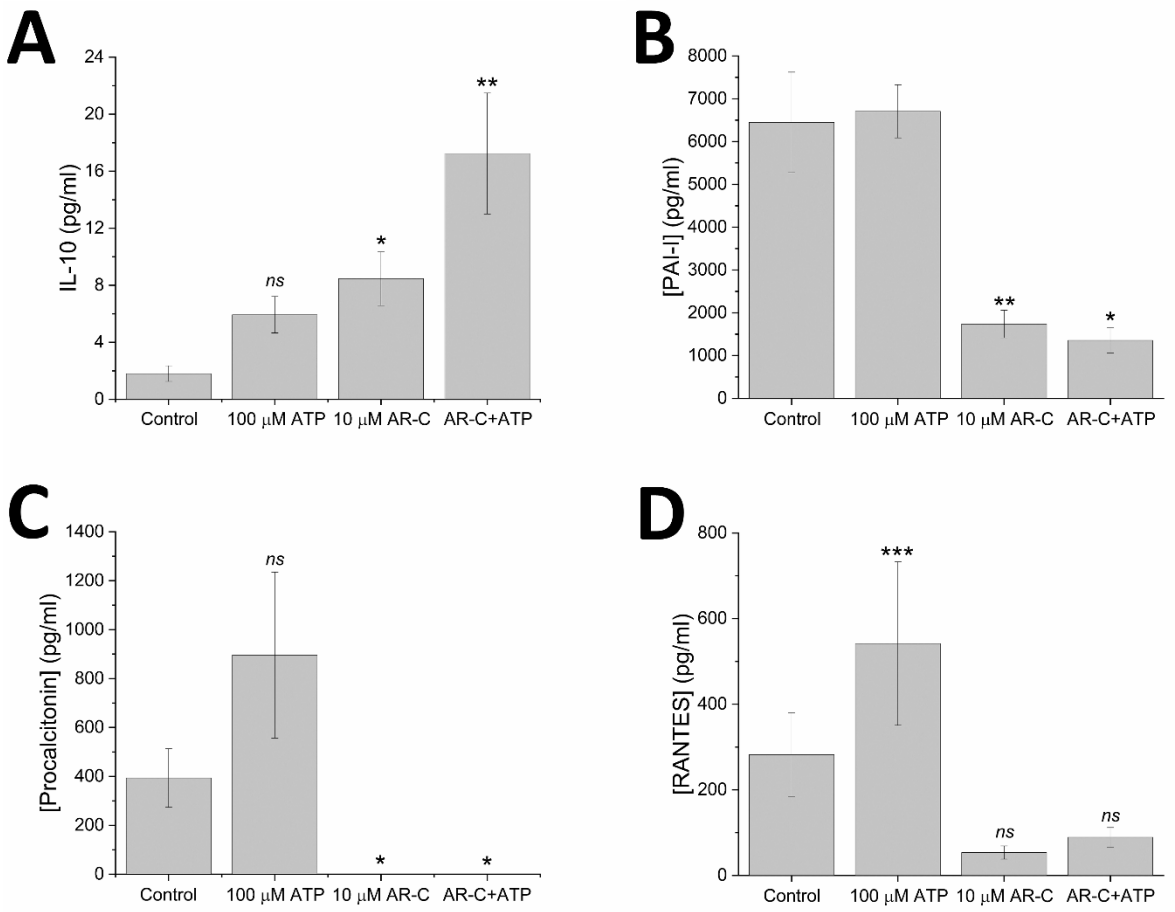

Figure 5.19 Inhibition of $P2Y_2$ receptors enhances the secretion of anti-inflammatory cytokines (IL-10), decreases expression of acute phase reactants (PAI-I and procalcitonin) and neutralises ATP-induced secretion of RANTES (*N*=4). Effect of singular treatment with 100 µM ATP, 10 µM AR-C118925XX ($P2Y_2$ receptor antagonist) and co-application of ATP and AR-C118925XX on the secretion of (A) interleukin 10 (IL-10), (B) plasminogen activator inhibitor-I (PAI-I), (C) procalcitonin and (D) RANTES from primary human *in vitro* differentiated adipocytes after 24 hours. All adipokines were quantified using a Human Obesity Array Q3 multiplex ELISA protein array from Ray Biotech. All data are expressed as mean ± SEM. **p*<0.05, ***p*<0.005, ****p*<0.001, *ns p*>0.05 versus secretion of each adipokine under control conditions (vehicle only).

5.14 After 24 hours, inhibition of $P2Y_2$ receptors enhances secretion of anti-lipolytic adipokines and decreases basal glycerol release

The results of the protein array appear to demonstrate that longer term (24 hours) treatment of primary human *in vitro* differentiated adipocytes with 10 µM AR-C118925XX promotes an anti-lipolytic phenotype, which is contrary to the earlier findings that indicate that inhibition of $P2Y_2$ receptors enhances basal lipolysis. Pharmacological inhibition of $P2Y_2$ dramatically enhances secretion of adipokines with anti-lipolytic activity including adiponectin (Qiao *et al.*, 2011; Wedellová *et al.*, 2011) and adipsin (Van Harmelen *et al.*, 1999; Ronti *et al.*, 2006; Liu *et al.*, 2015) (Figure 5.20). Although a slight increase in adiponectin secretion was observed in the presence of ATP alone, this increase was not significant and instead these data suggest inhibition of $P2Y_2$ receptors, irrespective of whether ATP is present or not, increases secretion of adiponectin (Figure 5.20A). Similarly, AR-C118925XX treatment with and without ATP caused an increase in adipsin secretion, although ATP alone also caused a significant increase (Figure 5.20B), which indicates that $P2Y_2$ activity may suppress adipsin secretion, while activation of another purinergic receptor may augment adipsin release. In addition to causing an increase in anti-lipolytic adipokine secretion, selective inhibition of $P2Y_2$ also led to a down-regulation of several adipokines that stimulate lipolysis, including angiopoietin-like 4 (ANGPTL4) protein (Gray *et al.*, 2012; La Paglia *et al.*, 2017), retinol-binding protein 4 (RBP4) (Lee *et al.*, 2016) and tumour necrosis factor α (TNFα) (H. H. Zhang *et al.*, 2002). The secretion of both ANGPTL4 and TNFα are non-significantly increased with ATP alone, but significantly decreased with AR-C118925XX treatment (Figure 5.20C,E), albeit in the case of TNFα the decrease observed is only statistically significant when the cells are treated with both ATP and AR-C118925XX simultaneously (Figure 5.20E). The fact that inhibition of $P2Y_2$ decreased release of ANGPTL4 and TNFα suggests that tonic $P2Y_2$ activity may encourage secretion of both adipokines and exogenous application of ATP may further augment secretion, but currently the data suggests exogenous ATP has no effect. Previous reports indicate that overexpression of human RBP4 in mouse adipocytes stimulates lipolysis via RBP4-induced inflammation (Lee *et al.*, 2016). RBP4 expression is also decreased following treatment with AR-C118925XX for 24 hours, but unlike, ANGPTL4 and TNFα, there is no indication that exogenous ATP may potentially influence RBP4 secretion (Figure 5.20D).

To test whether the augmented release of anti-lipolytic adipokines and diminished secretion of lipolytic adipokines (Figure 5.20) coincided with a reduction in basal glycerol release after 24 hours, the amount of glycerol in the supernatant was quantified following 0.5, 3.5 and 24.5 hours treatment with a singular dose of 10 µM AR-C118925XX. This demonstrated that there was a gradual accumulation of glycerol in the supernatant over time. Furthermore, it confirmed that blocking $P2Y_2$ receptor activity led to an increase in basal glycerol release after 0.5 and 3.5 hours,

but interestingly, it also established that selective antagonism of $P2Y_2$ caused a reduction in the glycerol concentration in the supernatant after 24.5 hours (Figure 5.21). These data indicate that acute inhibition of $P2Y_2$ receptors enhances lipolysis, whereas prolonged blockade of $P2Y_2$ receptors inhibits lipolysis. It is possible that this change in phenotype is due to the activation of feedback mechanisms triggered by an acute increase in lipolysis, which enhances the secretion of anti-lipolytic adipokines to overcome the lipolytic effects of $P2Y_2$ inhibition. However, to confirm this hypothesis additional experiments would be required.

In keeping with the energy storage theme of $P2Y_2$ receptor inhibition after 24 hours, selective antagonism of the receptor also seems to encourage the release of adipokines that may stimulate adipose tissue expansion and enhance glucose uptake (Figure 5.22). As well as being anti-lipolytic agents, both adiponectin and adipsin act to enhance glucose uptake (Sniderman and Cianflone, 1994; Tao *et al.*, 2014). In addition, a substantial increase in insulin-like growth factor (IGF) 1 and IGF binding protein (IGFBP) 1 and a decrease in IGFBP2 was detected after 24 hours in the presence of 10 µM AR-C118925XX (*N*=4; Figure 5.22). in addition, IGFBP2 secretion is enhanced by exogenous ATP treatment (Figure 5.22C). IGF-1 has been shown to be critical for cell proliferation and differentiation of adipocyte precursor cells (Smith *et al.*, 1988; Scavo *et al.*, 2004), as well as stimulating glucose uptake (Clemmons, 2004). The activity of IGF-1 is regulated by IGF binding proteins (IGFBP). Both IGFBP1 and IGFBP2 have been shown to inhibit the action of IGF-1, but IGFBP1 can also potentiate IGF-1 activity (Rajaram *et al.*, 1997).

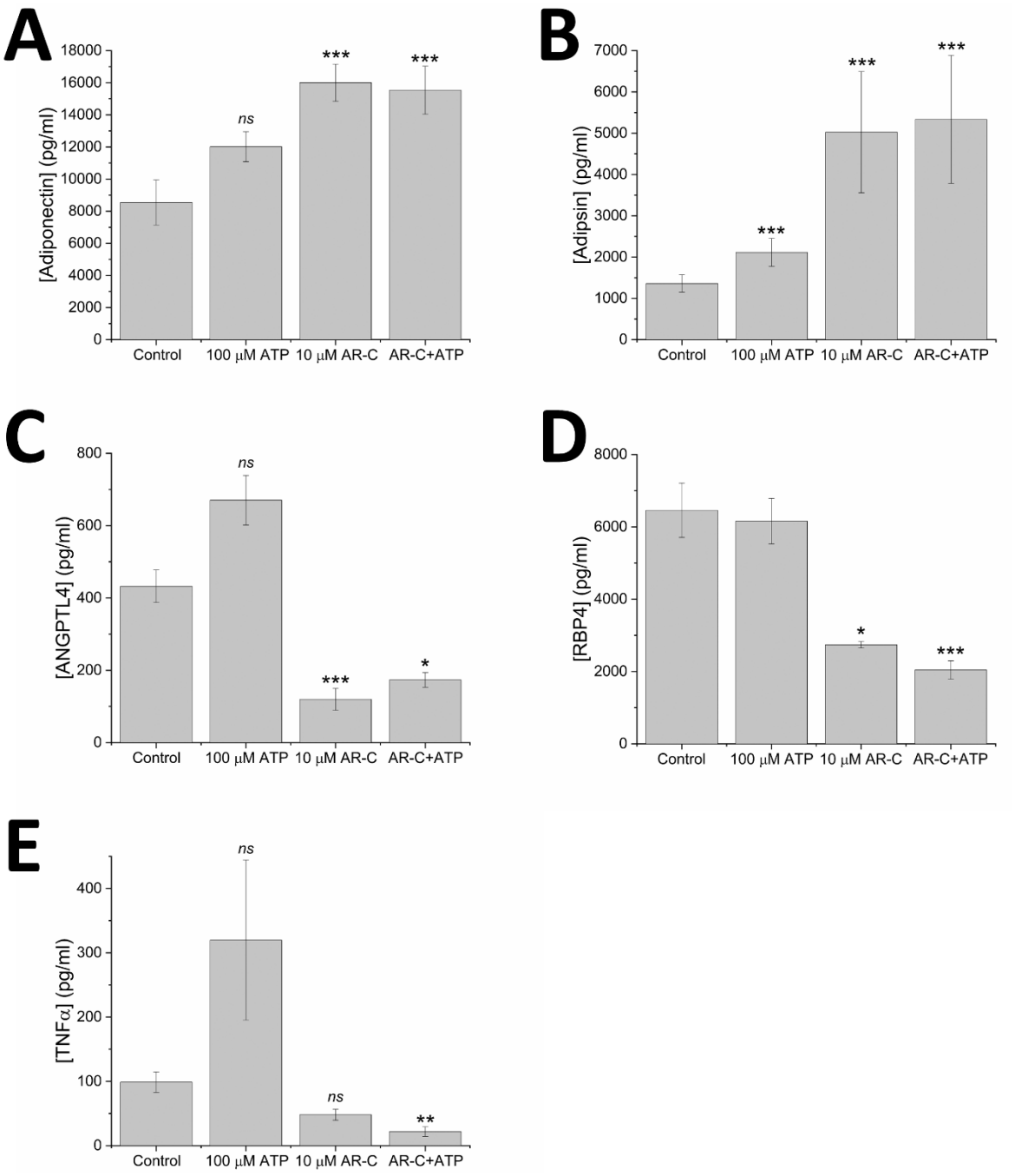

Figure 5.20 Inhibition of $P2Y_2$ receptors increases the release of anti-lipolytic adipokines and downregulates the secretion of lipolytic adipokines (*N*=4). Effect of singular treatment with 100 µM ATP, 10 µM AR-C118925XX ($P2Y_2$ receptor antagonist) and co-application of ATP and AR-C118925XX on the secretion of (A) adiponectin, (B) adipsin, (C) angiopoietin-like 4 (ANGPTL4), (D) retinol-binding protein 4 (RBP4) and (E) tumour necrosis factor α (TNFα). All adipokines were quantified using a Human Obesity Array Q3 multiplex ELISA protein array from Ray Biotech. All data are expressed as mean ± SEM. **p*<0.05, ***p*<0.005, ****p*<0.001, *ns p*>0.05 versus secretion of each adipokine under control conditions (vehicle only).

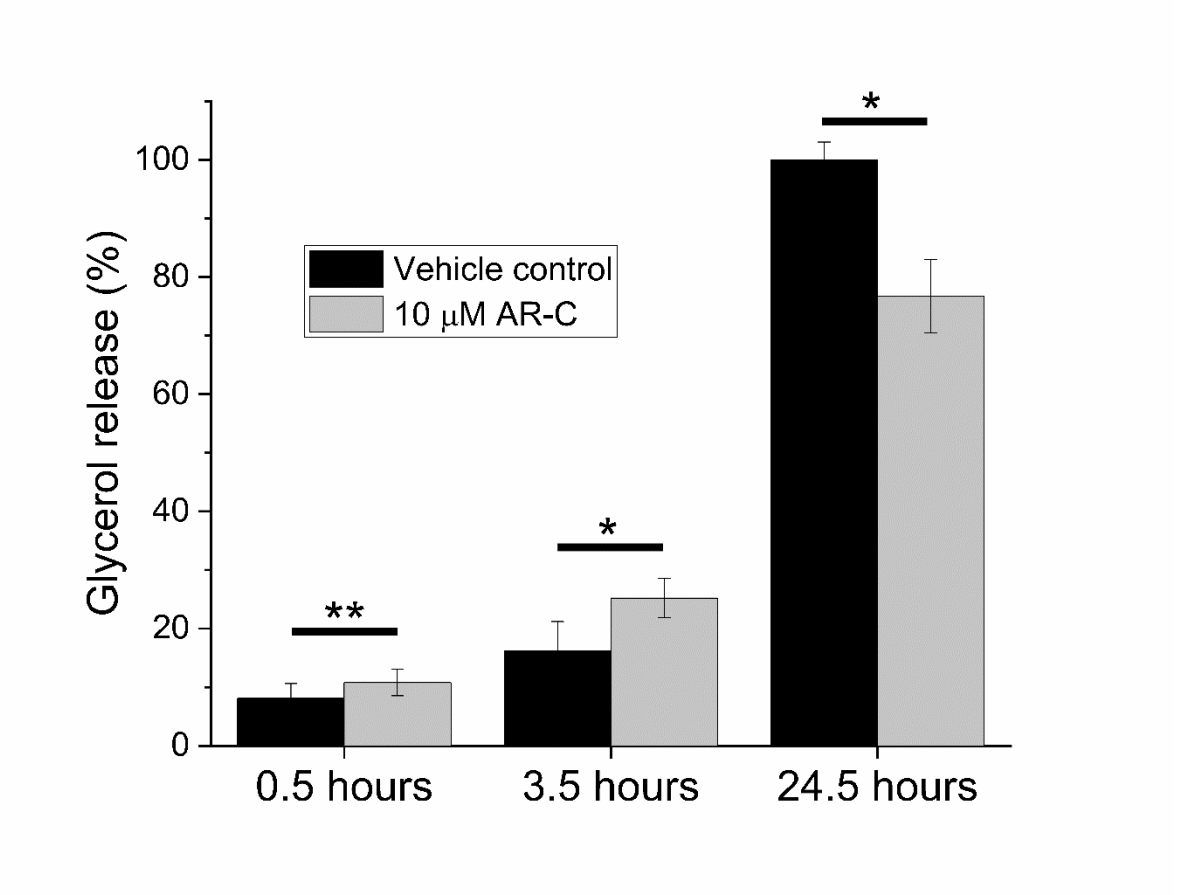

Figure 5.21 Pharmacological inhibition of $P2Y_2$ receptors in primary human *in vitro* differentiated adipocytes causes an acute increase in basal glycerol release, but longer-term receptor antagonism leads to a reduction in basal glycerol release (*N*=4). $P2Y_2$ receptors were inhibited with 10 μM AR-C118925XX (AR-C). All data are normalised to the glycerol release after 24 hours in the presence of vehicle only (control). *p<0.05, **p<0.005 signifies a significant difference between the two conditions under the line above the bars.

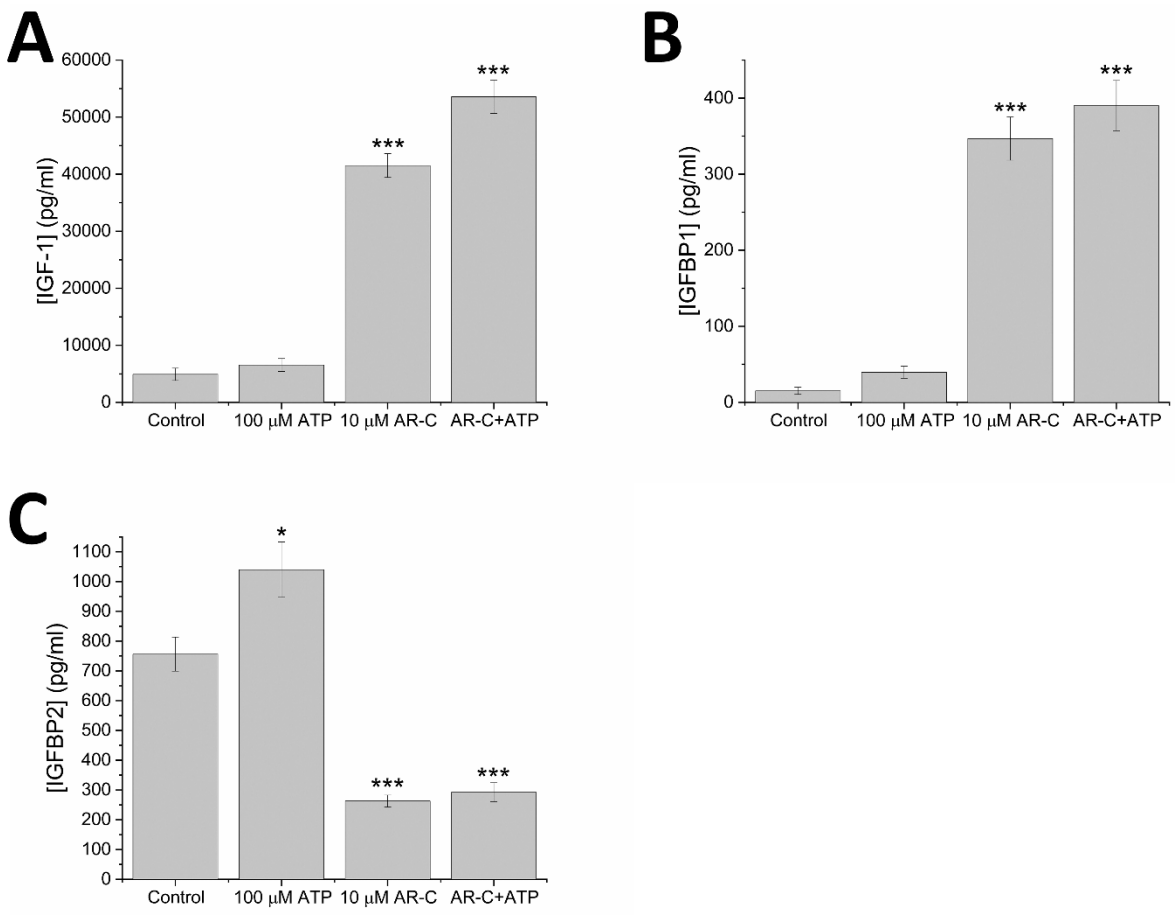

Figure 5.22 Inhibition of $P2Y_2$ receptors encourages release of adipokines that promote glucose uptake and tissue expansion after 24 hours (*N*=4). Effect of singular treatment with 100 μM ATP, 10 μM AR-C118925XX ($P2Y_2$ receptor antagonist) and co-application of ATP and AR-C118925XX on the secretion of (A) insulin-like growth factor 1 (IGF-1), (B) insulin-like growth factor binding protein 1 (IGFBP1) and (C) insulin-like growth factor binding protein 2 (IGFBP2). All adipokines were quantified using a Human Obesity Array Q3 multiplex ELISA protein array from Ray Biotech. All data are expressed as mean ± SEM. **p*<0.05, ***p*<0.005, ****p*<0.001, *ns p*>0.05 versus secretion of each adipokine under control conditions (vehicle only).

5.15 Selective antagonism of $P2Y_2$ receptors in primary human subcutaneous adipose tissue samples *ex vivo* causes a decrease in basal glycerol release

The results presented in thesis were almost exclusively obtained using primary human cells cultured *in vitro*. In order to determine whether the effects observed *in vitro* are mimicked *ex vivo*, small pieces of primary human subcutaneous adipose tissue were treated with 10 µM AR-C118925XX or vehicle and the amount of glycerol released into the supernatant was calculated. Via this method, it was evident that there were discrepancies between the *in vitro* and *ex vivo* model. Unlike the *in vitro* model, where inhibition of $P2Y_2$ receptors caused an acute increase in basal lipolysis (Figure 5.8), in the *ex vivo* model selective antagonism of $P2Y_2$ receptor caused an acute decrease in basal lipolysis (Figure 5.23). The differences between these two models may be due to numerous factors, including the fact that the *ex vivo* model contains multiple interacting cells types, whereas the *in vitro* cells are a relatively pure population of adipocytes, in addition the tissue is likely to have a much larger number of cells than the *in vitro* model. The differences between the two models will be discussed further in Chapter 6. It has already been confirmed that the lipolytic action of $P2Y_2$ inhibition is reversed with time, so it is evidently a dynamic process and these data may indicate that $P2Y_2$ receptors act as a 'molecular switch' that are capable of promoting or suppressing basal lipolysis in response to different conditions. It is possible that altering the *ex vivo* conditions may change the phenotype observed, however more research is needed to fully understand the mechanism that links $P2Y_2$ receptor activity and lipolysis. By understanding the mechanism fully, it may be possible to decipher how different factors such as interaction with other cell types or secretion of adipokines may influence this mechanism. Although the results suggest that there is disparity between the *in vitro* and *ex vivo* model, both models confirm that $P2Y_2$ receptors play a role in altering basal lipolysis, thus indicating that $P2Y_2$ receptors represent an interesting target to explore with a view to controlling triglyceride reserve usage.

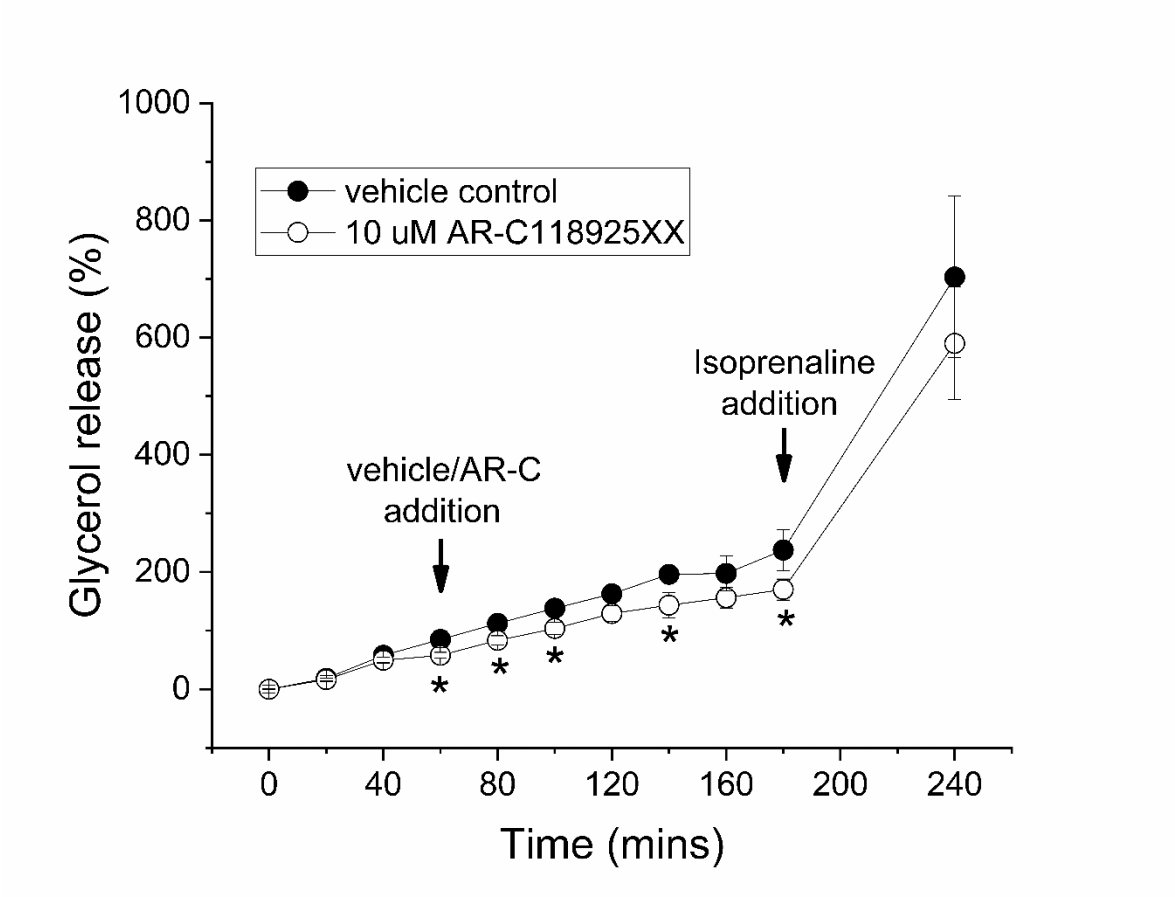

Figure 5.23 Inhibition of $P2Y_2$ receptors in primary human subcutaneous adipose tissue *ex vivo* causes a subtle decrease in basal glycerol release (*N*=3). $P2Y_2$ receptors were selectively antagonised with 10 µM AR-C118925XX. Basal samples were taken every 20 minutes for the first hour, then vehicle or antagonist was added, and samples were collected every 20 minutes for 2 hours. Finally, 1 µM isoprenaline was added as a positive control to verify that the tissue was capable of responding to a known lipolytic agent. Glycerol release was normalised to the weight of the tissue sample and the amount of glycerol present in the supernatant at time 0. **p*<0.05 versus glycerol release in the presence of vehicle only.

5.16 Summary

Utilising primary human *in vitro* differentiated subcutaneous adipocytes, it was determined that these cells are capable of secreting sufficiently high concentrations of ATP to activate $P2Y_2$ receptors expressed on the surface of the cells in an autocrine and/or paracrine manner. This means that under basal conditions $P2Y_2$ receptors may be constitutively active. $P2Y_2$ receptors primarily couple to G_q proteins, thus activation of these receptors leads to activation of PLC and subsequent production of IP_3 and DAG. The IP_3 is then able to bind to receptors on the surface of the endoplasmic reticulum, which initiate the release of calcium from the intracellular stores. Thus, constitutive $P2Y_2$ activity may be able to control calcium tone within primary human adipocytes. This maintenance of 'elevated' intracellular calcium levels inhibits calcium-sensitive isoforms of AC (AC5 and/or AC6), which limits the production of cAMP, which in turn means that $P2Y_2$ activity may control cytoplasmic cAMP tone within adipocytes as well. The limiting of cAMP accumulation means that PKA is not activated and therefore cannot phosphorylate CGI-58, perilipins or HSL, which in turn means that the extent of basal lipolysis is limited. This is evident in the fact that inhibition of $P2Y_2$ and shRNA-mediated knockdown of $P2Y_2$ receptor expression causes an increase in basal glycerol release, thus implying that constitutive $P2Y_2$ receptor activation limits basal glycerol release in primary human adipocytes. Furthermore, exogenous ATP application enhances the secretion of anti-lipolytic adiponectin, while also reducing the expression of lipolytic adipokines, such as chemerin, GH, leptin and resistin after 6 hours. This signifies that activation of purinergic signalling pathways promotes an anti-lipolytic phenotype in primary human adipocytes. Although currently it is not possible to ascribe these actions to $P2Y_2$ receptors specifically.

Although short-term inhibition of $P2Y_2$ (<4 hours) causes an increase in basal lipolysis, longer-term (24 hours) antagonism of $P2Y_2$ receptors appears to cause a decrease in basal glycerol release. This coincides with an enhancement in the secretion of anti-lipolytic adipokines, such as adiponectin and adipsin, while also reducing the expression of lipolytic adipokines, including ANGPTL4, RBP4 and TNFα. Longer term inhibition of $P2Y_2$ receptors also appears to promote a largely proinflammatory phenotype via augmented release of proinflammatory cytokines, chemokines and acute phase proteins. It is unclear whether these changes in the adipokine secretion profiles are directly due to inhibition of $P2Y_2$-mediated pathways or triggered by the activation of feedback mechanisms to rectify the loss of triglycerides due to $P2Y_2$-inhibition induced lipolysis. However, it is more likely that the effects are primarily due to the latter explanation. If the effects were predominantly due to direct inhibition of $P2Y_2$-mediated adipokine release or suppression, then it would be anticipated that knocking down $P2Y_2$ receptor expression would mimic the longer-term phenotype, rather than the shorter-term phenotype, which was not the case. However, irrespective of the cause, the development of a proinflammatory phenotype following treatment with a $P2Y_2$ antagonist proposes a potential hurdle for clinical use of $P2Y_2$ receptor antagonist, because it may

indicate that although inhibition of $P2Y_2$ receptors may be an attractive target for modulating basal lipolysis to control adipose tissue mass, this may also have unintended consequences such as inducing inflammation of adipose tissue, which is known to exacerbate the metabolically unfavourable consequences of obesity (Tilg and Moschen, 2008; Després, 2012). The adipocyte secretome is complex and highly regulated. A significant amount of additional work would be required to identify the exact mechanisms that lead to the up/down-regulation of each adipokine and how they may link to $P2Y_2$ receptor activity. The results of this protein array provide a good overview of some of the adipokines secreted after $P2Y_2$ receptors are inhibited, but the data presented here does not provide any definitive information regarding the mechanism that links $P2Y_2$ receptor activity and adipokine secretion. The protein array data presented in this Chapter should be viewed as an initial probe that highlights potential candidates for further investigation.

Despite the fact that all the data from the *in vitro* differentiated adipocytes suggests acute inhibition of $P2Y_2$ receptors enhances basal lipolysis, these findings were not replicated when primary human adipose tissue pieces were stimulated with AR-C118925XX (a $P2Y_2$ antagonist). In fact, using this *ex vivo* model, it was revealed that $P2Y_2$ receptor inhibition decreased basal glycerol release, which implies that constitutive $P2Y_2$ receptor activity enhances basal glycerol release, rather than limits it. Further experimentation is required to determine the reason for the differences observed between these two models. However, these results may suggest that $P2Y_2$ receptors may act as a 'molecular switch' in adipocytes that can promote or inhibit lipolysis under different conditions. Regardless of the discrepancies between the *in vitro* and *ex vivo* models, these data reveal $P2Y_2$ receptors as an interesting target for pharmacologically manipulating basal lipolysis in humans.

Chapter 6: Discussion

6.1 Project overview

Obesity is characterised by an excessive accumulation of adipose tissue that impacts of an individual's health. In recent years, there has been a global surge in the numbers of overweight and obese adults and children (WHO, 2018). This presents a substantial health issue, as obesity is linked to the development a number of chronic metabolic disorders, such as type 2 diabetes and cardiovascular disease. There is an almost log-linear increase in the risk of mortality as an individual's body weight increases over the healthy body mass index (BMI) range of 18 to 25 kg/m^2 (Di Angelantonio *et al.*, 2016), where each 5 kg/m^2 increase in BMI above the healthy range is associated with a 41% increase in risk of vascular mortality and 210% elevated probability of diabetic mortality, as well as a 29% higher risk of overall mortality (Whitlock *et al.*, 2009).

The global rise in the incidence of obesity has initiated a rise in research into adipose tissue biology to enable attempts to identify novel drug targets that can be of use in the fight against obesity and related comorbidities. It has been identified that adipose tissue expands through hyperplasia via stimulation of adipogenesis in tissue-resident adipocyte progenitor cells and hypertrophy of mature adipocytes due to enhanced storage of neutral lipids (White *et al.*, 2014). Although many efforts have been made to identify the cellular signalling mechanisms involved in adipose tissue regulation, very little research has been conducted to investigate the potential role of purinergic signalling in white adipose tissue (WAT). Cellular signalling mechanisms mediated via extracellular nucleotides have been implicated in a wide variety of physiological processes including smooth muscle contraction, immune responses, embryonic development and maintaining homeostasis (Yegutkin 2014). Purinergic receptors represent a very attractive drug target and they have been successfully targeted in other cell types for therapeutic gain. However, purinergic signalling in adipose tissue remains a largely unexplored area of research. Through this project, I hoped to characterise the molecular basis of nucleotide-evoked responses in primary human adipose-derived mesenchymal stromal cells (AD-MSCs) and in *in vitro* differentiated adipocytes and attribute the identified receptors to physiological functions within each cell type.

6.2 Key findings

6.2.1 $P2Y_2$ and $P2Y_6$ receptor activation elicits intracellular calcium responses in primary human adipose-derived mesenchymal stromal cells

Primary human AD-MSCs express all the known subtypes of P2 receptors, excluding P2X2, P2X3 and $P2Y_{12}$, although there is some heterogeneity in the expression of $P2Y_{11}$, $P2Y_{13}$ and $P2Y_{14}$ across

donors. Coupled with evidence of changes in intracellular calcium levels in response to exogenous nucleotide (ATP, ADP or UTP) application, positive identification of P2 receptors indicates that AD-MSCs possess functional purinergic receptors. These findings are supported by previous studies, which have also demonstrated evidence of functional purinergic responses in human AD-MSCs (Zippel *et al.*, 2012; Kotova *et al.*, 2018). However, the repertoire of P2 receptors detected differ slightly between this project and those previously reported. Zippel *et al.* (2012) identified mRNA expression of all P2 receptor subtypes, excluding P2X1 and P2X2, whereas Kotova *et al.* (2018) reported mRNA expression of P2X2, P2X4, P2X7 and all of the P2Y receptors except $P2Y_{12}$. It is perhaps unsurprising that there would be differences between the receptor profiles determined by different groups using different donor cells, as heterogeneity in receptor expression was even identified between the relatively small number of donors used within this study. Despite the slight variation in the receptor profiles identified, there is remarkable consistency in the functional evidence of the presence of purinergic receptors, with ATP, ADP and UTP, but not UDP, producing detectable changes in intracellular calcium levels both in this study and those previously reported by others (Zippel *et al.*, 2012; Kotova *et al.*, 2018).

Although AD-MSCs appear to express almost all known P2X receptor subtypes, the evidence presented in Chapter 3 demonstrates a clear predominance of metabotropic G_q-coupled P2Y receptors in the nucleotide-evoked calcium responses. This was demonstrated by the fact that the nucleotide responses persisted in the absence of extracellular calcium but were abolished when phospholipase C (PLC) and sarco/endoplasmic reticulum Ca^{2+}-ATPase, which are both downstream effectors of G_q-mediated signalling, were inhibited. In addition, subtype-selective antagonism of P2X4 and P2X7 receptors had no effect on the response to ATP in these cells. Taken together this data suggests the nucleotide-evoked calcium responses in primary human AD-MSCs are mediated by activation of P2Y receptors, with little/no contribution from the ionotropic P2X receptors present. These findings are supported by a study conducted by Kotova *et al.* (2018) which demonstrates that ATP-evoked calcium responses in human AD-MSCs are abolished by PLC and inositol triphosphate receptor inhibition, but persist when the extracellular calcium concentration was reduced (Kotova *et al.*, 2018). A lack of P2X5 and P2X6 receptor contribution is unsurprising, as these receptors are not functional in humans (Torres et al., 1999; Ormond, 2006; Kotnis et al., 2010). A possible explanation for the lack of P2X4 and P2X7 involvement may be that neither receptor is located at the cell surface under the conditions used in this study. P2X4 receptors are known to localise to lysosomes and traffic to and from the plasma membrane in other cell types (Ashour *et al.*, 2004; Stokes, 2013), so one explanation for the lack of effect of P2X4 receptor antagonism is that very few P2X4 receptors may be expressed at the cell surface. Other groups have demonstrated presence of P2X7 receptors in mesenchymal stem cells (Madec *et al.*, 2011), but in this study, we were unable to demonstrate functional P2X7 receptors, possibly due the use of

insufficiently elevated concentrations of ATP in this study or the unusual localisation of the P2X7 receptor in the nuclear/perinuclear region.

While all P2Y receptor subtypes (excluding $P2Y_{12}$ receptors) were detected in primary human AD-MSCs, the data suggests that only $P2Y_2$ and $P2Y_6$ receptors are involved in mediating nucleotide-evoked calcium responses. Possible explanations for these findings include limited cell surface expression of certain receptor subtypes and/or heterologous desensitisation due to $P2Y_2$ receptor activation (Govindan and Taylor, 2012). It is likely that the other P2 receptors (excluding $P2Y_2$ and $P2Y_6$) play a functional role in these cells, but this study suggests that they are not primarily involved in mediating changes in intracellular Ca^{2+} levels in response to exogenous nucleotide stimulation. They may be involved in non-Ca^{2+} dependent pathways, only activated under certain circumstances or have intracellular functions which are beyond the scope of this study.

Although inhibition of $P2Y_2$ receptors abolishes the response to UTP, approximately 25% of the peak ATP response is resistant to the effects of selective $P2Y_2$ antagonism. This residual response may be simply due to the competitive nature of the antagonist used (Rafehi *et al.*, 2017), ADP contamination of the ATP used or due to the liberation of ADP (and/or AMP and adenosine) from ATP by ectonucleotidases, such as CD39 (Kaebisch *et al.*, 2015; Kerkelä *et al.*, 2016), resulting in the activation of other P2 receptors. This may also explain the variation in the level of inhibition observed between donors, which may be due to the differing efficiencies of ectonucleotidase activity per donor. No genetic analysis of the donors used in this study was conducted, but previous reports suggest that mutations in the *ENTPD1* (CD39) gene can lead to a reduction in the activity of CD39 (Nardi-Schreiber *et al.*, 2017) and there have also been reports to suggest that CD39 surface expression levels are dynamic and can increase under certain conditions (Saldanha-Araujo *et al.*, 2011).

The presence of a UTP-evoked calcium response in human AD-MSCs may be indicative of $P2Y_4$ receptor involvement. Unfortunately, there is currently no commercially available selective antagonist for $P2Y_4$ receptors (Jacobson *et al.*, 2009), so it is not possible to conclusively eliminate the possibility that $P2Y_4$ receptors may have a role in the UTP-evoked calcium response, however the evidence presented here strongly supports the hypothesis that the ATP and UTP responses are mediated by $P2Y_2$ receptors. The calculated EC_{50} values for ATP and UTP and the IC_{50} values in the presence of a selective $P2Y_2$ receptor antagonist are comparable, which fits with reports that ATP and UTP act equipotently on $P2Y_2$ receptors (Parr *et al.*, 1994), whereas $P2Y_4$ receptors are antagonised by ATP (Kennedy *et al.*, 2000; Herold *et al.*, 2004). In addition, the ATP responses are blocked and the UTP responses are abolished by a $P2Y_2$ receptor selective antagonist, which strongly suggests $P2Y_2$ receptor involvement, and precludes $P2Y_4$ receptor contribution. It has recently been suggested that the $P2Y_2$ receptor may play a role in driving BM-MSC adipogenesis

while suppressing osteogenesis, without affecting the rate of cell proliferation (Li *et al.*, 2015). Although the role of $P2Y_2$ receptors in differentiation was not explored within the scope of this study, it was determined that $P2Y_2$ receptors are not involved in proliferation or migration of primary human AD-MSCs which supports some of the findings presented by Li *et al.* (2015). If $P2Y_2$ receptor-mediated signalling does promote adipogenesis in AD-MSCs, then this could provide an opportunity to develop pharmacological tools to target the $P2Y_2$ receptor specifically to drive MSCs towards/away from an adipogenic phenotype *in vivo*, thus providing a route to control the number of new adipocytes present in adipose tissue and potentially regulate weight gain.

AD-MSCs exhibited a robust ADP response, which was resistant to inhibition in the presence of all the subtype-selective antagonists tested, excluding AR-C118925XX ($P2Y_2$) and MRS2578 ($P2Y_6$). AR-C118925XX only significantly inhibited the net movement of Ca^{2+} in the latter decay phase of the response to ADP and not the initial peak. ADP is not the preferred agonist for $P2Y_2$ receptors, so these results may indicate indirect activation of the $P2Y_2$ receptor via ADP-induced release of ATP (Jiang, Mousawi, *et al.*, 2017). The ADP response was also inhibited by MRS2578. ADP has been shown to elicit a calcium response in 1321N1 astrocytoma cells over-expressing $P2Y_6$ receptors, but its effects are much less potent than the preferred agonist of $P2Y_6$ receptors, UDP (Communi *et al.*, 1996), so it was surprising that MRS2578 abolished the response to ADP in MSCs, when these cells lack a UDP-elicited Ca^{2+} response. It is important to note that UDP does elicit a Ca^{2+} response in MSCs, but only at very high agonist concentrations that are more than ten-fold higher than the concentration required to maximally activate the $P2Y_6$ receptor (Communi *et al.*, 1996). One possible explanation for this may be that $P2Y_6$ receptors may exist as a heterodimer thus altering the agonist profile in these cells. $P2Y_6$ receptors have been shown to form heterodimers with other GPCRs (D'Ambrosi *et al.*, 2007; Nishimura *et al.*, 2016) and hetero-oligomerization of other P2Y receptors can alter the agonist sensitivity of these receptors (Ecke *et al.*, 2008). After the initial peak, blockade of the ADP response with MRS2578 leads to a decrease in the concentration of intracellular Ca^{2+} to below baseline Ca^{2+} levels, suggesting there is either efflux or internalisation of Ca^{2+}. It is unclear why $P2Y_6$ receptor inhibition would have this effect and these observations imply that the role of the $P2Y_6$ receptor in MSCs is complex. Although, it was not possible to positively identify the functional role of $P2Y_6$ within the scope of this study, $P2Y_6$ receptors have been shown to promote osteogenesis in BM-MSCs (Noronha-Matos *et al.*, 2012) and have also been implicated in increasing IL-6 expression (Satrawaha *et al.*, 2011). It has been suggested that IL-6 is important for maintaining the immunoprivilege stasis of MSCs (Li *et al.*, 2013), so if $P2Y_6$ receptors are involved in IL-6 secretion it may prove to be a valuable target for prolonging AD-MSC viability for therapeutic use. However additional work is required to clarify both the molecular mechanism and functional role of $P2Y_6$ receptor activation in these cells.

The findings presented in Chapter 3 encompass a comprehensive characterisation of the functional P2 receptors expressed in primary human AD-MSCs, however caution must be applied when interpreting these results. Only female patients were recruited and no information about ethnicity or lifestyle was collected. The mean age of the recruited donors was 55.5 ± 1.4, and aging has been shown to increase cellular senescence and AD-MSCs extracted from elderly patients (age 60-73) have been shown to have diminished migration and differentiation capabilities (Liu *et al.*, 2017). The molecular mechanisms underlying these changes are not fully understood, so it is not possible to rule out potential changes in the P2 receptor expression and/or functioning as a possible cause. However, data presented by Zippel *et al.* (2012) included younger donors and they demonstrated functional responses to both ATP and UTP in AD-MSCs extracted from younger patients and they also detected a very similar P2 receptor profile to the profile determined in this study (Zippel *et al.*, 2012). However, it is important to note that Zippel et al. (2012) only used cells isolated from a total of three donors, so a much more extensive study would be required to clarify whether the results presented here are applicable to younger donors as well. In combination, these factors mean that the data presented here is limited to profiling the P2 receptor responses in AD-MSCs extracted from older women. Also, although all the recruited patients were cancer-free at the time of recruitment, each donor has been treated for breast cancer in the past. Although previous reports suggest some chemotherapeutic agents do not affect surface marker expression, proliferation and differentiation of AD-MSCs (Liang *et al.*, 2011), it is not known whether cancer and/or subsequent cancer treatment resulted in long-term alterations in the expression and function of purinergic receptors in these cells.

A key limitation of the study is the use of an *in vitro* system. Cell culture has been previously shown to cause changes in the behaviour of MSCs (Hagmann *et al.*, 2013; Lee *et al.*, 2014; Turinetto *et al.*, 2016), so this *in vitro* model may not accurately reflect conditions *in vivo*. This study depends heavily on the selectivity of available pharmacological probes and antibodies. Although all the pharmacological antagonists used in this study are reported to be selective for their target receptor, it is not possible to rule out the possibility that these antagonists affect non-specific targets in these cells. Similarly, despite the fact that the manufacturers of all of antibodies used throughout this study state that their antibodies specifically target the protein of interest and many of the antibodies used have been utilised in previously published reports, most of the antibodies have not been knockout validated. This introduces the possibility of non-specific antibody staining interfering with the accuracy of the immunocytochemistry, immunohistochemistry and flow cytometry data. In addition, although controls treated with secondary antibodies in the absence of primary antibodies were used to control for non-specific secondary antibody binding, neither western blotting nor positive or negative controls were performed to confirm the specificity of the primary

antibodies used. In particular, negative controls would have been an excellent addition to rule out non-specific primary antibody binding, however as purinergic receptors are rather ubiquitously expressed, it was difficult to locate human negative control cells or tissue. This study would greatly benefit from a thorough characterisation of the specificity of the primary antibodies used and/or the development of more specific antibodies. Although this is undoubtedly a limitation of this study, the substantial functional evidence of purinergic receptor activity conclusively demonstrates that purinergic receptors are present in human MSCs. Another limitation is that all of the pharmacological data presented here is based on analysis of a population level response, which does not account for cell-to-cell variation in response patterns. Single cell calcium imaging would be a good method to investigate any heterogeneity within the population.

6.2.2 $P2Y_1$, $P2Y_2$ and $P2Y_{12}$ receptor activation elicits intracellular calcium responses in primary human *in vitro* differentiated adipocytes

There are many similarities between the purinergic response characteristics in primary human AD-MSCs (Chapter 3) and *in vitro* differentiated adipocytes (Chapter 4), so to avoid repetition where possible general points that have already been explored in Section 6.2.1 will not be discussed again in this Section.

Primary human *in vitro* differentiated adipocytes express all known P2 receptor subtypes, excluding P2X1, P2X2, P2X3 and $P2Y_{14}$ receptors. This repertoire of receptors is largely supported by previous studies characterising the expression of P2 receptors in white adipocytes (Zippel *et al.*, 2012). Exogenous application of ATP, ADP and UTP produced transient increases in the concentration of intracellular calcium, whereas physiological concentrations of UDP and UDP-glucose did not alter intracellular calcium levels. The lack of a functional response to UDP-glucose is perhaps unsurprising as $P2Y_{14}$ receptor expression was not detected in most donors.

Like AD-MSCs, subtype-specific antagonism of P2X receptors and $P2Y_6$, $P2Y_{11}$ and $P2Y_{13}$ receptors had no effect on nucleotide-evoked responses, which suggests that these receptors are not functionally active under the conditions employed in this study. The molecular mechanisms underlying the lack of involvement of these receptors were not fully investigated, but possible explanations are discussed in Section 6.2.1. Although P2X receptors do not appear to be directly involved in initiating ATP-evoked calcium responses, the magnitude of the response to ATP is heavily dependent on the presence of extracellular calcium, so it is conceivable that the initial metabotropic response to ATP is potentiated by subsequent Ca^{2+} entry via P2X receptors.

The responses to ATP, ADP and UTP were all abolished by inhibition of PLC, which indicates a predominance of G_q-mediated signalling, however the responses to ADP and ATP were also substantially decreased, but not abolished, when G_i-signalling pathways were inhibited. This

suggests that multiple signalling pathways may be involved in the nucleotide-evoked calcium responses in human adipocytes. Indeed, subtype-selective antagonism revealed that a combination of classically G_q and G_i-coupled receptors are involved in the ATP and ADP response: $P2Y_1$, $P2Y_2$ and $P2Y_{12}$ receptors. It is not unprecedented that there may be crosstalk between P2Y receptor subtypes, for example it is well documented that $P2Y_1$ and $P2Y_{12}$ receptors work in coordination to sustain platelet aggregation (Jagroop *et al.*, 2003; Hardy *et al.*, 2004).

It is proposed here that the ATP response is partially mediated by $P2Y_2$ receptor activation. However, it is important to acknowledge that data from Chapter 5 demonstrates that selective inhibition of $P2Y_2$ receptors results in a reduction of the basal intracellular calcium level, and as the baseline is zeroed for the pharmacological data presented in Chapter 4 to normalise for the expected well-to-well variability in basal calcium concentrations, it is not possible to definitively conclude that the evident decrease in the responses is due to genuine $P2Y_2$ receptor contribution to ATP and UTP-evoked calcium responses. It is possible that the lower basal calcium concentrations prior to agonist application are responsible for the diminished magnitude of the nucleotide-evoked responses. Although the data from Chapter 5 raises some ambiguity regarding the contribution of $P2Y_2$ receptors in the exogenous nucleotide evoked Ca^{2+} responses, neither pharmacological inhibition of $P2Y_1$ nor $P2Y_{12}$ receptors had a significant effect on the basal calcium concentration. This indicates that the inhibitory effects of these antagonists on the ATP-evoked Ca^{2+} response imply $P2Y_1$ and $P2Y_{12}$ receptors play predominant roles in the ATP-evoked responses. As both $P2Y_1$ and $P2Y_{12}$ are preferentially activated by ADP, it is possible that this occurs via liberation of ADP from ATP by cell surface ectonucleotidases (Yegutkin, 2014). The ADP can then cause PLC-induced release of Ca^{2+} from the intracellular stores via activation of $P2Y_1$ receptors, while simultaneously activating $P2Y_{12}$ receptors to potentiate the level of intracellular calcium indirectly via modulation of cytosolic cAMP levels (Hardy *et al.*, 2004). However, an alternative explanation is that $P2Y_1$ and $P2Y_{12}$ receptors are activated by contaminating ADP in the ATP used in these experiments. However, the ATP used throughout this study was greater than 99% pure, so it is unlikely that this was the case. In addition, the effects of $P2Y_1$ and $P2Y_{12}$ antagonism are less potent on the ATP response than the ADP response. If there was ADP contamination of 30 µM ATP, then the concentration of ADP would be expected to be much lower than the 10 µM ADP that was used for the ADP experiments. As both antagonists are competitive (Kim *et al.*, 2003; Hoffmann *et al.*, 2009), logically a lower agonist concentration should result in more, not less, potent effects of competitive antagonism.

The expression of $P2Y_1$, $P2Y_2$ and $P2Y_{12}$ receptors was confirmed in primary human subcutaneous white adipose tissue sections, which suggests that there is some symmetry between the findings in the *in vitro* model and adipocytes in primary tissue. This also highlighted the morphological differences between mature adipocytes *in situ* and *in vitro* differentiated adipocytes, where the

white adipocytes *in situ* have a unilocular morphology, whereas the *in vitro* differentiated adipocytes are multilocular. Due to the technical difficulties of working with mature adipocytes, *in vitro* differentiated adipocytes are a commonly used model. However, it would be interesting to replicate key pharmacological assays on freshly isolated unilocular mature adipocytes to determine whether there are any differences, beyond the morphological differences, between the two models.

6.2.3 Constitutive $P2Y_2$ receptor activity regulates basal lipolysis in human adipocytes

Primary human *in vitro* differentiated adipocytes secrete sufficient concentrations of ATP to activate $P2Y_2$ receptors expressed on the surface of the cells (Lazarowski *et al.*, 1995). This is supported by previous reports that indicate that cells are capable of constitutively secreting ATP to regulate purinergic responses in an autocrine or paracrine manner (Corriden *et al.*, 2010; Sivaramakrishnan *et al.*, 2012; Campwala *et al.*, 2013). The presence of ATP in the microenvironment means that under basal conditions $P2Y_2$ receptors may be constitutively activated in human adipocytes. $P2Y_2$ receptors primarily couple to G_q proteins, thus activation of these receptor leads to activation of $G\alpha_q$-PLCβ-IP_3 pathway to initiate the release of calcium from the intracellular stores (Erb *et al.*, 2012), which suggests constitutive $P2Y_2$ activity may be able to control calcium tone within primary human adipocytes. This hypothesis is supported by the finding that pharmacological inhibition of $P2Y_2$ receptors caused a decrease in the basal intracellular calcium concentration. However, a change in basal calcium concentrations was not observed when $P2Y_2$ receptor expression was knocked down using shRNA (versus scrambled control cells). This may be, because 100% receptor knockdown was not achieved, resulting in a more subtle decrease in intracellular calcium levels that could not be detected due to the limited sensitivity of the assay used, or it may be due to unknown changes caused by the lentivirus-mediated shRNA knockdown procedure employed. It is not known whether lentiviral delivery of shRNA (scrambled and $P2Y_2$ shRNA) altered basal intracellular calcium levels, because control cells that were not treated with lentivirus/shRNA were not routinely included alongside the scrambled and $P2Y_2$ knockdown cells. However, the fact that there is good correlation (excluding the effects on basal intracellular calcium) between the pharmacological data using the adipocytes (non-shRNA treated cells) and the knockdown data is encouraging. It is also important to note that neither removal of extracellular ATP nor inhibition of $P2Y_2$ receptors was able to reduce basal cytoplasmic Ca^{2+} levels to zero, thus indicating that mechanisms independent of purinergic signalling are also involved in maintaining cytoplasmic Ca^{2+} tone, such as mechanisms involving Na^+/Ca^{2+} exchangers or voltage-gated Ca^{2+} channels (Pershadsingh *et al.*, 1989; Clapham, 2007), although this was not explored fully within this study. The pharmacological data suggests $P2Y_2$ receptor mediated maintenance of 'elevated' intracellular calcium levels inhibits calcium-sensitive isoforms of adenylate cyclase (AC5 and/or

AC6) (Guillou *et al.*, 1999; Sunahara and Taussig, 2002), which limits the production of cAMP, which in turn means that $P2Y_2$ activity may control cytoplasmic cAMP tone within adipocytes as well. An increase in intracellular cAMP levels was observed with both pharmacological inhibition of $P2Y_2$ receptors and shRNA-mediated knockdown of $P2Y_2$ receptor expression. The raw intracellular concentrations of cAMP varied between donors, so only the normalised data was included in Figure 5.3, however the absolute intracellular cAMP values for the adipocytes treated with vehicle control and scrambled shRNA were equivalent, which suggests that the process of lentivirus-mediated shRNA knockdown does not alter basal cAMP levels. However, it is not possible to conclusively rule this out, as control cells that were not treated with lentivirus/shRNA were not run alongside their shRNA-treated counterparts. It is important to note that although the basal cAMP concentrations were comparable between the two sets of control cells (vehicle control and scrambled control), shRNA-mediated knockdown of $P2Y_2$ receptor expression led to an almost three-fold increase in intracellular cAMP, whereas pharmacological inhibition of $P2Y_2$ receptors only led to an increase of approximately 33%. However, these disparities can be explained by donor-to-donor variation and/or the shorter timescale of pharmacological inhibition of $P2Y_2$ than shRNA-mediated receptor knockdown. Limiting of cAMP accumulation means that protein kinase A (PKA), a major effector of cAMP, is not activated and therefore cannot phosphorylate CGI-58, perilipins or hormone sensitive lipase (Miyoshi *et al.*, 2006, 2008; Schweiger *et al.*, 2006; Ahmadian *et al.*, 2010; Sahu-Osen *et al.*, 2015), which in turn means that extent of basal lipolysis is limited. This is evident in the fact that inhibition of $P2Y_2$ receptors using AR-C118925XX (a selective $P2Y_2$ antagonist) and shRNA-mediated knockdown of $P2Y_2$ receptor expression caused an increase in basal glycerol release, thus implying that constitutive $P2Y_2$ receptor activation limits basal glycerol release in primary human adipocytes. However, it is important to acknowledge that the enhancement of basal glycerol release was only observed with concentrations of AR-C118925XX that were greater than the reported IC_{50} for the antagonist (1 µM; Kemp *et al.*, 2004), and the majority of the glycerol release experiments were exclusively conducted with maximal concentrations of AR-C118925XX (10 µM). This concentration was selected, because it resulted in the largest increase in glycerol release, thus facilitating greater ease in identifying changes to this enhanced response. Although, it is a maximal concentration, previous selectivity studies conducted by Rafehi *et al.* (2018) suggest that the only P2 receptors that may be affected by 10 µM AR-C118925XX, other than $P2Y_2$, are P2X1, P2X3 and $P2Y_{11}$. Data presented in Chapter 4 indicates that P2X1 and P2X3 receptors are not expressed in the majority of human *in vitro* differentiated adipocytes tested, and the expression of $P2Y_{11}$ varied between donors, whereas $P2Y_2$ receptors were expressed in all donors tested, the effects of AR-C118925XX on basal lipolysis were consistently observed across donors and the effects were mimicked by shRNA-mediated knockdown of $P2Y_2$ receptor expression.

Furthermore, exogenous ATP application enhanced the secretion of anti-lipolytic adiponectin (Wedellová *et al.*, 2011), while also reducing the expression of lipolytic adipokines, such as chemerin (Fu *et al.*, 2016), growth hormone (Johansen *et al.*, 2003; Sakharova *et al.*, 2008), leptin (Ruud *et al.*, 2015) and resistin (Chen *et al.*, 2014) after 6 hours. This signifies that activation of purinergic signalling pathways promotes an anti-lipolytic phenotype in primary human adipocytes. Although currently it is not possible to ascribe the secretion of adipokines directly to $P2Y_2$ receptor activity, as the secretion of these adipokines may be indirectly due to enhanced $P2Y_2$ inhibition-induced lipolysis. AR-C118925XX, the $P2Y_2$ antagonist, used throughout this study, displays very high stability in mice and humans (Rafehi *et al.*, 2017), so although the amount of AR-C118925XX in the supernatant was not determined after three, six or 24 hours, it is possible that the antagonist may still be present despite the fact that the cells were only exposed to a singular dose. Alternatively, it is also possible that the antagonist is metabolised over time and the longer-term effects observed are largely due to the activation of homeostatic mechanisms within the cells to counteract the acute effects of $P2Y_2$ inhibition on basal lipolysis. It would be interesting to determine the stability of AR-C118925XX in this system, as this may help to decipher whether there is a direct or indirect relationship between $P2Y_2$ activity and adipokine secretion.

Although short-term inhibition of $P2Y_2$ (less than four hours) causes an increase in basal lipolysis, longer-term (24 hours) antagonism of $P2Y_2$ receptors appears to cause a decrease in basal glycerol release. This coincides with an enhancement in the secretion of anti-lipolytic adipokines, such as adiponectin (Wedellová *et al.*, 2011) and adipsin (Sniderman *et al.*, 1994), while also reducing the expression of lipolytic adipokines, including angiopoietin Like 4 (Gray *et al.*, 2012), retinol binding protein 4 (Lee *et al.*, 2016) and tumour necrosis factor α (H. H. Zhang *et al.*, 2002). Longer term inhibition of $P2Y_2$ receptors also appears to promote a largely proinflammatory phenotype via augmented release of proinflammatory cytokines, chemokines and acute phase proteins. It is unclear whether these changes in the adipokine secretion profiles are directly due to inhibition of $P2Y_2$-mediated pathways or triggered by the activation of feedback mechanisms to rectify the loss of triglycerides due to $P2Y_2$-inhibition induced lipolysis. Obese individuals have been shown to have enhanced basal lipolysis (Wang *et al.*, 2003), which elevate their levels of circulating free fatty acids (FFA) and high FFA levels are known to induce inflammation (Jiao *et al.*, 2011), it is perhaps not surprising that longer-term induction of enhanced basal lipolysis is associated with a proinflammatory phenotype. In support of the hypothesis that the changes in adipokine secretion observed are due to enhanced basal lipolysis rather than $P2Y_2$ activity directly, is the fact that shRNA-mediated knockdown of $P2Y_2$ receptor expression mimics the shorter-term lipolytic phenotype, rather than the longer term anti-lipolytic phenotype. However, irrespective of the cause, the development of a proinflammatory phenotype following treatment with a $P2Y_2$ antagonist proposes a potential hurdle for clinical use of a $P2Y_2$ receptor antagonist, because it may

indicate that although these findings suggest inhibition of $P2Y_2$ receptors may be an attractive target for modulating basal lipolysis to control adipose tissue mass, this may also have unintended consequences, such as inducing inflammation of adipose tissue, which is known to exacerbate the metabolically unfavourable consequences of obesity (Tilg *et al.*, 2008; Després, 2012). The adipocyte secretome is complex and highly regulated. A significant amount of additional work would be required to identify the exact mechanisms that lead to the up/down-regulation of each adipokine and how they may link to $P2Y_2$ receptor activity. The results of this protein array provide a good overview of some of the adipokines secreted after $P2Y_2$ receptors are inhibited, but the data presented here does not provide any definitive information regarding the mechanism that links $P2Y_2$ receptor activity and adipokine secretion. The protein array data presented in this Chapter should be viewed as an initial probe that highlights potential candidates for further investigation.

Despite the fact that all the data from the *in vitro* differentiated adipocytes suggests acute inhibition of $P2Y_2$ receptors enhances basal lipolysis, these findings were not replicated when primary human adipose tissue pieces were stimulated with AR-C118925XX (a $P2Y_2$ antagonist). In fact, using this *ex vivo* model, it was revealed that $P2Y_2$ receptor inhibition decreased basal glycerol release, which implies that constitutive $P2Y_2$ receptor activity enhances basal glycerol release, rather than limits it. Further experimentation is required to determine the reason for the differences observed between these two models. There are numerous possible explanations for the discrepancies between the *in vitro* and *ex vivo* models, including the fact that the *ex vivo* model contains multiple interacting cells types (Sheldon, 2011), whereas the *in vitro* cells are a relatively pure population of adipocytes, in addition the tissue is likely to have a much larger number of cells than the *in vitro* model. Furthermore, as discussed briefly in Section 6.2.2, there is a morphological difference between white adipocytes *in situ* and *in vitro* differentiated adipocytes, which may also play a role. Multiple smaller lipid droplets, such as in the *in vitro* model cells, have a larger surface area than a single large lipid droplet (*ex vivo* model), and are consequently more prone to lipolysis (Paar *et al.*, 2012). It has already be elucidated, in this study and previously, that adipokines influence lipolysis (Ronti *et al.*, 2006; Rosen *et al.*, 2006). It is likely that the adipokine profile is different for freshly dissected human subcutaneous adipose tissue sections than cells that have been maintained *in vitro* for an extended period (almost a month before experimental use), thus it would be interesting to characterise the adipokine profile to see whether this is a factor. Regardless of the discrepancies between the *in vitro* and *ex vivo* models, these data reveal $P2Y_2$ receptors as an interesting candidate for pharmacologically manipulating basal lipolysis in humans.

6.3 Future work

The research presented in this thesis provides an excellent insight into the complex roles of purinergic signalling in primary human adipose-derived mesenchymal stromal cells (AD-MSCs) and

in vitro differentiated adipocytes. However, the research presented here also exposes many potential avenues to pursue in the future. One of these potential areas of interest is determining the functional role of P2 receptors in primary human AD-MSCs. In this study, I was able to identify the expression of many P2 receptors, including $P2Y_2$ and $P2Y_6$ receptors, which appear to be involved in nucleotide-evoked calcium responses. However, neither receptor appeared to be involved in cell migration or proliferation, so it would be interesting to see whether $P2Y_2$ or $P2Y_6$ receptors (or indeed any other P2 receptors) play a role in differentiation or the immunomodulatory properties of MSCs. Similarly, many P2 receptors were identified in primary human *in vitro* differentiated adipocytes, but I was only able to determine the role of $P2Y_2$ receptors within the scope of this study. Further exploration of the possible functional roles of the other P2 receptors, in particular $P2Y_1$ and $P2Y_{12}$ receptors which appear to be involved in calcium signalling, would be an excellent way to extend the findings presented here. In addition, the adipokine protein array data presented here is very much an initial glimpse and it would be interesting to follow up the findings in a more comprehensive manner, using multiple agonists and/or antagonists, investigating additional timepoints and so on.

In the longer term, it would also be very interesting to explore the mechanisms underlying the differences between the *in vitro* and *ex vivo* model cells. Currently, there are some very interesting findings that suggest $P2Y_2$ global knockout mice are resistant to diet-induced obesity and that this may be achieved via enhanced metabolic activity in these mice (Kishore *et al.*, 2016). These findings correspond well with the *in vitro* results presented in this thesis. Gaining access to or developing in-house $P2Y_2$ knockout mice would greatly enhance the findings of this investigation by providing insight into the role of $P2Y_2$ *in vivo*. It would be particularly interesting to develop tissue-specific knockout of $P2Y_2$ in white adipose tissue to see whether the effects observed *in vitro* (or *ex vivo*) are replicated *in vivo*. It would also be fascinating to observe the effects of dosing wildtype and/or obese mice with a selective $P2Y_2$ antagonist to see whether this had any effect on the plasma free fatty acid, glycerol and adipokine levels, the mass of the white adipose tissue depots and overall weight of the mice. If these animal studies correlated well with the *in vitro* data presented in this thesis and no significant adverse effects were identified, then it would be extremely interesting to perform clinical trials on humans to see whether inhibiting $P2Y_2$ receptors may provide a novel method for stimulating weight loss. This would provide invaluable information regarding the potential usefulness and/or challenges of attempting to pharmacological manipulate $P2Y_2$ receptor mediated signalling in adipose tissue to control obesity.

6.4 Concluding remarks

In conclusion, the data presented in this thesis provides a much-needed insight into the role of purinergic signalling in primary human adipose-derived mesenchymal stromal cells and *in vitro* differentiated adipocytes. Despite the enormous potential of purinergic signalling and the societal need for solutions to the growing problem of obesity, there is currently very little literature surrounding the role of purinergic signalling in both cell types. It is hoped that the comprehensive pharmacological characterisation of the P2 receptors expressed in each cell type provided will provide a solid foundation upon which future research in this field can flourish.

At the beginning of this project, I set out to meet three key aims: to identify the molecular basis of nucleotide-evoked responses in primary human mesenchymal stromal cells, to characterise the P2 receptor profile in *in vitro* differentiated adipocytes and to determine the physiological role of P2 receptors in each cell type. Although, I was unable to uncover the physiological role of purinergic signalling in primary human AD-MSCs, I believe that I have successfully met all of my initial aims. During this study, I have determined that almost all the known subtypes of P2 receptors are expressed in both cell types, but only $P2Y_2$ and $P2Y_6$ receptors are involved in nucleotide-evoked calcium responses in AD-MSCs, whereas $P2Y_1$, $P2Y_2$ and $P2Y_{12}$ receptors are functionally active in human adipocytes. In addition, I have discovered that constitutive $P2Y_2$ receptor activity is important for the regulation of basal lipolysis in primary human adipocytes, thus proposing $P2Y_2$ receptors as a novel drug target for controlling the expansion of adipose tissue. I hope that this finding will help in future efforts to manage the detrimental effects of adipose tissue expansion observed in obesity.

As mentioned in Section 6.3, there is still much more research that needs to be done to fully elucidate the role of purinergic signalling in human AD-MSCs and adipocytes, but I believe that significant steps have been taken throughout the course of this study. I hope that the findings presented in this thesis will be useful to the wider scientific community and hopefully eventually the public too.

Appendix

Table A1 Adipokines secreted by primary human *in vitro* differentiated adipocytes following singular treatment with vehicle, 100 µM ATP and/or $P2Y_2$ receptor antagonist (10 µM AR-C118925XX (AR-C)) (*N*=4). Supernatant samples were collected from primary human *in vitro* differentiated adipocytes that had been incubated with DMEM (no serum) for two hours, then exposed to a singular dose of vehicle or antagonist for 30 minutes, and finally ATP or vehicle was added and the first samples were collected immediately. Adipokines are quantified by protein array and data are presented as mean ± SEM for four donors. % increase and decrease values show the statistically significant changes in expression versus the vehicle control levels. *NS* indicates no significant change. Cases of donor variation are indicated by an * near the adipokines name.

	Vehicle control (pg/ml)	100 µM ATP (pg/ml)	% increase or decrease	10 µM AR-C (pg/ml)	% increase or decrease	ATP and AR-C (pg/ml)	% increase or decrease
Adiponectin	4708.8 ± 437	5177.9 ± 525	*NS*	4494.6 ± 529	*NS*	5362.4 ± 870	*NS*
Adipsin	154.4 ± 21	234.2 ± 33	↑	446.1 ± 142	*NS*	571 ± 181	↑
AgRP	<14	<14	-	<14	-	<14	-
ANGPTL4	<137	<137	-	<137	-	<137	-
BDNF	<55	<55	-	<55	-	<55	-
Chemerin	<137	<137	-	<137	-	<137	-
CRP	<27	<27	-	<27	-	<27	-
GH	<27	<27	-	<27	-	<27	-
IFNγ	<14	<14	-	<14	-	<14	-
IGFBP-1	<27	<27	-	<27	-	<27	-
IGFBP-2	75.5 ± 16	104.6 ± 17	*NS*	15.3 ± 5	*NS*	18.2 ± 6	*NS*
IGF-1	4950.8 ± 1489	5863.1 ± 1528	*NS*	6931.8 ± 786	*NS*	123.4 ± 63	*NS*
IL-10	<3	<3	-	<3	-	<3	-
IL-12p40	<14	<14	-	<14	-	<14	-

IL-12p70	<3	<3	-	<3	-	<3	-
IL-1β	<3	<3	-	<3	-	<3	-
IL-1Ra	<27	<27	-	<27	-	<27	-
IL-6	66.1 ± 14	62.7 ± 6	*NS*	26.6 ± 3.6	↓	30.8 ± 4	↓
IL-8*	1.1 ± 0.5	2.5 ± 0.8	*NS*	2.3 ± 0.8	*NS*	1.4 ± 0.6	*NS*
Insulin	<274	<274	-	<274	-	<274	-
Leptin	<55	<55	-	<55	-	<55	-
Lipocalin-2	<3	<3	-	<3	-	<3	-
MSPα	<137	<137	-	<137	-	<137	-
OPG	75.1 ± 7	26.8 ± 6	↓	40.2 ± 12	*NS*	<27	↓
PAI-I	975.7 ± 98	1027 ± 136	*NS*	350.8 ± 87	↓	374.3 ± 123	*NS*
PDGF-BB	<3	<3	-	<3	-	<3	-
Pepsinogen 1	<27	<27	-	<27	-	<27	-
Pepsinogen 2	<55	<55	-	<55	-	<55	-
Procalcitonin	<137	<137	-	<137	-	<137	-
RANTES	<3	<3	-	<3	-	<3	-
RBP4	2317.7 ± 258	3345.0 ± 515	*NS*	1904.7 ± 109	*NS*	1844.6 ± 121	*NS*
Resistin	<55	<55	-	<55	-	<55	-
SAA	<137	<137	-	<137	-	<137	-
TGFβ1	<137	<137	-	<137	-	<137	-
TSP-1	111923.2 ± 14413	73501.6 ± 19053	*NS*	28104.9 ± 2523	↓	3217.6 ± 486	↓
TNF RI	<137	<137	-	<137	-	<137	-
TNF RII	26.0 ± 4	23.4 ± 5	-	2.9 ± 1	↓	2.8 ± 2	↓
TNFα	38.5 ± 11	55.6 ± 14	*NS*	9.3 ± 2	*NS*	3.0 ± 1	*NS*
VEGF	215.3 ± 20	284.2 ± 13	*NS*	73.6 ± 9	↓	55.2 ± 6	↓

* IL-8 was only detected in one of four donors.

Table A2 Adipokines secreted by primary human *in vitro* differentiated adipocytes following singular treatment with vehicle or 100 µM ATP for 6 hours (*N*=4). Supernatant samples were collected from primary human *in vitro* differentiated adipocytes that had been incubated with DMEM (no serum) for two hours, then exposed to a singular dose of 0.1% DMSO for 30 minutes, and finally ATP or vehicle was added, and the samples were collected after 6 hours. Adipokines are quantified by protein array and data are presented as mean ± SEM for four donors. % increase and decrease values show the statistically significant changes in expression versus the vehicle control levels. *NS* indicates no significant change.

	Vehicle control (pg/ml)	100 µM ATP (pg/ml)	% increase or decrease
Adiponectin	11164 ± 1527	15554 ± 1482	↑
Adipsin	2547.5 ± 867	2428.1 ± 782	*NS*
AgRP	<14	<14	-
ANGPTL4	<137	<137	-
BDNF	<55	<55	-
Chemerin	544.7 ± 148	114.1 ± 50	↓
CRP	<27	<27	-
GH	61.8 ± 15	26.3 ± 7	↓
IFNγ	<14	<14	-
IGFBP-1	49.5 ± 9	27.0 ± 8	*NS*
IGFBP-2	62.9 ± 7	63.4 ± 15	*NS*
IGF-1	24561.9 ± 7133	36907.2 ± 10376	*NS*
IL-10	<3	<3	-
IL-12p40	25.5 ± 3	7.4 ± 3	↓
IL-12p70	<3	<3	-
IL-1β	<3	<3	-
IL-1Ra	<27	<27	-
IL-6	120.8 ± 17	136.4 ± 24	*NS*
IL-8	11.0 ± 2	35.0 ± 11	*NS*
Insulin	<274	<274	-
Leptin	191.8 ± 26	34.3 ± 12	↓
Lipocalin-2	4.8 ± 0.9	1.6 ± 0.7	↓
MSPα	<137	<137	-
OPG	223.9 ± 36	126.6 ± 25	↓
PAI-I	2821.3 ± 688	1621.8 ± 212	*NS*
PDGF-BB	<3	<3	-
Pepsinogen 1	<27	<27	-
Pepsinogen 2	<55	<55	-
Procalcitonin	<137	<137	-
RANTES	<3	<3	-
RBP4	2724.1 ± 303	2535.8 ± 122	*NS*
Resistin	88.5 ± 18	25.5 ± 10	↓
SAA	200.0 ± 32	201.4 ± 59	*NS*
TGFβ1	<137	<137	-
TSP-1	95202.2 ± 16229	112023.9 ± 13362	↑

TNF RI	<137	<137	-
TNF RII	14.7 ± 3	3.1 ± 0.9	↓
TNFα	20.1 ± 5	15.7 ± 4	*NS*
VEGF	324.0 ± 75	358.7 ± 47	*NS*

References

Abbracchio, M. P., Boeynaems, J.-M., Barnard, E. A., Boyer, J. L., Kennedy, C., Miras-Portugal, M. T., King, B. F., Gachet, C., Jacobson, K. A., Weisman, G. A. and Burnstock, G. (2003) 'Characterization of the UDP-glucose receptor (re-named here the P2Y14 receptor) adds diversity to the P2Y receptor family.', *Trends in pharmacological sciences*, 24(2), pp. 52–5. doi: 10.1016/S0165-6147(02)00038-X.

Accurso, F. J., Moss, R. B., Wilmott, R. W., Anbar, R. D., Schaberg, A. E., Durham, T. A., Ramsey, B. W. and TIGER-1 Investigator Study Group (2011) 'Denufosol tetrasodium in patients with cystic fibrosis and normal to mildly impaired lung function.', *American journal of respiratory and critical care medicine*, 183(5), pp. 627–34. doi: 10.1164/rccm.201008-1267OC.

Adamson, S. E., Meher, A. K., Chiu, Y.-H., Sandilos, J. K., Oberholtzer, N. P., Walker, N. N., Hargett, S. R., Seaman, S. A., Peirce-Cottler, S. M., Isakson, B. E., McNamara, C. A., Keller, S. R., Harris, T. E., Bayliss, D. A. and Leitinger, N. (2015) 'Pannexin 1 is required for full activation of insulin-stimulated glucose uptake in adipocytes.', *Molecular metabolism*, 4(9), pp. 610–8. doi: 10.1016/j.molmet.2015.06.009.

Afshin, A., Forouzanfar, M. H., Reitsma, M. B., Sur, P., Estep, K., Lee, A., Marczak, L., Mokdad, A. H., Moradi-Lakeh, M., Naghavi, M., Salama, J. S., Vos, T., Abate, K. H., Abbafati, C., Ahmed, M. B., Al-Aly, Z., Alkerwi, A., Al-Raddadi, R., *et al.* (2017) 'Health Effects of Overweight and Obesity in 195 Countries over 25 Years', *New England Journal of Medicine*, 377(1), pp. 13–27. doi: 10.1056/NEJMoa1614362.

Ahima, R. S. and Flier, J. S. (2000) 'Adipose tissue as an endocrine organ.', *Trends in endocrinology and metabolism: TEM*, 11(8), pp. 327–32. Available at: http://www.ncbi.nlm.nih.gov/pubmed/10996528.

Ahmadian, M., Wang, Y. and Sul, H. S. (2010) 'Lipolysis in adipocytes', *International Journal of Biochemistry and Cell Biology*. Elsevier Ltd, 42(5), pp. 555–559. doi: 10.1016/j.biocel.2009.12.009.

Alessi, D. R., James, S. R., Downes, C. P., Holmes, A. B., Gaffney, P. R., Reese, C. B. and Cohen, P. (1997) 'Characterization of a 3-phosphoinositide-dependent protein kinase which phosphorylates and activates protein kinase Balpha.', *Current biology : CB*, 7(4), pp. 261–9. Available at: http://www.ncbi.nlm.nih.gov/pubmed/9094314.

Allender, S. and Rayner, M. (2007) 'The burden of overweight and obesity-related ill health in the UK', *Obesity Reviews*, 8(5), pp. 467–473. doi: 10.1111/j.1467-789X.2007.00394.x.

Di Angelantonio, E., Bhupathiraju, S. N., Wormser, D., Gao, P., Kaptoge, S., de Gonzalez, A. B., Cairns, B. J., Huxley, R., Jackson, C. L., Joshy, G., Lewington, S., Manson, J. E., Murphy, N., Patel, A. V, Samet, J. M., Woodward, M., Zheng, W., Zhou, M., *et al.* (2016) 'Body-mass index and all-cause

mortality: individual-participant-data meta-analysis of 239 prospective studies in four continents', *The Lancet*, 388(10046), pp. 776–786. doi: 10.1016/S0140-6736(16)30175-1.

Apovian, C. M. (2016) 'Obesity: definition, comorbidities, causes, and burden.', *The American journal of managed care*, 22(7 Suppl), pp. s176-85. Available at: http://www.ncbi.nlm.nih.gov/pubmed/27356115.

Appay, V. and Rowland-Jones, S. L. (2001) 'RANTES: a versatile and controversial chemokine.', *Trends in immunology*, 22(2), pp. 83–7. Available at: http://www.ncbi.nlm.nih.gov/pubmed/11286708.

Ashour, F. and Deuchars, J. (2004) 'Electron microscopic localisation of P2X4 receptor subunit immunoreactivity to pre- and post-synaptic neuronal elements and glial processes in the dorsal vagal complex of the rat', *Brain Research*, 1026(1), pp. 44–55. doi: 10.1016/j.brainres.2004.08.002.

Baer, P. C. and Geiger, H. (2012) 'Adipose-derived mesenchymal stromal/stem cells: tissue localization, characterization, and heterogeneity.', *Stem cells international*, 2012, p. 812693. doi: 10.1155/2012/812693.

Bagchi, S., Liao, Z., Gonzalez, F. A., Chorna, N. E., Seye, C. I., Weisman, G. A. and Erb, L. (2005) 'The P2Y2 nucleotide receptor interacts with alphav integrins to activate Go and induce cell migration.', *The Journal of biological chemistry*, 280(47), pp. 39050–7. doi: 10.1074/jbc.M504819200.

Balasubramanian, R., Robaye, B., Boeynaems, J.-M. and Jacobson, K. A. (2014) 'Enhancement of glucose uptake in mouse skeletal muscle cells and adipocytes by P2Y6 receptor agonists.', *PloS one*, 9(12), p. e116203. doi: 10.1371/journal.pone.0116203.

Barinaga, M. (1995) '"Obese" protein slims mice', *Science*, 269(5223), pp. 475–476. doi: 10.1126/science.7624769.

Bartness, T. J., Liu, Y., Shrestha, Y. B. and Ryu, V. (2014) 'Neural innervation of white adipose tissue and the control of lipolysis.', *Frontiers in neuroendocrinology*, 35(4), pp. 473–93. doi: 10.1016/j.yfrne.2014.04.001.

Bartness, T. J. and Bamshad, M. (1998) 'Innervation of mammalian white adipose tissue: implications for the regulation of total body fat.', *The American journal of physiology*, 275(5 Pt 2), pp. R1399-411. Available at: http://www.ncbi.nlm.nih.gov/pubmed/9791054.

Bartness, T. J. and Song, C. K. (2007) 'Thematic review series: adipocyte biology. Sympathetic and sensory innervation of white adipose tissue.', *Journal of lipid research*, 48(8), pp. 1655–72. doi: 10.1194/jlr.R700006-JLR200.

Beaucage, K. L., Xiao, A., Pollmann, S. I., Grol, M. W., Beach, R. J., Holdsworth, D. W., Sims, S. M., Darling, M. R. and Dixon, S. J. (2014) 'Loss of P2X7 nucleotide receptor function leads to abnormal fat distribution in mice.', *Purinergic signalling*, 10(2), pp. 291–304. doi: 10.1007/s11302-013-9388-

x.

Berridge, M. J., Bootman, M. D. and Roderick, H. L. (2003) 'Calcium signalling: dynamics, homeostasis and remodelling.', *Nature reviews. Molecular cell biology*, 4(7), pp. 517–29. doi: 10.1038/nrm1155.

Berridge, M. J., Lipp, P. and Bootman, M. D. (2000) 'The versatility and universality of calcium signalling', *Nature Reviews Molecular Cell Biology*. Macmillan Magazines Ltd., 1, p. 11. Available at: http://dx.doi.org/10.1038/35036035.

Bezaire, V., Mairal, A., Ribet, C., Lefort, C., Girousse, A., Jocken, J., Laurencikiene, J., Anesia, R., Rodriguez, A.-M., Ryden, M., Stenson, B. M., Dani, C., Ailhaud, G., Arner, P. and Langin, D. (2009) 'Contribution of adipose triglyceride lipase and hormone-sensitive lipase to lipolysis in hMADS adipocytes.', *The Journal of biological chemistry*, 284(27), pp. 18282–91. doi: 10.1074/jbc.M109.008631.

Biver, G., Wang, N., Gartland, A., Orriss, I., Arnett, T. R., Boeynaems, J.-M. and Robaye, B. (2013) 'Role of the P2Y13 receptor in the differentiation of bone marrow stromal cells into osteoblasts and adipocytes.', *Stem cells (Dayton, Ohio)*, 31(12), pp. 2747–58. doi: 10.1002/stem.1411.

Bjørndal, B., Burri, L., Staalesen, V., Skorve, J. and Berge, R. K. (2011) 'Different Adipose Depots: Their Role in the Development of Metabolic Syndrome and Mitochondrial Response to Hypolipidemic Agents', *Journal of Obesity*, 2011, pp. 1–15. doi: 10.1155/2011/490650.

Björntorp, P. (1990) '"Portal" adipose tissue as a generator of risk factors for cardiovascular disease and diabetes.', *Arteriosclerosis (Dallas, Tex.)*, 10(4), pp. 493–6. Available at: http://www.ncbi.nlm.nih.gov/pubmed/2196039.

Bleasdale, J. E. and Fisher, S. K. (1993) 'Use of U-73122 as an Inhibitor of Phospholipase C-Dependent Processes', *Neuroprotocols*, 3(2), pp. 125–133. doi: 10.1006/ncmn.1993.1046.

Bódis, K. and Roden, M. (2018) 'Energy metabolism of white adipose tissue and insulin resistance in humans', *European Journal of Clinical Investigation*, p. e13017. doi: 10.1111/eci.13017.

Boeynaems, J. M., Communi, D. and Robaye, B. (2012) 'Overview of the pharmacology and physiological roles of P2Y receptors', *Wiley Interdisciplinary Reviews: Membrane Transport and Signaling*, 1(5), pp. 581–588. doi: 10.1002/wmts.44.

Boura-Halfon, S. and Zick, Y. (2009) 'Phosphorylation of IRS proteins, insulin action, and insulin resistance.', *American journal of physiology. Endocrinology and metabolism*, 296(4), pp. E581-91. doi: 10.1152/ajpendo.90437.2008.

Bourdon, D. M., Mahanty, S. K., Jacobson, K. A., Boyer, J. L. and Harden, T. K. (2006) '(N)-methanocarba-2MeSADP (MRS2365) is a subtype-specific agonist that induces rapid desensitization of the P2Y1 receptor of human platelets.', *Journal of thrombosis and haemostasis : JTH*, 4(4), pp. 861–8. doi: 10.1111/j.1538-7836.2006.01866.x.

Brand, C. S., Hocker, H. J., Gorfe, A. A., Cavasotto, C. N. and Dessauer, C. W. (2013) 'Isoform

Selectivity of Adenylyl Cyclase Inhibitors: Characterization of Known and Novel Compounds', *Journal of Pharmacology and Experimental Therapeutics*, 347(2), pp. 265–275.

Buchthal, F. and Folkow, B. (1948) 'Interaction between acetylcholine and adenosine triphosphate in normal, curarised and denervated muscle.', *Acta physiologica Scandinavica*, 15(2), pp. 150–60. doi: 10.1111/j.1748-1716.1948.tb00492.x.

Burns, T. W., Langley, P. E. and Robison, G. A. (1975) 'Site of free-fatty-acid inhibition of lipolysis by human adipocytes', *Metabolism*, 24(3), pp. 265–276. doi: 10.1016/0026-0495(75)90108-0.

Burnstock, G., Campbell, G., Satchell, D. and Smythe, A. (1970) 'Evidence that adenosine triphosphate or a related nucleotide is the transmitter substance released by non-adrenergic inhibitory nerves in the gut.', *British journal of pharmacology*, 40(4), pp. 668–88. Available at: http://www.ncbi.nlm.nih.gov/pubmed/4322041.

Burnstock, G. (1972) 'Purinergic nerves.', *Pharmacological reviews*, 24(3), pp. 509–81. Available at: http://www.ncbi.nlm.nih.gov/pubmed/4404211.

Burnstock, G. (2007) 'Purine and pyrimidine receptors', *Cellular and Molecular Life Sciences*, 64(12), pp. 1471–1483. doi: 10.1007/s00018-007-6497-0.

Burnstock, G. (2014) 'Purinergic signalling: from discovery to current developments.', *Experimental physiology*, 99(1), pp. 16–34. doi: 10.1113/expphysiol.2013.071951.

Burnstock, G. and Verkhratsky, A. (2010) 'Long-term (trophic) purinergic signalling: purinoceptors control cell proliferation, differentiation and death', *Cell Death and Disease*, 1(1), p. e9. doi: 10.1038/cddis.2009.11.

Cammisotto, P. G. and Bukowiecki, L. J. (2004) 'Role of calcium in the secretion of leptin from white adipocytes.', *American journal of physiology. Regulatory, integrative and comparative physiology*, 287(6), pp. R1380-6. doi: 10.1152/ajpregu.00368.2004.

Campwala, H. and Fountain, S. J. (2013) 'Constitutive and agonist stimulated ATP secretion in leukocytes.', *Communicative & integrative biology*, 6(3), p. e23631. doi: 10.4161/cib.23631.

Cannon, B. and Nedergaard, J. (2004) 'Brown adipose tissue: function and physiological significance.', *Physiological reviews*, 84(1), pp. 277–359. doi: 10.1152/physrev.00015.2003.

Cao, H., Gerhold, K., Mayers, J. R., Wiest, M. M., Watkins, S. M. and Hotamisligil, G. S. (2008) 'Identification of a lipokine, a lipid hormone linking adipose tissue to systemic metabolism.', *Cell*, 134(6), pp. 933–44. doi: 10.1016/j.cell.2008.07.048.

Cao, H. (2014) 'Adipocytokines in obesity and metabolic disease.', *The Journal of endocrinology*, 220(2), pp. T47-59. doi: 10.1530/JOE-13-0339.

Carbonetti, N. H. (2010) 'Pertussis toxin and adenylate cyclase toxin: key virulence factors of Bordetella pertussis and cell biology tools', *Future Microbiology*, 5(3), pp. 455–469. doi: 10.2217/fmb.09.133.

Chen, H.-T., Lee, M.-J., Chen, C.-H., Chuang, S.-C., Chang, L.-F., Ho, M.-L., Hung, S.-H., Fu, Y.-C.,

Wang, Y.-H., Wang, H.-I., Wang, G.-J., Kang, L. and Chang, J.-K. (2012) 'Proliferation and differentiation potential of human adipose-derived mesenchymal stem cells isolated from elderly patients with osteoporotic fractures', *Journal of Cellular and Molecular Medicine*, 16(3), pp. 582–592. doi: 10.1111/j.1582-4934.2011.01335.x.

Chen, N., Zhou, L., Zhang, Z., Xu, J., Wan, Z. and Qin, L. (2014) 'Resistin induces lipolysis and suppresses adiponectin secretion in cultured human visceral adipose tissue.', *Regulatory peptides*, 194–195, pp. 49–54. doi: 10.1016/j.regpep.2014.10.001.

Chen, Y., Corriden, R., Inoue, Y., Yip, L., Hashiguchi, N., Zinkernagel, A., Nizet, V., Insel, P. A. and Junger, W. G. (2006) 'ATP release guides neutrophil chemotaxis via P2Y2 and A3 receptors.', *Science (New York, N.Y.)*, 314(5806), pp. 1792–5. doi: 10.1126/science.1132559.

Chhatriwala, M., Ravi, R. G., Patel, R. I., Boyer, J. L., Jacobson, K. A. and Harden, T. K. (2004) 'Induction of novel agonist selectivity for the ADP-activated P2Y1 receptor versus the ADP-activated P2Y12 and P2Y13 receptors by conformational constraint of an ADP analog.', *The Journal of pharmacology and experimental therapeutics*, 311(3), pp. 1038–43. doi: 10.1124/jpet.104.068650.

Cho, K.-J., Shim, J.-H., Cho, M.-C., Choe, Y.-K., Hong, J.-T., Moon, D.-C., Kim, J.-W. and Yoon, D.-Y. (2005) 'Signaling pathways implicated in alpha-melanocyte stimulating hormone-induced lipolysis in 3T3-L1 adipocytes.', *Journal of cellular biochemistry*, 96(4), pp. 869–78. doi: 10.1002/jcb.20561.

Cho, K.-S., Park, H.-K., Park, H.-Y., Jung, J. S., Jeon, S.-G., Kim, Y.-K. and Roh, H. J. (2009) 'IFATS Collection: Immunomodulatory Effects of Adipose Tissue-Derived Stem Cells in an Allergic Rhinitis Mouse Model', *Stem Cells*, 27(1), pp. 259–265. doi: 10.1634/stemcells.2008-0283.

Ciciarello, M., Zini, R., Rossi, L., Salvestrini, V., Ferrari, D., Manfredini, R. and Lemoli, R. M. (2013) 'Extracellular Purines Promote the Differentiation of Human Bone Marrow-Derived Mesenchymal Stem Cells to the Osteogenic and Adipogenic Lineages', *Stem Cells and Development*, 22(7), pp. 1097–1111. doi: 10.1089/scd.2012.0432.

Clapham, D. E. (2007) 'Calcium Signaling', *Cell*, 131(6), pp. 1047–1058. doi: 10.1016/j.cell.2007.11.028.

Clemmons, D. R. (2004) 'Role of insulin-like growth factor iin maintaining normal glucose homeostasis.', *Hormone research*, 62 Suppl 1, pp. 77–82. doi: 10.1159/000080763.

Cohen, M. V, Yang, X. and Downey, J. M. (2010) 'A(2b) adenosine receptors can change their spots.', *British journal of pharmacology*, 159(8), pp. 1595–7. doi: 10.1111/j.1476-5381.2010.00668.x.

Communi, D., Parmentier, M. and Boeynaems, J.-M. (1996) 'Cloning, Functional Expression and Tissue Distribution of the Human P2Y6Receptor', *Biochemical and Biophysical Research Communications*, 222(2), pp. 303–308. doi: 10.1006/bbrc.1996.0739.

Conroy, S., Kindon, N., Kellam, B. and Stocks, M. J. (2016) 'Drug-like Antagonists of P2Y

Receptors—From Lead Identification to Drug Development', *Journal of Medicinal Chemistry*. American Chemical Society, 59(22), pp. 9981–10005. doi: 10.1021/acs.jmedchem.5b01972.
Cooper, G. (2000) 'Pathways of Intracellular Signal Transduction.', in *The Cell: A Molecular Approach.* 2nd edn. Sunderland (MA): Sinauer Associates. Available at: https://www.ncbi.nlm.nih.gov/books/NBK9870/.
Copps, K. D. and White, M. F. (2012) 'Regulation of insulin sensitivity by serine/threonine phosphorylation of insulin receptor substrate proteins IRS1 and IRS2.', *Diabetologia*, 55(10), pp. 2565–2582. doi: 10.1007/s00125-012-2644-8.
Corriden, R. and Insel, P. A. (2010) 'Basal release of ATP: an autocrine-paracrine mechanism for cell regulation.', *Science signaling*, 3(104), p. re1. doi: 10.1126/scisignal.3104re1.
Cristancho, A. G. and Lazar, M. a. (2011) 'Forming functional fat: a growing understanding of adipocyte differentiation', *Nature Reviews Molecular Cell Biology*. Nature Publishing Group, 12(11), pp. 722–734. doi: 10.1038/nrm3198.
Cullen, B. R. (2004) 'Transcription and Processing of Human microRNA Precursors', *Molecular Cell*, 16(6), pp. 861–865. doi: 10.1016/j.molcel.2004.12.002.
Cullen, B. R. (2005) 'RNAi the natural way.', *Nature genetics*, 37(11), pp. 1163–5. doi: 10.1038/ng1105-1163.
Cypess, A. M., Lehman, S., Williams, G., Tal, I., Rodman, D., Goldfine, A. B., Kuo, F. C., Palmer, E. L., Tseng, Y.-H., Doria, A., Kolodny, G. M. and Kahn, C. R. (2009) 'Identification and importance of brown adipose tissue in adult humans.', *The New England journal of medicine*, 360(15), pp. 1509–17. doi: 10.1056/NEJMoa0810780.
Czech, M. P., Tencerova, M., Pedersen, D. J. and Aouadi, M. (2013) 'Insulin signalling mechanisms for triacylglycerol storage.', *Diabetologia*, 56(5), pp. 949–64. doi: 10.1007/s00125-013-2869-1.
D'Ambrosi, N., Iafrate, M., Saba, E., Rosa, P. and Volonté, C. (2007) 'Comparative analysis of P2Y4 and P2Y6 receptor architecture in native and transfected neuronal systems', *Biochimica et Biophysica Acta (BBA) - Biomembranes*, 1768(6), pp. 1592–1599. doi: 10.1016/j.bbamem.2007.03.020.
Dal Ben, D., Buccioni, M., Lambertucci, C., Marucci, G., Thomas, A. and Volpini, R. (2015) 'Purinergic P2X receptors: Structural models and analysis of ligand-target interaction', *European Journal of Medicinal Chemistry*, 89, pp. 561–580. doi: 10.1016/j.ejmech.2014.10.071.
Degerman, E., Belfrage, P. and Manganiello, V. C. (1997) 'Structure, Localization, and Regulation of cGMP-inhibited Phosphodiesterase (PDE3)', *Journal of Biological Chemistry*, 272(11), pp. 6823–6826. doi: 10.1074/jbc.272.11.6823.
Després, J.-P. (2012) 'Abdominal obesity and cardiovascular disease: is inflammation the missing link?', *The Canadian journal of cardiology*, 28(6), pp. 642–52. doi: 10.1016/j.cjca.2012.06.004.
Després, J.-P. and Lemieux, I. (2006) 'Abdominal obesity and metabolic syndrome.', *Nature*,

444(7121), pp. 881–887. doi: 10.1038/nature05488.

Deterding, R., Retsch-Bogart, G., Milgram, L., Gibson, R., Daines, C., Zeitlin, P. L., Milla, C., Marshall, B., Lavange, L., Engels, J., Mathews, D., Gorden, J., Schaberg, A., Williams, J., Ramsey, B. and Cystic Fibrosis Foundation Therapeutics Development Network (2005) 'Safety and tolerability of denufosol tetrasodium inhalation solution, a novel P2Y2 receptor agonist: results of a phase 1/phase 2 multicenter study in mild to moderate cystic fibrosis.', *Pediatric pulmonology*, 39(4), pp. 339–48. doi: 10.1002/ppul.20192.

Dixon, C. J., Bowler, W. B., Littlewood-Evans, A., Dillon, J. P., Bilbe, G., Sharpe, G. R. and Gallagher, J. A. (1999) 'Regulation of epidermal homeostasis through P2Y 2 receptors', *British Journal of Pharmacology*, 127(7), pp. 1680–1686. doi: 10.1038/sj.bjp.0702653.

Dominici, M., Le Blanc, K., Mueller, I., Slaper-Cortenbach, I., Marini, F. ., Krause, D. S., Deans, R. J., Keating, A., Prockop, D. J. and Horwitz, E. M. (2006) 'Minimal criteria for defining multipotent mesenchymal stromal cells. The International Society for Cellular Therapy position statement', *Cytotherapy*, 8(4), pp. 315–317. doi: 10.1080/14653240600855905.

Dong, Q., Ginsberg, H. N. and Erlanger, B. F. (2001) 'Overexpression of the A1 adenosine receptor in adipose tissue protects mice from obesity-related insulin resistance.', *Diabetes, obesity & metabolism*, 3(5), pp. 360–6. Available at: http://www.ncbi.nlm.nih.gov/pubmed/11703426.

Doris, R., Vernon, R. F., Houslay, M. D. and Kilgour, E. (1994) 'Growth hormone decreases the response to anti-lipolytic agonists and decreases the levels of G,2 in rat adipocytes', *Biochemical Journal*, 297, pp. 41–45.

Dorsam, R. T. and Kunapuli, S. P. (2004) 'Central role of the P2Y12 receptor in platelet activation.', *The Journal of clinical investigation*, 113(3), pp. 340–5. doi: 10.1172/JCI20986.

Drury, a N. and Szent-Györgyi, a (1929) 'The physiological activity of adenine compounds with especial reference to their action upon the mammalian heart.', *The Journal of physiology*, 68(3), pp. 213–237. doi: 10.1183/09031936.00137511.

DuBridge, R. B., Tang, P., Hsia, H. C., Leong, P. M., Miller, J. H. and Calos, M. P. (1987) 'Analysis of mutation in human cells by using an Epstein-Barr virus shuttle system.', *Molecular and cellular biology*, 7(1), pp. 379–87. Available at: http://www.ncbi.nlm.nih.gov/pubmed/3031469.

Dunkern, T. R. and Hatzelmann, A. (2007) 'Characterization of inhibitors of phosphodiesterase 1C on a human cellular system', *FEBS Journal*, 274(18), pp. 4812–4824. doi: 10.1111/j.1742-4658.2007.06001.x.

Ecke, D., Hanck, T., Tulapurkar, M. E., Schäfer, R., Kassack, M., Stricker, R. and Reiser, G. (2008) 'Hetero-oligomerization of the P2Y 11 receptor with the P2Y 1 receptor controls the internalization and ligand selectivity of the P2Y 11 receptor', *Biochemical Journal*, 409(1), pp. 107–116. doi: 10.1042/BJ20070671.

Eissing, L., Scherer, T., Tödter, K., Knippschild, U., Greve, J. W., Buurman, W. A., Pinnschmidt, H.

O., Rensen, S. S., Wolf, A. M., Bartelt, A., Heeren, J., Buettner, C. and Scheja, L. (2013) 'De novo lipogenesis in human fat and liver is linked to ChREBP-β and metabolic health.', *Nature communications*, 4, p. 1528. doi: 10.1038/ncomms2537.

Emery, A. C., Eiden, M. V and Eiden, L. E. (2013) 'A new site and mechanism of action for the widely used adenylate cyclase inhibitor SQ22,536.', *Molecular pharmacology*, 83(1), pp. 95–105. doi: 10.1124/mol.112.081760.

Emmelin, N. and Feldberg, W. (1948) 'Systemic effects of adenosine triphosphate.', *British journal of pharmacology and chemotherapy*, 3(4), pp. 273–84. Available at: http://www.ncbi.nlm.nih.gov/pubmed/18102596.

Endo, T. and Kobayashi, T. (2012) 'Expression of functional TSH receptor in white adipose tissues of hyt/hyt mice induces lipolysis in vivo.', *American journal of physiology. Endocrinology and metabolism*, 302(12), pp. E1569-75. doi: 10.1152/ajpendo.00572.2011.

Erb, L. and Weisman, G. A. (2012) 'Coupling of P2Y receptors to G proteins and other signaling pathways', *Wiley Interdisciplinary Reviews: Membrane Transport and Signaling*, 1(6), pp. 789–803. doi: 10.1002/wmts.62.

Eseonu, O. I. and De Bari, C. (2015) 'Homing of mesenchymal stem cells: mechanistic or stochastic? Implications for targeted delivery in arthritis', *Rheumatology*, 54(2), pp. 210–218. doi: 10.1093/rheumatology/keu377.

Evans, R. J. (2010) 'Structural interpretation of P2X receptor mutagenesis studies on drug action', *British Journal of Pharmacology*, 161(5), pp. 961–971. doi: 10.1111/j.1476-5381.2010.00728.x.

Fabre, J. E., Nguyen, M., Latour, A., Keifer, J. A., Audoly, L. P., Coffman, T. M. and Koller, B. H. (1999) 'Decreased platelet aggregation, increased bleeding time and resistance to thromboembolism in P2Y1-deficient mice.', *Nature medicine*, 5(10), pp. 1199–202. doi: 10.1038/13522.

Fagerberg, L., Hallström, B. M., Oksvold, P., Kampf, C., Djureinovic, D., Odeberg, J., Habuka, M., Tahmasebpoor, S., Danielsson, A., Edlund, K., Asplund, A., Sjöstedt, E., Lundberg, E., Szigyarto, C. A.-K., Skogs, M., Takanen, J. O., Berling, H., Tegel, H., *et al.* (2014) 'Analysis of the human tissue-specific expression by genome-wide integration of transcriptomics and antibody-based proteomics.', *Molecular & cellular proteomics : MCP*, 13(2), pp. 397–406. doi: 10.1074/mcp.M113.035600.

Fain, J. N. (1973) 'Biochemical Aspects of Drug and Hormone Action on Adipose Tissue', *Pharmacological Reviews*, 25(1), p. 67 LP-118. Available at: http://pharmrev.aspetjournals.org/content/25/1/67.abstract.

Fain, J. N. (2010) 'Release of Inflammatory Mediators by Human Adipose Tissue Is Enhanced in Obesity and Primarily by the Nonfat Cells: A Review', *Mediators of Inflammation*, 2010, pp. 1–20. doi: 10.1155/2010/513948.

Faulhaber-Walter, R., Jou, W., Mizel, D., Li, L., Zhang, J., Kim, S. M., Huang, Y., Chen, M., Briggs, J. P., Gavrilova, O. and Schnermann, J. B. (2011) 'Impaired glucose tolerance in the absence of adenosine A1 receptor signaling.', *Diabetes*, 60(10), pp. 2578–87. doi: 10.2337/db11-0058.

Feisst, V., Meidinger, S. and Locke, M. (2015) 'From bench to bedside: use of human adipose-derived stem cells', *Stem Cells and Cloning: Advances and Applications*, p. 149. doi: 10.2147/SCCAA.S64373.

Ferrari, D., Gulinelli, S., Salvestrini, V., Lucchetti, G., Zini, R., Manfredini, R., Caione, L., Piacibello, W., Ciciarello, M., Rossi, L., Idzko, M., Ferrari, S., Di Virgilio, F. and Lemoli, R. M. (2011) 'Purinergic stimulation of human mesenchymal stem cells potentiates their chemotactic response to CXCL12 and increases the homing capacity and production of proinflammatory cytokines.', *Experimental hematology*, 39(3), pp. 360–74, 374.e1–5. doi: 10.1016/j.exphem.2010.12.001.

Fishman, R. B. and Dark, J. (1987) 'Sensory innervation of white adipose tissue.', *The American journal of physiology*, 253(6 Pt 2), pp. R942-4. doi: 10.1152/ajpregu.1987.253.6.R942.

Fox, K. A. A., Després, J.-P., Richard, A.-J., Brette, S., Deanfield, J. E. and IDEA Steering Committee and National Co-ordinators (2009) 'Does abdominal obesity have a similar impact on cardiovascular disease and diabetes? A study of 91,246 ambulant patients in 27 European countries.', *European heart journal*, 30(24), pp. 3055–63. doi: 10.1093/eurheartj/ehp371.

Fox, S. C., Behan, M. W. H. and Heptinstall, S. (2004) 'Inhibition of ADP-induced intracellular Ca2+ responses and platelet aggregation by the P2Y12 receptor antagonists AR-C69931MX and clopidogrel is enhanced by prostaglandin E1.', *Cell calcium*, 35(1), pp. 39–46. Available at: http://www.ncbi.nlm.nih.gov/pubmed/14670370.

Frayn, K. N. (2002) 'Adipose tissue as a buffer for daily lipid flux.', *Diabetologia*, 45(9), pp. 1201–10. doi: 10.1007/s00125-002-0873-y.

Fredholm, B. and Hjemdahl, P. (1976) 'Cyclic AMP-dependent and independent inhibition of lipolysis by adenosine and decreased pH.', *Acta Physiologica Scandinavica*, 96(2), pp. 170–179. Available at: https://www.ncbi.nlm.nih.gov/pubmed/3945.

Fredholm, B. and Sollevi, A. (1977) 'Antilipolytic effect of adenosine in dog adipose tissue in situ', *Acta Physiologica*, 99(2), pp. 254–256. Available at: http://onlinelibrary.wiley.com/doi/10.1111/j.1748-1716.1977.tb10377.x/abstract.

Fredrikson, G., Tornqvist, H. and Belfrage, P. (1986) 'Hormone-sensitive lipase and monoacylglycerol lipase are both required for complete degradation of adipocyte triacylglycerol.', *Biochimica et biophysica acta*, 876(2), pp. 288–93. Available at: http://www.ncbi.nlm.nih.gov/pubmed/3955067.

Fu, Y.-Y., Chen, K.-L., Li, H.-X. and Zhou, G.-H. (2016) 'The adipokine Chemerin induces lipolysis and adipogenesis in bovine intramuscular adipocytes.', *Molecular and cellular biochemistry*, 418(1–2), pp. 39–48. doi: 10.1007/s11010-016-2731-0.

Van Gaal, L. F., Mertens, I. L. and De Block, C. E. (2006) 'Mechanisms linking obesity with cardiovascular disease.', *Nature*, 444(7121), pp. 875–880. doi: 10.1038/nature05487.
Gharibi, B., Abraham, A. A., Ham, J. and Evans, B. A. J. (2011) 'Adenosine receptor subtype expression and activation influence the differentiation of mesenchymal stem cells to osteoblasts and adipocytes.', *Journal of bone and mineral research : the official journal of the American Society for Bone and Mineral Research*, 26(9), pp. 2112–24. doi: 10.1002/jbmr.424.
Gharibi, B., Abraham, A. A., Ham, J. and Evans, B. A. J. (2012) 'Contrasting effects of A1 and A2b adenosine receptors on adipogenesis', *International Journal of Obesity*, 36(3), pp. 397–406. doi: 10.1038/ijo.2011.129.
Golan, R., Shelef, I., Rudich, A., Gepner, Y., Shemesh, E., Chassidim, Y., Harman-Boehm, I., Henkin, Y., Schwarzfuchs, D., Ben Avraham, S., Witkow, S., Liberty, I. F., Tangi-Rosental, O., Sarusi, B., Stampfer, M. J. and Shai, I. (2012) 'Abdominal Superficial Subcutaneous Fat: A putative distinct protective fat subdepot in type 2 diabetes', *Diabetes Care*, 35(3), pp. 640–647. doi: 10.2337/dc11-1583.
Gorini, S., Gatta, L., Pontecorvo, L., Vitiello, L. and la Sala, A. (2013) 'Regulation of innate immunity by extracellular nucleotides', *American Journal of Blood Research*, 3(1), pp. 14–28.
Govindan, S. and Taylor, C. W. (2012) 'P2Y receptor subtypes evoke different Ca2+ signals in cultured aortic smooth muscle cells', *Purinergic Signalling*, 8(4), pp. 763–777. doi: 10.1007/s11302-012-9323-6.
Graham, F. L., Smiley, J., Russell, W. C. and Nairn, R. (1977) 'Characteristics of a human cell line transformed by DNA from human adenovirus type 5.', *The Journal of general virology*, 36(1), pp. 59–74. doi: 10.1099/0022-1317-36-1-59.
Granneman, J. G., Moore, H.-P. H., Granneman, R. L., Greenberg, A. S., Obin, M. S. and Zhu, Z. (2007) 'Analysis of lipolytic protein trafficking and interactions in adipocytes.', *The Journal of biological chemistry*, 282(8), pp. 5726–35. doi: 10.1074/jbc.M610580200.
Gray, N. E., Lam, L. N., Yang, K., Zhou, A. Y., Koliwad, S. and Wang, J.-C. (2012) 'Angiopoietin-like 4 (Angptl4) protein is a physiological mediator of intracellular lipolysis in murine adipocytes.', *The Journal of biological chemistry*, 287(11), pp. 8444–56. doi: 10.1074/jbc.M111.294124.
van Greevenbroek, M. M. J., Schalkwijk, C. G. and Stehouwer, C. D. A. (2013) 'Obesity-associated low-grade inflammation in type 2 diabetes mellitus: causes and consequences.', *The Netherlands journal of medicine*, 71(4), pp. 174–87. Available at: http://www.ncbi.nlm.nih.gov/pubmed/23723111.
Grønning, L. M., Baillie, G. S., Cederberg, A., Lynch, M. J., Houslay, M. D., Enerbäck, S. and Taskén, K. (2006) 'Reduced PDE4 expression and activity contributes to enhanced catecholamine-induced cAMP accumulation in adipocytes from FOXC2 transgenic mice', *FEBS Letters*, 580(17), pp. 4126–4130. doi: 10.1016/j.febslet.2006.06.058.

Grynkiewicz, G., Poenie, M. and Tsien, R. Y. (1985) 'A new generation of Ca2+ indicators with greatly improved fluorescence properties.', *The Journal of biological chemistry*, 260(6), pp. 3440–50. Available at: http://www.ncbi.nlm.nih.gov/pubmed/3838314.

Guillou, J.-L. L., Nakata, H. and Cooper, D. M. F. (1999) 'Inhibition by Calcium of Mammalian Adenylyl Cyclases', *Journal of Biological Chemistry*, 274(50), pp. 35539–45. doi: 10.1074/jbc.274.50.35539.

El Hachmane, M. F., Ermund, A., Bränmark, C. and Olofsson, C. S. (2018) 'Extracellular ATP activates store-operated Ca 2+ entry in white adipocytes: functional evidence for STIM1 and ORAI1', *Biochemical Journal*, 475(3), pp. 691–704. doi: 10.1042/BCJ20170484.

Haemmerle, G., Zimmermann, R., Hayn, M., Theussl, C., Waeg, G., Wagner, E., Sattler, W., Magin, T. M., Wagner, E. F. and Zechner, R. (2002) 'Hormone-sensitive lipase deficiency in mice causes diglyceride accumulation in adipose tissue, muscle, and testis.', *The Journal of biological chemistry*, 277(7), pp. 4806–15. doi: 10.1074/jbc.M110355200.

Hagmann, S., Moradi, B., Frank, S., Dreher, T., Kämmerer, P. W., Richter, W. and Gotterbarm, T. (2013) 'Different culture media affect growth characteristics, surface marker distribution and chondrogenic differentiation of human bone marrow-derived mesenchymal stromal cells', *BMC Musculoskeletal Disorders*, 14(1), p. 223. doi: 10.1186/1471-2474-14-223.

Halberg, N., Wernstedt, I. and Scherer, P. E. (2008) 'The Adipocyte as an Endocrine Cell', *Endocrinology and metabolism clinics of North America*, 37(3), p. 753–xi. doi: 10.1016/j.ecl.2008.07.002.

Hamdi, M. and Rebecca, A. (2006) 'The Deep Inferior Epigastric Artery Perforator Flap (DIEAP) in Breast Reconstruction', *Seminars in Plastic Surgery*, 20(2), pp. 095-102. doi: 10.1055/s-2006-941716.

Hansen, T. K., Gravholt, C. H., ØRskov, H., Rasmussen, M. H., Christiansen, J. S. and Jørgensen, J. O. L. (2002) 'Dose dependency of the pharmacokinetics and acute lipolytic actions of growth hormone.', *The Journal of clinical endocrinology and metabolism*, 87(10), pp. 4691–8. doi: 10.1210/jc.2002-020563.

Hardy, A. R., Jones, M. L., Mundell, S. J. and Poole, A. W. (2004) 'Reciprocal cross-talk between P2Y1 and P2Y12 receptors at the level of calcium signaling in human platelets', *Blood*, 104(6), pp. 1745–1752. doi: 10.1182/blood-2004-02-0534.

Van Harmelen, V., Reynisdottir, S., Cianflone, K., Degerman, E., Hoffstedt, J., Nilsell, K., Sniderman, A. and Arner, P. (1999) 'Mechanisms involved in the regulation of free fatty acid release from isolated human fat cells by acylation-stimulating protein and insulin.', *The Journal of biological chemistry*, 274(26), pp. 18243–51. Available at: http://www.ncbi.nlm.nih.gov/pubmed/10373426.

Helal, C. J., Chappie, T. A., Humphrey, J. M., Verhoest, P. R. and Yang, E. (2012) 'Preparation of imidazo[5,1-f][1,2,4]triazines for the treatment of neurological disorders.' United Stated of

America.

Hernandez-Olmos, V., Abdelrahman, A., El-Tayeb, A., Freudendahl, D., Weinhausen, S. and Müller, C. E. (2012) 'N-Substituted Phenoxazine and Acridone Derivatives: Structure–Activity Relationships of Potent P2X4 Receptor Antagonists', *Journal of Medicinal Chemistry*, 55(22), pp. 9576–9588. doi: 10.1021/jm300845v.

Herold, C. L., Qi, A.-D., Harden, T. K. and Nicholas, R. A. (2004) 'Agonist Versus Antagonist Action of ATP at the P2Y 4 Receptor Is Determined by the Second Extracellular Loop', *Journal of Biological Chemistry*, 279(12), pp. 11456–11464. doi: 10.1074/jbc.M301734200.

Hidaka, H., Hayashi, H., Kohri, H., Kimura, Y., Hosokawa, T., Igawa, T. and Saitoh, Y. (1979) 'Selective inhibitor of platelet cyclic adenosine monophosphate phosphodiesterase, cilostamide, inhibits platelet aggregation.', *The Journal of pharmacology and experimental therapeutics*, 211(1), pp. 26–30. Available at: http://www.ncbi.nlm.nih.gov/pubmed/226672.

Hilger, D., Masureel, M. and Kobilka, B. K. (2018) 'Structure and dynamics of GPCR signaling complexes', *Nature Structural & Molecular Biology*, 25(1), pp. 4–12. doi: 10.1038/s41594-017-0011-7.

Hillgartner, F. B., Salati, L. M. and Goodridge, A. G. (1995) 'Physiological and molecular mechanisms involved in nutritional regulation of fatty acid synthesis.', *Physiological reviews*, 75(1), pp. 47–76. doi: 10.1152/physrev.1995.75.1.47.

Hoffmann, K., Baqi, Y., Morena, M. S., Glanzel, M., Muller, C. E. and von Kugelgen, I. (2009) 'Interaction of New, Very Potent Non-Nucleotide Antagonists with Arg256 of the Human Platelet P2Y12 Receptor', *Journal of Pharmacology and Experimental Therapeutics*, 331(2), pp. 648–655. doi: 10.1124/jpet.109.156687.

Hoffstedt, J., Arner, P., Hellers, G. and Lönnqvist, F. (1997) 'Variation in adrenergic regulation of lipolysis between omental and subcutaneous adipocytes from obese and non-obese men.', *Journal of lipid research*, 38(4), pp. 795–804. Available at: http://www.ncbi.nlm.nih.gov/pubmed/9144094.

Holton, P. (1959) 'The liberation of adenosine triphosphate on antidromic stimulation of sensory nerves.', *The Journal of physiology*, 145(3), pp. 494–504. Available at: http://www.ncbi.nlm.nih.gov/pubmed/13642316.

Hotamisligil, G. S. (2006) 'Inflammation and metabolic disorders', *Nature*, 444(7121), pp. 860–867. doi: 10.1038/nature05485.

Houtgraaf, J. H., den Dekker, W. K., van Dalen, B. M., Springeling, T., de Jong, R., van Geuns, R. J., Geleijnse, M. L., Fernandez-Aviles, F., Zijlsta, F., Serruys, P. W. and Duckers, H. J. (2012) 'First Experience in Humans Using Adipose Tissue–Derived Regenerative Cells in the Treatment of Patients With ST-Segment Elevation Myocardial Infarction', *Journal of the American College of Cardiology*, 59(5), pp. 539–540. doi: 10.1016/j.jacc.2011.09.065.

Hu, R., He, M.-L., Hu, H., Yuan, B.-X., Zang, W.-J., Lau, C.-P., Tse, H.-F. and Li, G.-R. (2009) 'Characterization of calcium signaling pathways in human preadipocytes.', *Journal of cellular physiology*, 220(3), pp. 765–70. doi: 10.1002/jcp.21823.

Ibrahim, M. M. (2010) 'Subcutaneous and visceral adipose tissue: structural and functional differences', *Obesity Reviews*, 11(1), pp. 11–18. doi: 10.1111/j.1467-789X.2009.00623.x.

Insel, P. A. and Ostrom, R. S. (2003) 'Forskolin as a Tool for Examining Adenylyl Cyclase Expression, Regulation, and G Protein Signaling', *Cellular and Molecular Neurobiology*, 23(3), pp. 305–314. doi: 10.1023/A:1023684503883.

Jacobson, K. A., Ivanov, A. A., de Castro, S., Harden, T. K. and Ko, H. (2009) 'Development of selective agonists and antagonists of P2Y receptors', *Purinergic Signalling*, 5(1), pp. 75–89. doi: 10.1007/s11302-008-9106-2.

Jacobson, K. A., Balasubramanian, R., Deflorian, F. and Gao, Z.-G. (2012) 'G protein-coupled adenosine (P1) and P2Y receptors: ligand design and receptor interactions.', *Purinergic signalling*, 8(3), pp. 419–36. doi: 10.1007/s11302-012-9294-7.

Jagroop, I. A., Burnstock, G. and Mikhailidis, D. P. (2003) 'Both the ADP receptors P2Y1 and P2Y12, play a role in controlling shape change in human platelets.', *Platelets*, 14(1), pp. 15–20. Available at: http://www.ncbi.nlm.nih.gov/pubmed/12623443.

Jensen, M. D. (1995) 'Gender differences in regional fatty acid metabolism before and after meal ingestion.', *The Journal of clinical investigation*, 96(5), pp. 2297–303. doi: 10.1172/JCI118285.

Jiang, L.-H., Mousawi, F., Yang, X. and Roger, S. (2017) 'ATP-induced Ca2+-signalling mechanisms in the regulation of mesenchymal stem cell migration', *Cellular and Molecular Life Sciences*, 74(20), pp. 3697–3710. doi: 10.1007/s00018-017-2545-6.

Jiang, L.-H., Hao, Y., Mousawi, F., Peng, H. and Yang, X. (2017) 'Expression of P2 Purinergic Receptors in Mesenchymal Stem Cells and Their Roles in Extracellular Nucleotide Regulation of Cell Functions.', *Journal of cellular physiology*, 232(2), pp. 287–297. doi: 10.1002/jcp.25484.

Jiao, P., Ma, J., Feng, B., Zhang, H., Diehl, J. A., Chin, Y. E., Yan, W., Xu, H., Alan Diehl, J., Eugene Chin, Y., Yan, W. and Xu, H. (2011) 'FFA-Induced Adipocyte Inflammation and Insulin Resistance: Involvement of ER Stress and IKKβ Pathways', *Obesity*, 19(3), pp. 483–491. doi: 10.1038/oby.2010.200.

Jin, J., Daniel, J. L. and Kunapuli, S. P. (1998) 'Molecular basis for ADP-induced platelet activation. II. The P2Y1 receptor mediates ADP-induced intracellular calcium mobilization and shape change in platelets.', *The Journal of biological chemistry*, 273(4), pp. 2030–4. Available at: http://www.ncbi.nlm.nih.gov/pubmed/9442040.

Jo, C. H., Lee, Y. G., Shin, W. H., Kim, H., Chai, J. W., Jeong, E. C., Kim, J. E., Shim, H., Shin, J. S., Shin, I. S., Ra, J. C., Oh, S. and Yoon, K. S. (2014) 'Intra-Articular Injection of Mesenchymal Stem Cells for the Treatment of Osteoarthritis of the Knee: A Proof-of-Concept Clinical Trial', *STEM*

CELLS, 32(5), pp. 1254–1266. doi: 10.1002/stem.1634.

Johansen, T., Richelsen, B., Hansen, H. S., Din, N. and Malmlöf, K. (2003) 'Growth hormone-mediated breakdown of body fat: effects of GH on lipases in adipose tissue and skeletal muscle of old rats fed different diets.', *Hormone and metabolic research = Hormon- und Stoffwechselforschung = Hormones et metabolisme*, 35(4), pp. 243–50. doi: 10.1055/s-2003-39481.

Johansson, S. M., Lindgren, E., Yang, J. N., Herling, A. W. and Fredholm, B. B. (2008) 'Adenosine A1 receptors regulate lipolysis and lipogenesis in mouse adipose tissue - Interactions with insulin', *European Journal of Pharmacology*. Elsevier B.V., 597(1–3), pp. 92–101. doi: 10.1016/j.ejphar.2008.08.022.

Jones, D. T. and Reed, R. R. (1989) 'Golf: an olfactory neuron specific-G protein involved in odorant signal transduction.', *Science (New York, N.Y.)*, 244(4906), pp. 790–5. Available at: http://www.ncbi.nlm.nih.gov/pubmed/2499043.

Kaebisch, C., Schipper, D., Babczyk, P. and Tobiasch, E. (2015) 'The role of purinergic receptors in stem cell differentiation', *Computational and Structural Biotechnology Journal*, 13, pp. 75–84. doi: 10.1016/j.csbj.2014.11.003.

Kahn, S. E., Hull, R. L. and Utzschneider, K. M. (2006) 'Mechanisms linking obesity to insulin resistance and type 2 diabetes.', *Nature*, 444(7121), pp. 840–846. doi: 10.1038/nature05482.

Kajimura, S., Spiegelman, B. M. and Seale, P. (2015) 'Brown and Beige Fat: Physiological Roles beyond Heat Generation', *Cell Metabolism*, 22(4), pp. 546–559. doi: 10.1016/j.cmet.2015.09.007.

Kalinovich, A. V., de Jong, J. M. A., Cannon, B. and Nedergaard, J. (2017) 'UCP1 in adipose tissues: two steps to full browning', *Biochimie*, 134, pp. 127–137. doi: 10.1016/j.biochi.2017.01.007.

Kamenetsky, M., Middelhaufe, S., Bank, E. M., Levin, L. R., Buck, J. and Steegborn, C. (2006) 'Molecular details of cAMP generation in mammalian cells: a tale of two systems.', *Journal of molecular biology*, 362(4), pp. 623–39. doi: 10.1016/j.jmb.2006.07.045.

Karantalis, V. and Hare, J. M. (2015) 'Use of mesenchymal stem cells for therapy of cardiac disease.', *Circulation research*, 116(8), pp. 1413–30. doi: 10.1161/CIRCRESAHA.116.303614.

Karastergiou, K., Smith, S. R., Greenberg, A. S. and Fried, S. K. (2012) 'Sex differences in human adipose tissues - the biology of pear shape.', *Biology of sex differences*, 3(1), p. 13. doi: 10.1186/2042-6410-3-13.

Katada, T., Tamura, M. and Ui, M. (1983) 'The A protomer of islet-activating protein, pertussis toxin, as an active peptide catalyzing ADP-ribosylation of a membrane protein.', *Archives of biochemistry and biophysics*, 224(1), pp. 290–8. Available at: http://www.ncbi.nlm.nih.gov/pubmed/6683482.

Kawano, S., Otsu, K., Kuruma, A., Shoji, S., Yanagida, E., Muto, Y., Yoshikawa, F., Hirayama, Y., Mikoshiba, K. and Furuichi, T. (2006) 'ATP autocrine/paracrine signaling induces calcium

oscillations and NFAT activation in human mesenchymal stem cells.', *Cell calcium*, 39(4), pp. 313–24. doi: 10.1016/j.ceca.2005.11.008.

Kawate, T., Robertson, J. L., Li, M., Silberberg, S. D. and Swartz, K. J. (2011) 'Ion access pathway to the transmembrane pore in P2X receptor channels.', *The Journal of general physiology*, 137(6), pp. 579–90. doi: 10.1085/jgp.201010593.

Kelley, D. E., Thaete, F. L., Troost, F., Huwe, T. and Goodpaster, B. H. (2000) 'Subdivisions of subcutaneous abdominal adipose tissue and insulin resistance.', *American journal of physiology. Endocrinology and metabolism*, 278(5), pp. E941-8. doi: 10.1152/ajpendo.2000.278.5.E941.

Kemp, P. A., Sugar, R. A. and Jackson, A. D. (2004) 'Nucleotide-mediated mucin secretion from differentiated human bronchial epithelial cells.', *American journal of respiratory cell and molecular biology*, 31(4), pp. 446–55. doi: 10.1165/rcmb.2003-0211OC.

Kennedy, C., Qi, a D., Herold, C. L., Harden, T. K. and Nicholas, R. a (2000) 'ATP, an agonist at the rat P2Y(4) receptor, is an antagonist at the human P2Y(4) receptor.', *Molecular pharmacology*, 57(5), pp. 926–931.

Kennedy, C. (2015) 'ATP as a cotransmitter in the autonomic nervous system.', *Autonomic neuroscience : basic & clinical*, 191, pp. 2–15. doi: 10.1016/j.autneu.2015.04.004.

Kerkelä, E., Laitinen, A., Räbinä, J., Valkonen, S., Takatalo, M., Larjo, A., Veijola, J., Lampinen, M., Siljander, P., Lehenkari, P., Alfthan, K. and Laitinen, S. (2016) 'Adenosinergic Immunosuppression by Human Mesenchymal Stromal Cells Requires Co-Operation with T cells', *Stem Cells*, 34(3), pp. 781–790. doi: 10.1002/stem.2280.

Kershaw, E. E., Hamm, J. K., Verhagen, L. A. W., Peroni, O., Katic, M. and Flier, J. S. (2006) 'Adipose triglyceride lipase: function, regulation by insulin, and comparison with adiponutrin.', *Diabetes*, 55(1), pp. 148–57. Available at: http://www.ncbi.nlm.nih.gov/pubmed/16380488.

Kersten, S. (2001) 'Mechanisms of nutritional and hormonal regulation of lipogenesis.', *EMBO reports*, 2(4), pp. 282–6. doi: 10.1093/embo-reports/kve071.

Kettlun, A. M., Uribe, L., Calvo, V., Silva, S., Rivera, J., Mancilla, M., Antonieta, M., Valenzuela and Traverso-Cori, A. (1982) 'Properties of two apyrases from Solanum tuberosum', *Phytochemistry*, 21(3), pp. 551–558. doi: 10.1016/0031-9422(82)83139-7.

Khor, V. K., Shen, W.-J. and Kraemer, F. B. (2013) 'Lipid droplet metabolism.', *Current opinion in clinical nutrition and metabolic care*, 16(6), pp. 632–7. doi: 10.1097/MCO.0b013e3283651106.

Kiefer, F. W. (2017) 'The significance of beige and brown fat in humans.', *Endocrine connections*, 6(5), pp. R70–R79. doi: 10.1530/EC-17-0037.

Kim, H. J. and Park, J.-S. (2017) 'Usage of Human Mesenchymal Stem Cells in Cell-based Therapy: Advantages and Disadvantages', *Development & Reproduction*, 21(1), pp. 1–10. doi: 10.12717/DR.2017.21.1.001.

Kim, H. S., Ohno, M., Xu, B., Kim, H. O., Choi, Y., Ji, X. D., Maddileti, S., Marquez, V. E., Harden, T. K.

and Jacobson, K. A. (2003) '2-Substitution of adenine nucleotide analogues containing a bicyclo[3.1.0]hexane ring system locked in a northern conformation: enhanced potency as P2Y1 receptor antagonists.', *Journal of medicinal chemistry*, 46(23), pp. 4974–87. doi: 10.1021/jm030127+.

Kim, S. and Moustaid-moussa, N. (2000) 'Secretory , Endocrine and Autocrine / Paracrine Function of the Adipocyte', *The Journal of nutrition*, pp. 3110–3115.

Kim, Y.-C., Lee, J.-S., Sak, K., Marteau, F., Mamedova, L., Boeynaems, J.-M. and Jacobson, K. A. (2005) 'Synthesis of pyridoxal phosphate derivatives with antagonist activity at the P2Y13 receptor', *Biochemical Pharmacology*, 70(2), pp. 266–274. doi: 10.1016/j.bcp.2005.04.021.

Kishore, B. K., Zhang, Y. and Ecelbarger, C. M. (2016) 'COMPOSITION AND METHODS FOR THE PREVENTION AND TREATMENT OF DETINDUCED OBESTY'. United States: United States of America. Available at: https://patentimages.storage.googleapis.com/40/81/d3/c81717f4c22ec0/US20160377598A1.pdf.

Kissebah, A. H., Vydelingum, N., Murray, R., Evans, D. J., Hartz, A. J., Kalkhoff, R. K. and Adams, P. W. (1982) 'Relation of body fat distribution to metabolic complications of obesity.', *The Journal of clinical endocrinology and metabolism*, 54(2), pp. 254–60. doi: 10.1210/jcem-54-2-254.

Kissebah, A. H., Freedman, D. S. and Peiris, A. N. (1989) 'Health risks of obesity.', *The Medical clinics of North America*, 73(1), pp. 111–38. Available at: http://www.ncbi.nlm.nih.gov/pubmed/2643000.

Klok, M. D., Jakobsdottir, S. and Drent, M. L. (2007) 'The role of leptin and ghrelin in the regulation of food intake and body weight in humans: a review', *Obesity Reviews*, 8(1), pp. 21–34. doi: 10.1111/j.1467-789X.2006.00270.x.

Kolditz, C.-I. and Langin, D. (2010) 'Adipose tissue lipolysis.', *Current opinion in clinical nutrition and metabolic care*, 13(4), pp. 377–81. doi: 10.1097/MCO.0b013e32833bed6a.

Konige, M., Wang, H. and Sztalryd, C. (2014) 'Role of adipose specific lipid droplet proteins in maintaining whole body energy homeostasis', *Biochimica et Biophysica Acta (BBA) - Molecular Basis of Disease*, 1842(3), pp. 393–401. doi: 10.1016/j.bbadis.2013.05.007.

Köster, A., Chao, Y. B., Mosior, M., Ford, A., Gonzalez-DeWhitt, P. A., Hale, J. E., Li, D., Qiu, Y., Fraser, C. C., Yang, D. D., Heuer, J. G., Jaskunas, S. R. and Eacho, P. (2005) 'Transgenic angiopoietin-like (angptl)4 overexpression and targeted disruption of angptl4 and angptl3: regulation of triglyceride metabolism.', *Endocrinology*, 146(11), pp. 4943–50. doi: 10.1210/en.2005-0476.

Kotnis, S., Bingham, B., Vasilyev, D. V., Miller, S. W., Bai, Y., Yeola, S., Chanda, P. K., Bowlby, M. R., Kaftan, E. J., Samad, T. A. and Whiteside, G. T. (2010) 'Genetic and Functional Analysis of Human P2X5 Reveals a Distinct Pattern of Exon 10 Polymorphism with Predominant Expression of the Nonfunctional Receptor Isoform', *Molecular Pharmacology*, 77(6), pp. 953–960. doi:

10.1124/mol.110.063636.
Kotova, P. D., Bystrova, M. F., Rogachevskaja, O. A., Khokhlov, A. A., Sysoeva, V. Y., Tkachuk, V. A. and Kolesnikov, S. S. (2018) 'Coupling of P2Y receptors to Ca 2+ mobilization in mesenchymal stromal cells from the human adipose tissue', *Cell Calcium*, 71, pp. 1–14. doi: 10.1016/j.ceca.2017.11.001.
Kristiansen, K. (2004) 'Molecular mechanisms of ligand binding, signaling, and regulation within the superfamily of G-protein-coupled receptors: molecular modeling and mutagenesis approaches to receptor structure and function', *Pharmacology & Therapeutics*, 103(1), pp. 21–80. doi: 10.1016/j.pharmthera.2004.05.002.
von Kügelgen, I. and Hoffmann, K. (2016) 'Pharmacology and structure of P2Y receptors', *Neuropharmacology*, 104, pp. 50–61. doi: 10.1016/j.neuropharm.2015.10.030.
Kwok, K. H. M., Lam, K. S. L. and Xu, A. (2016) 'Heterogeneity of white adipose tissue: molecular basis and clinical implications', *Experimental &Amp; Molecular Medicine*. The Author(s), 48, p. e215. Available at: http://dx.doi.org/10.1038/emm.2016.5.
Lafferty, M. J., Bradford, K. C., Erie, D. A. and Neher, S. B. (2013) 'Angiopoietin-like protein 4 inhibition of lipoprotein lipase: evidence for reversible complex formation.', *The Journal of biological chemistry*, 288(40), pp. 28524–34. doi: 10.1074/jbc.M113.497602.
Lago, F., Dieguez, C., Gómez-Reino, J. and Gualillo, O. (2007) 'Adipokines as emerging mediators of immune response and inflammation.', *Nature clinical practice. Rheumatology*. Nature Publishing Group, 3(12), pp. 716–24. doi: 10.1038/ncprheum0674.
Langenbach, F. and Handschel, J. (2013) 'Effects of dexamethasone, ascorbic acid and β-glycerophosphate on the osteogenic differentiation of stem cells in vitro.', *Stem cell research & therapy*, 4(5), p. 117. doi: 10.1186/scrt328.
Langin, D. (2006) 'Control of fatty acid and glycerol release in adipose tissue lipolysis.', *Comptes rendus biologies*, 329(8), pp. 598-607; discussion 653–5. doi: 10.1016/j.crvi.2005.10.008.
Laplante, M. A., Monassier, L., Freund, M., Bousquet, P. and Gachet, C. (2010) 'The purinergic P2Y1 receptor supports leptin secretion in adipose tissue', *Endocrinology*, 151(5), pp. 2060–2070. doi: 10.1210/en.2009-1134.
Lau, O. C. F., Samarawickrama, C. and Skalicky, S. E. (2014) 'P2Y2 receptor agonists for the treatment of dry eye disease: a review.', *Clinical ophthalmology (Auckland, N.Z.)*, 8, pp. 327–34. doi: 10.2147/OPTH.S39699.
Layland, J., Carrick, D., Lee, M., Oldroyd, K. and Berry, C. (2014) 'Adenosine: physiology, pharmacology, and clinical applications.', *JACC. Cardiovascular interventions*, 7(6), pp. 581–91. doi: 10.1016/j.jcin.2014.02.009.
Lazarowski, E. R., Watt, W. C., Stutts, M. J., Boucher, R. C. and Harden, T. K. (1995) 'Pharmacological selectivity of the cloned human P2U-purinoceptor: potent activation by

diadenosine tetraphosphate', *British Journal of Pharmacology*, 116(1), pp. 1619–1627. doi: 10.1111/j.1476-5381.1995.tb16382.x.

Lean, M. E. J., Han, T. S. and Morrison, C. E. (1995) 'Waist circumference as a measure for indicating need for weight management', *BMJ*. BMJ Publishing Group Ltd, 311(6998), pp. 158–161. doi: 10.1136/bmj.311.6998.158.

Lecoultre, V. and Ravussin, E. (2011) 'Brown adipose tissue and aging.', *Current opinion in clinical nutrition and metabolic care*, 14(1), pp. 1–6. doi: 10.1097/MCO.0b013e328341221e.

Lee, K. S., Kang, H. W., Lee, H. T., Kim, H.-J., Kim, C.-L., Song, J.-Y., Lee, K. W. and Cha, S.-H. (2014) 'Sequential sub-passage decreases the differentiation potential of canine adipose-derived mesenchymal stem cells', *Research in Veterinary Science*, 96(2), pp. 267–275. doi: 10.1016/j.rvsc.2013.12.011.

Lee, P., Swarbrick, M. M. and Ho, K. K. Y. (2013) 'Brown Adipose Tissue in Adult Humans: A Metabolic Renaissance', *Endocrine Reviews*, 34(3), pp. 413–438. doi: 10.1210/er.2012-1081.

Lee, S.-A., Yuen, J. J., Jiang, H., Kahn, B. B. and Blaner, W. S. (2016) 'Adipocyte-specific overexpression of retinol-binding protein 4 causes hepatic steatosis in mice.', *Hepatology (Baltimore, Md.)*, 64(5), pp. 1534–1546. doi: 10.1002/hep.28659.

Lee, S.-Y., Lim, J., Khang, G., Son, Y., Choung, P.-H., Kang, S.-S., Chun, S. Y., Shin, H.-I., Kim, S.-Y. and Park, E. K. (2009) 'Enhanced Ex Vivo Expansion of Human Adipose Tissue–Derived Mesenchymal Stromal Cells by Fibroblast Growth Factor-2 and Dexamethasone', *Tissue Engineering Part A*, 15(9), pp. 2491–2499. doi: 10.1089/ten.tea.2008.0465.

Lee, S. C. and Pappone, P. A. (1997) 'Membrane responses to extracellular ATP in rat isolated white adipocytes.', *Pflügers Archiv : European journal of physiology*, 434(4), pp. 422–8. Available at: http://www.ncbi.nlm.nih.gov/pubmed/9211808 (Accessed: 22 April 2015).

Lemaire, A., Vanorlé, M., Horckmans, M., di Pietrantonio, L., Clouet, S., Robaye, B., Boeynaems, J.-M. and Communi, D. (2017) 'Mouse P2Y4 Nucleotide Receptor Is a Negative Regulator of Cardiac Adipose-Derived Stem Cell Differentiation and Cardiac Fat Formation.', *Stem cells and development*, 26(5), pp. 363–373. doi: 10.1089/scd.2016.0166.

Lenain, N., Freund, M., Léon, C., Cazenave, J.-P. and Gachet, C. (2003) 'Inhibition of localized thrombosis in P2Y1-deficient mice and rodents treated with MRS2179, a P2Y1 receptor antagonist.', *Journal of thrombosis and haemostasis : JTH*, 1(6), pp. 1144–9. Available at: http://www.ncbi.nlm.nih.gov/pubmed/12871312.

Léon, C., Freund, M., Ravanat, C., Baurand, A., Cazenave, J. P. and Gachet, C. (2001) 'Key role of the P2Y(1) receptor in tissue factor-induced thrombin-dependent acute thromboembolism: studies in P2Y(1)-knockout mice and mice treated with a P2Y(1) antagonist.', *Circulation*, 103(5), pp. 718–23. Available at: http://www.ncbi.nlm.nih.gov/pubmed/11156884.

Lessard, J., Laforest, S., Pelletier, M., Leboeuf, M., Blackburn, L. and Tchernof, A. (2014) 'Low

abdominal subcutaneous preadipocyte adipogenesis is associated with visceral obesity, visceral adipocyte hypertrophy, and a dysmetabolic state', *Adipocyte*, 3(3), pp. 197–205. doi: 10.4161/adip.29385.

Li, P., Li, S.-H., Wu, J., Zang, W.-F., Dhingra, S., Sun, L., Weisel, R. D. and Li, R.-K. (2013) 'Interleukin-6 downregulation with mesenchymal stem cell differentiation results in loss of immunoprivilege', *Journal of Cellular and Molecular Medicine*, p. n/a-n/a. doi: 10.1111/jcmm.12092.

Li, W., Wei, S., Liu, C., Song, M., Wu, H. and Yang, Y. (2015) 'Regulation of the osteogenic and adipogenic differentiation of bone marrow-derived stromal cells by extracellular uridine triphosphate: The role of P2Y2 receptor and ERK1/2 signaling', *International journal of molecular medicine*, 37(1), pp. 63–73. doi: 10.3892/ijmm.2015.2400.

Liang, W., Xia, H., Li, J. and Zhao, R. C. (2011) 'Human adipose tissue derived mesenchymal stem cells are resistant to several chemotherapeutic agents', *Cytotechnology*, 63(5), pp. 523–530. doi: 10.1007/s10616-011-9374-5.

Liao, Z., Seye, C. I., Weisman, G. A. and Erb, L. (2007) 'The P2Y2 nucleotide receptor requires interaction with alpha v integrins to access and activate G12.', *Journal of cell science*, 120(Pt 9), pp. 1654–62. doi: 10.1242/jcs.03441.

Lillie, R. D. and Ashburn, L. L. (1943) 'Super-saturated solutions of fat stains in dilute isopropanol for demonstration of acute fatty degenerations not shown by Herxheimer technique.', *Archives of Pathology*, 36, pp. 432–440.

Lim, S. S., Vos, T., Flaxman, A. D., Danaei, G., Shibuya, K., Adair-Rohani, H., Amann, M., Anderson, H. R., Andrews, K. G., Aryee, M., Atkinson, C., Bacchus, L. J., Bahalim, A. N., Balakrishnan, K., Balmes, J., Barker-Collo, S., Baxter, A., Bell, M. L., *et al.* (2012) 'A comparative risk assessment of burden of disease and injury attributable to 67 risk factors and risk factor clusters in 21 regions, 1990-2010: a systematic analysis for the Global Burden of Disease Study 2010.', *Lancet (London, England)*, 380(9859), pp. 2224–60. doi: 10.1016/S0140-6736(12)61766-8.

Litosch, I., Hudson, T. H., Mills, I., Li, S. Y. and Fain, J. N. (1982) 'Forskolin as an activator of cyclic AMP accumulation and lipolysis in rat adipocytes.', *Molecular pharmacology*, 22(1), pp. 109–15. Available at: http://www.ncbi.nlm.nih.gov/pubmed/6289066.

Liu, M., Lei, H., Dong, P., Fu, X., Yang, Z., Yang, Y., Ma, J., Liu, X., Cao, Y. and Xiao, R. (2017) 'Adipose-Derived Mesenchymal Stem Cells from the Elderly Exhibit Decreased Migration and Differentiation Abilities with Senescent Properties', *Cell Transplantation*, 26(9), pp. 1505–1519. doi: 10.1177/0963689717721221.

Liu, Z., Xu, J., He, J., Liu, H., Lin, P., Wan, X., Navone, N. M., Tong, Q., Kwak, L. W., Orlowski, R. Z. and Yang, J. (2015) 'Mature adipocytes in bone marrow protect myeloma cells against chemotherapy through autophagy activation.', *Oncotarget*, 6(33), pp. 34329–41. doi:

10.18632/oncotarget.6020.
Livak, K. J. and Schmittgen, T. D. (2001) 'Analysis of Relative Gene Expression Data Using Real-Time Quantitative PCR and the 2−ΔΔCT Method', *Methods*, 25(4), pp. 402–408. doi: 10.1006/meth.2001.1262.
Lytton, J., Westlin, M. and Hanley, M. R. (1991) 'Thapsigargin Inhibits the Sarcoplasmic or Endoplasmic Reticulum Ca-ATPase Family of Calcium Pumps', *Journal of Biological Chemistry*, 266(26), pp. 17067–17071.
MacKenzie, S. and Houslay, M. D. (2000) 'Action of rolipram on specific PDE4 cAMP phosphodiesterase isoforms and on the phosphorylation of cAMP-response-element-binding protein (CREB) and p38 mitogen-activated protein (MAP) kinase in U937 monocytic cells', *Biochemical Journal*, 347, pp. 571–578.
Madec, S., Rossi, C., Chiarugi, M., Santini, E., Salvati, A., Ferrannini, E. and Solini, A. (2011) 'Adipocyte P2X7 receptors expression: A role in modulating inflammatory response in subjects with metabolic syndrome?', *Atherosclerosis*. Elsevier Ireland Ltd, 219(2), pp. 552–558. doi: 10.1016/j.atherosclerosis.2011.09.012.
Mahaut-Smith, M., Ennion, S., Rolf, M. and Evans, R. (2000) 'ADP is not an agonist at P2X(1) receptors: evidence for separate receptors stimulated by ATP and ADP on human platelets', *British journal of pharmacology*, 131(1), pp. 108–14.
Mamedova, L. K., Joshi, B. V, Gao, Z.-G., von Kügelgen, I. and Jacobson, K. A. (2004) 'Diisothiocyanate derivatives as potent, insurmountable antagonists of P2Y6 nucleotide receptors', *Biochemical Pharmacology*, 67(9), pp. 1763–1770. doi: 10.1016/j.bcp.2004.01.011.
Manolopoulos, K. N., Karpe, F. and Frayn, K. N. (2012) 'Marked resistance of femoral adipose tissue blood flow and lipolysis to adrenaline in vivo.', *Diabetologia*, 55(11), pp. 3029–37. doi: 10.1007/s00125-012-2676-0.
Marinou, K., Hodson, L., Vasan, S. K., Fielding, B. A., Banerjee, R., Brismar, K., Koutsilieris, M., Clark, A., Neville, M. J. and Karpe, F. (2014) 'Structural and functional properties of deep abdominal subcutaneous adipose tissue explain its association with insulin resistance and cardiovascular risk in men.', *Diabetes care*, 37(3), pp. 821–9. doi: 10.2337/dc13-1353.
van Marken Lichtenbelt, W. D., Vanhommerig, J. W., Smulders, N. M., Drossaerts, J. M. A. F. L., Kemerink, G. J., Bouvy, N. D., Schrauwen, P. and Teule, G. J. J. (2009) 'Cold-activated brown adipose tissue in healthy men.', *The New England journal of medicine*, 360(15), pp. 1500–8. doi: 10.1056/NEJMoa0808718.
Martinez-Botas, J., Anderson, J. B., Tessier, D., Lapillonne, A., Chang, B. H., Quast, M. J., Gorenstein, D., Chen, K. H. and Chan, L. (2000) 'Absence of perilipin results in leanness and reverses obesity in Lepr(db/db) mice.', *Nature genetics*, 26(4), pp. 474–9. doi: 10.1038/82630.
McAllister, E. J., Dhurandhar, N. V, Keith, S. W., Aronne, L. J., Barger, J., Baskin, M., Benca, R. M.,

Biggio, J., Boggiano, M. M., Eisenmann, J. C., Elobeid, M., Fontaine, K. R., Gluckman, P., Hanlon, E. C., Katzmarzyk, P., Pietrobelli, A., Redden, D. T., Ruden, D. M., *et al.* (2009) 'Ten putative contributors to the obesity epidemic.', *Critical reviews in food science and nutrition*, 49(10), pp. 868–913. doi: 10.1080/10408390903372599.

Meghani, P. (2002) 'The design of P2Y2 antagonists for the treatment of inflammatory diseases.', in *American Chemical Society Division of Medicinal Chemistry Abstracts of 224th ACS National Meeting*.

Meis, S., Hamacher, A., Hongwiset, D., Marzian, C., Wiese, M., Eckstein, N., Royer, H.-D., Communi, D., Boeynaems, J.-M., Hausmann, R., Schmalzing, G. and Kassack, M. U. (2010) 'NF546 [4,4'-(Carbonylbis(imino-3,1-phenylene-carbonylimino-3,1-(4-methyl-phenylene)-carbonylimino))-bis(1,3-xylene- , '-diphosphonic Acid) Tetrasodium Salt] Is a Non-Nucleotide P2Y11 Agonist and Stimulates Release of Interleukin-8 from Human Monocyte-Deri', *Journal of Pharmacology and Experimental Therapeutics*, 332(1), pp. 238–247. doi: 10.1124/jpet.109.157750.

Misra, A., Vikram, N. K., Gupta, R., Pandey, R. M., Wasir, J. S. and Gupta, V. P. (2005) 'Waist circumference cutoff points and action levels for Asian Indians for identification of abdominal obesity', *International Journal Of Obesity*. Nature Publishing Group, 30, p. 106. Available at: http://dx.doi.org/10.1038/sj.ijo.0803111.

Miyoshi, H., Souza, S. C., Zhang, H.-H., Strissel, K. J., Christoffolete, M. A., Kovsan, J., Rudich, A., Kraemer, F. B., Bianco, A. C., Obin, M. S. and Greenberg, A. S. (2006) 'Perilipin promotes hormone-sensitive lipase-mediated adipocyte lipolysis via phosphorylation-dependent and -independent mechanisms.', *The Journal of biological chemistry*, 281(23), pp. 15837–44. doi: 10.1074/jbc.M601097200.

Miyoshi, H., Perfield, J. W., Obin, M. S. and Greenberg, A. S. (2008) 'Adipose triglyceride lipase regulates basal lipolysis and lipid droplet size in adipocytes.', *Journal of cellular biochemistry*, 105(6), pp. 1430–6. doi: 10.1002/jcb.21964.

Mizuno, N. and Itoh, H. (2009) 'Functions and regulatory mechanisms of Gq-signaling pathways.', *Neuro-Signals*, 17(1), pp. 42–54. doi: 10.1159/000186689.

Monzon, J. R., Basile, R., Heneghan, S., Udupi, V. and Green, A. (2002) 'Lipolysis in adipocytes isolated from deep and superficial subcutaneous adipose tissue.', *Obesity research*, 10(4), pp. 266–9. doi: 10.1038/oby.2002.36.

Morgan, A. J., Murray, K. J. and Challiss, R. A. (1993) 'Comparison of the effect of isobutylmethylxanthine and phosphodiesterase-selective inhibitors on cAMP levels in SH-SY5Y neuroblastoma cells.', *Biochemical pharmacology*, 45(12), pp. 2373–80. Available at: http://www.ncbi.nlm.nih.gov/pubmed/7687130.

Nardi-Schreiber, A., Sapir, G., Gamliel, A., Kakhlon, O., Sosna, J., Gomori, J. M., Meiner, V., Lossos, A. and Katz-Brull, R. (2017) 'Defective ATP breakdown activity related to an ENTPD1 gene

mutation demonstrated using 31 P NMR spectroscopy', *Chemical Communications*, 53(65), pp. 9121–9124. doi: 10.1039/C7CC00426E.

Nelson, D. W., Gregg, R. J., Kort, M. E., Perez-Medrano, A., Voight, E. A., Wang, Y., Grayson, G., Namovic, M. T., Donnelly-Roberts, D. L., Niforatos, W., Honore, P., Jarvis, M. F., Faltynek, C. R. and Carroll, W. A. (2006) 'Structure−Activity Relationship Studies on a Series of Novel, Substituted 1-Benzyl-5-phenyltetrazole P2X 7 Antagonists', *Journal of Medicinal Chemistry*, 49(12), pp. 3659–3666. doi: 10.1021/jm051202e.

Ng, M., Fleming, T., Robinson, M., Thomson, B., Graetz, N., Margono, C., Mullany, E. C., Biryukov, S., Abbafati, C., Abera, S. F., Abraham, J. P., Abu-Rmeileh, N. M. E., Achoki, T., AlBuhairan, F. S., Alemu, Z. A., Alfonso, R., Ali, M. K., Ali, R., *et al.* (2014) 'Global, regional, and national prevalence of overweight and obesity in children and adults during 1980-2013: a systematic analysis for the Global Burden of Disease Study 2013.', *Lancet (London, England)*, 384(9945), pp. 766–81. doi: 10.1016/S0140-6736(14)60460-8.

Nicholls, D. G. and Rial, E. (2016) 'A novel regulatory mechanism for the brown-fat uncoupling protein?', *Nature Structural &Amp; Molecular Biology*. Nature Publishing Group, a division of Macmillan Publishers Limited. All Rights Reserved., 23, p. 364. Available at: http://dx.doi.org/10.1038/nsmb.3221.

Nielsen, T. S., Jessen, N., Jorgensen, J. O. L., Moller, N. and Lund, S. (2014) 'Dissecting adipose tissue lipolysis: molecular regulation and implications for metabolic disease', *Journal of Molecular Endocrinology*, 52(3), pp. R199–R222. doi: 10.1530/JME-13-0277.

Ning, H., Lin, G., Lue, T. F. and Lin, C.-S. (2006) 'Neuron-like differentiation of adipose tissue-derived stromal cells and vascular smooth muscle cells', *Differentiation*, 74(9–10), pp. 510–518. doi: 10.1111/j.1432-0436.2006.00081.x.

Nishimura, A., Sunggip, C., Tozaki-Saitoh, H., Shimauchi, T., Numaga-Tomita, T., Hirano, K., Ide, T., Boeynaems, J.-M., Kurose, H., Tsuda, M., Robaye, B., Inoue, K. and Nishida, M. (2016) 'Purinergic P2Y6 receptors heterodimerize with angiotensin AT1 receptors to promote angiotensin II-induced hypertension', *Science Signaling*, 9(411), pp. ra7-ra7. doi: 10.1126/scisignal.aac9187.

Noronha-Matos, J. B., Costa, M. A., Magalhães-Cardoso, M. T., Ferreirinha, F., Pelletier, J., Freitas, R., Neves, J. M., Sévigny, J. and Correia-de-Sá, P. (2012) 'Role of ecto-NTPDases on UDP-sensitive P2Y 6 receptor activation during osteogenic differentiation of primary bone marrow stromal cells from postmenopausal women', *Journal of Cellular Physiology*, 227(6), pp. 2694–2709. doi: 10.1002/jcp.23014.

Noronha-Matos, J. B., Coimbra, J., Sá-e-Sousa, A., Rocha, R., Marinhas, J., Freitas, R., Guerra-Gomes, S., Ferreirinha, F., Costa, M. A. and Correia-de-Sá, P. (2014) 'P2X7-induced zeiosis promotes osteogenic differentiation and mineralization of postmenopausal bone marrow-derived mesenchymal stem cells.', *FASEB journal : official publication of the Federation of American*

Societies for Experimental Biology, 28(12), pp. 5208–22. doi: 10.1096/fj.14-257923.
North, R. a (2002) 'Molecular physiology of P2X receptors', *Physiological reviews*, 82(4), p. 1013–67. doi: 10.1152/physrev.00015.2002.
Nuttall, F. Q. (2015) 'Body Mass Index: Obesity, BMI, and Health: A Critical Review.', *Nutrition today*, 50(3), pp. 117–128. doi: 10.1097/NT.0000000000000092.
O'Doherty, U., Swiggard, W. J. and Malim, M. H. (2000) 'Human immunodeficiency virus type 1 spinoculation enhances infection through virus binding.', *Journal of virology*, 74(21), pp. 10074–80. Available at: http://www.ncbi.nlm.nih.gov/pubmed/11024136.
Ohisalo, J. J. (1981) 'Effects of Adenosine on Lipolysis in Human Subcutaneous Fat Cells*', *The Journal of Clinical Endocrinology & Metabolism*, 52(2), pp. 359–363. doi: 10.1210/jcem-52-2-359.
Omatsu-Kanbe, M., Inoue, K., Fujii, Y., Yamamoto, T., Isono, T., Fujita, N. and Matsuura, H. (2006) 'Effect of ATP on preadipocyte migration and adipocyte differentiation by activating P2Y receptors in 3T3-L1 cells.', *The Biochemical journal*, 393(Pt 1), pp. 171–180. doi: 10.1042/BJ20051037.
Onogi, Y., Wada, T., Kamiya, C., Inata, K., Matsuzawa, T., Inaba, Y., Kimura, K., Inoue, H., Yamamoto, S., Ishii, Y., Koya, D., Tsuneki, H., Sasahara, M. and Sasaoka, T. (2017) 'PDGFRβ Regulates Adipose Tissue Expansion and Glucose Metabolism via Vascular Remodeling in Diet-Induced Obesity.', *Diabetes*, 66(4), pp. 1008–1021. doi: 10.2337/db16-0881.
Ormond, S. J. (2006) 'An Uncharged Region within the N Terminus of the P2X6 Receptor Inhibits Its Assembly and Exit from the Endoplasmic Reticulum', *Molecular Pharmacology*, 69(5), pp. 1692–1700. doi: 10.1124/mol.105.020404.
Paar, M., Jüngst, C., Steiner, N. A., Magnes, C., Sinner, F., Kolb, D., Lass, A., Zimmermann, R., Zumbusch, A., Kohlwein, S. D. and Wolinski, H. (2012) 'Remodeling of lipid droplets during lipolysis and growth in adipocytes.', *The Journal of biological chemistry*, 287(14), pp. 11164–73. doi: 10.1074/jbc.M111.316794.
La Paglia, L., Listì, A., Caruso, S., Amodeo, V., Passiglia, F., Bazan, V. and Fanale, D. (2017) 'Potential Role of ANGPTL4 in the Cross Talk between Metabolism and Cancer through PPAR Signaling Pathway', *PPAR Research*, 2017, pp. 1–15. doi: 10.1155/2017/8187235.
Parr, C. E., Sullivan, D. M., Paradiso, A. M., Lazarowski, E. R., Burch, L. H., Olsen, J. C., Erb, L., Weisman, G. A., Boucher, R. C. and Turner, J. T. (1994) 'Cloning and expression of a human P2U nucleotide receptor, a target for cystic fibrosis pharmacotherapy.', *Proceedings of the National Academy of Sciences*, 91(8), pp. 3275–3279. doi: 10.1073/pnas.91.8.3275.
Pchelintseva, E. and Djamgoz, M. B. A. (2018) 'Mesenchymal stem cell differentiation: Control by calcium-activated potassium channels.', *Journal of cellular physiology*, 233(5), pp. 3755–3768. doi: 10.1002/jcp.26120.
Peng, H., Hao, Y., Mousawi, F., Roger, S., Li, J., Sim, J. A., Ponnambalam, S., Yang, X. and Jiang, L.-H. (2016) 'Purinergic and Store-Operated Ca(2+) Signaling Mechanisms in Mesenchymal Stem Cells

and Their Roles in ATP-Induced Stimulation of Cell Migration.', *Stem cells (Dayton, Ohio)*, 34(8), pp. 2102–14. doi: 10.1002/stem.2370.

Pershadsingh, H. A., Lee, L. Y. and Snowdowne, K. W. (1989) 'Evidence for a sodium/calcium exchanger and voltage-dependent calcium channels in adipocytes.', *FEBS letters*, 244(1), pp. 89–92. Available at: http://www.ncbi.nlm.nih.gov/pubmed/2538354.

Petersen, R. K., Madsen, L., Pedersen, L. M., Hallenborg, P., Hagland, H., Viste, K., Doskeland, S. O. and Kristiansen, K. (2008) 'Cyclic AMP (cAMP)-Mediated Stimulation of Adipocyte Differentiation Requires the Synergistic Action of Epac- and cAMP-Dependent Protein Kinase-Dependent Processes', *Molecular and Cellular Biology*, 28(11), pp. 3804–3816. doi: 10.1128/MCB.00709-07.

Pierce, K. L., Premont, R. T. and Lefkowitz, R. J. (2002) 'Seven-transmembrane receptors', *Nature Reviews Molecular Cell Biology*. Nature Publishing Group, 3, p. 639. Available at: http://dx.doi.org/10.1038/nrm908.

Poirier, P. (2007) 'Adiposity and cardiovascular disease: are we using the right definition of obesity?', *European Heart Journal*, 28(17), pp. 2047–2048. doi: 10.1093/eurheartj/ehm321.

Post, S. R., Rump, L. C., Zambon, A., Hughes, R. J., Buda, M. D., Jacobson, J. P., Kao, C. C. and Insel, P. A. (1998) 'ATP activates cAMP production via multiple purinergic receptors in MDCK-D1 epithelial cells. Blockade of an autocrine/paracrine pathway to define receptor preference of an agonist.', *The Journal of biological chemistry*, 273(36), pp. 23093–7. Available at: http://www.ncbi.nlm.nih.gov/pubmed/9722536.

Postic, C. and Girard, J. (2008) 'Contribution of de novo fatty acid synthesis to hepatic steatosis and insulin resistance: lessons from genetically engineered mice.', *The Journal of clinical investigation*, 118(3), pp. 829–38. doi: 10.1172/JCI34275.

Purves, D., Augustine, G. and Fitzpatrick, D. (2001) 'Receptor Types.', in *Neuroscience.* 2nd editio. Sunderland (MA): Sinauer Associates. Available at: https://www.ncbi.nlm.nih.gov/books/NBK10989/.

Qiao, L., Lee, B., Kinney, B., Yoo, H. S. and Shao, J. (2011) 'Energy intake and adiponectin gene expression.', *American journal of physiology. Endocrinology and metabolism*, 300(5), pp. E809-16. doi: 10.1152/ajpendo.00004.2011.

Qiu, Y., Liu, Y., Li, W.-H., Zhang, H.-Q., Tian, X.-X. and Fang, W.-G. (2018) 'P2Y2 receptor promotes the migration and invasion of breast cancer cells via EMT-related genes Snail and E-cadherin.', *Oncology reports*, 39(1), pp. 138–150. doi: 10.3892/or.2017.6081.

Rafehi, M., Burbiel, J. C., Attah, I. Y., Abdelrahman, A. and Müller, C. E. (2017) 'Synthesis, characterization, and in vitro evaluation of the selective P2Y2 receptor antagonist AR-C118925', *Purinergic Signalling*, 13(1), pp. 89–103. doi: 10.1007/s11302-016-9542-3.

Rajaram, S., Baylink, D. J. and Mohan, S. (1997) 'Insulin-Like Growth Factor-Binding Proteins in Serum and Other Biological Fluids: Regulation and Functions*', *Endocrine Reviews*, 18(6), pp. 801–

831. Available at: http://dx.doi.org/10.1210/edrv.18.6.0321.

Ranganathan, G., Unal, R., Pokrovskaya, I., Yao-Borengasser, A., Phanavanh, B., Lecka-Czernik, B., Rasouli, N. and Kern, P. A. (2006) 'The lipogenic enzymes DGAT1, FAS, and LPL in adipose tissue: effects of obesity, insulin resistance, and TZD treatment.', *Journal of lipid research*, 47(11), pp. 2444–50. doi: 10.1194/jlr.M600248-JLR200.

Rao, D. D., Vorhies, J. S., Senzer, N. and Nemunaitis, J. (2009) 'siRNA vs. shRNA: Similarities and differences', *Advanced Drug Delivery Reviews*, 61(9), pp. 746–759. doi: 10.1016/j.addr.2009.04.004.

Ratjen, F., Durham, T., Navratil, T., Schaberg, A., Accurso, F. J., Wainwright, C., Barnes, M., Moss, R. B. and TIGER-2 Study Investigator Group (2012) 'Long term effects of denufosol tetrasodium in patients with cystic fibrosis.', *Journal of cystic fibrosis : official journal of the European Cystic Fibrosis Society*, 11(6), pp. 539–49. doi: 10.1016/j.jcf.2012.05.003.

Reddix, R. and Pacheco, M. A. (2007) 'Second Messengers', in *xPharm: The Comprehensive Pharmacology Reference*. Elsevier, pp. 1–7. doi: 10.1016/B978-008055232-3.60008-X.

Rodrigues, A. R., Almeida, H. and Gouveia, A. M. (2013) 'Alpha-MSH signalling via melanocortin 5 receptor promotes lipolysis and impairs re-esterification in adipocytes.', *Biochimica et biophysica acta*, 1831(7), pp. 1267–75. Available at: http://www.ncbi.nlm.nih.gov/pubmed/24046867.

Roh, H. C., Tsai, L. T. Y., Shao, M., Tenen, D., Shen, Y., Kumari, M., Lyubetskaya, A., Jacobs, C., Dawes, B., Gupta, R. K. and Rosen, E. D. (2018) 'Warming Induces Significant Reprogramming of Beige, but Not Brown, Adipocyte Cellular Identity', *Cell Metabolism*, 27(5), p. 1121–1137.e5. doi: 10.1016/j.cmet.2018.03.005.

Ronti, T., Lupattelli, G. and Mannarino, E. (2006) 'The endocrine function of adipose tissue: an update.', *Clinical endocrinology*, 64(4), pp. 355–65. doi: 10.1111/j.1365-2265.2006.02474.x.

Rosen, E. D. and Spiegelman, B. M. (2006) 'Adipocytes as regulators of energy balance and glucose homeostasis.', *Nature*, 444(7121), pp. 847–853. doi: 10.1038/nature05483.

Rutkowski, J. M., Stern, J. H. and Scherer, P. E. (2015) 'The cell biology of fat expansion', *The Journal of Cell Biology*, 208(5), pp. 501–512. doi: 10.1083/jcb.201409063.

Ruud, J. and Brüning, J. C. (2015) 'Light on leptin link to lipolysis', *Nature*. Nature Publishing Group, a division of Macmillan Publishers Limited. All Rights Reserved., 527, p. 43. Available at: http://dx.doi.org/10.1038/527043a.

Sadana, R. and Dessauer, C. W. (2009) 'Physiological Roles for G Protein-Regulated Adenylyl Cyclase Isoforms: Insights from Knockout and Overexpression Studies', *Neuro-Signals*, 17(1), pp. 5–22. doi: 10.1159/000166277.

Sage, S. O., Yamoah, E. H. and Heemskerk, J. W. (2000) 'The roles of P(2X1)and P(2T AC)receptors in ADP-evoked calcium signalling in human platelets.', *Cell calcium*, 28(2), pp. 119–26. doi: 10.1054/ceca.2000.0139.

Sahu-Osen, A., Montero-Moran, G., Schittmayer, M., Fritz, K., Dinh, A., Chang, Y.-F., McMahon, D., Boeszoermenyi, A., Cornaciu, I., Russell, D., Oberer, M., Carman, G. M., Birner-Gruenberger, R. and Brasaemle, D. L. (2015) 'CGI-58/ABHD5 is phosphorylated on Ser239 by protein kinase A: control of subcellular localization.', *Journal of lipid research*, 56(1), pp. 109–21. doi: 10.1194/jlr.M055004.

Sakharova, A. A., Horowitz, J. F., Surya, S., Goldenberg, N., Harber, M. P., Symons, K. and Barkan, A. (2008) 'Role of growth hormone in regulating lipolysis, proteolysis, and hepatic glucose production during fasting.', *The Journal of clinical endocrinology and metabolism*, 93(7), pp. 2755–9. doi: 10.1210/jc.2008-0079.

Saldanha-Araujo, F., Ferreira, F. I. S., Palma, P. V., Araujo, A. G., Queiroz, R. H. C., Covas, D. T., Zago, M. A. and Panepucci, R. A. (2011) 'Mesenchymal stromal cells up-regulate CD39 and increase adenosine production to suppress activated T-lymphocytes', *Stem Cell Research*, 7(1), pp. 66–74. doi: 10.1016/j.scr.2011.04.001.

Sassone-Corsi, P. (2012) 'The cyclic AMP pathway.', *Cold Spring Harbor perspectives in biology*, 4(12). doi: 10.1101/cshperspect.a011148.

Satrawaha, S., Wongkhantee, S., Pavasant, P. and Sumrejkanchanakij, P. (2011) 'Pressure induces interleukin-6 expression via the P2Y6 receptor in human dental pulp cells', *Archives of Oral Biology*, 56(11), pp. 1230–1237. doi: 10.1016/j.archoralbio.2011.05.003.

Scavo, L. M., Karas, M., Murray, M. and Leroith, D. (2004) 'Insulin-like growth factor-I stimulates both cell growth and lipogenesis during differentiation of human mesenchymal stem cells into adipocytes.', *The Journal of clinical endocrinology and metabolism*, 89(7), pp. 3543–53. doi: 10.1210/jc.2003-031682.

Schödel, J., Weise, I., Klinger, R. and Schmidt, M. (2004) 'Stimulation of lipogenesis in rat adipocytes by ATP, a ligand for P2-receptors', *Biochemical and Biophysical Research Communications*, 321(4), pp. 767–773. doi: 10.1016/j.bbrc.2004.06.179.

Schweiger, M., Schreiber, R., Haemmerle, G., Lass, A., Fledelius, C., Jacobsen, P., Tornqvist, H., Zechner, R. and Zimmermann, R. (2006) 'Adipose triglyceride lipase and hormone-sensitive lipase are the major enzymes in adipose tissue triacylglycerol catabolism.', *The Journal of biological chemistry*, 281(52), pp. 40236–41. doi: 10.1074/jbc.M608048200.

Scott, M. A., Nguyen, V. T., Levi, B. and James, A. W. (2011) 'Current Methods of Adipogenic Differentiation of Mesenchymal Stem Cells', *Stem Cells and Development*, 20(10), pp. 1793–1804. doi: 10.1089/scd.2011.0040.

Sengenès, C., Berlan, M., De Glisezinski, I., Lafontan, M. and Galitzky, J. (2000) 'Natriuretic peptides: a new lipolytic pathway in human adipocytes.', *FASEB journal : official publication of the Federation of American Societies for Experimental Biology*, 14(10), pp. 1345–51. Available at: http://www.ncbi.nlm.nih.gov/pubmed/10877827.

Sengenès, C., Bouloumié, A., Hauner, H., Berlan, M., Busse, R., Lafontan, M. and Galitzky, J. (2003) 'Involvement of a cGMP-dependent Pathway in the Natriuretic Peptide-mediated Hormone-sensitive Lipase Phosphorylation in Human Adipocytes', *Journal of Biological Chemistry*, 278(49), pp. 48617–48626. doi: 10.1074/jbc.M303713200.

Serradeil-Le Gal, C., Lafontan, M., Raufaste, D., Marchand, J., Pouzet, B., Casellas, P., Pascal, M., Maffrand, J. P. and Le Fur, G. (2000) 'Characterization of NPY receptors controlling lipolysis and leptin secretion in human adipocytes.', *FEBS letters*, 475(2), pp. 150–6. Available at: http://www.ncbi.nlm.nih.gov/pubmed/10858507.

Sheldon, H. (2011) 'Morphology of adipose tissue: a microscopic anatomy of fat', in *Comprehensive Physiology*. Hoboken, NJ, USA: John Wiley & Sons, Inc. doi: 10.1002/cphy.cp050113.

Shi, H., Halvorsen, Y. D., Ellis, P. N., Wilkison, W. O. and Zemel, M. B. (2000) 'Role of intracellular calcium in human adipocyte differentiation.', *Physiological genomics*, 3(2), pp. 75–82. doi: 10.1152/physiolgenomics.2000.3.2.75.

Shonberg, J., Kling, R. C., Gmeiner, P. and Löber, S. (2015) 'GPCR crystal structures: Medicinal chemistry in the pocket.', *Bioorganic & medicinal chemistry*, 23(14), pp. 3880–906. doi: 10.1016/j.bmc.2014.12.034.

Siehler, S. (2009) 'Regulation of RhoGEF proteins by G12/13-coupled receptors.', *British journal of pharmacology*, 158(1), pp. 41–9. doi: 10.1111/j.1476-5381.2009.00121.x.

Sivaramakrishnan, V., Bidula, S., Campwala, H., Katikaneni, D. and Fountain, S. J. (2012) 'Constitutive lysosome exocytosis releases ATP and engages P2Y receptors in human monocytes.', *Journal of cell science*, 125(Pt 19), pp. 4567–75. doi: 10.1242/jcs.107318.

Skurk, T., Mack, I., Kempf, K., Kolb, H., Hauner, H. and Herder, C. (2009) 'Expression and secretion of RANTES (CCL5) in human adipocytes in response to immunological stimuli and hypoxia.', *Hormone and metabolic research = Hormon- und Stoffwechselforschung = Hormones et metabolisme*, 41(3), pp. 183–9. doi: 10.1055/s-0028-1093345.

Slakey, L. L., Dickinson, E. S., Goldman, S. J., Gordon, E. L., Meghji, P. and Pearson, J. D. (1997) 'The Hydrolysis of Extracellular Adenine Nucleotides by Cultured Vascular Cells and Cardiac Myocytes', in Plesner, L., Kirley, T. L., and Knowles, A. F. (eds) *Ecto-ATPases: Recent Progress on Structure and Function*. Boston, MA: Springer US, pp. 27–32. doi: 10.1007/978-1-4615-5955-9_4.

Slawik, M. and Vidal-Puig, A. J. (2007) 'Adipose tissue expandability and the metabolic syndrome', *Genes and Nutrition*, 2(1), pp. 41–45. doi: 10.1007/s12263-007-0014-9.

Smith, P. J., Wise, L. S., Berkowitz, R., Wan, C. and Rubin, C. S. (1988) 'Insulin-like growth factor-I is an essential regulator of the differentiation of 3T3-L1 adipocytes.', *The Journal of biological chemistry*, 263(19), pp. 9402–8. Available at: http://www.ncbi.nlm.nih.gov/pubmed/2967822.

Smith, S. J., Cieslinski, L. B., Newton, R., Donnelly, L. E., Fenwick, P. S., Nicholson, A. G., Barnes, P.

J., Barnette, M. S. and Giembycz, M. A. (2004) 'Discovery of BRL 50481 [3-(N,N-dimethylsulfonamido)-4-methyl-nitrobenzene], a selective inhibitor of phosphodiesterase 7: in vitro studies in human monocytes, lung macrophages, and CD8+ T-lymphocytes.', *Molecular pharmacology*, 66(6), pp. 1679–89. doi: 10.1124/mol.104.002246.

Smith, S. R., Lovejoy, J. C., Greenway, F., Ryan, D., DeJonge, L., de la Bretonne, J., Volafova, J. and Bray, G. A. (2001) 'Contributions of total body fat, abdominal subcutaneous adipose tissue compartments, and visceral adipose tissue to the metabolic complications of obesity.', *Metabolism: clinical and experimental*, 50(4), pp. 425–35. doi: 10.1053/meta.2001.21693.

Smyth, J. T., Hwang, S.-Y., Tomita, T., DeHaven, W. I., Mercer, J. C. and Putney, J. W. (2010) 'Activation and regulation of store-operated calcium entry.', *Journal of cellular and molecular medicine*, 14(10), pp. 2337–49. doi: 10.1111/j.1582-4934.2010.01168.x.

Sniderman, A. D. and Cianflone, K. (1994) 'The Adipsin-ASP Pathway and Regulation of Adipocyte Function', *Annals of Medicine*. Taylor & Francis, 26(6), pp. 389–393. doi: 10.3109/07853899409148358.

Snyder, P. B., Esselstyn, J. M., Loughney, K., Wolda, S. L. and Florio, V. A. (2005) 'The role of cyclic nucleotide phosphodiesterases in the regulation of adipocyte lipolysis', *Journal of Lipid Research*, 46(3), pp. 494–503. doi: 10.1194/jlr.M400362-JLR200.

Sollevi, A., Hjemdahl, P. and Fredholm, B. (1981) 'Endogenous adenosine inhibits lipolysis induced by nerve stimulation without inhibiting noradrenaline release in canine subcutaneous adipose tissue in vivo', *Naunyn-Schmiedeberg's Archive of Pharmacology*, 316(2), pp. 112–119. Available at: http://link.springer.com/article/10.1007/BF00505303.

Song, H. and Yang, P.-C. (2010) 'Construction of shRNA lentiviral vector', *North American Journal of Medical Sciences*, pp. 598–601. doi: 10.4297/najms.2010.2598.

Spalding, K. L., Arner, E., Westermark, P. O., Bernard, S., Buchholz, B. A., Bergmann, O., Blomqvist, L., Hoffstedt, J., Näslund, E., Britton, T., Concha, H., Hassan, M., Rydén, M., Frisén, J. and Arner, P. (2008) 'Dynamics of fat cell turnover in humans', *Nature*, 453(7196), pp. 783–787. doi: 10.1038/nature06902.

Stewart, S. A., Dykxhoorn, D. M., Palliser, D., Mizuno, H., Yu, E. Y., An, D. S., Sabatini, D. M., Chen, I. S. Y., Hahn, W. C., Sharp, P. A., Weinberg, R. A. and Novina, C. D. (2003) 'Lentivirus-delivered stable gene silencing by RNAi in primary cells.', *RNA (New York, N.Y.)*, 9(4), pp. 493–501. doi: 10.1261/rna.2192803.

Stokes, L. (2013) 'Rab5 regulates internalisation of P2X4 receptors and potentiation by ivermectin', *Purinergic Signalling*, 9(1), pp. 113–121. doi: 10.1007/s11302-012-9336-1.

Stokoe, D., Stephens, L. R., Copeland, T., Gaffney, P. R., Reese, C. B., Painter, G. F., Holmes, A. B., McCormick, F. and Hawkins, P. T. (1997) 'Dual role of phosphatidylinositol-3,4,5-trisphosphate in the activation of protein kinase B.', *Science (New York, N.Y.)*, 277(5325), pp. 567–70. Available at:

http://www.ncbi.nlm.nih.gov/pubmed/9228007.

Styner, M., Sen, B., Xie, Z., Case, N. and Rubin, J. (2010) 'Indomethacin promotes adipogenesis of mesenchymal stem cells through a cyclooxygenase independent mechanism', *Journal of Cellular Biochemistry*, 111(4), pp. 1042–1050. doi: 10.1002/jcb.22793.

Sunahara, R. K. and Taussig, R. (2002) 'Isoforms of mammalian adenylyl cyclase: multiplicities of signaling.', *Molecular interventions*, 2(3), pp. 168–84. doi: 10.1124/mi.2.3.168.

Surprenant, A. and North, R. A. (2009) 'Signaling at Purinergic P2X Receptors', *Annual Review of Physiology*, 71(1), pp. 333–359. doi: 10.1146/annurev.physiol.70.113006.100630.

Swinburn, B. A., Sacks, G., Hall, K. D., McPherson, K., Finegood, D. T., Moodie, M. L. and Gortmaker, S. L. (2011) 'The global obesity pandemic: shaped by global drivers and local environments.', *Lancet (London, England)*, 378(9793), pp. 804–14. doi: 10.1016/S0140-6736(11)60813-1.

Tansey, J. T., Sztalryd, C., Gruia-Gray, J., Roush, D. L., Zee, J. V, Gavrilova, O., Reitman, M. L., Deng, C. X., Li, C., Kimmel, A. R. and Londos, C. (2001) 'Perilipin ablation results in a lean mouse with aberrant adipocyte lipolysis, enhanced leptin production, and resistance to diet-induced obesity.', *Proceedings of the National Academy of Sciences of the United States of America*, 98(11), pp. 6494–9. doi: 10.1073/pnas.101042998.

Tao, C., Sifuentes, A. and Holland, W. L. (2014) 'Regulation of glucose and lipid homeostasis by adiponectin: effects on hepatocytes, pancreatic β cells and adipocytes.', *Best practice & research. Clinical endocrinology & metabolism*, 28(1), pp. 43–58. doi: 10.1016/j.beem.2013.11.003.

Tchoukalova, Y. D., Votruba, S. B., Tchkonia, T., Giorgadze, N., Kirkland, J. L. and Jensen, M. D. (2010) 'Regional differences in cellular mechanisms of adipose tissue gain with overfeeding', *Proceedings of the National Academy of Sciences*, 107(42), pp. 18226–18231. doi: 10.1073/pnas.1005259107.

Thesleff, T., Lehtimäki, K., Niskakangas, T., Mannerström, B., Miettinen, S., Suuronen, R. and Öhman, J. (2011) 'Cranioplasty with adipose-derived stem cells and biomaterial: a novel method for cranial reconstruction.', *Neurosurgery*, 68(6), pp. 1535–40. doi: 10.1227/NEU.0b013e31820ee24e.

Tilg, H. and Moschen, A. R. (2008) 'Inflammatory mechanisms in the regulation of insulin resistance.', *Molecular medicine (Cambridge, Mass.)*, 14(3–4), pp. 222–31. doi: 10.2119/2007-00119.Tilg.

Tonelli, F. M. P., Santos, A. K., Gomes, D. A., da Silva, S. L., Gomes, K. N., Ladeira, L. O. and Resende, R. R. (2012) 'Stem Cells and Calcium Signaling', *Advances in Experimental Medicine and Biology*, 740, pp. 891–916. doi: 10.1007/978-94-007-2888-2_40.

Torres, G. E., Egan, T. M. and Voigt, M. M. (1999) 'Hetero-oligomeric Assembly of P2X Receptor Subunits', *Journal of Biological Chemistry*, 274(10), pp. 6653–6659. doi: 10.1074/jbc.274.10.6653.

Tozzi, M. and Novak, I. (2017) 'Purinergic Receptors in Adipose Tissue As Potential Targets in Metabolic Disorders', *Frontiers in Pharmacology*, 8. doi: 10.3389/fphar.2017.00878.

Turinetto, V., Vitale, E. and Giachino, C. (2016) 'Senescence in Human Mesenchymal Stem Cells: Functional Changes and Implications in Stem Cell-Based Therapy', *International Journal of Molecular Sciences*, 17(7), p. 1164. doi: 10.3390/ijms17071164.

Uccelli, A., Moretta, L. and Pistoia, V. (2008) 'Mesenchymal stem cells in health and disease.', *Nature reviews. Immunology*, 8(9), pp. 726–36. doi: 10.1038/nri2395.

Uhlén, M., Fagerberg, L., Hallström, B. M., Lindskog, C., Oksvold, P., Mardinoglu, A., Sivertsson, Å., Kampf, C., Sjöstedt, E., Asplund, A., Olsson, I., Edlund, K., Lundberg, E., Navani, S., Szigyarto, C. A.-K., Odeberg, J., Djureinovic, D., Takanen, J. O., *et al.* (2015) 'Proteomics. Tissue-based map of the human proteome.', *Science (New York, N.Y.)*, 347(6220), p. 1260419. doi: 10.1126/science.1260419.

Ungefroren, H., Gieseler, F., Fliedner, S. and Lehnert, H. (2015) 'Obesity and cancer', *Hormone Molecular Biology and Clinical Investigation*, 21(1). doi: 10.1515/hmbci-2014-0046.

Unger, R. H., Scherer, P. E. and Holland, W. L. (2013) 'Dichotomous roles of leptin and adiponectin as enforcers against lipotoxicity during feast and famine.', *Molecular biology of the cell*, 24(19), pp. 3011–5. doi: 10.1091/mbc.E12-10-0774.

Vaughan, M. (1962) 'The production and release of glycerol by adipose tissue incubated in vitro', *The Journal of biological chemistry*, 237(11), pp. 3354–3358. Available at: http://www.ncbi.nlm.nih.gov/pubmed/13996476.

Virtanen, K. A., Lidell, M. E., Orava, J., Heglind, M., Westergren, R., Niemi, T., Taittonen, M., Laine, J., Savisto, N.-J., Enerbäck, S. and Nuutila, P. (2009) 'Functional brown adipose tissue in healthy adults.', *The New England journal of medicine*, 360(15), pp. 1518–25. doi: 10.1056/NEJMoa0808949.

Wahrenberg, H., Lönnqvist, F. and Arner, P. (1989) 'Mechanisms underlying regional differences in lipolysis in human adipose tissue.', *Journal of Clinical Investigation*, 84(2), pp. 458–467. doi: 10.1172/JCI114187.

Wajchenberg, B. L. (2000) 'Subcutaneous and visceral adipose tissue: their relation to the metabolic syndrome.', *Endocrine reviews*, 21(6), pp. 697–738. doi: 10.1210/edrv.21.6.0415.

Walker, G. E., Verti, B., Marzullo, P., Savia, G., Mencarelli, M., Zurleni, F., Liuzzi, A. and Di Blasio, A. M. (2007) 'Deep subcutaneous adipose tissue: a distinct abdominal adipose depot.', *Obesity (Silver Spring, Md.)*, 15(8), pp. 1933–43. doi: 10.1038/oby.2007.231.

Wallentin, L., Becker, R. C., Budaj, A., Cannon, C. P., Emanuelsson, H., Held, C., Horrow, J., Husted, S., James, S., Katus, H., Mahaffey, K. W., Scirica, B. M., Skene, A., Steg, P. G., Storey, R. F. and Harrington, R. A. (2009) 'Ticagrelor versus Clopidogrel in Patients with Acute Coronary Syndromes', *New England Journal of Medicine*, 361(11), pp. 1045–1057. doi:

10.1056/NEJMoa0904327.

Wang, P., Henning, S. M. and Heber, D. (2010) 'Limitations of MTT and MTS-based assays for measurement of antiproliferative activity of green tea polyphenols.', *PloS one*, 5(4), p. e10202. doi: 10.1371/journal.pone.0010202.

Wang, S. P., Laurin, N., Himms-Hagen, J., Rudnicki, M. A., Levy, E., Robert, M. F., Pan, L., Oligny, L. and Mitchell, G. A. (2001) 'The adipose tissue phenotype of hormone-sensitive lipase deficiency in mice.', *Obesity research*, 9(2), pp. 119–28. doi: 10.1038/oby.2001.15.

Wang, Y., Sullivan, S., Trujillo, M., Lee, M.-J., Schneider, S. H., Brolin, R. E., Kang, Y. H., Werber, Y., Greenberg, A. S. and Fried, S. K. (2003) 'Perilipin expression in human adipose tissues: effects of severe obesity, gender, and depot.', *Obesity research*, 11(8), pp. 930–6. doi: 10.1038/oby.2003.128.

Wang, Z. V. and Scherer, P. E. (2016) 'Adiponectin, the past two decades', *Journal of Molecular Cell Biology*, 8(2), pp. 93–100. doi: 10.1093/jmcb/mjw011.

Wedellová, Z., Dietrich, J., Siklová-Vítková, M., Kološtová, K., Kováčiková, M., Dušková, M., Brož, J., Vedral, T., Stich, V. and Polák, J. (2011) 'Adiponectin inhibits spontaneous and catecholamine-induced lipolysis in human adipocytes of non-obese subjects through AMPK-dependent mechanisms.', *Physiological research*, 60(1), pp. 139–48. Available at: http://www.ncbi.nlm.nih.gov/pubmed/20945960.

Weyer, C., Foley, J. E., Bogardus, C., Tataranni, P. A. and Pratley, R. E. (2000) 'Enlarged subcutaneous abdominal adipocyte size, but not obesity itself, predicts type II diabetes independent of insulin resistance.', *Diabetologia*, 43(12), pp. 1498–506. doi: 10.1007/s001250051560.

Whicher, J., Bienvenu, J. and Monneret, G. (2001) 'Procalcitonin as an acute phase marker.', *Annals of clinical biochemistry*, 38(Pt 5), pp. 483–93. doi: 10.1177/000456320103800505.

White, M. F. (1998) 'The IRS-signalling system: a network of docking proteins that mediate insulin action.', *Molecular and cellular biochemistry*, 182(1–2), pp. 3–11. Available at: http://www.ncbi.nlm.nih.gov/pubmed/9609109.

White, U. A. and Tchoukalova, Y. D. (2014) 'Sex dimorphism and depot differences in adipose tissue function.', *Biochimica et biophysica acta*, 1842(3), pp. 377–92. doi: 10.1016/j.bbadis.2013.05.006.

Whitlock, G., Lewington, S., Sherliker, P., Clarke, R., Emberson, J., Halsey, J., Qizilbash, N., Collins, R., Peto, R. and Collaboration, P. S. (2009) 'Body-mass index and cause-specific mortality in 900 000 adults: collaborative analyses of 57 prospective studies.', *Lancet (London, England)*, 373(9669), pp. 1083–96. doi: 10.1016/S0140-6736(09)60318-4.

WHO (2016) *Obesity and overweight*. Available at: http://www.who.int/news-room/fact-sheets/detail/obesity-and-overweight (Accessed: 1 August 2018).

WHO (2018) *Obesity and overweight fact sheet*, *World Health Organisation*. Available at: http://www.who.int/en/news-room/fact-sheets/detail/obesity-and-overweight (Accessed: 27 June 2018).

Wu, F., Song, G., de Graaf, C. and Stevens, R. C. (2017) 'Structure and Function of Peptide-Binding G Protein-Coupled Receptors.', *Journal of molecular biology*, 429(17), pp. 2726–2745. doi: 10.1016/j.jmb.2017.06.022.

Xie, R., Xu, J., Wen, G., Jin, H., Liu, X., Yang, Y., Ji, B., Jiang, Y., Song, P., Dong, H. and Tuo, B. (2014) 'The P2Y 2 Nucleotide Receptor Mediates the Proliferation and Migration of Human Hepatocellular Carcinoma Cells Induced by ATP', *Journal of Biological Chemistry*, 289(27), pp. 19137–19149. doi: 10.1074/jbc.M113.540047.

Xu, D., Isaacs, C., Hall, I. and CW, E. (2001) 'Human airway smooth muscle expresses 7 isoforms of adenylyl cyclase: a dominant role for isoform V.', *American Journal of Physiology - Lung Cellular and Molecular Physiology*, 821(4), pp. L832–L843. Available at: http://ajplung.physiology.org/content/281/4/L832.long.

Xue, B., Greenberg, A. G., Kraemer, F. B. and Zemel, M. B. (2001) 'Mechanism of intracellular calcium ([Ca2+]i) inhibition of lipolysis in human adipocytes.', *FASEB journal : official publication of the Federation of American Societies for Experimental Biology*, 15(13), pp. 2527–9. doi: 10.1096/fj.01-0278fje.

Yang, S., Mulder, H., Holm, C. and Edén, S. (2004) 'Effects of growth hormone on the function of beta-adrenoceptor subtypes in rat adipocytes.', *Obesity research*, 12(2), pp. 330–9. doi: 10.1038/oby.2004.41.

Yang, X., Lee, F. Y. and Wand, G. S. (1997) 'Increased expression of Gs(alpha) enhances activation of the adenylyl cyclase signal transduction cascade.', *Molecular endocrinology (Baltimore, Md.)*, 11(8), pp. 1053–61. doi: 10.1210/mend.11.8.9957.

Yegutkin, G. G. (2014) 'Enzymes involved in metabolism of extracellular nucleotides and nucleosides: Functional implications and measurement of activities', *Critical Reviews in Biochemistry and Molecular Biology*, 49(6), pp. 473–497. doi: 10.3109/10409238.2014.953627.

Yerxa, B. R., Sabater, J. R., Davis, C. W., Stutts, M. J., Lang-Furr, M., Picher, M., Jones, A. C., Cowlen, M., Dougherty, R., Boyer, J., Abraham, W. M. and Boucher, R. C. (2002) 'Pharmacology of INS37217 [P1-(Uridine 5')-P4- (2'-deoxycytidine 5')tetraphosphate, Tetrasodium Salt], a Next-Generation P2Y2 Receptor Agonist for the Treatment of Cystic Fibrosis', *Journal of Pharmacology and Experimental Therapeutics*, 302(3), pp. 871–880. doi: 10.1124/jpet.102.035485.

Yilmaz, M., Claiborn, K. C. and Hotamisligil, G. S. (2016) 'De Novo Lipogenesis Products and Endogenous Lipokines.', *Diabetes*, 65(7), pp. 1800–7. doi: 10.2337/db16-0251.

Yu, F., Ji, S., Su, L., Wan, L., Zhang, S., Dai, C., Wang, Y., Fu, J. and Zhang, Q. (2015) 'Adipose-derived mesenchymal stem cells inhibit activation of hepatic stellate cells in vitro and ameliorate

rat liver fibrosis in vivo.', *Journal of the Formosan Medical Association = Taiwan yi zhi*, 114(2), pp. 130–8. doi: 10.1016/j.jfma.2012.12.002.

Yu, J. and Li, P. (2017) 'The size matters: regulation of lipid storage by lipid droplet dynamics', *Science China Life Sciences*, 60(1), pp. 46–56. doi: 10.1007/s11427-016-0322-x.

Yu, Z. and Jin, T. (2010) 'Extracellular high dosages of adenosine triphosphate induce inflammatory response and insulin resistance in rat adipocytes', *Biochemical and Biophysical Research Communications*. Elsevier Inc., 402(3), pp. 455–460. doi: 10.1016/j.bbrc.2010.10.028.

Zech, G., Hessler, G., Evers, A., Weiss, T., Florian, P., Just, M., Czech, J., Czechtizky, W., Görlitzer, J., Ruf, S., Kohlmann, M. and Nazaré, M. (2012) 'Identification of High-Affinity P2Y 12 Antagonists Based on a Phenylpyrazole Glutamic Acid Piperazine Backbone', *Journal of Medicinal Chemistry*, 55(20), pp. 8615–8629. doi: 10.1021/jm300771j.

Zechner, R., Zimmermann, R., Eichmann, T. O., Kohlwein, S. D., Haemmerle, G., Lass, A. and Madeo, F. (2012) 'FAT SIGNALS--lipases and lipolysis in lipid metabolism and signaling.', *Cell metabolism*, 15(3), pp. 279–91. doi: 10.1016/j.cmet.2011.12.018.

Zhang, D., Gao, Z.-G., Zhang, K., Kiselev, E., Crane, S., Wang, J., Paoletta, S., Yi, C., Ma, L., Zhang, W., Han, G. W., Liu, H., Cherezov, V., Katritch, V., Jiang, H., Stevens, R. C., Jacobson, K. A., Zhao, Q., *et al.* (2015) 'Two disparate ligand-binding sites in the human P2Y1 receptor', *Nature*. Nature Publishing Group, a division of Macmillan Publishers Limited. All Rights Reserved., 520, p. 317. Available at: http://dx.doi.org/10.1038/nature14287.

Zhang, D., Zhao, Q. and Wu, B. (2015) 'Structural Studies of G Protein-Coupled Receptors.', *Molecules and cells*, 38(10), pp. 836–42. doi: 10.14348/molcells.2015.0263.

Zhang, H., Kolb, F. A., Brondani, V., Billy, E. and Filipowicz, W. (2002) 'Human Dicer preferentially cleaves dsRNAs at their termini without a requirement for ATP', *The EMBO Journal*, 21(21), pp. 5875–5885. doi: 10.1093/emboj/cdf582.

Zhang, H. H., Halbleib, M., Ahmad, F., Manganiello, V. C. and Greenberg, A. S. (2002) 'Tumor necrosis factor-alpha stimulates lipolysis in differentiated human adipocytes through activation of extracellular signal-related kinase and elevation of intracellular cAMP.', *Diabetes*, 51(10), pp. 2929–35. Available at: http://www.ncbi.nlm.nih.gov/pubmed/12351429.

Zhang, J., Zhang, K., Gao, Z.-G., Paoletta, S., Zhang, D., Han, G. W., Li, T., Ma, L., Zhang, W., Müller, C. E., Yang, H., Jiang, H., Cherezov, V., Katritch, V., Jacobson, K. A., Stevens, R. C., Wu, B. and Zhao, Q. (2014) 'Agonist-bound structure of the human P2Y12 receptor.', *Nature*, 509(7498), pp. 119–22. doi: 10.1038/nature13288.

Zhang, Y., Proenca, R., Maffei, M., Barone, M., Leopold, L. and Friedman, J. M. (1994) 'Positional cloning of the mouse obese gene and its human homologue.', *Nature*, 372(6505), pp. 425–32. doi: 10.1038/372425a0.

Zhao, D. (2013) 'Adipose tissue dysfunction and the pathogenesis of metabolic syndrome', *World*

Journal of Hypertension, 3(3), p. 18. doi: 10.5494/wjh.v3.i3.18.
Zimmermann, H. (2001) 'Ectonucleotidases: Some recent developments and a note on nomenclature', *Drug Development Research*, 52(1–2), pp. 44–56. doi: 10.1002/ddr.1097.
Zimmermann, R., Strauss, J. G., Haemmerle, G., Schoiswohl, G., Birner-Gruenberger, R., Riederer, M., Lass, A., Neuberger, G., Eisenhaber, F., Hermetter, A. and Zechner, R. (2004) 'Fat mobilization in adipose tissue is promoted by adipose triglyceride lipase.', *Science (New York, N.Y.)*, 306(5700), pp. 1383–6. doi: 10.1126/science.1100747.
Zippel, N., Limbach, C. A., Ratajski, N., Urban, C., Luparello, C., Pansky, A., Kassack, M. U. and Tobiasch, E. (2012) 'Purinergic Receptors Influence the Differentiation of Human Mesenchymal Stem Cells', *Stem Cells and Development*, 21(6), pp. 884–900. doi: 10.1089/scd.2010.0576.
Zorina, Y., Iyengar, R. and Bromberg, K. D. (2010) 'Effectors of Gαo', in *Handbook of Cell Signaling*. Elsevier, pp. 1655–1663. doi: 10.1016/B978-0-12-374145-5.00203-5.